NOTE TO USERS

IMPROVED MEMBRANE FILTRATION FOR WATER AND WASTEWATER USING AIR SPARGING AND BACKFLUSHING

A

Thesis

Presented to the Faculty

of the University of Alaska Fairbanks

in Partial Fulfillment of the Requirements

for the Degree of

DOCTOR OF PHILOSOPHY

By

Christian Psoch

Dipl. Ing. (equiv. to BS+MS)

Fairbanks, Alaska

May 2005

IMPROVED MEMBRANE FILTRATION FOR WATER AND WASTEWATER

USING AIR SPARGING AND BACKFLUSHING

By

Christian Psoch

RECOMMENDED:

Advisory Committee Chair

Chair, Department of Civil and Environmental Engineering

APPROVED:

Dean, College of Engineering and Mines

Dean of the Graduate School

April 21, 2005

Date

Abstract

The goal of this research was to investigate methods and techniques that enhance mass transfer through the membranes. Two general types of fluids were investigated: synthetic wastewater treated in a membrane bioreactor (MBR) and natural and simulated river water. For both fluids, a wide range of solid concentrations (up to 18 g/L) were tested. The membranes investigated were all tubular modules at pilot scale between 0.75 and 1.20 m length, with tubular diameters of 5.5-6.3 mm, 0.2 μm pore size, and membrane surface areas of 0.036-0.1 m^2.

For flux enhancement, two techniques were applied: air sparging (AS), and backflushing (BF). Both techniques were compared with the sponge ball cleaning method. The experimental temperature ranged between 10 and 30°C, cross-flow velocities (CFV) ranged between 0.5 and 5.2 m/s, and transmembrane pressure (TMP) ranged between 30 and 350 kPa.

Research results showed, that AS was able to enhance the conventional flux over weeks to months up to factor of 4.5 for river water and a factor of 3 for wastewater. At modest CFV of 1.5- 2 m/s, AS was as successful as BF. If higher CFV (up to 5.2 m/s) were supplied for BF, this technique could enhance the wastewater flux by factor 4.5. The supply of AS and BF combined was superior to the single application even at moderate CFV. The major finding of this research was that cake thickness on the membrane surface was decreased by AS, contrary to research by other authors. AS can be used as substitute aeration in MBRs, without impairing the degradation

performance. The combination of AS and BF generated the least filter cake, but the lowest fouling was observed for AS. An empirical equation was proposed to calculate the viscosity in a sidestream MBR depending on reactor temperature and mixed liquor suspended solids (MLSS).

Table of Contents

List of Figures

List of Tables

List of Appendices

Acknowledgement

The submitted document comprises my work at WERC during the years 2002-2005 and was supported by a USGS grant, an EPSCOR start up grant and a thesis completion fellowship, for which I am very grateful. I would like to thank my supervisor, Dr. Silke Schiewer, for the opportunity to work independently. She demonstrated trust and confidence for my work and skills.

I would also like to thank my advisory committee for the extra mile they went for me and their dedication to support my work (even if the meeting times were often before the early birds get up).

Special thanks to Lewis Pane from PCI Membranes Inc. and Mr. Hubold from the Microdyn-Nadir who fostered my work with advice and donations of membranes.

An extra thanks to Michael Rasmussen from the Grundfos Company who generously supported my work with indispensable advice and equipment way beyond my research budget.

Furthermore, I am happy to thank Eric Johansen who designed the air sparging system and helped me several times, especially when the setup failed.

Finally, I would like to thank my girlfriend, all my friends, and the WERC research community for their given mental support and critical comments about my work.

Zum Schluss möchte ich meinen Eltern und meiner Schwester herzlichen Dank zuteil werden lassen, die mir durch finanzielle Zuwendungen und Ratschläge, insbesondere in den schwierigen Tagen des Beginns eine grosse Unterstützung waren.

Preface

According to the Water Supply & Sanitation Collaborative Council, more than 2 million people die every year from waterborne disease. Today's water supplies are limited by quantity and/or quality, particularly on a global perspective when considering world population growth.

Water resources are unevenly distributed over land masses. In addition, humankind has caused quality-based water scarcities by seriously polluting available fresh water supplies.

In many areas of the world where water scarcity is prevalent, a reuse of conventionally treated municipal wastewater for indirect potable use or direct industrial reuse seems advantageous. Furthermore, internal industrial recycling has become more attractive as a substitute for existing water supplies as water prices increase worldwide. This is especially true in industrial countries where about 60% of the water consumption is drawn for cooling purposes.

Membrane processes can play a key role in future water supply. They may be used to treat wastewaters, recover materials from industrial processes, and treat waters for drinking purposes.

However, membrane operation is limited by fouling, the major problem associated with this technology. Therefore, the main intention of this work, was to fight fouling in membrane filtration for water treatment with experimental methods.

Objective of the work

Improve the performance of membrane filtration for water and wastewater treatment.

The aim of this thesis was to investigate what options to overcome fouling are available to enhance water and wastewater membrane filtration. The research was empirical. It was assumed, that through providing certain features to the system and combining/optimizing them higher fluxes were possible.

The following attempts were made toward the overall objective of the work:

1. operate a membrane bioreactor (MBR) in the conventional way
2. investigate air sparging (AS) in the context of fouling prevention
3. investigate the combination of air sparging and backflushing (BF) for the fouling prevention
4. compare AS and BF with each other and their overall impact on the fouling process
5. investigate the potential of air sparged enhanced water filtration by example of river water filtration

Hypotheses

Based on literature study, the following hypotheses were postulated and provided the basis for this work:

- It is possible to enhance the process membrane flux in the treatment of potable water and wastewater with air sparging (AS) to maintain stable fluxes over longer time frames.
- It is possible to substitute AS in a membrane bioreactor (MBR) for conventional aeration.
- Degradation performance in a MBR is not affected adversely by substitution of conventional aeration for AS
- The combination of AS with backflushing (BF) is even more successful than just AS or BF alone.
- AS can reduce cake layers as external fouling
- AS is particularly effective to increase flux for waters with a strong fouling potential

1 Introduction

1.1 Membrane filtration

1.1.1 General introduction and definitions

Today, membrane filtration is on the verge of becoming a mainstream filtration process and is already competing with conventional techniques. Membranes are often times the first choice because of their decreasing costs and superior performance for improving a broad range of water qualities. Many new large capacity municipal water and wastewater treatment facilities in North America implement membrane filtration units.

Increasingly stringent disinfection and disinfection by-product standards support the use of membrane filtration. Many state and federal regulatory agencies opt for membrane application based on their high credits for pathogen removal as compared to conventional treatment. An additional benefit is the subsequent use of less disinfection chemicals and hence smaller storage tanks and feed facilities.

The effluent from a membrane filtration process is relatively constant and not very susceptible to changes in feedwater quality.

Finally, membrane filtration plants are easier to operate and monitor, and require less supervision than conventional plants, making remote control possible [1].

Before discussing published results on improved membrane filtration, it is reasonable to define a few of the terms used in this thesis more closely. If the definitions remain ambiguous, please refer to the context (topic) of this work.

1.1.1.1 Filtration

Filtration can be defined as a process to separate dispersed immiscible particles from a dispersing fluid by means of porous media based on size differences. The dispersing medium can be either a gas or a liquid. Under phenomenological aspects, the filtration process can be characterized by several parameters such as the pressure drop over the filter. This is defined below by eq. 1.1.

$$\Delta p = p_1 - p_2 \qquad \text{(eq. 1.1)}$$

In this case p_1 represents the pressure before the filter and p_2 the pressure behind the filter. The difference in pressure depends on the properties of the fluid and on the properties of the porous medium, which serves as the filter. This statement is only valid at time zero of the filtration process; for any time thereafter, particle deposition on the surface of the filtration material has to be taken into consideration [2-3].

Filtration is one of the principal methods for the treatment of potable water and wastewater. Nowadays, filtration is extensively used for supplemental removal of suspended solids (including particulate BOD = Biochemical Oxygen Demand, measured as the dissolved oxygen used by microorganisms in the biochemical oxidation of organic matter) from wastewater treatment plant effluents [4].

1.1.1.2 Membrane

A membrane [Lat. membrana, skin] is a selective barrier between two fluid phases. An artificial or synthetic membrane is a structure formed by a process not occurring in nature. It has lateral dimensions much greater than the thickness of the structure through which mass transfer occurs.

Membrane processes are driven by differences in some driving force such as the pressure, concentration, or voltage of the individual components across the membrane [5].

1.1.1.3 Ideal membranes and membrane materials

An ideal membrane is an impermeable barrier to one or more components to be separated from a fluid mixture.

Ideal membranes should have A) high flux; B) high selectivity (rejection); C) mechanical stability; D) tolerance to all feed stream components, including high fouling resistance; E) tolerance to temperature variations; F) manufacturing reproducibility; G) low manufacturing costs and H) ability to be packed into high surface area modules [5].

Membrane materials used for industrial membrane filtration can be made out of a steady increasing number of components such as: cellulose acetate, polysulfone, polyamide and ceramics.

1.1.1.4 Membrane filtration

Membrane filtration is the extension of the filtration term to applications that include the separation of dissolved solutes in liquid streams and separation of gaseous mixtures [2].

The membrane is the heart of every membrane process and can be understood as a semiselective barrier between two phases. In Fig. 1.1 a schematic expression is shown for a two component system. The feed side (phase 1) represents the random distribution of particles before the separation process and the permeate side (phase 2) shows the result of the separation process realized by a driving force. The membrane is ideally only permeable for one of the two components. The level of permeability is limited by a number of factors such as pore size. The driving force is often times a pressure gradient between both phases.

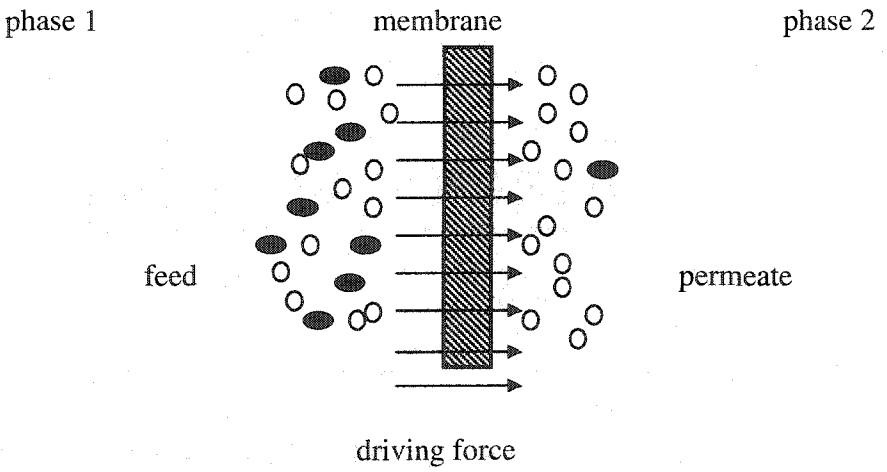

Fig. 1.1. Schematic principle of a two phase system separated by a membrane [6]

Figure 1.2 shows the basic membrane filtration processes, their pore and particle size ranges, range of method deployments, as well as comparison to common particles.

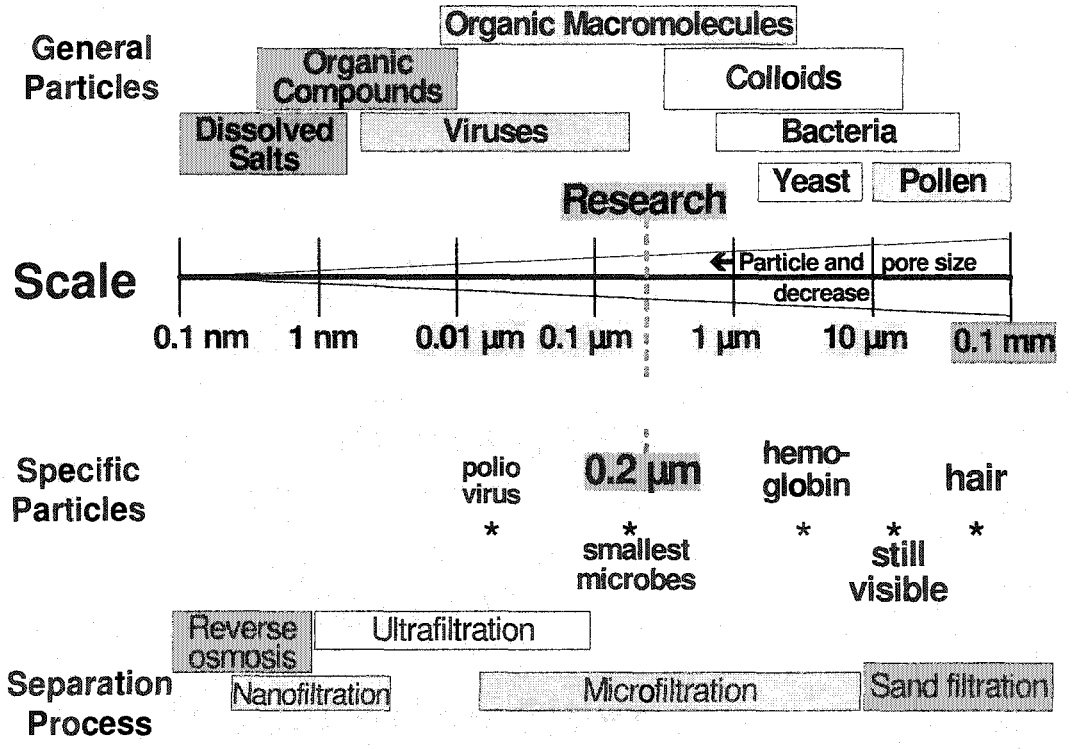

Fig. 1.2. Separation processes, specific and general particles in scale context

As evident from the logarithmic depiction in Fig. 1.2, membrane filtration spreads over a wide range of pore sizes, resulting in applications in all fields of science and industry. The most common way to define membrane filtration is by pore

size or by what components can be separated from the fluid. Hence, a short overview about the pressure driven membrane processes should be given.

The nature of the membrane itself determines which components permeate the filter and which are retained on the filter. An ideal example is reverse osmosis (pore size = 0.1-1 nm) which retains all components other than the solvent, which is mostly water. Thus, reverse osmosis (RO) can be considered as a dewatering technology. Nanofiltration is a comparably new process, which uses charged membranes with larger pore sizes than in RO, to retain sugars, divalent salts, and dissociated acids. However, unlike RO, nanofiltration allows the permeation of monovalent salts and undissociated acids. Ultrafiltration cannot retain any of the before mentioned compounds but is able to retain macromolecules or particles larger than about 10-200 Angstroms (depending on the shape of the particle). Microfiltration is deployed to separate particles in the range of 0.1 – 5 μm. Larger particles are better separated with conventional granular filtration technology.

Membrane technology is the call for the future. According to Prof. Enrico Drioli in his keynote lecture at the Water Environment Membrane Technology Conference 2004 in Seoul, South Korea: ". . . in 30 years, 50% of all separation processes will be accomplished by membranes."

1.1.2 Membrane filtration principles

1.1.2.1 Dead-End filtration

Dead-end flow is the conventional filtration process in liquid filtration. It is the familiar filtration principle used for instance in filtering coffee through filter paper or straining spaghetti. The flow is normal to the filter surface as shown in Fig. 1.3. Permeate and feed flow (bulk stream) directions are parallel to each other. The process is usually characterized by a thick filter cake (generated by separated particles on top of the membrane), which takes over a substantial part of the filtration itself and causes increasingly higher pressure drops across the continuously growing filter, made of filter material and cake. All of the fluid entering the filter is either retained or emerges on the permeate side. The conversion can reach 100% [7].

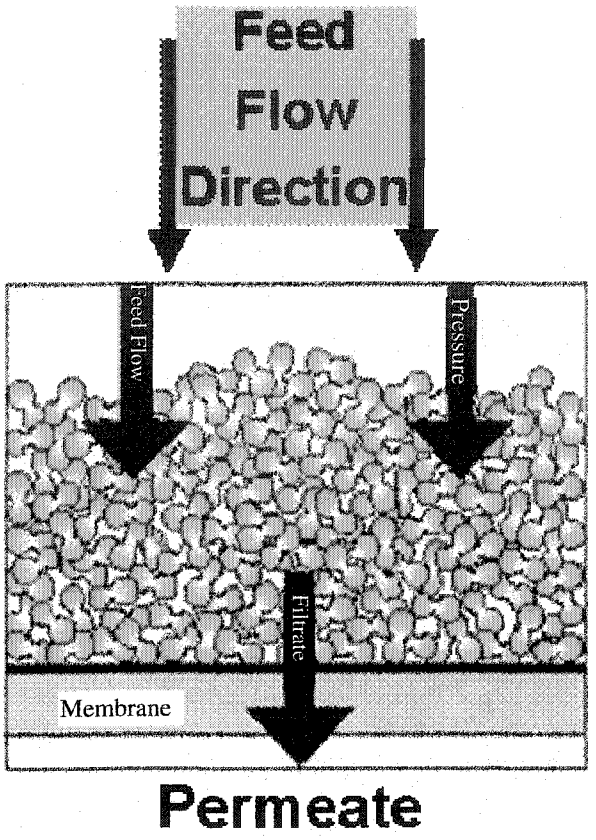

Fig. 1.3. Conventional or dead-end filtration

1.1.2.2 Cross-Flow filtration

In cross-flow filtration, the main flow directions, i. e. feed flow and permeate flow, stand perpendicular to each other. By maintaining the cross-flow velocity above the membrane material, the components which are retained by the membrane are swept off its surface. Thus, there is less accumulation on top of the membrane, which results in a lower filter cake thickness than in the dead-end filtration. This is illustrated by the differences in Fig. 1.4 compared to Fig. 1.3. With a thinner filter

cake, there is less tendency to "blind" (clog) the membrane. This helps to maintain the output of cross-flow filtration at higher levels than for dead-end filtration.

In cross-flow filtration, far more of the feed stream passes along the membrane than passes through it. Even if many membranes are operated in series, a mass less than 20% of the fluid passes through the membrane per passage. This output can be improved toward higher conversion rates via recirculation of the stream (stream recycling).

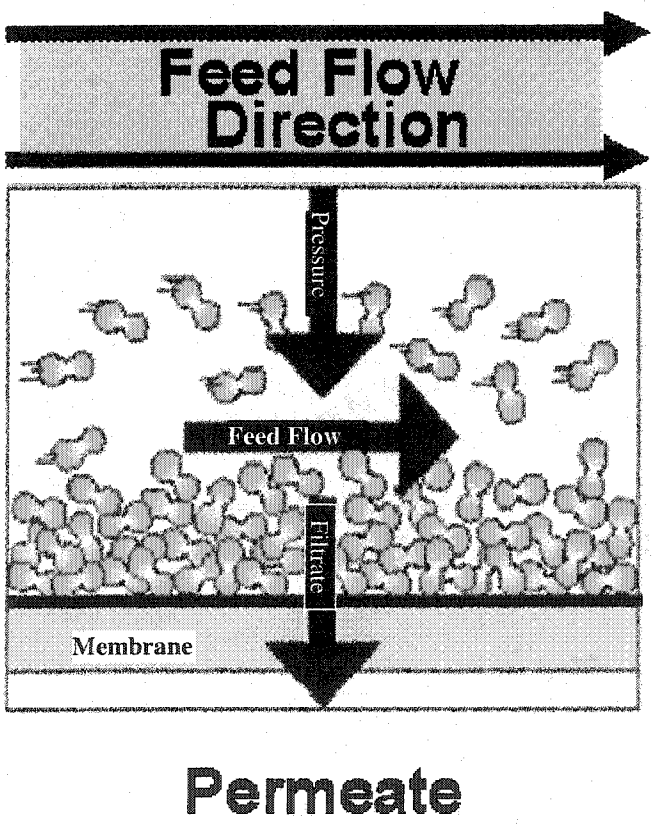

Fig. 1.4. Cross-flow filtration

1.1.3 Wastewater treatment via membrane filtration

1.1.3.1 General wastewater treatment

Wastewater treatment is grouped into primary, secondary, and advanced treatment. Primary treatment comprises physical operations such as screening and sedimentation to remove floatable and settleable solids from the water. Secondary treatment uses biological and chemical processes to reduce the load of organic matter in the water. Advanced (tertiary) treatment further aims to remove other constituents like nitrogen and phosphorus [4].

The conventional activated sludge process, commercialized in 1920 as a continuous process, is the most common biological process able to handle secondary and advanced treatment [8]. Although well understood and mathematically modeled, the use of the activated sludge process is constrained by several factors. Those factors are a relatively large area for the process setup, large volumes for the aeration and sedimentation tanks, further treatment of excess sludge, required adaptation to fluctuations in the loading rate, and frequent problems with sludge separation problems due to bulking and foaming [9].

1.1.3.2 Membrane bioreactors (MBR)

As an alternative technology to the activated sludge process, researchers became interested about 35 years ago in combining membranes with biological processes. MBR consists of a bioreactor and a membrane filtration unit, which replaces the step

of the secondary clarification for biomass separation. Fig. 1.5 and 1.6 show two possible configurations.

MBR for wastewater treatment are one of the fastest growing technologies in municipal and industrial wastewater treatment, especially for effluent reuse. If space restrictions apply, as in densely populated areas and on-board ships, MBR are a superior alternative due to small footprints [10].

The advantages of MBR compared to the conventional activated sludge process are a complete solid removal, quicker startup, the possibility of modular plant extension, and higher loading rates [11].

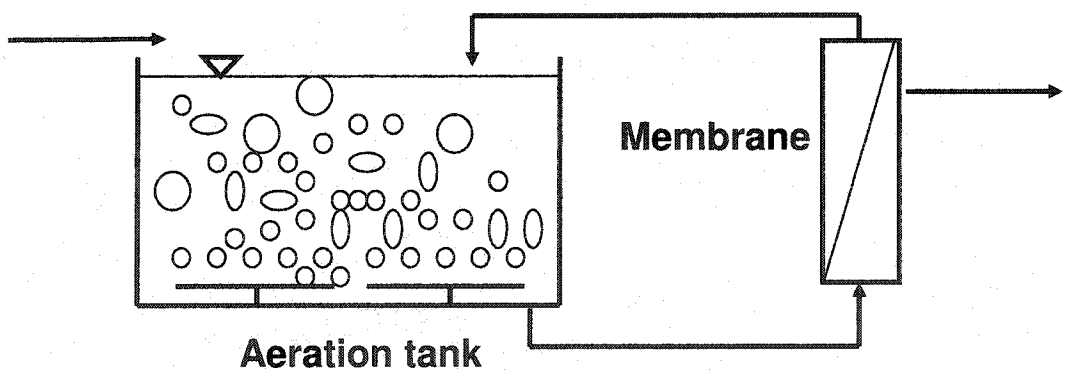

Fig. 1.5. Sidestream MBR as used in this work.

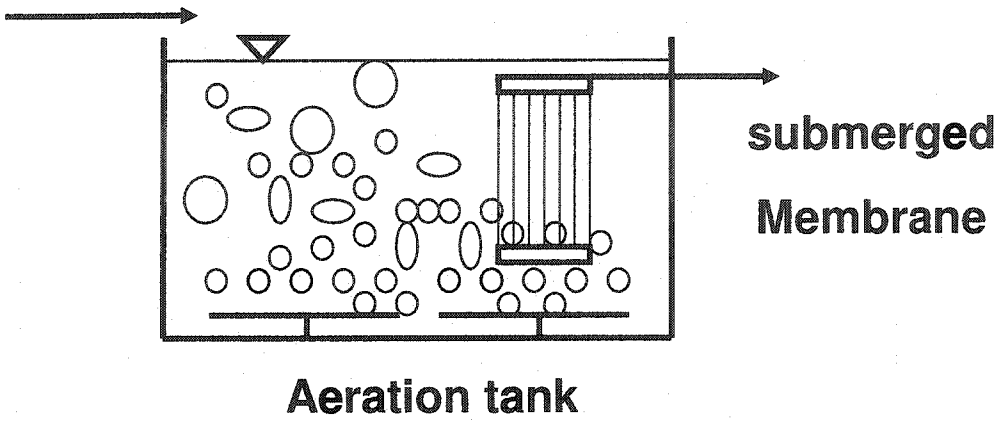

Fig. 1.6. Submerged MBR

MBR have been used commercially for a little over 20 years. Nowadays, far more than 1000 MBR plants are installed worldwide. In the last 14 years, submerged configurations (Fig. 1.6) have also been available [12].

The advantages of MBR are well documented. However, there are disadvantages as well. The productivity of MBR is constrained by membrane fouling. This is especially challenging since high concentrations of mixed liquor suspended solids (MLSS), dissolved extracellular polymeric substances (EPS) in combination with colloids, which are widely acknowledged as key foulants in MBR processes, lead to fouling as the major challenge during MBR operations [13-15].

MBR can be operated in sidestream and submerged configurations. Sidestream MBR show, as opposed to submerged reactors, high fluxes and excellent hydrodynamic control, but at the expense of low permeability. For conventional operation, the difference between the permeability of sidestream to the submerged

MBR can be anything between 2 and 20 in favor of the submerged system at equivalent gas velocity (submerged) and cross-flow velocity (CFV) (sidestream). The basis for the superior performance of the submerged system is the considerably enhanced mass transfer by the outside air sparging. With air sparging, submerged systems with bulk velocities half those of corresponding sidestream MBR still offer higher permeate flow rates [12].

The advantage of the submerged system may diminish if air sparging is supplied for the sidestream reactor. In this case, air sparging generates a two-phase flow inside the membrane for an inside-out system. This principle is one of the key research areas of this thesis and is further elucidated in section 1.3.4. The main advantage of the sidestream air sparging application is the more direct contact of the air bubbles on the membrane surface. In submerged systems, the membrane fibers often do evasive movements, which reduce the efficiency of the air sparging considerably. In sidestream air sparged systems, a maximum of shear force can be transferred from the air bubble in the slug flow regime (see section 1.3.4) to the top layers of the membrane. This enhances the permeability of the membrane by at least 100% (see chapters 3 and 7).

1.1.4 Potable water membrane filtration

One of the major driving forces for potable water treatment with membranes are the increased stringent drinking water standards. Many regulatory and governmental

institutions are giving more pathogen removal credits for membrane separation technology than for conventional treatment, which has the disadvantage of disinfection byproducts.

Finished water quality from a membrane treatment system shows considerably constant water quality, independent of the feedwater quality. Thus, especially for treating raw water supplies with fluctuating qualities, membrane filtration is the first choice. Additionally, the same advantages that apply for wastewater treatment with membranes apply also in potable water membrane filtration. These are significantly smaller footprints, less chemical use, easier operation, and less necessary supervision [1].

1.2 Membrane fouling

1.2.1 General

Fouling is the major problem in all membrane applications. Fouling changes the pore size and the pore size distribution. This causes problems in measuring and interpreting pore sizes. In microfiltration (0.01-10μm) (which is about the range of this research at 0.2 μm) and ultrafiltration (1-100nm), the pore size is usually not uniform. Thus, fouling affects pores differently. Four cases of fouling in micro and ultrafiltration should be distinguished [7].

A) Pore narrowing

- mainly due to adsorption, it begins by narrowing of the pore diameter due to particle adsorption onto the pore walls; particle diameter is considerably smaller than the pore diameter
- later, the pore gets clogged due to several adsorption layers; occlusion of the pore occurs

B) Pore plugging (also called Pore blockage)

- pore blockage by particles with about the same diameter as the pore

C) Gel/Cake layer formation

- particles with diameter much larger than the pore diameter deposit on top of the membrane and build a cake with several layers

D) Selective plugging of larger pores (especially for ultrafiltration)

- the particle diameter is bigger than the average pores and clogs only the largest pores

For simplicity and for practical reasons the fouling is often times only separated into internal and external fouling, or gel/cake (fouling) and (internal) fouling. This is because it is almost impossible to distinguish between the different types of fouling in practice.

To put the fouling phenomena into the context of mass transfer and membrane filtration calculations, the popular resistance in series model, as shown in eq. 1.2

should be introduced. The model only separates the fouling into cake layer and (real) internal fouling [6]:

$$J = \frac{TMP}{\mu * R_t} = \frac{TMP}{\mu * (R_m + R_c + R_f)} \qquad \text{eq. 1.2}$$

where J is the flux [L/(m²*h)], TMP is the applied transmembrane pressure [Pa], μ is the liquid viscosity [Pas], R_t is the total or overall resistance of the system [m^{-1}]. The total resistance can be split into R_m, the intrinsic membrane resistance, R_c, the cake resistance, and R_f, the fouling resistance. R_c and R_f increase over time.

1.2.2 External fouling or fouling resistance R_c

If the suspension has particulates with diameters larger than the membrane pores, the surface mechanism of sieving occurs. A cake layer grows on the membrane surface based on the retained particles. The cake provides an additional resistance to filtration. Hence this is called cake resistance, Rc. For Dead-End filtration the cake continuously grows but in crossflow operation the tangential shear stress may arrest the cake growth and extended operation is possible. Under the assumption of an incompressible cake, its porosity and resistance are independent of pressure. The specific cake resistance per unit thickness can be estimated (very roughly) by a

variation of the Carman-Kozeny equation (see Chapter 6) if further parameters such as particle diameters, etc. are known [16].

1.2.3 Internal fouling or fouling resistance R_f

Contrary to cake fouling or cake resistance, the internal fouling or actual fouling resistance, R_f, is considered more severe. Cake resistance, R_c, can be more easily removed by shear stress and or chemicals than the fouling resistance, R_f. The fouling resistance can be well characterized by fouling types A+B as described in the general explanation (section 1.2.1), which happens below the top level of the membrane, including partial pore blocking and especially adsorption. It is comparably harder to get rid of the internal fouling because it is (if the system is not suitable for backflushing) not easy to wash cleaning residues off the membrane as a cake just using overflow. Further, it is more complicated to reach all meso and micro pores with the chemical cleaning agent. If some membrane pores/areas can not be accessed by the cleaning agent, a loss of total membrane capacity, which is expressed as decreasing initial flux, is the result. Thus the treatment of internal fouling is essential for the life expectancy of the membrane and should be carefully carried out.

1.3 Measures against membrane fouling

1.3.1 General

Several strategies to maximize flux (in other words to control fouling) exist. Most of the measures involve fluid movements while others suggest moving the membrane (rotating disc principle). Turbulence has a huge impact on the mass transfer through the membrane. Agitation and mixing "sweeps" away accumulated solute, reducing the hydraulic resistance of the cake. Moreover, a thinner boundary layer and less concentration polarization are the result. Providing turbulence and flow instabilities is one of the simplest and most effective methods to enhance flux and control fouling. Following are some additional techniques to control flux decline over time [2].

1.3.2 Air sparging (AS)

Air sparging in this context is defined as the injection of air into the channels of a liquid stream. As Fig. 1.7 shows, the injection of air into a liquid stream generates a two phase flow with different possible flow patterns.

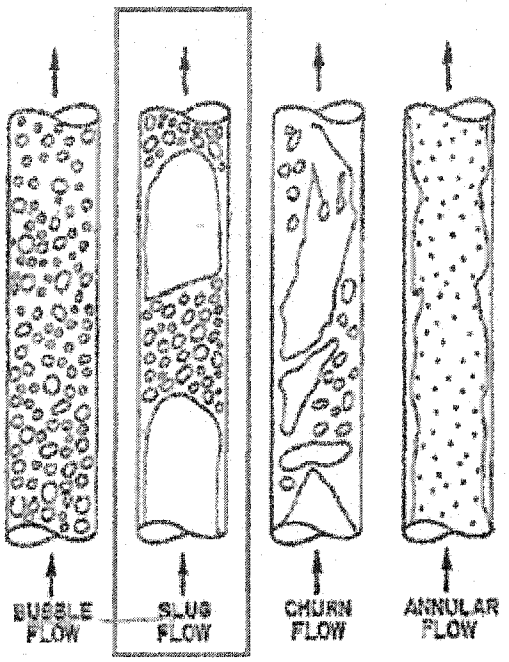

Fig. 1.7. Two phase flow pattern in upward flow according to *Salomon Levy* [17]

The flow patterns (also called flow regimes) depend on the air injection ratio ε, which is defined according to eq. 1.3 and on the inclination of the pipe

$$\varepsilon = \frac{v_{gas}}{v_{gas} + v_{liquid}} \qquad \text{eq. 1.3}$$

with:

v_{gas} = superficial gas velocity

v_{liquid} = superficial liquid velocity

In vertical upward filtration, which was mainly investigated in this thesis, for air injection ratios smaller than 0.2, bubble flow is the usually prevalent flow regime. At air injection ratios between 0.2 and 0.9, slug flow is prevalent. If ε is larger than 0.9,

churn flow is prevalent and the switch from liquid as the continuous phase to gas occurs. Annular flow at ε values clearly above 0.9 shows only little water moving in waves onto the channel walls upwards [18].

Lee et al. [19] published one of the first papers in 1993 about air slugs and enhancement of filtration by 50%. In 1994, *Cui and Wright* [20] reported on AS enhanced filtration with benefit of 60-113%.

From the mid nineties until today more research groups picked up on the topic of air sparging. As a result, it could be confirmed that the slug flow regime in upward flow has the most benefit for the membrane filtration with an optimum mass transfer at an air injection ratio between $\varepsilon = 0.55$ and $\varepsilon = 0.7$. If the gas slugs move upward, a thin water film (secondary flow) moves downward on the membrane surface causing high shear stress, which fights concentration polarization and enhances mass transport through the membrane. In the trail of the gas slug many micro bubbles are generated due to the pressure difference between the end of the gas slug and the following liquid slug. The micro bubbles, which are moving in wild turbulent movements in the trace of the gas slug are taken up by the next gas slug. The train of single air slugs, which are often times called Taylor bubbles, is moving faster than the liquid slugs [21-30].

As several researchers showed, AS in slug flow regime is even able to generate a suction pressure beyond the pressure fluctuation on the top layers of the membrane,

which is able to dislocate particles and cell debris that are already deposited or about to clog pores [31-33].

While the above reported results where only validated for tubular membranes (more than 4 mm diameter) and hollow fiber (less than 1 mm diameter) geometries, *Laborie et al.* [34] presented similar results for capillary membranes (4 mm > diameter > 1 mm).

Smith [35] pointed out the minor differences between the flow regimes in tubular and hollow fiber dimensions. In tubular slug flow, the bubble wake is very pronounced and the secondary flow in wake and gas slug has a substantial contribution to the flux enhancement. In hollow fibers, a wake actually doesn't exist and the enhanced mass transfer relies largely on the dynamic shear stress on the bubble nose and tail region. The surface tension in hollow fibers causes lower film velocities, which results in less shear stress. To optimize AS in hollow fibers, shorter and more frequent bubbles are required as compared to tubular dimensions.

Most of the literature relates to vertical upward flow because early investigations [20] have already shown that upward flow is more successful than horizontal flow. Nevertheless, *Cui and Wright* [36] showed that in downwards cross-flow with AS enhancement under certain circumstances (low velocities), very good results are possible as well. For more practical upward flow an inclination might be advantageous, as *Cheng et al.* [37-38] suggested.

Mikulasek and Pospisil [39] and *Cabassud et al.* [40] revealed research results on filter cake characteristics based on non direct methods. Both research groups claimed

that AS cross-flow filtration of inorganic suspensions generates a more porous but thicker filter cake than the conventional cross-flow filtration.

Vera et al. [41-42] and *Verberk et al.* [43-44] were better able to characterize AS through application of dimensionless numbers.

In regards to AS, not many studies present attempts on modeling the flow. *Mikulasek et al.* [45] and *Pospisil et al.* [46] tried with reasonable success to model flux results for inorganic suspension based on simple correlations and assumptions. More elaborate and scientific approaches were undertaken by *Taha and Cui* [33] and *Smith* [35] to model air sparged cross flow filtration with the help of computational fluid dynamics (CFD).

While *Lee et al.* [19] investigated flat channels of polysulfone membranes and *Cui et al.* [20] tubular PVDF (polyvinyliden fluoride) membranes, Mercier extended the application on mineral tubular membranes. Additionally, *Bellara et al.* [22] were the first to report on AS in polysulfone hollow fibers and *Li et al.* [48] documented work on polyethersulfone flat sheet membranes, which shows that AS works for a variety of different membrane materials and geometries.

During the last twelve years a wide variety of liquids was tested for the application of AS. From the successful filtration of bacteria cells [19], yeast [49] and different types of proteins such as bovine serum albumin, human serum albumin, human immunoglobulin and lysozyme [47], AS has proven to be a powerful enhancement technique without negatively impacting the properties of the components [47]. Not only biological model solutions as municipal [27; 50] and oily

wastewater [51], but also inorganic suspensions such as clay slurries [40; 55] and titanium dioxide [26; 39] were successfully investigated.

Cui et al. [52] and *Laborie et al.* [53] claim that the application of AS might even under economic aspects be advantageous compared to conventional filtration in addition to the reported benefits.

Finally, a few disadvantages and limitations for AS exist as well. *Bellara et al.* [54] reported on the problem of foam production in the context of treating protein solutions. *Bellara et al.* and *Majewska-Nowak et al.* [55] discovered less selectivity resulting in a decrease of the sieving coefficient (sieving coefficient= permeate concentration/feed concentration). *Cheng et al.* [56] and *Ducom and Cabassud* [57] found that if there is very little boundary layer resistance (concentration polarization), the effect of AS is limited.

1.3.3 Backflushing (BF)

Backflushing or backwashing (depending on the author and/or definition) is a periodic reversal of the filtrate flow (permeate) back into the feed channel. This technique has been commonly practiced in the industry for many years and is a fairly simple effective way to fight fouling. The backflushing can be accomplished with gas or liquid and it is even possible under certain circumstances to add a cleaning agent to the backflush fluid. It is assumed that backflushing both pushes particles out of clogged membrane pores and dislodges accumulated particles from the membrane

surface. Thus, backflushing is able to overcoming pore blockage, which is not possible with other cleaning strategies without process disturbance. Some disadvantages of BF are the product loss and the fact that only the part of the module which has the lower TMP (due to pressure drop over the membrane in flow direction) substantially benefits from the procedure. To be effective, the backflush pressure should be greater than the regular operating inlet pressure [2]. The investigation of BF was a major goal of this thesis, especially in combination with air sparging on which *Chang and Judd* first reported in 2002 [50].

1.3.4 Critical flux

The term critical flux was first defined by *R. Field et al.* in 1995 [58]. The postulation of the critical flux was based on the observation that at certain low fluxes no flux decline at constant pressure occurred with time. This lead to the following definition [58]:

"The critical flux hypothesis for microfiltration is that on start-up there exists a flux below which a decline of flux with time does not occur, above it fouling is observed. This flux is the critical flux and its value depends on the hydrodynamics and probably other variables."

The reevaluation of this statement almost 10 years later showed that after a long enough time a flux decline is *always* observed, due to mass transfer phenomena, even if the Peclet number (bulk mass transfer/diffusive mass transfer) is below the critical

value (the critical Peclet number was determined to describe the critical flux) [59]. However, the principle to operate a system under very low pressure as the subcritical flux approaches is proven to be very successful in practice [60].

1.3.5 Chemical cleaning

Def. [2]: *Cleaning is the removal of foreign material from the surface and body of the membrane.*

Problems are often times described as fouling problems but it is actually a cleaning problem since certain accumulation within the membrane can not be removed.

The frequency of cleaning is an important economical factor and impacts the life of the membrane.

Membrane cleaning may be advantageous for several reasons:

- assures germ growth does not exceed hygienic requirements and prevention of contamination of already treated sections of the product stream
- process optimization (it might be better to stop and clean for the advantage of obtaining a higher flux instead proceeding with a low flux)

Three properties characterize a clean membrane:

- **physically clean,** means free from visible impurities and foreign matter
- **chemically clean**, means *all* foulants and impurities are removed
- **biologically clean** or "**sanitized**", means the membrane is free of all viable microorganisms

After the first application of a new membrane, the initial water flux cannot be reestablished even after thoroughly chemical cleaning. The initial water flux drops to a stable value after a few operation cycles. However, it is important that the previous process flux be restored. This was the fact on which this research was based.

Operational rules for chemical cleaning and important factors during cleaning [2]:

- It is important to keep in mind that cleaning from the permeate side is just as necessary as from the feed stream side.
- The type of foulant determines if a solubilizer or disperser should be used, since a reprecipitation during rinsing is possible.
- The membrane must withstand the cleaning agent without any damage.
- Cleaning should be processed under turbulent conditions ($3000 \leq Re \leq 5000$).
- The time should not exceed 30-60 min, since most of the cleaning agents do their job within this time; prolonged cleaning may cause refouling.
- Maintain high temperatures using Van't Hoff's law (increase of temperature by 10°C yields in doubling of the reaction velocity), but 55-60°C is acceptable. Higher temperature of chemicals leads to faster reactions and thus better cleaning since the cleaning times are limited. During cleaning time, the system cannot operate and thus the downtime should be as short as possible.
- The usage of deionized (DI) water for rinsing.
- The pH of the cleaning solutions or rinsing water should be adapted according to the foulant.

1.3.6 Alternative anti fouling measures

1.3.6.1 Sponge balls

In tubular membrane systems it is possible to use oversized (about 10% larger dimensions than the tube) sponge balls to achieve a mechanical cleaning of the membrane surface. The cleaning frequency and hardness of the sponge balls can be adjusted according to the needs. Usually very good results can be obtained [6].

1.3.6.2 Turbulence promoters and local vortex promotion

Some authors described designs of concentric screws threads in tubular membranes, which have a clearance to the wall to permit leakage flow in the resulting annular gap. This results in corkscrew vortexes superimposed on the helical flow, generating a helical mixing of the flow field [61].

1.3.6.3 Helical baffles, stamped membranes and curved membranes (membrane helix)

These techniques are similar to the application of spacers in spiral wound modules. Significant flux improvements were reported up to a factor of 6 compared to smooth wall membranes [61-63].

1.3.6.4 Electrical fields

This technique uses the fact that many foulant particles in the solutions are charged. Next to the bulk flow and parallel to the membrane surface, a convective flow towards the porous surface exists, transporting particles laterally toward the membrane. The convective flow can be (more or less) counterbalanced by electrophoretic velocity by application of an electrical field [62].

1.4 Mass balances

1.4.1 MBR balance

The reactor mass balance is based on the general balance equation 1.4 and 1.5. Without running the equipment for a longer time it would be difficult to determine values for individual terms in equation 1.6, which is an adaptation of the general balance equation for the membrane bioreactor. Only experience made it possible to quantify elements of this detailed reactor balance.

Storage = Transport $\pm$ Conversion eq. 1.4

Accumulation or Depletion = In – Out $\pm$ Source or Sink eq. 1.5

$$S = \sum_{0}^{k} In - \sum_{0}^{n} Out - Sinks \qquad \text{eq. 1.6}$$

Whereby:

S = Storage volume (Accumulation or Depletion) of liquid in the tank

Input terms:

$$\sum_{1}^{k} In$$

With 1-k:

1 = Concentrated feed (about 450 mL/day)

2 = Dilution water (about 500 mL/day)

3 = BF water, (about 2 L/day)

4 = Rinsing water (volume varied, occasionally)

5 = Condensation water from cooling

Output terms:

$$\sum_{1}^{n} Out$$

1 = Sampling (less than 50 ml/day)

2 = Sludge (2L/day)

3 = Spilling (volume varied, occasionally)

4 = Permeate, depending on type of operation (volume varied every day)

Sinks (~500 mL/day): Evaporation + microbial respiration

1.4.2 River water or potable water treatment

In the case of river water filtration, eq. 1.6, included fewer terms:

S = Storage (Accumulation or Depletion) volume of liquid in the tank

Input terms

$$\sum_{1}^{k} In$$

With 0-k:

1 = Refill of water or model solution

2 = Condensation water from cooling

Output terms:

$$\sum_{1}^{n} Out$$

1 = Sampling

2 = Spelling (volume varied, occasionally)

3 = Permeate, depending on type of operation (volume varied every day)

Sinks (not determined):

Evaporation

1.5 Undertaken research

1.5.1 Relevance of this research

As described in Section 1.3 several methods mitigate fouling. Most of the described techniques were applied in the frame of this work with an emphasis on air sparging and backflushing. All cited papers which report on AS, with the exception of one, investigated short term application with less than 8 hour durations. This thesis reports on long term experiments between 5 days and 190 days, which distinguishes this work from other research. Especially for instable fluctuating conditions as in multiphase-flow, it is very challenging to operate a system on a permanent basis, which might reflect in the small number of published papers reporting on extended time frames. Moreover this thesis presents research results on combining AS (inside of the membrane) and BF - a successful approach not very often pursued in the past except by *Chang and Judd* [50]. Finally the application of AS in the context of potable water filtration is very seldom reported.

Turbulence: The rather general statement that increased turbulence is capable in minimizing fouling during solid liquid membrane filtration is basically in all the papers included (Chapter 2 – 8). Within Chapters 2 and 3 considerations are made regarding the influence of turbulence on the fouling under the special circumstances.

Air sparging: All of the papers in this thesis include the application of air sparging as a successful technique to suppress fouling. Chapter 2, 3 and 8 focus on the application of AS as the only enhancement technique.

Backflushing: Chapters 4-7 describe the investigations of maintaining flux at higher levels by deployment of backflushing in addition or in comparison to AS.

Critical flux: Chapter 7 reports on system operation under subcritical flux conditions to avoid flux decline at different levels.

Chemical cleaning: Chapters 5, 6 and 8 contain observations about chemical cleaning with different cleaning solutions and membrane fouling caused by different types of raw water and wastewater.

Sponge balls: Chapters 6 and 8 include tests with sponge ball applications and the results for cleaning membranes from wastewater filtration (Chapter 6) and river water filtration (Chapter 8).

1.5.2 Overview of the papers embedded in this thesis as Chapters 2 to 8

Chapter 2 shows initial results which show that air sparging as a measure against fouling works with the chosen setup. The whole paper is based on intermittent AS in an MBR. The feed (synthetic wastewater) for the MBR had to be optimized and adapted to the microbial growth. The experiments ran for up to more than six months.

Chapter 3 is based on the results of Chapter 2 and focuses more on dimensionless numbers. A new approach which is not only applicable to AS is proposed resulting in a changed dimensionless number. Chapter 2 and Chapter 3 show the results of investigations in regard to turbulence and fouling indicators as the Shear Stress Number and the Fouling Number.

Chapter 4 shows first results of the combination of air sparging and backflushing for synthetic wastewater, to address internal and external fouling separately. First time results also show the comparison between enhanced and non-enhanced filtration. The duration for the compared test was about one week. Furthermore, the effects of varied air injection ratios on flux improvement were investigated.

Chapter 5 shows the results of degradation measurements in an air sparged MBR using synthetic wastewater. Observations regarding pure water flux are represented. Comparisons between only air sparging and only backflushing enhanced flux are made and further compared to conventional treatment. The impact of high liquid cross-flow velocity is tested as well. Finally, models for flux declines depending on the type of applications and time frame are suggested. As a byproduct of this study, an equation for estimation of the dynamic viscosity of activated sludge depending on MLSS and temperature is given. In Chapter 5 and 6 the chemical cleaning of membranes after wastewater filtration is discussed.

Chapter 6 shows the results of a quantitative split into internal and external fouling (cake deposition) for different filtration modes. The experimental results served as validation for a comprehensive study on theoretical and half empirical determination of the cake resistance. The experiments reveal the advantages and disadvantages of the different anti fouling measures. Literature results for cake thickness based on theoretical solutions are critically evaluated with the help of sponge ball applications for AS membrane filtration. Indirect conclusions of the cake thickness via flux measurements are compared by direct measurements of the cake

thickness through the SEM. Furthermore, the backflush resistances of the BF versus the AS+BF membrane were compared.

Chapter 7 reflects the investigations of critical flux tests for conventional and enhanced filtration. A stepwise pressure increase was provided for constant flux filtration of different methods. Under the aspect of critical flux, a constant pressure filtration was investigated as well. Prior to the tests the limiting flux was determined. Chapter 7 also evaluated postulations made in past literature regarding the relationship between limiting and critical flux for wastewater membrane filtration.

Chapter 8 is the only paper which investigates natural or synthetic river water. A comparison between air sparged and non-air sparged filtration is given for different time frames with different types of water and thus different fouling propensities. Comparison is made between the effect of sponge ball application and air sparged system versus application on a conventional membrane system. Further changes of the river water fouling potential over the course of a summer are reported. Finally, a model for flux prediction of long term measurements is given.

1.6 References

[1] S. Duranceau, Membrane Practices for Water Treatment. American Water Works Association, Denver Colorado, first edition, (2001), ISBN: 1-58321-147-0.

[2] M. Cheryan, Ultrafiltration and Microfiltration Handbook. Technomic Publishing Co., Inc. Lancaster, Basel (1998), ISBN: 1-56676-598-6.

[3] M. Matteson and Clyde Orr, Filtration: Principles and Practices. Marcel Dekker, Marcel Dekker, New York, second edition, (1987), ISBN: 0824775821.

[4] Metcalf & Eddy, edited by G. Tchobanoglous, and F. Burton, Wastewater Engineering, Treatment, Disposal and Reuse. McGraw-Hill, Boston, 3rd edition, (1991), ISBN 0-07-041690-7.

[5] I. Pinnau, Workshop organized by the NAMS: Polymeric and Inorganic Membrane Materials and Membrane Formation. Jackson Hole, (2004).

[6] M. Mulder, Basic Principles of Membrane Technology, Kluwer Academic Publishers Dordrecht/Boston/London second edition, (1996), ISBN: 0-7923-4247-X.

[7] W. Eykamp, Microfiltration and Ultrafiltration, In: R. Noble and S. Stern (Ed.), Membrane Separations Technology – Principles and Applications. Elsevier, Amsterdam (1995), pp.1-43, ISBN: 0-444-81633-X.

[8] M. Kraume, U. Bracklow, A. Drews and M. Vocks, Nutrients removal in MBRs for municipal wastewater treatment. Keynote, IWA Special. Conf. WEMT Seoul, Korea, (2004).

[9] Le Clech, P., PhD thesis: Process configuration and fouling in membrane bioreactors. Cranfield University, UK, (2002).

[10] H. Ng and W. Hermanowicz, Membrane bioreactor at short mean cell residence times – a new mode of operation. IWA Special. Conf. WEMT Seoul, Korea, (2004).

[11] T. Stephenson, S. Judd, B. Jefferson and K. Brindle, Membrane bioreactors for wastewater treatment. IWA Publishing, London, UK, (2000).

[12] S. Judd, Fouling control in submerged membrane bioreactors. Keynote, IWA Special. Conf. WEMT Seoul, Korea, (2004).

[13] I. Chang and C. Lee, Membrane filtration characteristics in membrane-coupled activated sludge system – the effect of physiological states of activated sludge on membrane fouling. Desalination, 120 (3), (1998), 221-233.

[14] E. Bouhabila, R. Ben Aim and H. Buisson, Fouling characterization in membrane bioreators. Separation and Purification Technology, 22-23, (2001), pp. 123-132.

[15] I. Chang, P. Le Clech, B. Jefferson and S. Judd, Membrane fouling in membrane bioreactors for wastewater treatment. J. Environ. Eng. ASCE, (2002), 128, (11), pp. 1018-1029.

[16] G. Belfort, R. Davis and A. Zydney, Review: The behavior of suspensions and macromolecular solutions in crossflow microfiltration. J. Membr. Sci., 96, (1994), pp. 1-58.

[17] S. Levy, Two-Phase Flow in Complex Systems. Interscience, (1999), ISBN: 0471329673.

[18] N. Cheremisinoff and R. Gupta, Handbook of fluids in motion. Ann Arbor Science, (1983), ISBN: 0250404583

[19] C. Lee, W. Chang and Y. Ju, Air slugs entrapped cross-flow filtration of bacterial suspensions. Biotechnology and Bioengineering, 41, (1993) pp. 525-530

[20] Z. Cui and K. Wright, Gas-liquid two-phase cross-flow ultrafiltration of BSA and dextran solutions. J. Membr. Sci., 90, (1994), pp. 183-189

[21] M. Mercier, C. Fonade and C. Lafforgue-Delorme, Influence of the flow regime on the efficiency of a gas liquid two phase medium filtration. Biotechnology Techniques, 12, (1995), pp. 853-858

[22] Q. Li, Z. Cui and D. Pepper, Effect of bubble size and frequency on the permeate flux of gas sparged ultrafiltration with tubular membranes. Chem. Eng. J., 67, (1997), pp. 71-75

[23] C. Cabassud, S. Laborie and J. Laine, How slug flow can improve ultrafiltration flux in organic hollow fibres. J. Membr. Sci., 128, (1997), pp. 93-101.

[24] M. Mecier, C. Fonade and C. Lafforgue-Delorme, How Slug flow can enhance the ultrafiltration flux in mineral tubular membranes, J. Membr. Sci., 128, (1997), pp. 103-113.

[25] R. Ghosh and Z. Cui, Mass transfer in gas-sparged ultrafiltration: upward slug flow in tubular membranes. J. Membr. Sci., 162, (1999), pp. 91-102.

[26] P. Mikulasek, J. Cakl, P. Pospisil and P. Dolecek, The use of flux enhancement methods for high flux cross-flow membrane microfiltration systems. Chem. Biochem. Eng., 14, 4, (2000), pp. 117-123

[27] L. Vera, S. Delgado and S. Elmaleh, Gas sparged cross-flow microfiltration of biologically treated wastewater. Water Science and Technology, 41, 10/11, (2000), pp. 173-180

[28] S. Chang and A. Fane, Filtration of biomass with axial inter-fibre upward slug flow: performance and mechanisms, J. Membr. Sci., 180, (2000), pp. 57-68

[29] M. Um, S. Yoon, C. Lee, K. Chung and J. Kim, Flux enhancement with gas injection in crossflow ultrafiltration of oily wastewater. Wat. Res., 35, 17 (2001), pp. 4095-4101

[30] P. Le-Clech, H. Alvarez-Vasquez, B. Jefferson and S. Judd, Fluid hydrodynamics in submerged and sidestream membrane bioreactors. Water Science and Technology, 48, 3, (2003), pp. 113-119

[31] M. Mercier-Bonin, C. Maranges, C. Lafforgue, C. Fonade and A. Laine, Hydrodynamics of slug flow applied to cross-flow filtration in narrow tubes, AIChE, 46, 3, (2000) pp. 476-488

[32] G. Ducom, F. Puech and C. Cabassud, Air sparging with flat sheet nanofiltration: a link between wall shear stresses and flux enhancement. Desal., 145, (2002), pp. 97-102

[33] T. Taha and Z. Cui, CFD modelling of gas-sparged ultrafiltration in tubular membranes. J. Membr. Sci., 210, (2002), pp. 13-27

[34] S. Laborie, C. Cabassud, L Durand Bourlier and J. Laine, Characterization of gas-liquid two-phase flow inside capillaries. Chem. Engin. Sci., 54, (1999), pp. 5723-5735.

[35] S. Smith, Lumen-side gas bubbling for enhancement of hollow fibre membrane filtration, Membrane Quarterly, 19, 2, (2004), pp. 12-16

[36] Z. Cui and K. Wright, Flux enhancement with gas sparging in downwards crossflow ultrafiltration: performance and mechanism. J. Membr. Sci., 117, (1996) pp. 109-116.

[37] T. Cheng, H. Yeh and J. Wu, Effects of gas slugs and inclination angle on the ultrafiltration flux in tubular membrane module. J. Membr. Sci., 158, (1999), pp. 223-234

[38] T. Cheng, Influence of inclination on gas-sparged cross-flow ultrafiltration through an inorganic tubular membrane. J. Membr. Sci., 196, (2002), pp. 103-110

[39] P. Mikulasek and P. Pospisil, Influence of two-phase gas –liquid flow on permeate flux and cake characteristics in ceramic membrane crossflow microfiltration. Scientific Papers of the Univ. of Pardubice, Series A, Faculty of Chemical Technology 6, (2000), pp. 79-94

[40] C. Cabassud, S. Laborie,L Durand Bourlier and J. Laine, Air sparging in ultrafiltration hollow fibers: relationship between flux enhancement, cake characteristics and hydrodynamic parameters. J. Membr. Sci., 181, (2001), pp. 57-69.

[41] L. Vera, R. Villarroel, S. Delgado and S. Elmaleh, Enhancing microfiltration through an inorganic tubular membrane by gas sparging. J. Membr. Sci., 165, (2000), pp. 47-57

[42] L. Vera, S. Delgado and S. Elmaleh, Dimensionless numbers for the steady-state flux of cross-flow microfiltration and ultrafiltration with gas sparging. Chem. Engin. Sci., 55, (2000), pp. 3419-3428

[43] J. Verberk, G. Worm, H. Futselaar and J. van Dijk, Combined air-water flush in dead-end ultrafiltration. Water Science and Technology, 1, 5/6, (2001), pp. 393-402

[44] J. Verberk, P. Hoogeveen, H. Futselaar and J. van Dijk, Hydraulic distribution of water and air over a membrane module using AirFlush. Water Science and Technology, 2, 2, (2002), pp. 297-304

[45] P. Mikulasek, P. Pospisil, P. Dolecek and Jiri Cakl, Gas-liquid two-phase flow in microfiltration mineral tubular membranes: relationship between flux enhancement and hydrodynamic parameters. Desal., 146, (2002) pp. 103-109

[46] P. Pospisil, R. Wakeman, I. Hodgson and P. Mikulasek, Shear stress-based modelling of steady state permeate flux in microfiltration enhanced by two-phase flows. Chemical Engineering Journal, 97, (2004), pp. 257-263

[47] Q. Li, Z. Cui and D. Pepper, Fractionation of HSA and IgG by gas sparged ultrafiltration. J. Membr. Sci., 121, (1997), pp. 181-190.

[48] Q. Li, R. Ghosh, S. Bellara, Z. Cui and D. Pepper, Enhancement of ultrafiltration by gas sparging with flat sheet membrane modules. Separation and Purification Technology, 14, (1998), pp. 79-83

[49] H. Sur and Z. Cui, Experimental study on the enhancement of yeast microfiltration with gas sparging. J. Chem. Technol. Biotechnol., 76, (2001), pp. 477-484

[50] I. Chang and S. Judd, Air sparging of a submerged MBR for municipal wastewater treatment. Process Biochemistry, 37, (2002), pp. 915-920

[51] G. Ducom, H. Matamoros and C. Cabassud, Air sparging for flux enhancement in nanofiltration membranes: application to O/W stabilised and non-stabilised emulsions. J. Membr. Sci., 204, (2002), pp. 221-236

[52] Z. Cui, S. Bellara and Homewood, Airlift crossflow membrane filtration – a feasibility study with dextran ultrafiltration. J. Membr. Sci., 128, (1997), pp. 83-91

[53] S. Laborie, C. Cabassud, L. Durand-Bourlier and J. Laine, Fouling control by air sparging inside hollow fibre membranes – effects on energy consumption. Desal., 118, (1998), pp. 189-196

[54] S. Bellara, Z. Cui and D. Pepper, Gas sparging to enhance permeate flux in ultrafiltration using hollow fiber membranes. J. Membr. Sci., 121, (1996), pp. 175-184.

[55] K. Majewska-Nowak, M. Kabsch-Korbutowicz and T. Winnicki, The effect of gas bubble flow on ultrafiltration efficiency. Desal., 126, (1999), pp. 187-192

[56] T. Cheng, H. Yeh and C. Gau, Enhancement of permeate Flux by gas slugs for crossflow ultrafiltration in tubular membrane modules. Separation. Science and Technology, 33, 15, (1998) pp. 2295-2309

[57] G. Ducom and C. Cabassud, Possible effects of air sparging for nanofiltration of salted solutions. Desal., 156, (2003), pp. 267-274

[58] R. Field, D. Wu, J. Howell and B. Gupta, Critical flux concept for microfiltration fouling, J. Membr. Sci., 100 (1995), pp. 259-272

[59] P. Bacchin, D. Si-Hassen, V. Starov, M. Clifton, P. Aimar, A unifying model for concentration polarization, gel-layer formation and particle deposition in cross-

flow membrane filtration of colloidal suspensions, Chem. Eng. Sci., 57, (2002), pp. 77-91

[60] J. Howell, Sub-critical flux operation of microfiltration, J. Membr. Sci., 107, (1995), pp. 165-171

[61] N. Al-Bastaki and A. Abbas, Use of fluid instabilities to enhance membrane performance: a review. Desalination 136, (2001), pp. 255-262

[62] R. Wakemann, C. Williams, Additional techniques to improve microfiltration, Separation and Purification Technology, 26, (2002), pp. 3-18.

[63] C. Guigui, V. Bonnelye, L. Durand-Bourlier, N. Abidine, J. Rouch and P. Aptel, A novel approach for the ultrafiltration of surface water: combination of coagulation and Dean vortices in a feed-and-bleed process configuration, AWWW Membrane Technology Conference, (2001) Texas, USA

2 Long-term study of an intermittent air sparged MBR for synthetic wastewater treatment[1]

C. Psoch and S. Schiewer*

Department of Civil & Environmental Engineering; WERC, University of Alaska Fairbanks, AK 99775; USA

Abstract

Membrane bioreactors (MBR) combine biological processes with membrane filtration. Advantages of MBR in municipal wastewater treatment include high effluent quality and reduced space requirements. Steady operation of membrane plants requires careful management of membrane fouling. Even though it might be impossible to prevent, fouling can be limited by techniques such as gas sparging. The injection of gas bubbles increases the shear stress and removes fouling material from the membrane surface. Most cited literature on air sparging refers to short-term experiments, often times in bench scale. The aim of this study was therefore long-term investigations in pilot plant scale of a 70 L reactor fed with glucose-based synthetic wastewater. The main focus was on enhancing permeate flux by air sparging. The results showed that using air sparging significantly increased the permeate flux was doubled even over several weeks. The findings were interpreted using the dimensionless fouling and shear stress number. The fouling resistance was found to decrease significantly with air injection ratios between 0.4 and 0.5. When air

[1] Journal of Membrane Science, Elsevier (in press) 2005

sparging was applied after a period without air sparging, the shear stress number doubled. This increase in shear led to a reduction of the fouling number by approximately 30%. During several weeks air sparging only a slow fouling number increase was. In contrast to that after air sparging was ceased, an exponential increase of the fouling number was observed.

Keywords: membrane bioreactor, fouling air sparging, microfiltration, synthetic wastewater

* Corresponding author; Tel.: (907) 474-2620; fax: (907) 474-6087, E-mail address: ffsos@uaf.edu

2.1 Introduction

Membrane bioreactors (MBR) are modified activated sludge plants whereby a membrane replaces the secondary sedimentation for the solid/liquid separation. MBR feature a compact volume and high loading rate capacity [1]. Since microorganisms are largely retained by the membrane, high concentrations of well-adapted microorganisms can be achieved in the reactor. Thus, a more efficient biological treatment with a better disinfected wastewater results [2].

Even though MBR are already established in commercial application for more than a decade, fouling remains the most crucial problem limiting wider application of membrane filtration. The rate of fouling and permeate flux decrease, or conversely the required increase of the transmembrane pressure (TMP) to maintain the flux, depends on the operating flux, the turbulence intensity on the membrane surface, and the viscosity of the wastewater [3, 4].

Consequently careful fouling management is required for consistent operations of membrane plants. Several models exist to describe fouling and to distinguish between different fouling components [5], such as external and internal fouling, as suggested by *Wakemann and Williams* [6].

The main focus of this study was to investigate a technique to counter external fouling, which is due to cake formation on the membrane surface, or, more specifically, a gel layer and concentration polarization on top of the gel layer [7].

Several techniques exist to reduce external fouling, one of which is gas sparging. This method disrupts the concentration polarization layer by improving the cross flow hydrodynamics near the membrane surface. Gas sparging (i.e. injecting gas into the feed of a tubular membrane module to generate a gas liquid two phase cross-flow operation) helps maintain a stable permeate flux over longer time periods. It can even, to a minor degree, reduce internal fouling on the membrane surface due to generation of suction pressure [8-10].

If liquid and gas flow together in a tube, the interface between the phases follows a variety of flow patterns, depending on the ratio of gas and liquid flow rates, on the pipe diameter, interfacial tension and inclination. In the literature the following flow regimes are described:

- Bubble flow
- Slug flow
- Churn flow
- Annular flow

The predominant factor determining the flow pattern is the void fraction in the pipe, which depends directly on the gas and liquid phase velocities, and is defined as follows:

$$\varepsilon = \frac{u_{Gas}}{(u_{Gas} + u_{Liquid})} \qquad \text{eq. 2.1}$$

with:

ε = void fraction [-]

u_{Gas} = superficial gas velocity, i.e. velocity if only gas was in the channel [m/s]

u_{Liquid} = superficial liquid velocity, i.e. velocity if only liquid was in the channel [m/s]

The void fraction increases from bubble ($0 < \varepsilon < 0.2$) over slug flow ($0.2 < \varepsilon < 0.9$) to annular and churn flow ($0.9 < \varepsilon < 1.0$) [11-16].

Slug flow delivers the most impact on shear stress to the wall, according to studies of *Cabassud et al, Li et al. and Vera et al.* [9; 17; 18].

Under slug flow conditions water and air slugs fight cake layer build up by inducing shear stress. Additionally, a water film flows in countercurrent parallel to the rising gas slugs [19]. Gas and liquid slugs cause different turbulence intensities, which influence the concentration polarization layer strongly [20, 21]. This influence might cause a slightly deteriorated selectivity of the membranes [22]. The most severe turbulence phenomena occur within the wake zone of the gas slugs, where, in tubular membranes, smaller gas bubbles moving after the gas slugs in heavily turbulent movements [23]. These turbulent movements, associated with small gas bubbles, are to some extent able to dislocate and remove cell debris and particles, which accumulate and partially clog the pore channels [24].

Even though it is possible to calculate different Reynolds numbers for the gas and liquid slugs, it is common to use a mixture Reynolds number ($Re_{mixture}$) to characterize the two phase flow [25, 26]:

$$Re_{mixture} = \frac{\rho_{Liquid} * (u_{Liquid} + u_{Gas}) * L}{\mu_{Liquid}} \qquad \text{eq. 2.2}$$

with:

$Re_{(mixture)}$ = two phase Reynolds number [dimensionless]

ρ = density [kg/m³]

u = superficial velocity of the phase [m/s]

L = characteristic length, here diameter of the channel [m]

μ = dynamic viscosity [Pas]

Gas sparging in tubular applications has proven to be an effective, cost-saving enhancement technique, but is not yet frequently applied [27, 28, 29]. If the chosen gas is air, an additional benefit of air sparging is that this contributes to the oxygen supply, which is necessary for the biological degradation processes in the reactor. For first prediction models for two phase flow in membrane filtration, see, for instance, *Mikulasek et al.* [30].

In the literature, no research on tubular membranes in combination with air sparging exceeded time frames of one day except investigations from the *Stork Company* on x-flow membranes and studies accomplished by *Chang and Judd*, [29; 31]. In the study by *Chang and Judd* one of the modules failed after about two weeks of operation due to very challenging operation conditions. The lack of data and need for long-term investigations on fluid instabilities to enhance membrane performance was pointed out in a comprehensive literature review by *Al-Bastaki and Abbas* [32].

In industrial membrane applications, membranes are typically operated for several weeks before chemical cleaning. Therefore, research on the effectiveness of air sparging over a period of weeks or months rather than hours is necessary.

The objective of this study was correspondingly to operate an air sparged tubular membrane filtration system over time periods of several months. The main focus was on monitoring the flux development with and without air sparging and to determine the impacts on the biodegradation in a membrane bioreactor fed with synthetic wastewater. It was intended to operate the system below the critical flux value [33] to maintain comparable conditions throughout the whole observation period. The use of antifoam substances was avoided to prevent negative impact on the membranes [34]. Prior investigations [35] were extended, and the fouling and shear stress numbers according to *Vera et al.* [36] were used for a more generalized and better interpretation of the observed behavior.

2.2 Materials and methods

For the experimental setup, as shown in Fig. 2.1, an activated sludge tank was used with a volume of 60 - 80 liters. The wastewater and activated sludge were pumped with a submerged pump (Grundfos MP1). Because the pump is actually designed for cold ground water, a cooling cycle with a thermostat was necessary. The applied transmembrane pressure (TMP) for the filtration was between 140 and 200 kPa.

The pump speed (and thus the volume stream) could be regulated over a variable frequency drive (Grundfos). In the interest of a longer pump life, the system was controlled by a timer, which shut the pump on and off every other hour. Another timer task was to control a solenoid valve, which connected the air supply with the loop. Air was only supplied if the pump was working. The oxygen content in the vessel was monitored by a semi-automatic oxygen probe which also measured the temperature.

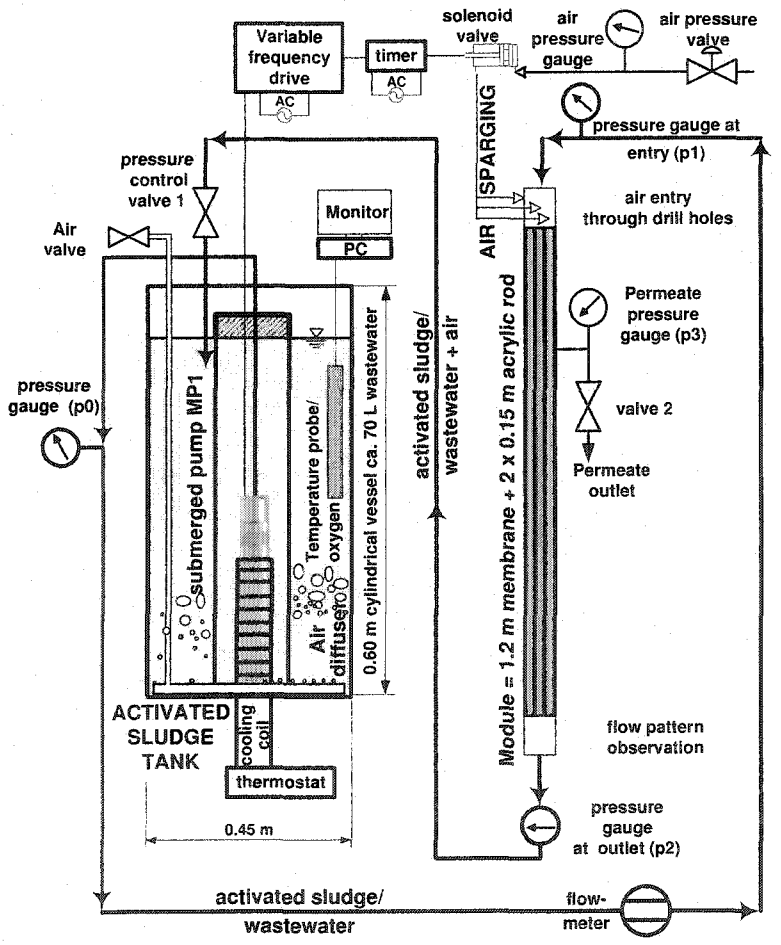

Fig. 2.1. Scheme of experimental setup, with activated sludge tank and membrane

The polymer membrane (PCI) had a length of 1.20 m and a pore size of 0.2 μm. The module was made of five tubes, each with an inner diameter of 6.35 mm, yielding a membrane surface area of 0.1 m^2. On each side of the module, the membrane tubes were extended by about 10 cm through an acrylic rod. The acrylic extensions, with drill holes in the same diameter as the membrane tubes, served for the air supply and for observation of the flow pattern in the unit. Fig. 2.2 shows the acrylic rod with wastewater and air bubbles. Each tube featured its own connection to the air supply, with separately adjustable air volume stream.

A hose diffuser with numerous air outlets of 1.6 mm diameter served for the aeration in experimental sections where no air sparging was supplied. The hose was mounted like an annulus at the inner circumference of the bottom of the cylindrical vessel.

The water flow velocity within the membrane tubes was between 0.7 and 1.05 m/s. The maximum velocity was limited by the ability to observe the flow pattern, which was invisible to the naked eye. The flow was controlled with photographs using a digital still camera, a Sony FD Mavica with 10 x optical zoom (see Fig. 2.2). At flow velocities exceeding 1 m/s it was no longer possible to monitor the flow pattern in the system.

A glucose-based synthetic wastewater was prepared as described in Table 2.1, based on the composition in experiments carried out by Shim et al. [37]. At first, a batch trial was launched to build up a high amount of biomass, indicated by the amount of mixed liquor suspended solids (MLSS). The inoculation of the synthetic

wastewater tank with microbes was achieved by adding 2 L of fresh drawn activated sludge from the local municipal wastewater treatment plant.

For determining the MLSS the standard methods [38] were used. The initial amount of MLSS was slightly above 2 g/L.

Within the first nineteen days the loading was about 600 mg/L COD, which is close to typical wastewater concentrations for the US [39]. Subsequently the glucose feed load was increased in three steps, from 1.6 g/day up to about 26 g/day to maintain the MLSS above 2 g/L (see Table 2.1), with sludge withdrawal of 2 L/day occurring from day 80 on.

Results from the biodegradation of the bioreactor are revealed in *Psoch and Schiewer* [40].

Throughout the whole test series of about 190 days no membrane cleaning or chemical application was performed.

Table 2.1. Nutrients added to the reactor of about 60-80 L at different process stages, altered according to *Shim et al.* [36].

	Day 1 – 19	Day 20 – 27	Day 28 - 111	Day 112 - 122	Day 123 - 128	Day 129 - 190
Substance	**Amount added [mg/day]**	**Amount added [mg/day]**	**Amount added [mg/day]**	**Amount added [mg/day]**	**Amount added [mg/day]**	**Amount added [mg/day]**
Glucose	*1600*	*2800*	*5600*	*15600*	*20600*	*25600*
Ammonium acetate	513	912	1824	1824	1824	1824
Glutamic acid	666	1184	2368	2368	2368	2368
NH_4Cl	77	138	275	275.2	275.2	275.2
KH_2PO_4	27	48	96	96	96	96
K_2HPO_4	36	64	128	128	128	128
$CaCl_2$	36	64	128	128	128	128
$MgSO_4$	59	106	211	211.2	211.2	211.2
$NaHCO_3$	3375	6000	4000	4000	4000	4000
NaCl	45	80	160	160	160	160
MLSS [g/L]	1.5-2.5	1.5-3.1*	2.5-3.5**	2.6-2.9	2.9	2.9-6.0

* Between day 19 and 24 an enrichment process was conducted, not refilling the volume which was withdrawn as permeate, resulting in an increase of MLSS up to 3.1 g/L.

** Taking out every day 2 L of sludge starting at day 82 decreased the MLSS until more stable conditions were achieved at MLSS of about 2.5 g/L.

2.3 Results and discussion

2.3.1 Degradation performance and general observations

Air sparged aeration allowed the same successful degradation performance as conventional aeration for the MBR, even under increasing loads as described in

Table 2.1. Effluent COD removal rates were consistently above 90% [40]. The oxygen content in the reactor was meanwhile higher during air sparging, although air was supplied to the reactor only every other hour [40]. The higher efficiency of air sparging for aeration is due to smaller bubbles between the air slugs compared to bubble sizes in conventional aeration (see Fig. 2.2). Furthermore the contact time between air and water within the loop is longer than for conventional aeration. During the sections when air sparging was supplied, heavy foam production occurred, which resulted after 40 days in the collapse of the pump. Subsequently an insertion tube of about 0.15 m diameter was deployed (see Fig. 2.1) with ground clearance of 0.08 m to prevent air suction by the pump, giving the setup the character of a loop reactor.

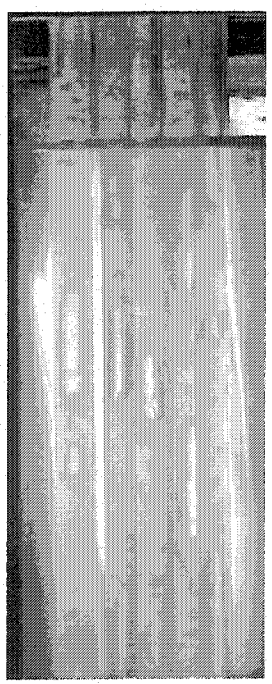

Fig. 2.2. Slug flow observation at the outlet of the tubular membrane, channel diameter 6 mm

2.3.2 Flux development and process parameters vs time

In Fig. 2.3 the measured values of the flux and TMP are pictured. Between Section I and Section IV the mixed liquor suspended solids (MLSS) were between 1.4 and 3.5 g/L and seemed not to have significant impact on the permeate flux. In Section V the MLSS increased from 2.4 to 6.1 g/L.

2.3.2.1 Changes of permeate flux over time

Within the first eleven days (first section), no air sparging was supplied and the flux decreased significantly until it approached a fairly stable value. The initial experiments without air sparging were performed in order to create a reference value and to demonstrate clearly the efficiency of subsequent air sparging on a pre-fouled membrane.

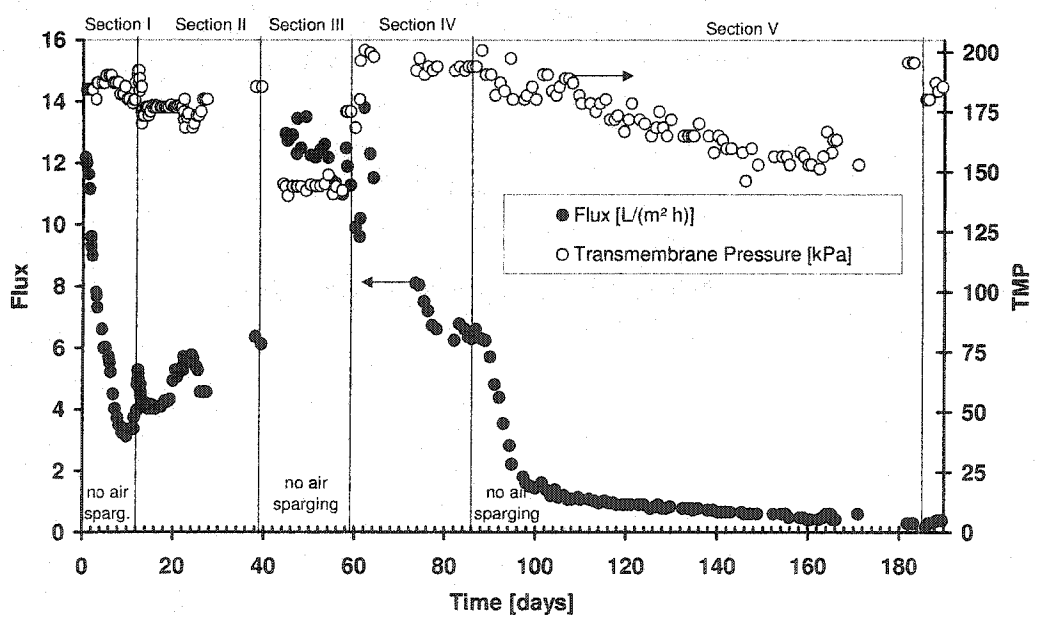

Fig. 2.3. Flux development with and without air sparging

With the beginning of the 12th day (second section) air sparging was deployed and the flux increased after a time lag, as similarly observed for short time investigations by Cabassud et al. [9] and Sur & Cui [41]. The flux was highest near the end of Section II, when the velocity of the gas had approached that of the liquid (Fig. 2.4). Comparison between Section I and II shows that air sparging can increase the flux by about a factor of two with other process parameters remaining about constant. The liquid cross flow velocity increases slightly from section I (CFV = 0.70 m/s) to the end of section II (CFV = 0.80 m/s) as shown in Fig. 2.4. Due to the fact that membrane filtration heavily depends on the operation history, the positive impact of air sparging in the second section is very significant.

In the third section no air sparging was supplied, due to technical problems and to allow development of a new cake layer on the membrane surface. The fairly high flux values are related to significantly higher cross flow velocities (compare Fig. 2.4).

In Section IV the superficial liquid velocity was reduced to values close to those in Section I and II and air sparging was again applied. The flux decreased after a few days. Nevertheless, after 14 days of air sparging the flux values in Section IV were appreciably higher than after 11 days without air sparging (Section I) under comparable conditions. The liquid velocity in section IV is with about 0.80 m/s only slightly higher as in section II, where average values are about 0.75 m/s. The general flux decrease within Section IV is related to a lower liquid velocity than in Section III and to a non-optimized flow pattern, in contrast to Section II. By continuously readjusting the flow patterns during Section II, the best flux results were achieved

when the length of the air bubble and the length of the liquid slug were about equal. This was the case, for example, at days 18-24, when a particularly high flow rate was achieved. This observation agrees with findings of Gosh and Cui [23]. Long term investigations condensed by Roest et al. [29] revealed that tubular modules are not very suitable to handle permeate flux variations of > 1.5 and run best in continuous permeation mode.

In Section V no air sparging was deployed, and the flux started to significantly drop after 4 days. After 7 more days, the flux was about 1.5 L/(m² h) and decreased gradually within the next 80 days to 0.3 L/(m² h).

After Section V air sparging was supplied again, to explore whether a flux increase was possible. Five days later the test was abandoned because the permeate flow did not rise; in fact it stayed below the economically reasonable range. This observation can be attributed to the totally blocked pores; it was not possible to increase the flux by removing the external fouling layer because the main resistance was due to internal fouling. This observation highlights the need to supply air sparging on a regular basis to reduce the fouling occurrence in the first place.

2.3.2.2 Effect of TMP

Measurements showed that within the first two sections no significant changes of the TMP values occurred, except for short time fluctuations at the onset of air sparging at the beginning of Section II, due to instabilities of the flow regimes. After about 22 to 24 days at comparatively high flux values, the flow patterns were

optimized and stable so that the TMP even dropped slightly. In Section II the TMP was almost constantly slightly below the values of Section I. In Section III the TMP was clearly at its lowest values throughout the whole test series. A fairly stable flux indicates that the operation mode, which is affected by cross flow velocity, TMP and MLSS, is close to the critical flux value for which stable flux is achieved [33].

In Section IV the highest TMP was observed but the flux dropped significantly. The initial flux of Section IV was apparently above the critical flux, and so it was impossible to maintain the initial flux for this section. Air sparging was not able to overcome the combined impacts of increasing internal fouling, stronger gel layer, and concentration polarization due to higher TMP. Gosh and Cui [23] observed that air sparging was particularly effective under conditions such as high TMP and high foulant concentration, where strong external fouling can be expected without air sparging. Compared to Section I, where conditions similar to those of Section IV were present, the effectiveness of air sparging is apparent. However, air sparging (sections II and IV) is apparently less effective than an increase of the liquid flow rate, as in Section III. The high superficial liquid velocity of Section III was not maintained because it did not allow the observation of the flow pattern with the available photographic equipment.

In Section V the pump started to show attrition, and so the TMP decreased steadily without the change of other parameters. A pressure increase at the end of Section V after repairing the pump could not raise the flux.

2.3.2.3 Effect of superficial liquid and gas velocity

In Fig. 2.4 the flux and the superficial liquid and gas velocity are depicted -- both are highly important parameters in determining the flux. In sections II and IV, days 22 to 24 and days 59 to 64, where the superficial gas and liquid velocities were about equal, the highest flux values were achieved. It was notable that after previous cake deposition from unsparged sections, a time delay of several hours was observed to remove the cake layer. These observations agree with results from short term analyses of less than 10 hours by *Cabassud et al.* [9].

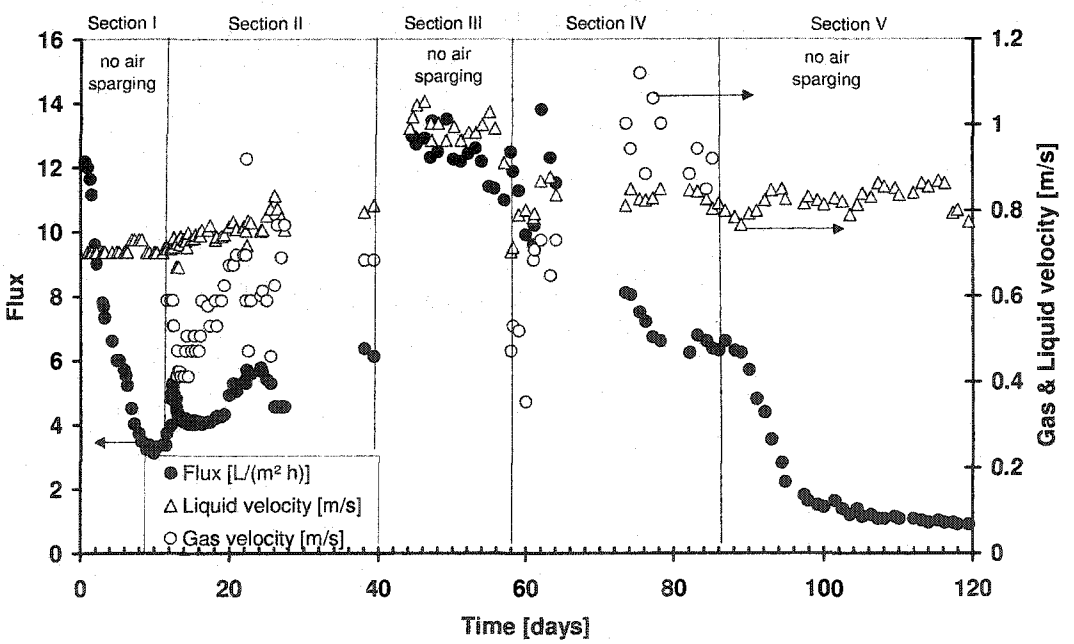

Fig. 2.4. Flux development related to superficial liquid and gas velocity

Even though in Section IV the flux dropped while air sparging was supplied -- presumably due to lower liquid velocity combined with non-optimized relations between flux, liquid velocity and TMP -- within the first 6 days the flux was close to the measured values for Section III but with clearly less liquid velocity, which points to less energy consumption [27].

Fig. 2.5 shows the Reynolds numbers on the left y-axis; meanwhile the air injection ratio ε is depicted on the right y-axis; both parameters are plotted against time. The measured flux values are included to show the relationship between Re, ε, and flux. For the single phase flow the Reynolds number is:

$$\mathrm{Re} = \frac{\rho * u_{Liquid} * L}{\mu} \qquad \text{eq. 2.3}$$

with:

ρ = density [kg/m³]

u = velocity [m/s]

L = characteristic length, here channel diameter [m]

μ = dynamic viscosity [Pas]

In Section I, the Reynolds numbers for the one phase flow are about 2100 and still in the laminar range (by convention under 2300 is laminar).

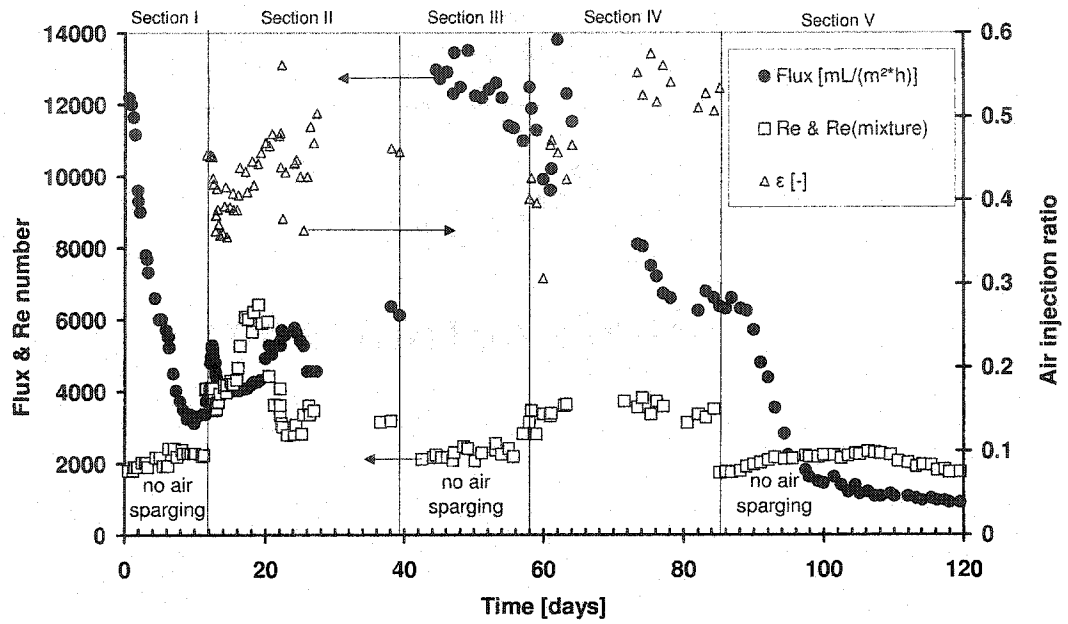

Fig. 2.5. Flux, Re and $Re_{(mixture)}$ (for air sparging sections) and air injection ratio ε vs. time

For Section II, the two-phase mixture Reynolds number is calculated according to Equation 2. The calculated values show the flow was highly turbulent. It is assumed that a time delay between the highest fluxes and optimized flow conditions exists. Air injection ratios at about 0.45 in combination with high mixture Reynolds numbers yield significantly increased flux values. The flux, after optimized conditions, stays constant about one more day, then drops afterwards. However, the dependence of flux on the mixture Reynolds number and air injection ratio (ε) deserves more study in order to better confirm the effect of these parameters on the flux. Therefore further experiments on these parameters are currently underway.

In Section III the system was on the threshold of turbulent flow conditions. That observation is well-supported by the high fluxes observed, which prove that there was significantly less cake deposition.

In Section IV the lowest Reynolds numbers are also well above the laminar threshold, and the flow conditions are clearly in the turbulent range. Because the mixture Reynolds number stays about constant for the whole section, the air injection ratio ε is one factor that can explain why the flux significantly varied; another is the lag effects after the decrease in liquid velocity compared to Section III. From Fig. 2.5, the conclusion can be drawn that at moderate turbulent, mixture Reynolds numbers, ε values below 0.5 are more supportive of high fluxes than ε values above 0.5. This conclusion seems to be supported by comparison with the data from Section II, where the highest fluxes were achieved under similar conditions.

In Section V the flow is settled back to laminar conditions, which favors cake deposition, as evidenced by the strong flux decrease.

2.3.3 Process analysis by use of dimensionless numbers

In order to draw more general conclusions from the data about the effect of flow rates and TMP on fouling, dimensionless parameters were used, as proposed by Vera et al. [14, 17]. Fig. 2.6 shows the dimensionless shear stress numbers, Ns and Ns' respectively, for air sparging sections on the left y-axis and the dimensionless fouling

number Nf on the right y-axis over time. Again the flux is included in the figure for better data interpretation.

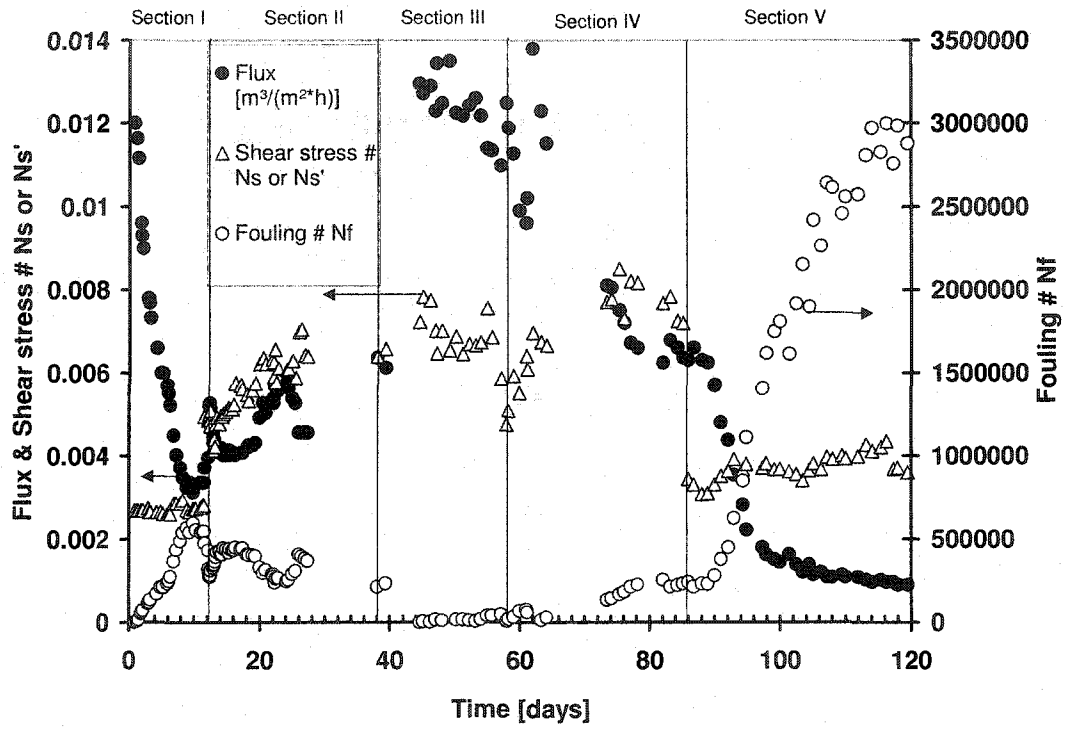

Fig. 2.6. Flux and shear stress numbers, Ns and Ns' (for air sparging sections) and fouling number N_f vs. time

For the calculation of the shear stress number the following equation applies [17]:

$$N_S = \frac{\rho_{Liquid} * u_{Liquid}^2}{TMP} \qquad \text{eq. 2.4}$$

If air sparging is supplied, some of the variables in eq. 2.4 have to be modified to represent two phase flow conditions and e 2.5 applies, where the mixture density

$\rho_{mixture}$ according Equation 6 is used in place of the liquid density, and the mixture velocity $u_{mixture}$ is calculated according to Equation 2.7.

$$N_S' = \frac{\rho_{mixture} * u_{mixture}^2}{TMP} \qquad \text{eq. 2.5}$$

with

$$\rho_{mixture} = \frac{\rho_{Liquid} * u_{Liquid} + \rho_{Gas} * u_{Gas}}{u_{mixture}} \qquad \text{eq. 2.6}$$

and

$$u_{mixture} = u_{Gas} + u_{Liquid} \qquad \text{eq. 2.7}$$

For the calculation of the fouling number as in Vera et al. [17], the row resistance model for fouling has to be applied.

$$R_t = R_m + R_f \qquad \text{eq. 2.8}$$

with

R_t = total resistance

R_m = membrane resistance at initial conditions

R_f = fouling resistance at time t, additional to the initial resistance

R_m is calculated according to the following equation:

$$R_m = \frac{TMP}{\mu * J_0} \qquad \text{eq. 2.9}$$

with:

μ = dynamic viscosity [Pas]

J_0 = intial flux [L/(m² h)]

The fouling resistance is determined as follows:

$$R_f = \frac{TMP}{\mu * J} - R_m \qquad \text{eq. 2.10}$$

with:

J = the flux at any time larger than zero during the filtration process

The dimensionless fouling number is calculated as follows, according Vera et al. [17]

$$N_f = \frac{\mu * R_f * u_{Liquid}}{u_{mixture}} \qquad \text{eq. 2.11}$$

A general drawback in the definition of the fouling number is that flux increases above the initial flux level due to altered boundary conditions cannot be reasonably accounted for. Therefore, the fouling number had to be calculated separately for two ranges, with range A (sections I and II) covering the first 40 days, where the flux was consistently below the initial flux, and range B (sections III-V) for the remaining time, where the flux decreased from a highest value after 45 days (where the liquid velocity was increased) to the end at 190 days.

From Fig. 2.6 it can be concluded that after the flux drop within the first section, where only low shear stress values were applied, for sections II – IV comparably high shear stress values are calculated. The flux development fits the shear stress development very well. In sections II-IV with high shear stress numbers, the highest

fluxes where achieved and the fouling number remains low. In Section V the shear stress number was significantly decreased again, since air sparging was discontinued, leading to a significant increase of the fouling number over several orders of magnitude in Section V. For optimal flux conditions the shear stress number obviously has to be within a certain range.

Fig. 2.7 shows the impact of the shear stress number on the fouling number N_f for the first 40 days. Throughout the first section, the fouling number increased over time, reflecting accumulating cake layer formation due to a constant, low, shear stress number of approximately 0.0025-0.003. In the second section, where the shear stress number was about twice as high, ranging between 0.004 and 0.007, the fouling number was -- even under more challenging membrane history conditions -- substantially lower than at the end of the unsparged section. This demonstrates how increased shear due to air sparging can reduce fouling.

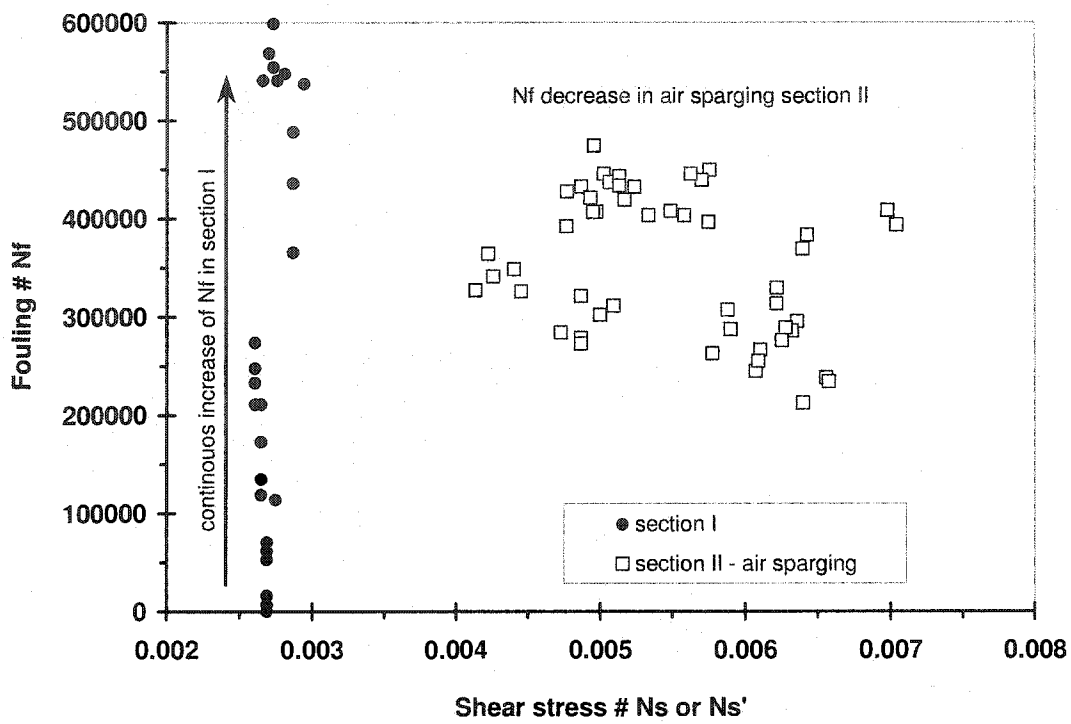

Fig. 2.7. Fouling number N_f vs. shear stress numbers Ns and Ns' respectively, for sections I and II

That effect is even more apparent in Fig. 2.8, where the fouling vs. shear stress numbers are depicted for sections III-V. Here the lower fouling numbers and the higher shear stress numbers for the air air-sparged Section IV, compared to the non-sparged Section V, are even more obvious. In Section 3 the higher liquid velocity increases the shear stress number to similar values as obtained by air sparging with lower liquid velocities, also resulting in low fouling numbers. This illustrates the usefulness of dimensionless numbers, which show that in spite of different conditions in sections III and IV, similar results for shear stress and fouling numbers are achieved.

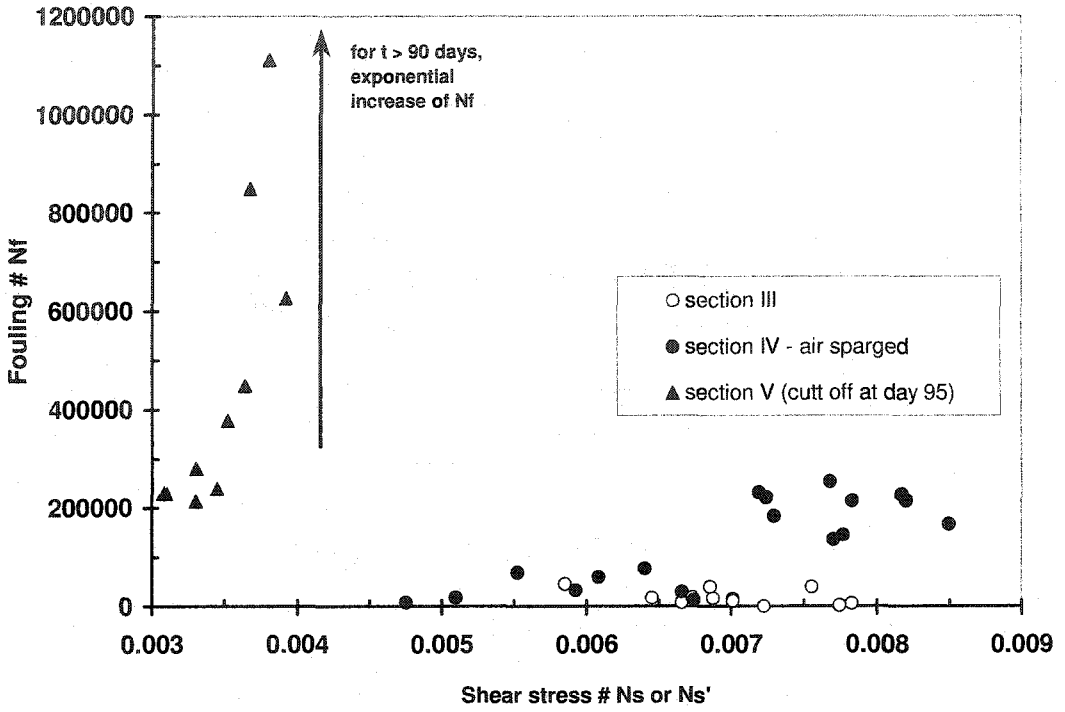

Fig. 2.8. Fouling number N_f vs. shear stress numbers Ns and Ns' respectively, for sections III-V

In Fig. 2.9 the total resistance R_t is plotted against the liquid velocity. As explained above, it was necessary to separate the data field in two ranges, before day 40 and afterwards, due to flux increases above the initial flux. To make data comparable, only the data with air sparging are depicted. For Section II, the total resistance decreases with increasing liquid velocity at average gas velocities of 0.57 m/s. For Section IV, the total resistance does not change noticeably with changing liquid velocity at average gas velocities of 0.79 m/s. This may be due to the fact that the total resistance is already so low that it is hard to achieve further improvements.

Possibly the remaining resistance is associated with internal fouling, which cannot be removed by air sparging.

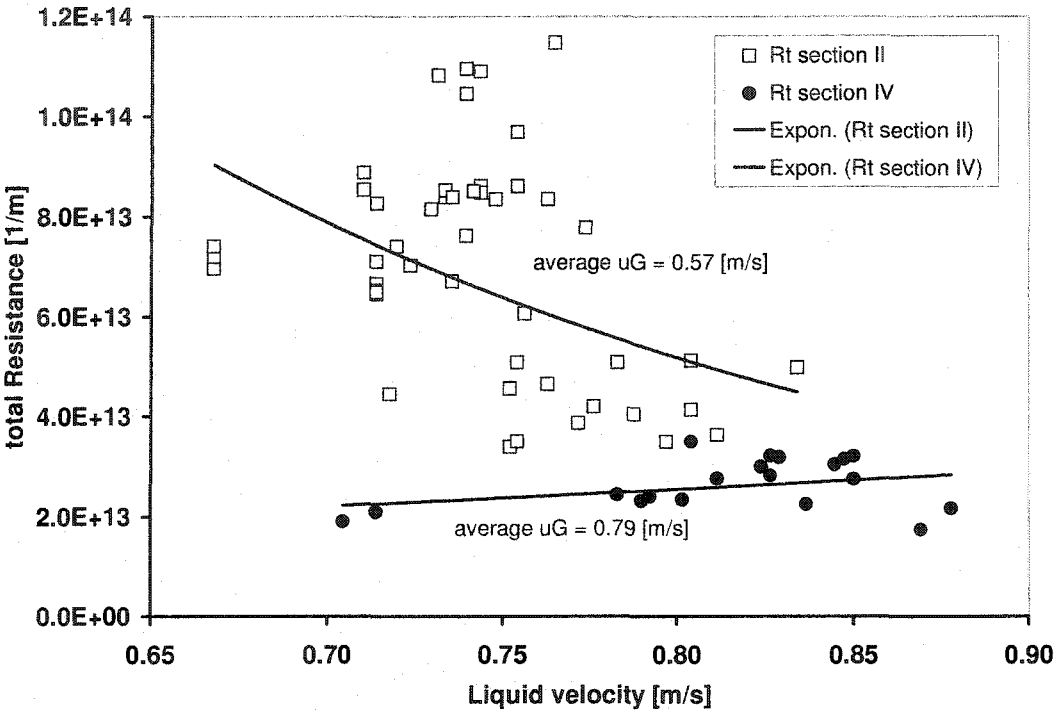

Fig. 2.9. Total Resistance vs. liquid velocity, sections II and IV

Fig. 2.10 shows a comparison of total resistance to the gas velocity for sections II and IV. For Section II, with an average liquid velocity of 0.73 m/s, there is clearly the trend of higher gas velocity toward lower total resistance. For Section IV, with an average liquid velocity of 0.81 m/s, the increase in gas velocity does not lead to a decrease in total resistance. Again, the gas velocity's reduced influence may be due to the fact that the resistance is already low and possibly due to internal fouling, which cannot be alleviated by optimizing the gas velocity.

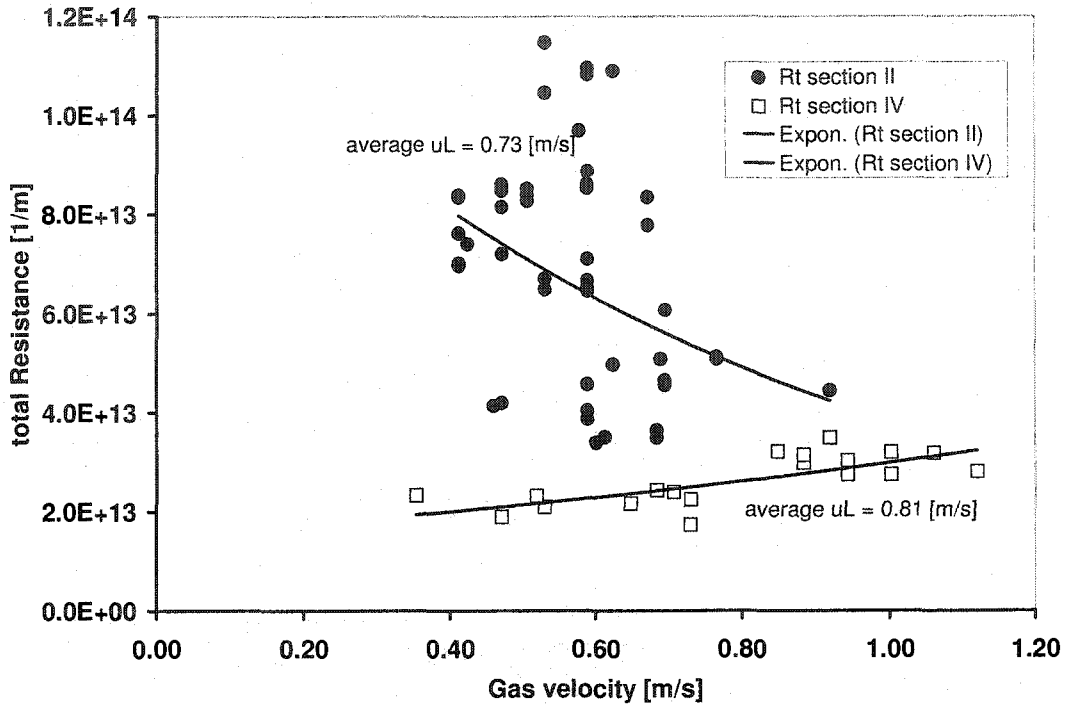

Fig. 2.10. Total Resistance vs. gas velocity, sections II and IV

In Fig. 2.11 the air injection ratio ε and total resistance R_t are plotted against time. The results are only shown up to day 100 for a better illustration, because the total resistance increases within Section V exponentially. In Section I the total resistance increases as anticipated. In Section II the total resistance drops at first, then increases from day 12 up to about day 18, temporarily even above the total resistance from Section I. Between days 18 and 24 the total resistance significantly drops to a third of its value. In Section III, when a new initial flux as a reference value to calculate the resistance is chosen, the total resistance is smaller than in Section II, but

increases again as anticipated due to cake deposition. Since the membrane was not cleaned during the whole test series, internal fouling resistance increases, which is largely unaffected by air sparging. This continuous increase in internal fouling resistance steadily raises the total fouling resistance in sections III and IV, independently of flow conditions, until values at the end of Section IV approach the final values of Section II. The air injection ratio ε varies in Section II between 0.37 and 0.57 and in Section IV between 0.31 and 0.58. The crush of the total resistance in Section II appears at ε values of about 0.43 – 0.48. The lowest values for the total resistance from the whole Section II are at day 24 and day 39, when ε is roughly 0.45. For Section IV the same observations have been made: The lowest total resistance for Section IV is calculated for day 62-63, when the air injection ratio was close to 0.45. This suggests that the air injection ratio 0.45 may represent an optimum value.

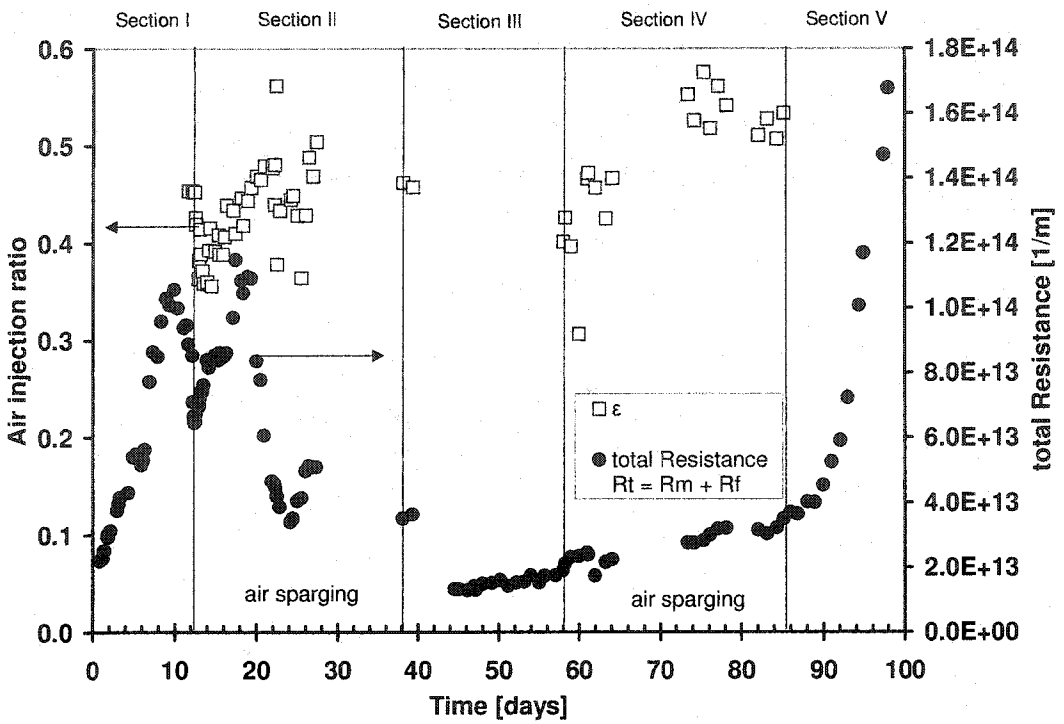

Fig. 2.11. Air injection ratio ε and total Resistance R_t vs. time – comparison of air sparged to non-sparged sections

2.4 Conclusions

Air sparging seems to be an effective aeration technique for biodegradation in a membrane bioreactor. The supplied oxygenation with air sparging is sufficient for the microbial performance without additional conventional aeration.

Air sparging has proven over several weeks in increasing the permeate flux in membrane filtration of synthetic wastewater significantly.

Shear stress numbers between 0.004 and 0.007, which resulted either from air sparging or from increased liquid velocity, lead to significantly lower fouling

numbers than those observed after a period with lower shear stress numbers. Increasing liquid velocity lead to lower fouling resistance, unless the resistance was already so low that internal fouling dominated, which could not be affected by characteristics of the feed flow. Further, it is suggested that turbulent flow conditions below Re = 4000 are sufficient to maintain high fluxes in combination with an optimized air injection ratio.

If the superficial liquid and gas velocities are fairly close to each other, the highest flux values are achievable. This test series suggests that an optimum air injection ratio exists at $\varepsilon = 0.45$.

After deployment of air sparging, a lag time (from several hours up to days) exists before the advantages of scouring air bubbles become apparent. This underlines the importance of long-term studies such as in this work.

Systematic investigations of the effect of gas and liquid superficial velocities and the air injection ratio on permeate flux are currently in progress based on the results of this study.

Nomenclature

ε	Void fraction of the pipe also called injection ratio = $u_g/(u_g+u_L)$ [dimensionless]
μ	Dynamic viscosity [Pas]
ρ	Density [kg/m³]
J	Flux at time t > zero [L/(m²*h)] or [mL/(m²*h)] or [m³/(m²*h)]
J_0	Initial Flux [L/(m²*h)] or [mL/(m²*h)] or [m³/(m²*h)]
L	Characteristic length, here channel diameter [m]
MLSS	Mixed liquor suspended solids [g/L]
Nf	Fouling number [dimensionless]
Ns	Shear stress number [dimensionless]
Ns'	Shear stress number while air sparging is supplied [dimensionless]
Re	Reynolds number [dimensionless]
Re_m	Mixture Reynolds number for the air/water two phase flow [dimensionless]
R_t	Total Resistance [1/m]
R_m	Membrane resistance at initial time [1/m]
R_f	Fouling resistance additional to the membrane resistance [1/m]
Temperature	[°C]
TMP	Transmembrane pressure [kPa]
u	Superficial velocity [m/s]

Acknowledgements

The authors would like to thank PCI Membrane Incorporated for the donation of the membrane module and valuable suggestions. Moreover, we are especially

thankful to the GRUNDFOS Company, which served our research with high quality equipment and excellent technical advice. We would also like to acknowledge a USGS National Institutes of Water Research grant, which funds this work.

2.5 References

[1] T. Stephenson, S. Judd, B. Jefferson, K. Brindle, Membrane Bioreactors for Wastewater Treatment, IWA Publishing, London (2000), ISBN: 1900222078.

[2] N. Cicek, et al., Effectiveness of the membrane bioreactor in the biodegradation of high molecular weight compounds Water Research, 32:5 (1998) 1553-1563.

[3] E. Tardieu, A. Grasmick, V. Geaugey, J. Manem, Influence of hydrodynamics on fouling velocity in a recirculated MBR for wastewater treatment, J. Membr. Sci. 156 (1999) 131-140.

[4] P. Le-Clech, P.; H. Alvarez–Vazquez, B. Jefferson, S. Judd, Fluid hydrodynamics in submerged and sidestream membrane bioreactors, Water Science and Technology, 48:3 (2003) 113-119.

[5] M. Cheryan, Ultrafiltration and Microfiltration Handbook, Technomic Publishing Co., Inc. Lancaster, Basel (1998), ISBN: 1-56676-598-6.

[6] R. Wakemann, C. Williams, Additional techniques to improve microfiltration, Separation and Purification Technology, 26 (2002) 3-18.

[7] M. Mulder, Basic Principles of Membrane Technology, Kluwer Academic Publishers, Dordrecht/Boston/London (1996), second edition, ISBN: 0-7923-4247-X.

[8] T. Taha, Z. Cui, CFD modeling of gas-sparged ultrafiltration in tubular membranes, J. Membr. Sci., 210 (2002) 13 – 27.

[9] C. Cabassud, S. Laborie, J. M. Laine, How slug flow can improve ultrafiltration flux in organic hollow fibres, J. Membr. Sci. 128 (1997) 93-101.

[10] C. Cabassud, G. Ducom, S. Laborie, Measurement and comparison of wall shear stresses in a gas/liquid two-phase flow for two module configurations, 2003 Conference Proceedings for IMSTEC, Sydney, paper 163, pg. 6.

[11] S. Levy, Two-Phase Flow in Complex Systems, Interscience, (1999) ISBN: 0471329673.

[12] H.-Q. Zhang, Q. Wang, C.Sarica, J. Brill, A unified mechanistic model for slug liquid holdup and transition between slug and dispersed bubble flows, International Journal of Multiphase Flow, 29 (2003) 97-107.

[13] A. Soleimani, T. Hanratty, Critical liquid flows for the transition from the pseudo-slug and stratified patterns to slug flow, International Journal of Multiphase Flow, 29 (2003) 51-67.

[14] L. Vera, S. Delgado, D. Elmaleh, Dimensionless numbers for the steady-state flux of cross-flow microfiltration and ultrafiltration with gas sparging, Chemical Engineering Science, 55 (2000) 3419-3428.

[15] J. Verberk, G. Worm, H. Futselaar, J. van Dijk, Combined air-water flush in dead-end ultrafiltration, Water Science and Technology: Water Supply, 1:5/6 393-402.

[16] M. Mercier, C. Fonade, C. Lafforgue-Delorme, Influence of the flow regime on the efficiency of a gas-liquid two-phase medium filtration, Biotechnology Techniques, 9:12 (Dec 1995) 853-858.

[17] L. Vera, R. Villarroel, S. Delgado, S. Elmaleh, Enhancing microfiltration through an inorganic tubular membrane by gas sparging, J. Membr. Sci., 165 (2000) 47-57.

[18] Q. Li, Z. Cui, D. Pepper, Effect of bubble size and frequency on the permeate flux of gas sparged ultrafiltration with tubular membranes, Chemical Engineering Journal, 67 (1997) 71-75.

[19] C. Cabassud, S. Laborie, L. Durand-Bourlier, J. Laine, Air sparging in ultrafiltration hollow fibers: relationship between flux enhancement, cake characteristics and hydrodynamic parameters, J. Membr. Sci., 181 (2001) 57-69.

[20] S. Bellara, Z. Cui, D. Pepper, Gas sparging to enhance permeate flux in ultrafiltration using hollow fiber membranes, J. Membr. Sci., 121 (1996) 175-184.

[21] G. Ducom, C. Cabassud, Possible effects of air sparging for nanofiltration of salted solutions, Desalination, 156 (2003) 267-274.

[22] K. Majewska-Nowak, M. Kabsch-Korbutowicz, T. Winnicki, The effect of gas bubble flow on ultrafiltration efficiency, Desalination, 126 (1999) 187-192.

[23] R. Ghosh, Z. Cui, Mass transfer in gas-sparged ultrafiltration: upward slug flow in tubular membranes, J. Membr. Sci., 162 (1999) 91-102.

[24] T. Cheng, Influence of inclination on gas-sparged cross-flow ultrafiltration through an inorganic tubular membrane, J. Membr. Sci., 196 (2002) 103-110.

[25] J. Verberk, P. Hoogeveen, H. Futselaar, J. van Dijk, Hydraulic distribution of water and air over a membrane module using AirFlush, Water Science and Technology: Water Supply, V2:2 (2001) 297-304.

[26] J. Verberk, H. van Dijk, Research on AirFlush: Distribution of water and air in tubular capillary membrane modules, *Berichte aus dem IWW Rheinisch-Westfälischen Institut für Wasserforschung gemeinnützige GmbH Band 37a, Mühlheim an der Ruhr, (2002) ISSN 0941-0961.*

[27] S. Laborie, C. Cabassud, L.Durand-Bourlier, J. Laine, Fouling control by air sparging inside hollow fibre membranes – effects on energy consumption, Desalination, 118 (1998) 189-196.

[28] P. Mikulasek, J. Cakl, P. Pospisil, P. Dolecek, The Use of Flux Enhancement Methods for High Flux Cross-flow Membrane Microfiltration Systems, Chem. Biochem. Eng. 14:4 (2000) 117-123.

[29] H.F. Roest, D.P. Lawrence, A.G.N. Bentem, Membrane bioreactors for municipal wastewater treatment, IWA Publishing, STOWA Report, (2002) ISBN: 1843390116.

[30] P. Mikulasek, P. Pospisil, P. Dolecek, J. Cakl, Gas-liquid two-phase flow in microfiltration mineral tubular membranes: relationship between flux enhancement and hydrodynamic parameters; Desalination, 146 (2002) 103-109.

[31] I. Chang, S. Judd, Air sparging of a submerged MBR for municipal wastewater treatment, Process Biochemistry, 37 (2002) 915-920.

[32] N. Al-Bastaki, A. Abbas, Use of fluid instabilities to enhance membrane performance: a review, Desalination, 136 (2001) 255-262.

[33] Le-Clech P.; Jefferson, B.; Chang, I.S.; Judd, S.; Critical flux determination by the flux-step method in a submerged membrane bioreactor, J. Membr. Sci., 227(2003) 81-93.

[34] C. Psoch, S. Schiewer, Strategies for enhanced performance of wastewater treatment in membrane bioreactors, Proceedings of 2003 ASCE/EWRI World Water & Environmental Resources Congress, Philadelphia, 10 pp.

[35] C. Psoch, S. Schiewer, Air sparged membrane bioreactors for performance increase and less fouling, Proceedings of the 2003 IMSTEC,Sydney Australia, paper 195, 6 pp.

[36] L. Vera, S. Delgado, D. Elmaleh, Gas sparged cross-flow microfiltration of biologically treated wastewater, Water Science and Technology, 41:10/11 (2000) 173-180.

[37] J. Shim, I. Yoo, Y. Lee, Design and operation considerations for wastewater treatment using a flat submerged membrane bioreactor, Process Biochemistry, 38 (2002) 279-285.

[38] APHA-AWWA-WEF, Standard Methods for the Examination of Water and Wastewater, A. Eaton, L. Clesceri, A. Greenberg, (Eds.), 19th ed. (1995) Washington DC.

[39] Metcalf & Eddy, revised by G. Tchobanoglous and F. Burton, Wastewater Engineering – Treatment, Disposal and Reuse, 3rd ed., Mc Graw Hill, New York (1991).

[40] C. Psoch and S. Schiewer, Long term investigation of aeration and flux improvement by air sparging and backflushing for membrane bioreactor, Water Research (to be submitted 2005).

[41] H. Sur, Z. Cui, Experimental study on the enhancement of yeast microfiltration with gas sparging, Journal of Chemical Technology and Biotechnology, 76 (2001) 477-484.

3 Dimensionless numbers for the analysis of air sparging aimed to reduce fouling in tubular membranes of a membrane bioreactor[2]

C. Psoch and S. Schiewer*

Department of Civil & Environmental Engineering; Water & Environmental Research Center, University of Alaska Fairbanks, AK 99775; USA

Abstract

Membrane bioreactors (MBR) combine conventional wastewater treatment and membrane filtration to create a system that uses very efficient, specialized microbes, produces a high quality effluent, and leaves small footprint. Fouling remains the major drawback of membrane processes, including MBR systems. Recently, one of the more frequent strategies employed to combat fouling and flux decrease is air sparging, in which injecting gas bubbles to the membrane generates high shear stress and scours cake layers from the membrane surface. This study mainly focused on permeate flux enhancement by air sparging. The results showed that air sparging over several weeks significantly increased permeate flux. In interpreting the findings, the dimensionless Fouling and Shear stress numbers are utilized. The Fouling number is the ratio of the Peclet number for mass transfer and the Sherwood number. It was found that fouling resistance significantly decreased with air injection ratios between 0.4 and 0.5. This paper introduces a new approach: dividing the Fouling number by the Reynolds number, which basically corresponds to the ratio of the Schmidt and

[2] Desalination, Elsevier (in preparation for resubmission) 2005

Sherwood numbers. That dimensionless number, subsequently called the Viscous Fouling number, shows qualitatively the same graph as the Fouling number if viscosity remains constant. If viscosity changes during the filtration process, the Fouling number and the Viscous Fouling number diverge from each other. Using the Viscous Fouling number instead of the Fouling number may be especially useful for processes where fluctuations in viscosity are significant, as they are in MBR.

Keywords: membrane bioreactor, fouling, air sparging, tubular membrane, synthetic wastewater

* Corresponding author: Tel.: (907) 474-2620; fax: (907) 474-6087, E-mail address: ffsos@uaf.edu

3.1 Introduction

The use of membrane bioreactors (MBR) for wastewater treatment has rapidly increased in the last decade. One reason for this growing popularity is that the membrane eliminates the need for a secondary sedimentation tank for solid/liquid separation after biological treatment. Furthermore, retention of microbes by the membrane enables not only establishment of higher biomass concentrations, which in turn lead to a compact volume and high loading rate capacity [1], but also to establishment of a well adapted microbial community and partial disinfection of the wastewater [2].

The main challenge still facing MBR is membrane fouling. Factors determining the severity of fouling include the operating flux, turbulence intensity on the membrane surface, and viscosity of the wastewater [3; 4]. Since fouling is the main obstacle to a more widespread application of membrane processes, it is important to control fouling to ensure steady operation of membrane plants [5]. Further investigations are necessary to investigate the effectiveness of anti-fouling measures. In this respect, two main types of fouling are distinguished: internal fouling in the pores of the membrane, and external fouling on the membrane surface due to a cake layer, or, more specifically, a gel layer and concentration polarization on top of the gel layer [6].

This study focused on investigating gas sparging as a technique to reduce external fouling and describing the results with the use of dimensionless numbers. In

gas sparging, gas is injected into the feed stream inside a tubular membrane. The two-phase flow generated helps maintain a stable permeate flux over longer time periods [7-9].

The interface for this gas-liquid two-phase flow in tubular membranes follows a variety of flow patterns. The predominant factor determining flow regime is the void fraction in the pipe, which depends directly on the gas and liquid phase velocities. With increasing void fraction, the flow pattern changes from bubble flow ($0 < \varepsilon < 0.2$) over slug flow ($0.2 < \varepsilon < 0.9$) to annular and churn flow ($0.9 < \varepsilon < 1.0$) [10-15]. Slug flow is the most effective flow pattern for reducing cake layer build up; this is due to high shear stress induced by water and air slugs, according to studies of Cabassud et al., Li et al., and Vera et al. [8; 16; 17].

Additionally, a water film flows parallel to the gas slugs, which is countercurrent, (i.e. downward in upward filtration) [18]. Gas and liquid slugs cause different turbulence intensities, which strongly influence the concentration polarization layer [19; 20]. This influence may cause membrane selectivity to deteriorate slightly [21]. In tubular membranes, the most severe turbulence phenomena occur within the wake zone of the gas slugs, where smaller gas bubbles follow the gas slugs in heavily turbulent movements [22]. These turbulent movements, associated with small gas bubbles, are to some extent able to dislocate and remove the cell debris and particles that have accumulated and partially clogged the pore channels [23].

If the chosen gas is air, an additional benefit of air sparging is increased oxygen supply, which is necessary for the reactor's biological degradation processes.

In industrial membrane applications, membranes are typically operated for several weeks before chemical cleaning. One objective of this study was, correspondingly, to operate an air sparged tubular membrane filtration system over time periods of several months.

The main focus was on monitoring the flux development with and without air sparging and to interpret the findings by using dimensionless numbers like the Shear stress number and Fouling number, as suggested by *Vera et al.* [24].

3.2 Materials and methods

The experimental setup, as shown in Fig. 3.1, used an activated sludge tank with a volume of 60 - 80 liters. The wastewater and activated sludge were circulated with a submerged pump (Grundfos MP1). The applied transmembrane pressure (TMP) for the filtration was between 140 and 200 kPa.

The pump speed, and therefore the volume stream, could be regulated over a variable frequency drive (Grundfos). In the interest of a longer pump life, the system was controlled by a timer, which shut the pump on and off every other hour. The timer also controlled a solenoid valve, which connected the air supply with the loop. Air was supplied only when the pump was operating. A semi-automatic oxygen probe that also measured the temperature monitored the oxygen content in the vessel.

The polymer membrane (PCI) had a length of 1.20 m and a pore size of 0.2 μm. The module was made up of five tubes, each with an inner diameter of 6.35 mm, yielding a membrane surface area of 0.1 m^2. On each side of the module, the membrane tubes were extended by about 10 cm through an acrylic rod. The acrylic extensions, with drill holes in the same diameter as the membrane tubes, served for the air supply and for observation of the flow pattern in the unit. Each tube had its own connection to the air supply, with a separately adjustable air volume stream.

A hose diffuser with numerous air outlets of 1.6 mm diameter served for aeration in those experimental sections where no air sparging was supplied. This hose was

mounted like an annulus at the inner circumference of the bottom of the cylindrical vessel.

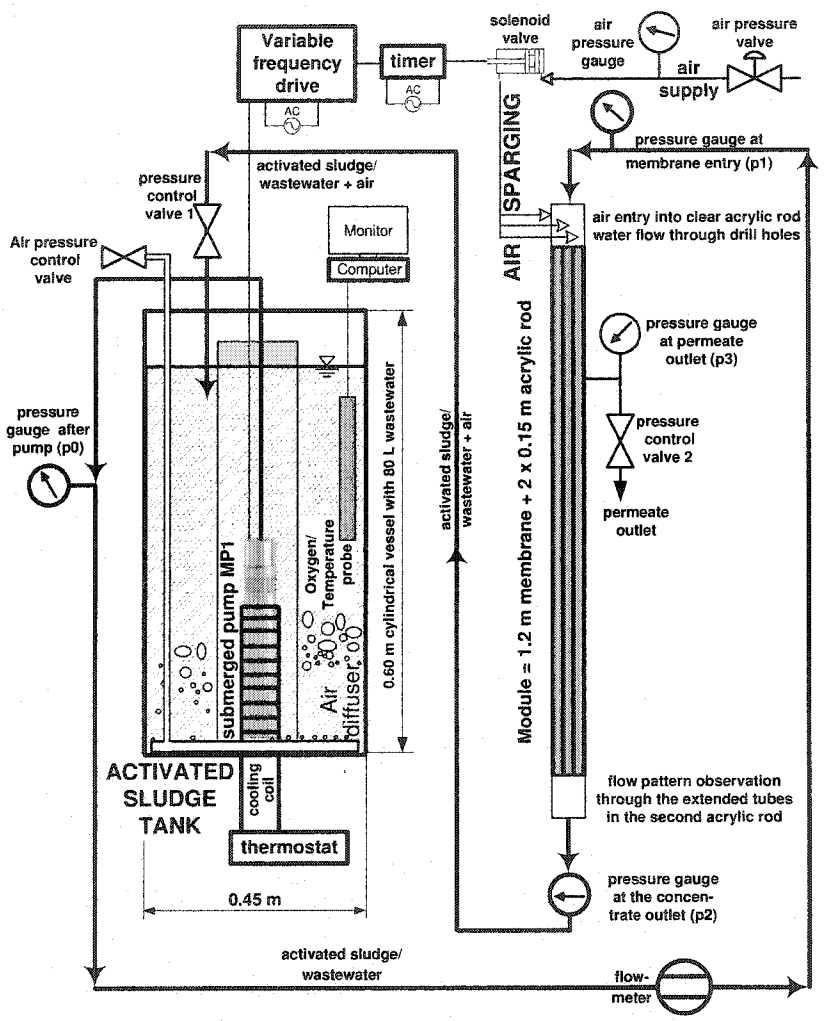

Fig. 3.1. Experimental setup schematically with activated sludge tank and membrane

The water flow velocity within the membrane tubes was between 0.6 and 1.05 m/s. The maximum velocity was limited by the ability to observe the flow pattern, which generally moved too quickly for the naked eye. The flow was adjusted based

on photographs taken with a digital still camera, (a Sony FD Mavica; 10 x optical zoom). When flow velocities exceeded 1 m/s it was no longer possible to monitor the flow pattern in the system, even with the camera's help.

A glucose-based synthetic wastewater was prepared as described in *Psoch & Schiewer* [25], based on the composition in experiments carried out by *Shim et al.* [26]. At first, a batch trial was launched to build up a high amount of biomass, indicated by the amount of mixed liquor suspended solids (MLSS). For determining the MLSS amounts, the standard methods [38] were used. The initial amount of MLSS was slightly above 2 g/L.

Throughout the whole test series (about 190 days), no membrane cleaning or chemical application was performed. No data were collected from days 28 to 37 and 65 to 72, due to conference attendances, and from days 40 to 45 and 167 to 181, due to pump repair.

3.3 Results and discussion

3.3.1 General observations

When the reactor was aerated only by air sparging, the oxygen supply for the degradation performance within the reactor was sufficient, even with aeration limited to every other hour and under increasing loads, as reported in *Psoch & Schiewer* [27].

In Fig. 3.2, flux, Reynolds number and liquid velocity are plotted versus time. The liquid velocity stayed between 0.65 and 0.85 m/s, except in Section III, where the

liquid flow velocity reached about 1 m/s. Based on the convention that laminar flow prevails at Reynolds numbers below 2300, the majority of the data points in the non-air-sparged sections (I, III and V) are in the laminar range. For one phase flow the Reynolds number is calculated as:

$$\mathrm{Re} = \frac{\rho * u_{Liquid} * L}{\mu} \qquad \text{eq. 3.1}$$

with:

ρ = density [kg/m³]

u_{Liquid} = liquid velocity [m/s]

L = characteristic length, here channel diameter [m]

μ = dynamic viscosity [Pas]

The dynamic viscosity was estimated after a correlation related to the mixed liquor suspended solid content as explained in Psoch & Schiewer [27].

For the two-phase flow in sections II and IV, the calculation of the mixture Reynolds number is as follows:

$$\mathrm{Re}_{mixture} = \frac{\rho_{Liquid} * (u_{Liquid} + u_{Gas}) * L}{\mu_{Liquid}} \qquad \text{eq. 3.2}$$

with:

$\mathrm{Re}_{(mixture)}$ = two phase Reynolds number [dimensionless]

u = superficial velocity of the phase [m/s]

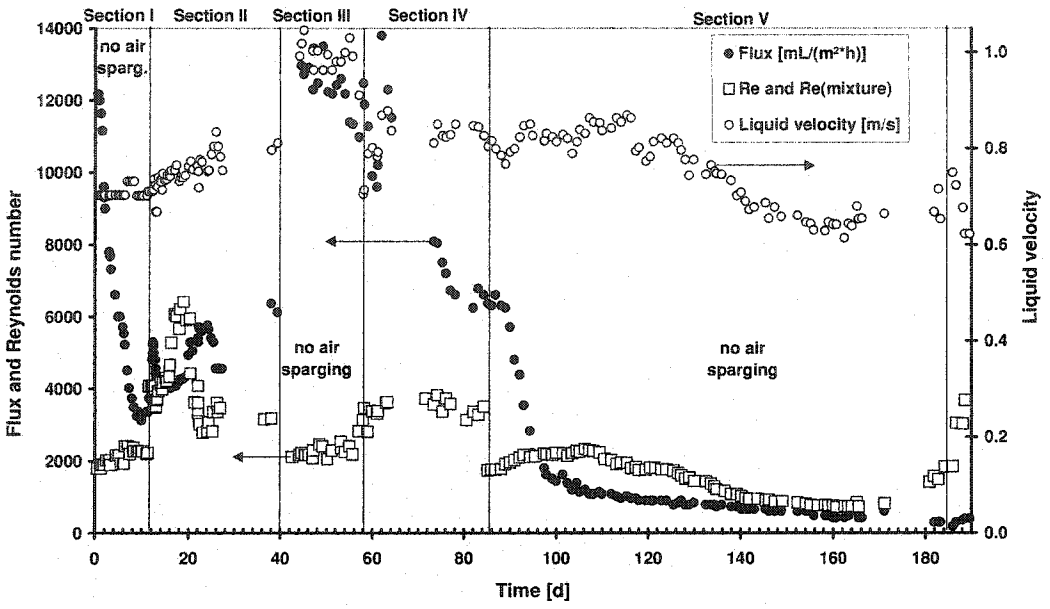

Fig. 3.2. Flux, Reynolds number, and liquid velocity vs. time

As one can see in Fig. 3.2, for the one-phase flow fouling can not be predicted from the Reynolds number, because this parameter does not change significantly within sections I, III and V, but the flux fluctuates significantly.

In Section II the mixture Reynolds number ramps up to about 6000, and with some delay the flux increases accordingly. In Section IV the mixture Reynolds numbers are substantially lower but clearly in the turbulent range. However, the highest flux values are observed in sections III and IV.

For the relationship between flux and resistance, the following equation is valid [6]:

$$J = \frac{TMP}{\mu * R_t} \qquad \text{eq. 3.3}$$

with:

J = the flux at any time larger than zero during the filtration process [$m^3/(m^2\ s)$]

μ = dynamic viscosity [Pas]

R_t = total resistance [1/m]

For the total resistance, the row resistance model is applied:

$$R_t = R_m + R_f \qquad \text{eq. 3.4}$$

with

R_m = initial membrane resistance

R_f = fouling resistance at time t, additional to the initial resistance

R_m is calculated according to the following equation:

$$R_m = \frac{TMP}{\mu * J_0} \qquad \text{eq. 3.5}$$

with:

J_0 = initial flux [$L/(m^2\ h)$]

The fouling resistance is determined as follows:

$$R_f = \frac{TMP}{\mu * J} - R_m \qquad \text{eq. 3.6}$$

with:

J = the flux at any time larger than zero during the filtration process [$m^3/(m^2\ s)$]

With eq. 3.5 substituted in eq. 3.6 we obtain:

$$R_f = \frac{TMP}{\mu}\left(\frac{1}{J} - \frac{1}{J_0}\right) \qquad \text{eq. 3.7}$$

The row resistance model shows a certain weakness; namely that this model can't accommodate flux increases above the initial values, which may occur due to altered process parameters. At the beginning of Section III the liquid flow velocity is significantly increased compared to Section I and II, thus the flux is higher. Moreover the initial flux of Section III is the highest throughout the whole time span of the observations. Due to this circumstance, in order to apply the row resistance model it was necessary to divide the test series into two segments. Segment A includes the first two sections and segment B, sections III to V. Consequently for all resistance calculations in segment A the initial flux at Section I is the reference value, and for the calculations in segment B the initial flux in Section III is the reference value.

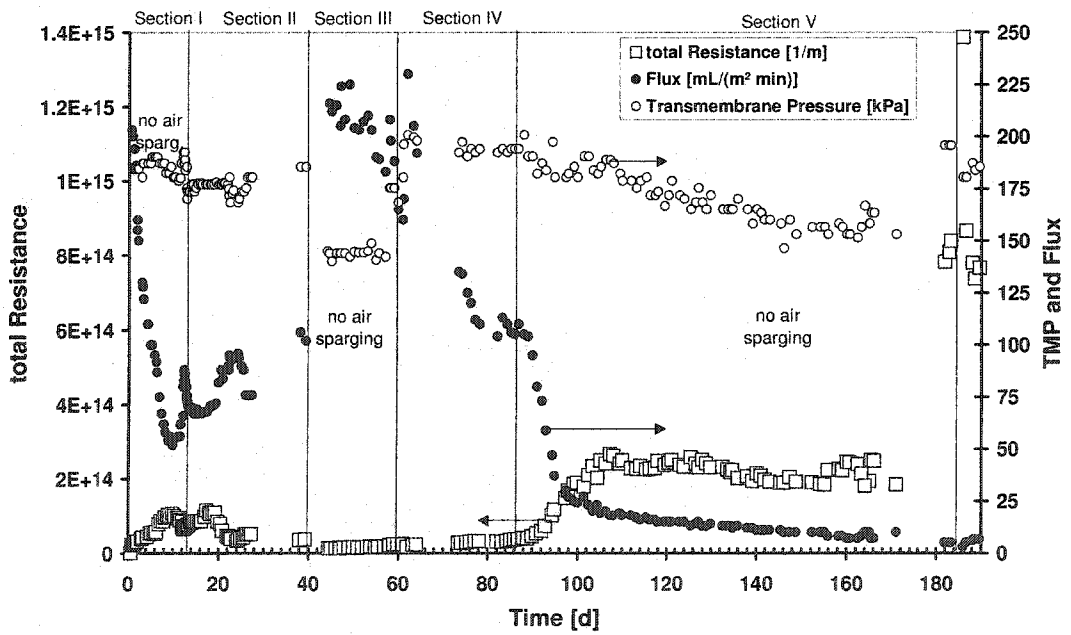

Fig. 3.3. Total Resistance R_t of the Membrane, TMP and Flux vs time.

In Fig. 3.3, the measured flux and TMP and the calculated values for the total membrane resistance are pictured. The chart is divided in five sections with air sparging applied in every second section.

For the duration of the experiment the TMP did not vary by more than 12 %, except for Section III, where the lowest pressures (about 140 kPa) were imposed. Nevertheless, the highest fluxes were achieved in this section, due to high crossflow velocity, which significantly increased the critical flux line.

Within the first twelve days (Section I), no air sparging was provided and the flux plunged to about 25 % of its initial values due to intensive fouling unmitigated by any remedial action. That is congruent with the total resistance increase within Section I. Between days 12 and 40 (Section II) air sparging was supplied; the flux increased and was even -- after 40 days -- significantly higher than at the end of Section I with similar conditions in both sections. The decrease of the total resistance reflects that observation. Between days 40 and 59 (Section III) no air sparging was supplied, but the liquid velocity was significantly increased compared to sections I and II, as one can easily see from Fig. 3.2. Consequently the flux increased further and the total resistance reached its lowest level. In Section IV (days 59 to 86), air sparging was again supplied with conditions similar to sections I and II. The flux decreased after three days due to an un-optimized flow pattern and increasing internal fouling of the membrane, which caused a slow, steady increase of the total membrane resistance. In Section V (days 86 to 185), when air sparging was discontinued, the flux dropped below the levels from Section I. The total resistance in Section V (after 100 days)

reaches a plateau value and remains constant up to day 167. Some pump adjustments at the end of the section and renewed air sparging after Section V were unable to raise the flux again.

Fig. 3.4 depicts the air injection ratio and the fouling resistance for the first 100 days of the experiments. The air injection ratio ε is calculated as follows:

$$\varepsilon = \frac{u_{\text{Gas}}}{(u_{Gas} + u_{Liquid})} \qquad \text{eq. 3.8}$$

with:

ε = void fraction in the tube [-]

u_{Gas} = superficial gas velocity, i.e. velocity if only gas was in the channel [m/s]

u_{Liquid} = superficial liquid velocity, i.e. velocity if only liquid was in the channel [m/s]

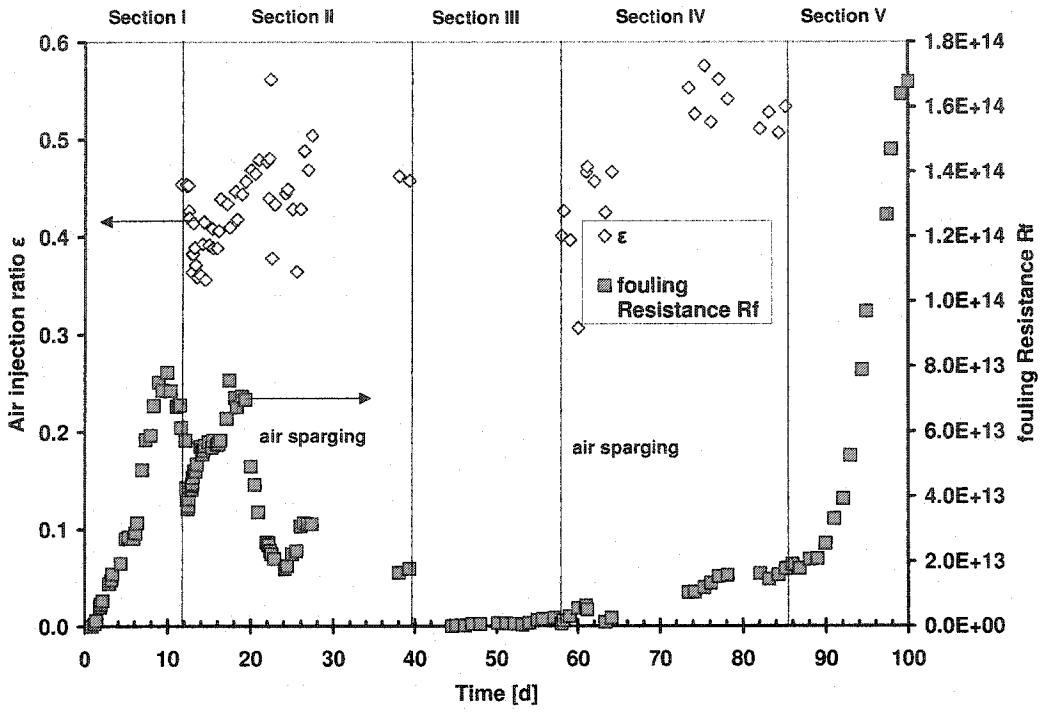

Fig. 3.4. Air injection ratio ε and fouling Resistance R_f vs time.

Within the first section, the fouling resistance reflects the flux decrease without any remedial action and a slight decrease of the MLSS (compare Fig. 3.6) and, consequently, viscosity, toward the end of the section. In Section II the fouling resistance drops down immediately after air sparging is supplied. With an enrichment of MLSS the viscosity increased between days 20 and 24, and the fouling resistance nevertheless significantly decreased due to air sparging. At the end of Section II the highest fluxes were achieved, so the fouling resistance was very small. In Section III no air sparging was supplied, but high shear stresses due to comparatively high cross flow velocities (compare to Fig. 3.2) were exerted. Hence the fouling number during

the whole section was almost constant at very low values. In Section IV the fouling resistance steadily increases due to gradual accumulation of internal fouling. In Section V the fouling resistance increases over several orders of magnitude. For better visualization only the first 14 days (Day 86 to Day 100) are depicted. The strong increase in membrane fouling is based on internal fouling. Therefore imparting high shear stress, which is mainly a measure against external fouling, was not very effective (Fig. 3.2 & 3.3, Section IV).

In the air sparging sections, the lowest fouling resistance was observed at air injection ratios of about 0.45 (Day 24 and Day 62), indicating that for the operated setup there is an optimal ε value for the air sparging.

3.3.2 Data interpretation via dimensionless parameters

To achieve more general information from the data about the effect of flow rates and TMP on fouling, dimensionless parameters were used, as proposed by *Vera et al.* [13; 16; 24]. Fig. 3.5 shows the dimensionless Shear Stress numbers, Ns and Ns' for air sparging sections on the x-axis and the dimensionless Fouling number N_f on the y-axis. For the calculation of the shear stress number the following equation applies [24]:

$$N_S = \frac{\rho_{Liquid} * u^2_{Liquid}}{TMP} \qquad \text{eq. 3.9}$$

If air sparging is supplied, density and velocity have to be modified in this equation to represent two-phase flow conditions and eq. 3.10 applies, where the

mixture density $\rho_{mixture}$ according to eq. 3.11 is used in place of the liquid density, and the mixture velocity $u_{mixture}$ is calculated according to eq. 3.12.

$$N_S' = \frac{\rho_{mixture} * u_{mixture}^2}{TMP} \qquad \text{eq. 3.10}$$

with

$$\rho_{mixture} = \frac{\rho_{Liquid} * u_{Liquid} + \rho_{Gas} * u_{Gas}}{u_{mixture}} \qquad \text{eq. 3.11}$$

and

$$u_{mixture} = u_{Gas} + u_{Liquid} \qquad \text{eq. 3.12}$$

The calculation of the dimensionless Fouling number is according to *Vera et al.*[24] in eq. 3.13 and 3.14 explained:

$$N_f = \frac{\mu * R_f * u_{Liquid}}{TMP} \qquad \text{eq. 3.13}$$

With eq. 3.7 substituted in eq. 3.13 and rearranged we obtain:

$$N_f = u_{Liquid} * \left(\frac{1}{J} - \frac{1}{J_0} \right) \qquad \text{eq. 3.14}$$

The Fouling number can, according to *Vera et al.* [24], be understood as the inverse of the Stanton number for mass transfer, which is a function of the Peclet und Sherwood number:

$$Pe = \mathrm{Re} * Sc = \frac{u_{Liquid} * L}{\nu} * \frac{\nu}{D} = \frac{bulkMassTransfer}{diffusiveMassTransfer} \qquad \text{eq. 3.15}$$

with:

ν = kinematic viscosity [m²/s]

L = characteristic length, here tube diameter [m]

D = diffusivity [m²/s]

and

Re = Reynolds number according to eq. 3.1 and Sc = Schmidt number according to:

$$Sc = \frac{\nu}{D} \qquad \text{eq. 3.16}$$

furthermore

$$Sh = \frac{k * l}{D} = \frac{massDiffusivity}{molecularDiffusivity} \qquad \text{eq. 3.17}$$

and

k = diffusion rate [m/s]

l = characteristic length, here the film thickness [m]

with eq. 3.15 and eq. 3.17 we obtain [24]:

$$N_f = \frac{1}{St} = \frac{Pe}{Sh} = \frac{\mathrm{Re} * Sc}{Sh} = \frac{u_{Liquid} * L}{k * l} = \frac{bulkMassTransfer}{massDiffusivity} \qquad \text{eq. 3.18}$$

St = Stanton number

According to Baehr & Stephan [28] and Mulder [6], the Sherwood number can be expressed as a function of the Reynolds and Schmidt number with:

$$Sh = c * \mathrm{Re}^{n} * Sc^{m} \qquad \text{eq. 3.19}$$

Here c, n, and m are constants depending on the system and the predominant flow regime.

When the above expression is inserted in eq. 3.18, the following result for the Fouling number as a function of the Reynolds and Schmidt number will be obtained:

$$N_f = \frac{\mathrm{Re} * Sc}{c * \mathrm{Re}^{n} * Sc^{m}} = C * \mathrm{Re}^{(1-n)} * Sc^{(1-m)} \qquad \text{eq. 3.20}$$

with:

C = constant

One way to obtain a new dimensionless number is to divide the Fouling number N_f by the ordinary Reynolds number. This term shall be called Viscous Fouling number (N_{vf}). Substitution of eq. 3.17 and 3.18 into this equation yields:

$$N_{vf} = \frac{N_f}{\mathrm{Re}} = \frac{Sc}{Sh} = \frac{\nu}{D} * \frac{D}{k * l} = \frac{kinematicViscosity}{massDiffusivity} \qquad \text{eq. 3.21}$$

Another expression for the Viscous Fouling number is obtained by combining eq. 3.1 and eq. 3.14:

$$N_{vf} = \frac{N_f}{\mathrm{Re}} = \frac{\nu}{L} * \left(\frac{1}{J} - \frac{1}{J_0} \right) \qquad \text{eq. 3.22}$$

If eq. 3.19 is substituted into eq. 3.21 the following relationship will be found,

$$N_{vf} = \frac{N_f}{\mathrm{Re}} = \frac{Sc}{Sh} = \frac{Sc}{c * \mathrm{Re}^n * Sc^m} = \frac{Sc^{(1-m)}}{c * \mathrm{Re}^n} = C * \frac{Sc^{(1-m)}}{\mathrm{Re}^n} \qquad \text{eq. 3.23}$$

Comparing eq. 3.14 and 3.22, as well as eq. 3.20 and 3.23 shows the Viscous Fouling number has a different character than the conventional Fouling number.

The Fouling number N_f depends directly on the liquid velocity, whereas the Viscous Fouling number N_{vf} depends directly on the kinematical viscosity. This difference is also evident from the verbal expressions of eq. 3.18 and eq. 3.21.

In Fig. 3.5, the three non-sparged sections are shown as separate series and the air sparged sections are shown as the same category of dots. In Section I the liquid velocity stayed constant; hence the Shear Stress number expressed no significant fluctuation. The Fouling number increased significantly due to permanent flux decrease in Section I. The Shear Stress number in sections II, III and IV fluctuates significantly due to changes in the liquid or mixture velocity. In all of these three sections the Shear Stress numbers are comparatively high. Consequently the Fouling numbers remain at fairly low values. In the air sparged sections (II and IV) the Fouling numbers are mostly higher than in Section III, where the highest liquid velocities were measured (compare Fig. 3.2). That is inherent in the calculation of the Fouling number, which implies that the highest fluxes are always at the beginning of a measurement at constant boundary conditions.

Because the expression in parenthesis in eq. 3.14 increases with ongoing time more, than the velocity in Section IV decreases, compared to Section III, the Fouling number increases too. Thus the Fouling numbers in Section IV are generally higher than in Section III. Meanwhile the flux rise from Section II to Section III overcomes the impact of the higher liquid velocity. Thus Section II has higher Fouling numbers compared to Section III.

In Section V the velocity decreases slightly, as well as the transmembrane pressure, and so the Shear Stress numbers don't fluctuate too much, but the Fouling number increases significantly due to severe flux decrease.

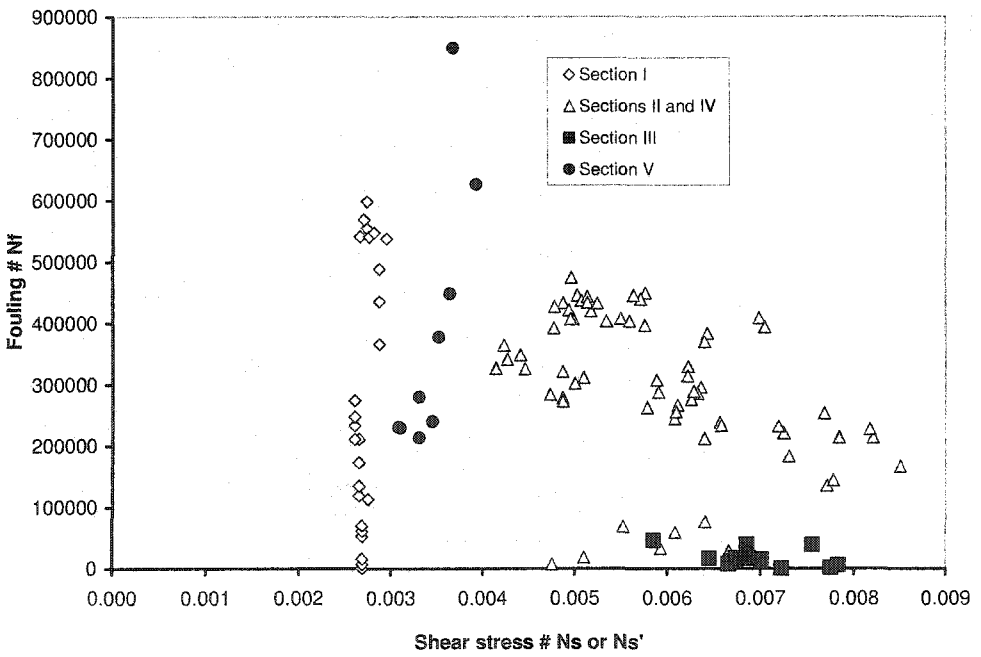

Fig 3.5. Shear stress number vs Fouling number

In Fig. 3.6 to 3.8, the Fouling number and the Viscous Fouling number and Reynolds numbers are depicted. For better data interpretation, the flux and MLSS are shown too.

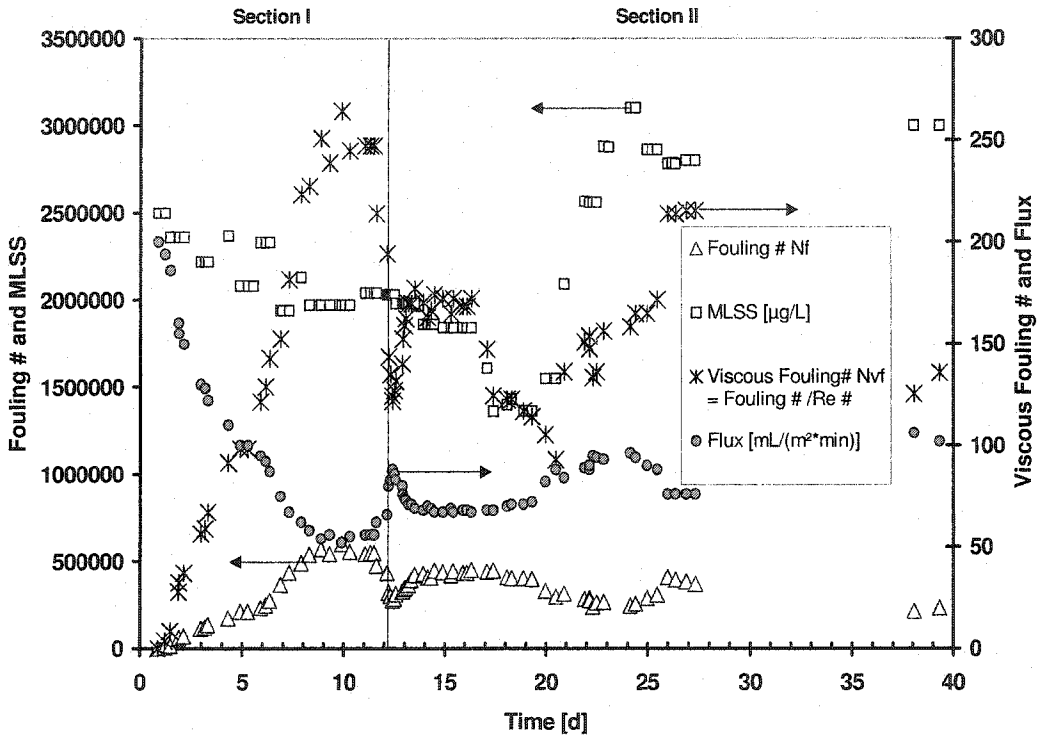

Fig. 3.6. Comparison of Fouling number N_f and Viscous Fouling number $N_{vf} = N_f/Re$ related to MLSS and flux for days 0 to 40.

Fig. 3.6 shows the first 40 days of the Fouling and Viscous Fouling number, inclusive of flux and MLSS. Both dimensionless numbers show similar graphs but a different intensity of the amplitude. Between days 21 and 24, both graphs show opposite trends due to the fact that the MLSS noticeably increased and, correspondingly, the viscosity of the liquid. The MLSS changed within this 40 days, between 1.3 and 3.1 g/L respectively 1,300,000 and 3,100,000 µg/L.

In Fig. 3.7, Day 40 to Day 90 is presented. In Section III Fouling number and Viscous Fouling number do not diverge much from each other. That is explained, because the Fouling number is subject to a decrease in liquid velocity in a similar manner as the Viscous Fouling number is subject to a decrease of kinematic viscosity ν, while both are affected by decreasing flux (eq. 3.14 and 3.22).

Throughout the whole of Section IV and the beginning of Section V, the Fouling number increases less than the Viscous Fouling number due to the fact that the cross flow velocity in Section IV is noticeably smaller than in Section III. Meanwhile the changes in MLSS and therefore the viscosity variation are negligible. The rise of N_{vf} compared to N_f becomes even more pronounced when the MLSS rises, as for instance in Section IV up to Day 82 and in Section V.

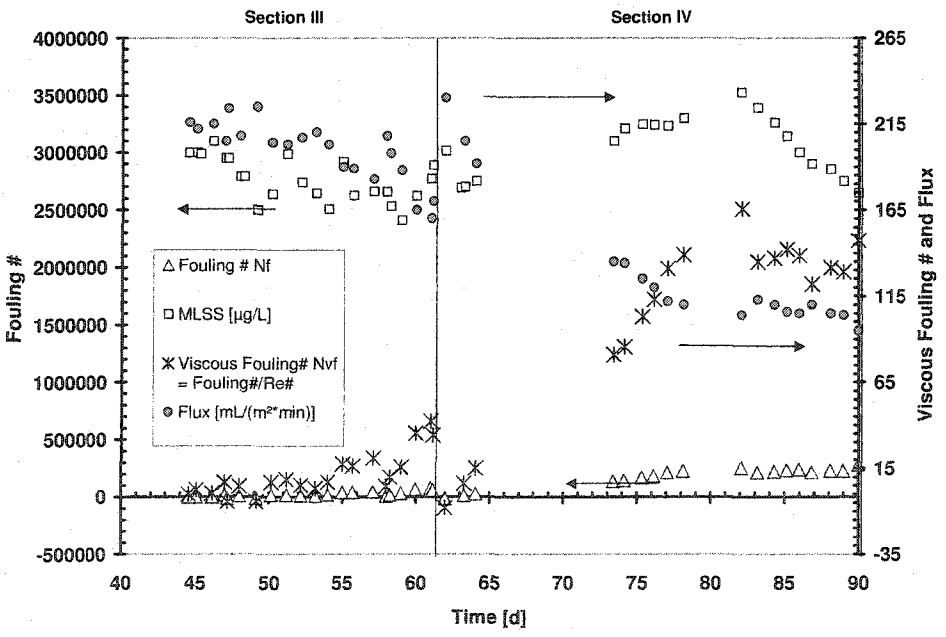

Fig. 3.7. Comparison of Fouling number N_f and Viscous Fouling number N_{vf} =Fouling number/Re number with MLSS and flux for days 40 to 90.

Fig. 3.8 shows the calculated Fouling and Viscous Fouling Number for days 90 to 190. Up to Day 130, both dimensionless numbers show the same behavior, due to favorable depiction, even exactly the same shape. That is explicable by basically constant liquid velocity and almost unchanged MLSS. The only variable that changes for both dimensionless numbers is the decreasing flux, which raises both dimensionless numbers, according to eq. 3.14 and 3.22.

From Day 130 up to Day 167, as long as the setup worked properly, both parameters show different trends with significantly higher increases of the Viscous Fouling Number. The increase is due to a steadily rising MLSS, from 3.25 g/L at Day 130 to about 5.65 g/L at Day 166, and a decrease of cross flow velocity, from 0.87 to 0.65 m/s. Measurements beyond this time only confirm this explanation, because the MLSS decreased after a peak at Day 174, again to 2.2 g/L and the flow velocity increased slightly, and so the dimensionless numbers approached each other again.

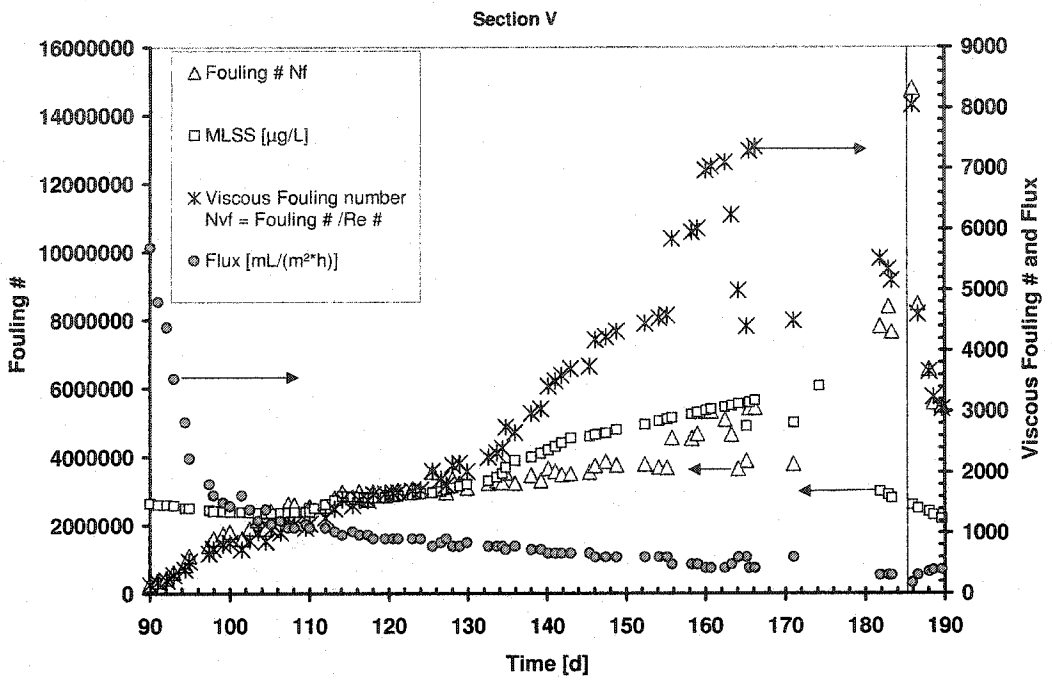

Fig. 3.8. Comparison of Fouling number N_f and Viscous Fouling number N_{vf} =Fouling #/Re # with MLSS for days 90 to 190.

3.4 Conclusions

Air sparging provided sufficient aeration for microbial biodegradation in the membrane bioreactor without additional conventional aeration. Air sparging applied over several weeks has proven to raise the permeate flux in membrane filtration of synthetic wastewater. When the superficial liquid and gas velocity are fairly close to each other, the highest flux values are achievable. The test series suggests that an optimum air injection ratio exists at $\varepsilon = 0.45$. The one- phase and two-phase mixture Reynolds number gives only limited information about the fouling tendency of the system. For the two-phase mixture Reynolds numbers in the moderate turbulent range

the highest fluxes where obtained. The dimensionless Fouling number seems to be a good tool to reflect the flux decrease in a system with synthetic wastewater. A further dimensionless parameter was introduced by dividing the dimensionless Fouling number by the ordinary Reynolds number. Throughout this paper, this dimensionless number is labeled the Viscous Fouling number. Advantages of using this Viscous Fouling number compared to the common Fouling number are:

- Substantially smaller, more manageable dimensionless numbers
- If the liquid viscosity remains constant, similar behavior as for the Fouling number
- If the viscosity changes, the Viscous Fouling number reacts differently, proving more sensitive to the altered viscosity

Acknowledgements

The authors would like to thank the PCI Membrane Incorporated for donating the membrane module and for their valuable suggestions. Moreover, we are especially thankful to the GRUNDFOS Company, which served our research with high quality equipment and excellent technical advice. We would also like to acknowledge a USGS NIWR grant for funding this research.

3.5 References

[1] T. Stephenson, S. Judd, B. Jefferson and K. Brindle, Membrane Bioreactors for Wastewater Treatment, IWA Publishing, London (2000), ISBN: 1900222078.

[2] N. Cicek, H. Winnen, B. Wrenn, V. Urbain and J. Manem, Effectiveness of the Membrane Bioreactor in the biodegradation of high molecular weight compounds Water Research, Vol. 32, No. 5 (1998) 1553-1563.

[3] E. Tardieu, A. Grasmick, V. Geaugey and J. Manem, Influence of hydrodynamics on fouling velocity in a recirculated MBR for wastewater treatment, J. Membr. Sci., 156 (1999) 131-140.

[4] P. Le-Clech, P., H. Alvarez–Vazquez, B. Jefferson and S. Judd, Fluid hydrodynamics in submerged and sidestream membrane bioreactors Water Science and Technology, Vol 48 No 3 (2003) 113-119.

[5] R. Wakemann and C. Williams, Additional techniques to improve microfiltration, Separation and Purification Technology, 26 (2002) 3-18.

[6] M. Mulder, Basic Principles of Membrane Technology, Kluwer Academic Publishers Dordrecht/Boston/London (1996), second edition, ISBN: 0-7923-4247-X.

[7] T. Taha, and Z. Cui, CFD modeling of gas-sparged ultrafiltration in tubular membranes, J. Membr. Sci., 210 (2002) 13 – 27.

[8] C. Cabassud, S. Laborie, and J. M. Laine, How slug flow can improve ultrafiltration flux in organic hollow fibres, J. Membr. Sci. 128 (1997) 93-101.

[9] C. Cabassud, G. Ducom and S. Laborie, Measurement and comparison of wall shear stresses in a gas/liquid two-phase flow for two module configurations, Conference proceedings IMSTEC Sydney, paper 163 (2003) 6 pages.

[10] S. Levy, Two-Phase Flow in Complex Systems, Interscience, (1999), ISBN: 0471329673.

[11] H.-Q. Zhang, Q. Wang, C.Sarica and J. Brill, A unified mechanistic model for slug liquid holdup and transition between slug and dispersed bubble flows, International Journal of Multiphase Flow 29 (2003) 97-107.

[12] A. Soleimani, and T. Hanratty, Critical liquid flows for the transition from the pseudo-slug and stratified patterns to slug flow", International Journal of Multiphase Flow 29 (2003) 51-67.

[13] L. Vera, S. Delgado and D. Elmaleh, Dimensionless numbers for the steady-state flux of cross-flow microfiltration and ultrafiltration with gas sparging Chemical Engineering Science 55 (2000) 3419-3428.

[14] J. Verberk, G. Worm, H. Futselaar and J. van Dijk, Combined air-water flush in dead-end ultrafiltration, Water Science and Technology: Water Supply, Vol 1, No 5/6 (2001) 393-402.

[15] M. Mercier, C. Fonade, and C. Lafforgue-Delorme, Influence of the flow regime on the efficiency of a gas-liquid two-phase medium filtration, Biotechnology Techniques, Vol. 9 no. 12 (Dec.1995) 853-858.

[16] L. Vera, R. Villarroel, S. Delgado and S. Elmaleh, Enhancing microfiltration through an inorganic tubular membrane by gas sparging, J. Membr. Sci., 165 (2000) 47-57.

[17] Q. Li, Z. Cui, and D. Pepper, Effect of bubble size and frequency on the permeate flux of gas sparged ultrafiltration with tubular membranes, Chem. Engin. Journ., 67 (1997) 71-75.

[18] C. Cabassud, S. Laborie, L. Durand-Bourlier and J. Laine, Air sparging in ultrafiltration hollow fibers: relationship between flux enhancement, cake characteristics and hydrodynamic parameters, J. Membr. Sci., 181 (2001) 57-69.

[19] S. Bellara, Z. Cui, and D. Pepper, Gas sparging to enhance permeate flux in ultrafiltration using hollow fiber membranes J. Membr. Sci., 121 (1996) 175-184.

[20] G. Ducom, and C. Cabassud, "Possible effects of air sparging for nanofiltration of salted solutions"; Desalination 156 (2003) 267-274.

[21] K. Majewska-Nowak, M. Kabsch-Korbutowicz, and T. Winnicki, "The effect of gas bubble flow on ultrafiltration efficiency, Desalination 126 (1999) 187-192.

[22] R. Ghosh, and Z. Cui, Mass transfer in gas-sparged ultrafiltration: upward slug flow in tubular membranes, J. Membr. Sci., 162 (1999) 91-102.

[23] T. Cheng, Influence of inclination on gas-sparged cross-flow ultrafiltration through an inorganic tubular membrane, J. Membr. Sci., 196 (2002) 103-110.

[24] L. Vera, S. Delgado, and D. Elmaleh, Gas sparged cross-flow microfiltration of biologically treated wastewater, Water Science and Technology, Vol. 41, No 10 (2000) 173-180.

[25] C. Psoch and S. Schiewer, Long-term trial of intermittent air sparging for fouling reduction in a MBR, J. Membr. Sci., submitted for publication.

[26] J. Shim, I. Yoo, and Y. Lee, Design and operation considerations for wastewater treatment using a flat submerged membrane bioreactor, Process Biochemistry, 38 (2002) 279-285.

[27] C. Psoch and S. Schiewer, Flux improvement in a MBR by air sparging in sidestream, Water Research, submitted for publication.

[28] H. Baehr, and K. Stephan, Wärme und Stoffübertragung, Springer-Verlag (1994), Berlin, 1st edition, ISBN: 3-540-55086-0.

4 Anti-fouling application of air sparging and backflushing for MBR[3]

C. Psoch,[1] and S. Schiewer[2*]

[1] Water & Environmental Research Center, University of Alaska Fairbanks, P.O. Box 750725, Fairbanks, AK 99775, USA, Phone (907) 474-6234; Fax (907) 474-7979; email: ftcp@uaf.edu

[2*]Department of Civil & Environmental Engineering, University of Alaska Fairbanks, Duckering Building, P.O. Box 755900, Fairbanks, AK 99775-5900, USA; email: ffsos@uaf.edu

Abstract

In membrane processes, fouling remains the main drawback and the toughest challenge at present and in the foreseeable future. The aim of this work was to combine anti fouling strategies. In a membrane bioreactor (MBR) fed with synthetic wastewater, the clear/wastewater separation took place through a tubular membrane in side stream. For longer sustainable flux, air sparging was supplied to fight external fouling with the scouring effect of slug flow. Additional to that, backflushing was provided as a technique against internal fouling. The combination of both techniques showed very promising results in a range from 3 to 9 g/L mixed liquor suspended solids (MLSS). The combination of air sparging and backflushing is superior to the operation of only one flux enhancement technique and yields about 3 times higher

[3] Water Research, Elsevier (to be submitted) 2005

fluxes compared to the NON-enhanced application after continuous filtration for 8 days. Minimal backflush pressures reduce the product loss due to backflushing while accomplishing significant flux increases.

Keywords: Air sparging, minimal backflushing, external & internal fouling, MBR, synthetic wastewater

4.1 Introduction

The permanent operation of membrane plants requires careful management of membrane fouling, which remains a major drawback of the membrane technology. Several models are utilized to describe fouling and subdivide it into different components (Cheryan, 1998) such as external and internal fouling, suggested by *Wakemann and Williams* (2002).

Several approaches exist to mitigate the inevitable. For external fouling, gas sparging can be an efficient application to reduce fouling (Bellara et al., 1996) In the case of tubular membranes as in this study, gas is injected into the membrane with the feed stream to generate a gas liquid two-phase flow, leading to higher shear stress near the membrane surface (Cabassud et al., 2003). If liquid and gas flow together in a pipe, depending on the ratio of gas and liquid mass flow and the inclination of the tube, different flow regimes can develop (Levy, 1999). The flow pattern with the most significant impact on the wall shear stress and on the flux rates is "Slug-flow".

Water and gas slugs fight cake layer build up with different intensities, depending on the flow velocity. Additionally, a water film flows parallel to the gas slugs, which is actually counter current in upward filtration (Cabassud et al., 1997). Gas and liquid slugs cause different Reynolds-numbers and different turbulence patterns (Verberk et al., 2002), which influence the concentration polarization layer strongly. However, the most severe turbulence phenomena occur within the wake zone of the gas slugs, where smaller gas bubbles are moving in the trail of the gas slugs in heavily turbulent vortexes (Gosh and Cui, 1997; Taha and Cui, 2002). These turbulent movements, combined with small gas bubbles, partially dislocate and remove cell debris and particles, which are accumulated on the feed side of clogged pore channels. The primary objective of air sparging is to affect the cake layer and the first sections of the membrane pores on the feed side (external fouling). The cake layer consists of a gel layer with a concentration polarisation on top of it (Mulder, 1996). For wastewater applications, an improved aeration can be observed, if the chosen gas is air, which is subsequently called air sparging (AS).

Another anti-fouling technique is backflushing (BF). Backflushing pushes clear water, for instance permeate, back into the feed stream and is applied to minimize pore blockage (internal fouling) in the deeper layers of the membrane and channel clogging near the membrane surface. Its influence decreases with growing layer thickness, due to pressure drop and velocity loss. A disadvantage of backflushing is product loss, which can severely decrease the recovery rate at higher flow volumes in reverse direction.

The objective of this investigation was to compare both methods of fouling reduction in a pilot scale membrane bioreactor fed with synthetic wastewater (Cicek et al., 1998). The glucose based synthetic wastewater was anticipated to lead to high fouling propensity for longer time periods (Le-Clech, 2003a). Comparably high MLSS values yield non-Newtonian behaviour for wastewater at low shear rates (Le-Clech, 2003b), as encountered near the membrane surface, and decrease the flux significantly, so that synergistic effects of AS and BF are particularly noticeable.

While each of these techniques has shown promise in fouling reduction, their combination, air sparging focuses on external fouling and backflushing addresses internal fouling, has not yet been investigated extensively. Moreover, very few studies besides *Chang and Judd* (2002) report observation periods of more than 24 hours for air sparging. Consequently a need for long-term studies exists, as pointed out in a review by *Al-Bastaki and Abbas* (2001).

With the help of dimensionless numbers, derived from non air sparged processes and extended to air sparged applications, according to *Vera et al.* (2000a, b), the data was analysed and interpreted.

4.2 Materials and methods

For the experimental setup, as shown in Fig. 4.1., an activated sludge tank with 60 - 80 liters was used. The wastewater, respectively the activated sludge, was pumped with a multistage pump (Grundfos) through braided hoses of ½ inch

diameters to the membranes and back to the bioreactor. With a thermostat the reactor temperature was maintained at a temperature of 15°C, which is typical for municipal wastewater.

The majority of the experiments were carried out with a single membrane. This module was utilized throughout all experiments and was featured with an air sparging system: On each side of the module, a 15 cm long acrylic rod extended the membrane tubes. The acrylic extensions with drill holes in the same diameter as the membrane tubes served for the air supply and for observation of the flow pattern in the unit. Each tube features its own connection to the air supply, with separately adjustable air volume stream. The air volume stream was monitored by a flow meter and pressure gauge. The air pressure was between 245 kPa at an aeration rate of 8 L/min and 285 kPa at an aeration rate of 15 L/min. Fluctuation of the airflow was prevented by a mass flow meter.

Later the experimental setup was extended to three membrane modules that were deployed in parallel. Each polymer membrane (Microdyn-Nadir) has a length of 0.75 m and a pore size of 0.2 μm. The modules were made of three tubes each with a channel diameter of 5.5 mm, yielding a membrane surface area of 0.036 m^2 per module.

Flow velocities of the water within the membrane tubes were about 1.5 m/s. The flow pattern was observed with a stroboscope. Observations with the naked eye were impossible. With flow velocities exceeding 1 m/s, monitoring of the flow pattern in the system was a challenge. The application of a stroboscope brings some remedy,

but the flow patterns varied too rapidly to obtain good photographs with a conventional camera.

The pump speed and thus the pressure for the backflush pump (submerged pump, MP1, Grundfos) were regulated over a variable frequency drive. The backflush pressure applied was 250 kPa throughout the whole set of experiments. The experiments were carried out with the lowest backflush pressure possible, 35 to 45 kPa above the transmembrane pressure (TMP), to minimize the product loss.

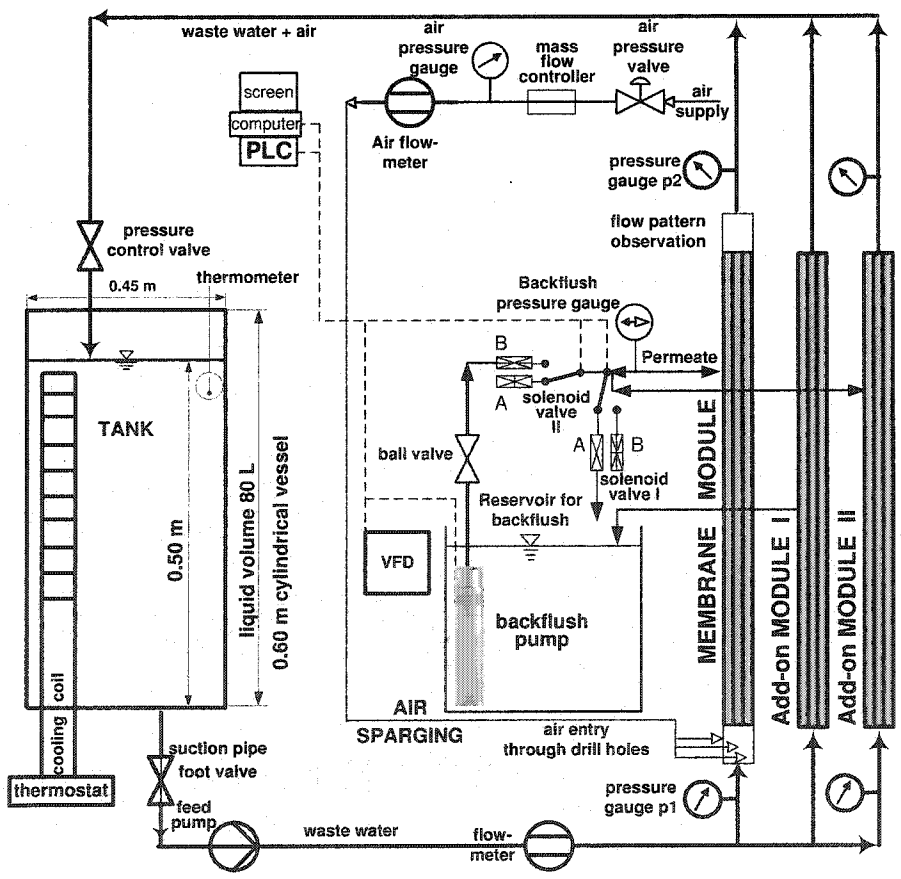

Fig. 4.1. Experimental setup scheme with activated sludge tank and three membranes in parallel

With a programmable logic controller connected to a personal computer with additional software, the backflush cycle was regulated and two solenoid valves (solenoid valve I and II) were opened and shut alternatively to allow a reversal of the normal flow direction within the membrane. The backflush procedure superimposed the continuously running air sparging every 30 minutes for 15 seconds.

Synthetic wastewater was prepared as described in *Psoch and Schiewer* (2004). The main carbon and energy source for the microbes in the reactor was supplied by a dosage of 20 - 60 g glucose per day, depending on the MLSS content in the reactor, determined according to the *Standard Methods* (APHA, 1995). In addition to that, a mixture of synthetic wastewater was fed to supply trace elements and different sources of carbon, nitrogen and phosphorus for sustainable microbial growth. The MLSS was developing from about 3 g/L at the first data series with wastewater to about 9.5 g/L at the end of the investigations.

Within this study, each data set was based on membrane operation for 8 days under approximately constant conditions. Prior to a new data set, a chemical cleaning of the membrane was conducted to achieve largely the same initial conditions at each test series. The cleaning was accomplished by soaking the membrane in hot NaOH at about 60°C from the permeate side for an hour, followed by an intensive flush with deionised water for 4 hours.

At first, ten test series were performed with only one module, which was equipped with air sparging. Out of these ten experiments, two were carried out with wastewater without flux enhancement (NON) and eight with a combination of AS

and BF. Afterwards, three new membrane modules were installed in parallel. This allowed a direct comparison of the fluxes for one module with only air sparging, one with only backflushing and one without any flux enhancement technique.

4.3 Results and discussion

At first, clear water tests were performed for 11.4 days. Within this time the flux decreased from more than 1000 L/(m² h) to 8.5 L/(m² h), below the initial value of wastewater flux after chemical cleaning.

After the clear water tests, wastewater at an MLSS content of 3 g/L was filtered without any flux enhancement techniques for 8 days to serve as a baseline for subsequent investigations. Next a combination of AS and BF was applied. Even at significantly higher MLSS contents compared to the reference values, the combination of AS and BF achieved higher fluxes in any case. The air injection ratio ε (see eq. 4.1) was varied for each test series and the MLSS increased gradually with time.

$$\varepsilon = \frac{u_{Gas}}{(u_{Gas} + u_{Liquid})} \qquad \text{eq. 4.1}$$

with:

ε = void fraction [-]

u_{Gas} = superficial gas velocity, i.e. velocity if only gas was in the channel [m/s]

u_{Liquid} = superficial liquid velocity, i.e. velocity if only liquid was in the channel [m/s]

Towards the end of the study, when the MLSS reached about 8.5 g/L, another reference test without any enhancement technique was conducted. Fig. 4.2 and 4.3 show the results for the reference tests compared to the enhanced filtration.

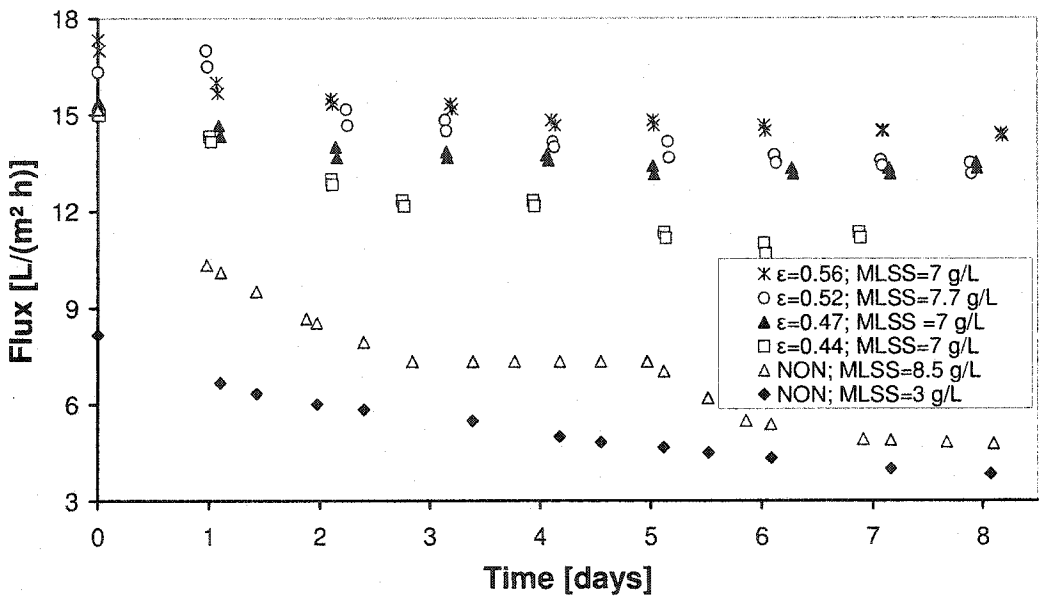

Fig. 4.2. Comparison of flux with NON-enhancement to combination of air sparging (AS) and backflushing (BF) at different air injection ratios

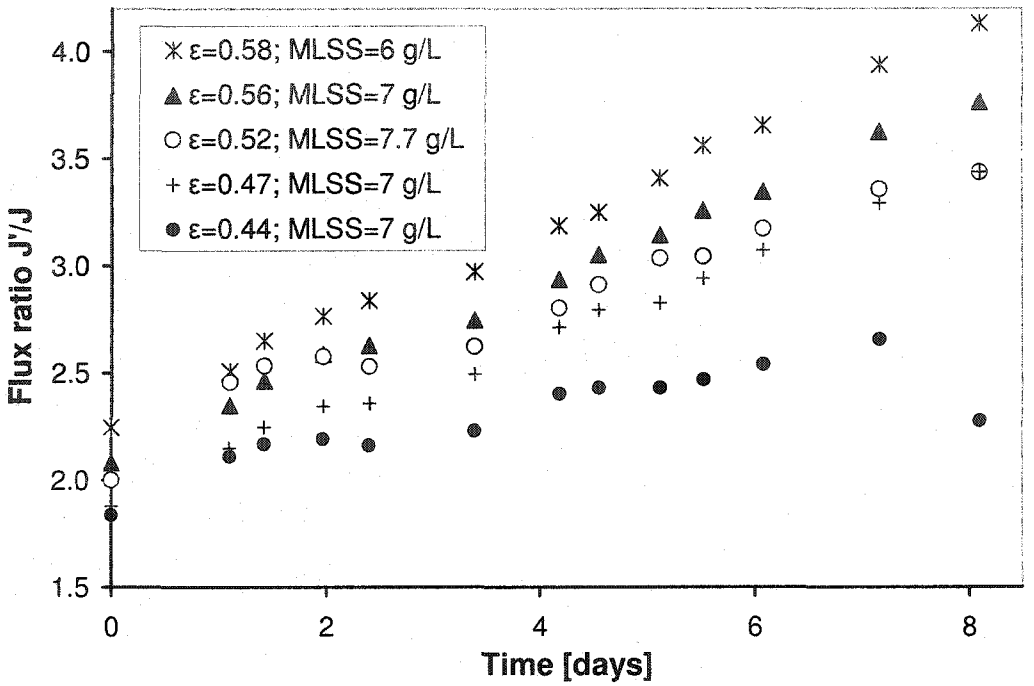

Fig. 4.3. Flux ratios J'/J (between enhanced flux J' and NON-enhanced flux J) for a combination of AS and BF at different air injection ratios

The initial flux for the wastewater tests at 3 g/L MLSS content without any enhancement (NON) was lower than the initial flux for all other tests. That can be explained by existing biofilms (Flemming, 1995), which were organoleptic, identified in the tank after 11 days of clear water filtration and were assumed to be present on the membrane surface as well. The initial flux for the wastewater of 8.5 g/L without enhancement (NON) started as all other tests, immediately after a chemical cleaning according to the standard procedure, but dropped within 8 days to about the same values as the wastewater flux at 3 g/L MLSS, which confirms the flux results for the reference value especially for the end of the test series after 8 days.

Fig. 4.2. shows that within the generated slug flow regime (slug flow exists between $0.25 < \varepsilon < 0.9$, (Vera, 2000b) increasing air injection ratios achieve higher fluxes if all other parameters remain approximately constant.

Fig. 4.3 shows the flux ratio J'/J. That is the quotient between enhanced flux J' (at approximately constant MLSS) and NON-enhanced flux J. The NON-enhanced flux represents the results of wastewater filtration with 3 g/L MLSS. The ratios compare the flux results achieved after the same period of wastewater filtration. The enhanced flux is significantly increased up to 4 times compared to the conventional wastewater filtration after 8 days when the air injection ratio ε rises up to 0.58.

Fig. 4.4 and 4.5 depict the flux ratios related to the MLSS in the MBR. Fig. 4.4 shows how the flux ratio increases, if the air injection ratio stays constant and the sludge gets thicker indicated by higher MLSS values. At higher solid content in the wastewater, the efficient deployment of the synergistic effects of AS and BF is clearly more emphasized. After 8 days a flux ratio between about 3.5 (at 7 g/L MLSS) and 2.7 (at 4.6 g/L MLSS) was obtained.

Fig. 4.5 shows that the flux ratio significantly increases with rising air injection ratios both for high (approximately 7 g/L) and low (approximately 5 g/L) sludge concentrations. At high sludge concentrations the advantages of the air sparging were most pronounced. High air injection ratios within the slug flow regime and high MLSS give the best flux ratios if all other parameters remain approximately constant.

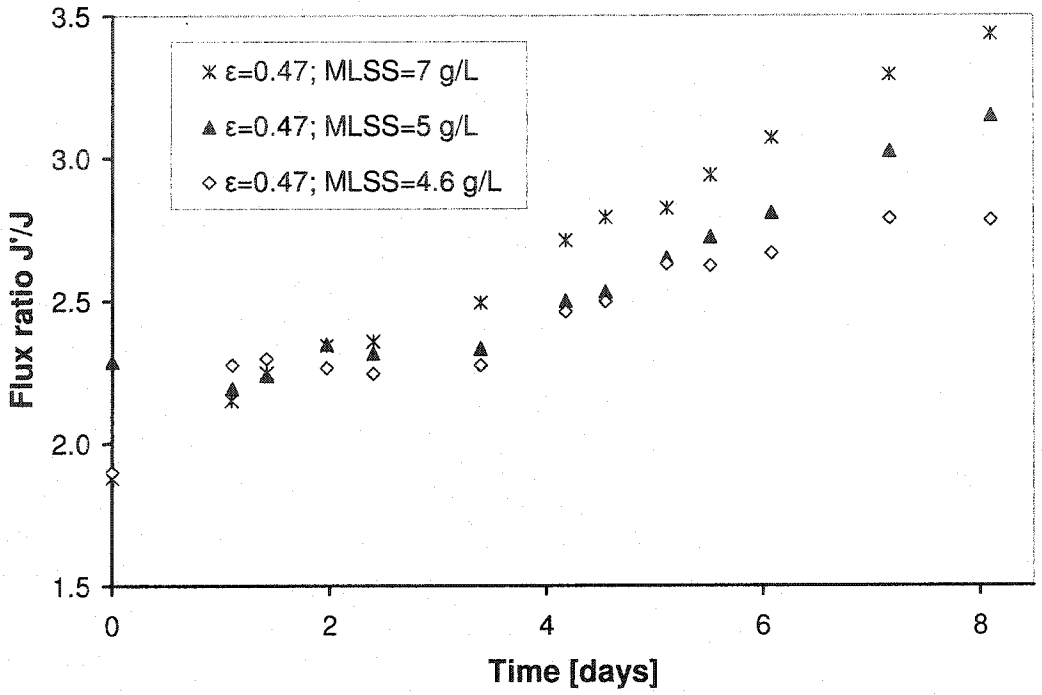

Fig. 4.4. Flux ratios for combination of air sparging and backflushing at constant air injection ratio and increasing MLSS

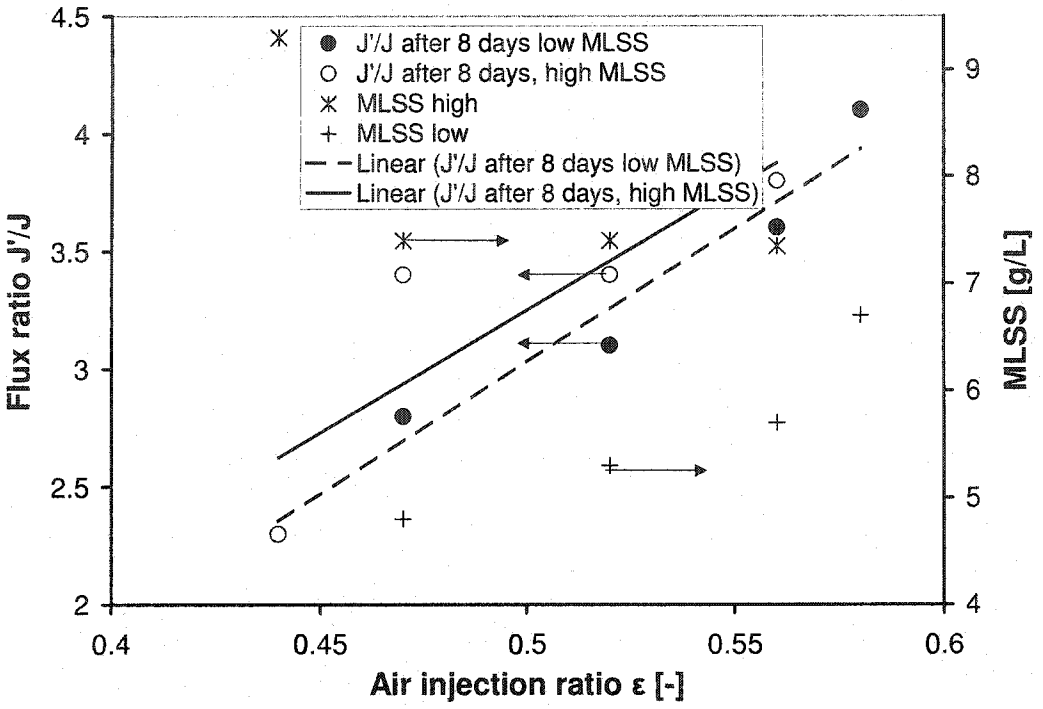

Fig. 4.5. Flux ratio trends at different air injection ratios and changing MLSS content in the MBR

In Fig. 4.6 the dimensionless Fouling number is plotted against the dimensionless Shear stress number. According to *Vera et al.* (2000c) both variables are calculated, as described below. For the Shear stress number N_s [-] equation 4.2 applies:

$$N_S = \frac{\rho_{Liquid} * u^2_{Liquid}}{TMP} \qquad \text{eq. 4.2}$$

with:

ρ_{Liquid} = liquid density [kg/m³]

TMP = transmembrane pressure [Pa]

This equation applies for single phase flow, as for the NON-enhanced wastewater filtration. If air sparging is supplied, density and velocity have to be modified in this equation to represent two-phase flow conditions and eq. 4.3 applies, where the mixture density $\rho_{mixture}$, according to eq. 4.4, is used in place of the liquid density, with ρ_{Gas} as the gas density [kg/m³]. The mixture velocity $u_{mixture}$ is calculated according to eq. 4.5.

$$N_S = \frac{\rho_{mixture} * u_{mixture}^2}{TMP} \qquad \text{eq. 4.3}$$

with:

$$\rho_{mixture} = \frac{\rho_{Liquid} * u_{Liquid} + \rho_{Gas} * u_{Gas}}{u_{mixture}} \qquad \text{eq. 4.4}$$

$$u_{mixture} = u_{Gas} + u_{Liquid} \qquad \text{eq. 4.5}$$

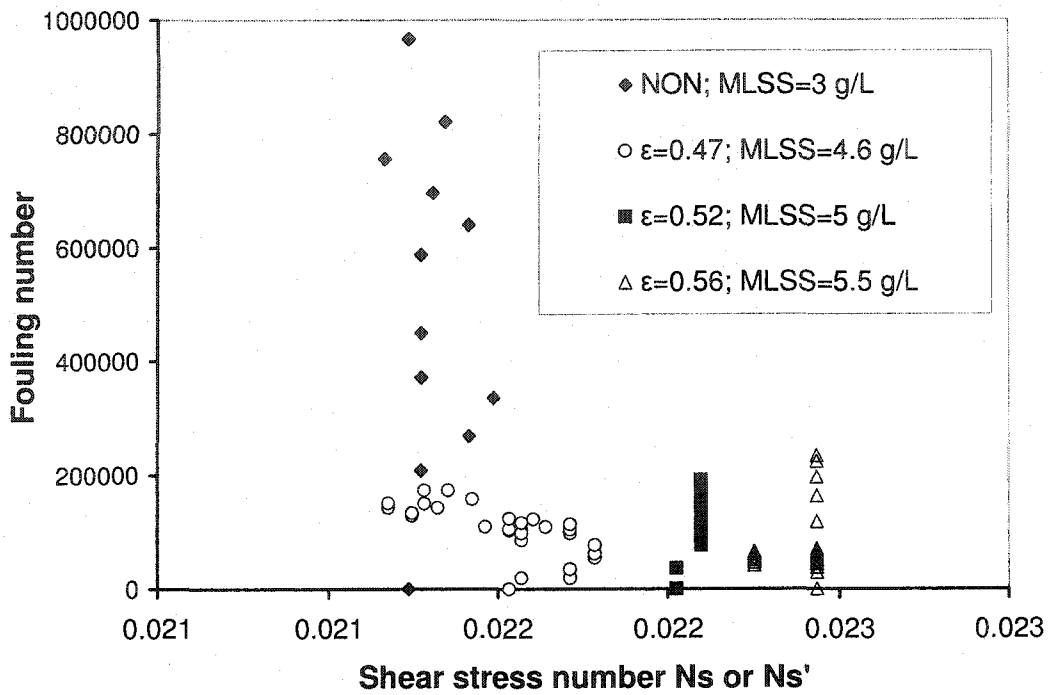

Fig. 4.6. Influence of Shear stress number and air injection ratio on the Fouling number at comparable low MLSS values

For the Fouling number N_F [-] eq. 4.6 applies:

$$N_F = u_{Liquid} * \left(\frac{1}{J} - \frac{1}{J_0} \right) \qquad \text{eq. 4.6}$$

with:

J = flux at any time t > zero [$m^3/(m^2\ s)$]

J_0 = initial flux at time t = zero [$m^3/(m^2\ s)$]

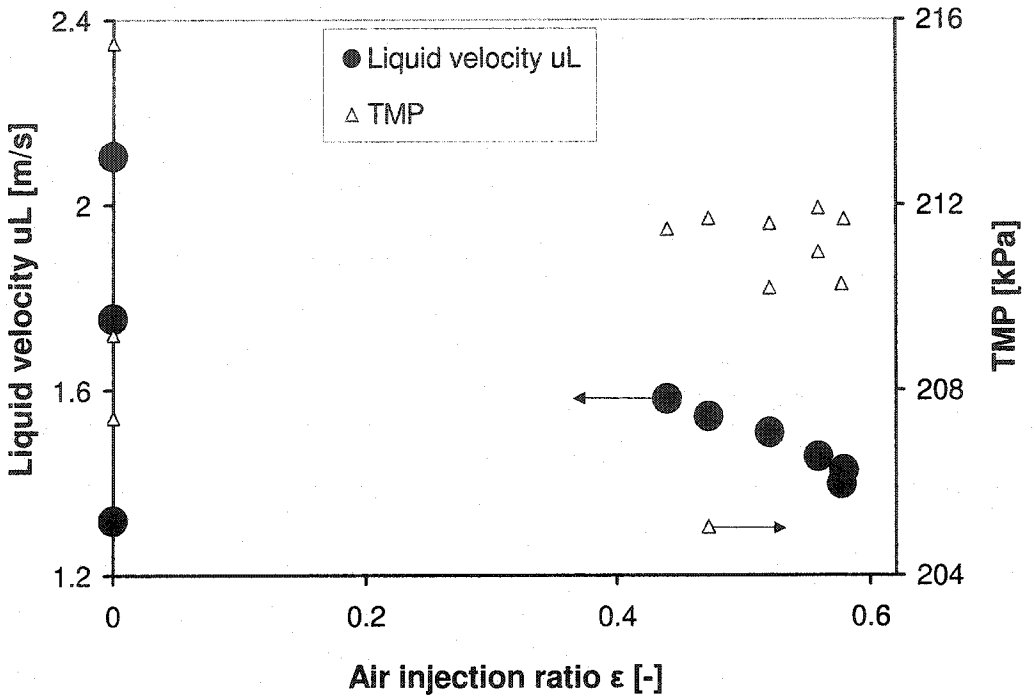

Fig. 4.7. Liquid velocity u_L as a function of air injection ratio ε at largely constant TMP

Fig. 4.6 shows that the shear stress number increases with higher air injection ratios. The Fouling number for NON-enhanced filtration at 3 g/L MLSS increases over one order of magnitude within 8 days, even though the liquid velocity was at 2.1 m/s, significantly higher than in the air sparged trials, which supports less flux decrease due to higher critical flux values (see Fig. 4.7). For the air sparged tests the Fouling number rises up to about 200000 (Fig. 4.6) but does not significantly change at higher air injection ratios since the latter are compensated by higher MLSS and lower liquid velocities (Fig. 4.7). Higher shear stress counteracts flux decrease.

In Fig. 4.7 the average values of the liquid velocity and transmembrane pressure of all test series are plotted versus the air injection ratio. The NON air sparged tests were carried out at 1.31; 1.75 and 2.10 m/s. They show a range in TMP between 207 and 215.5 kPa. The air sparged trials show that with increasing air injection ratio the liquid velocity decreased, nevertheless the average TMP remained fairly constant between 205 and 212 kPa. For the air injection ratios 0.47; 0.52; 0.56 and 0.58 the trials were performed twice at different sludge concentrations with comparable TMP.

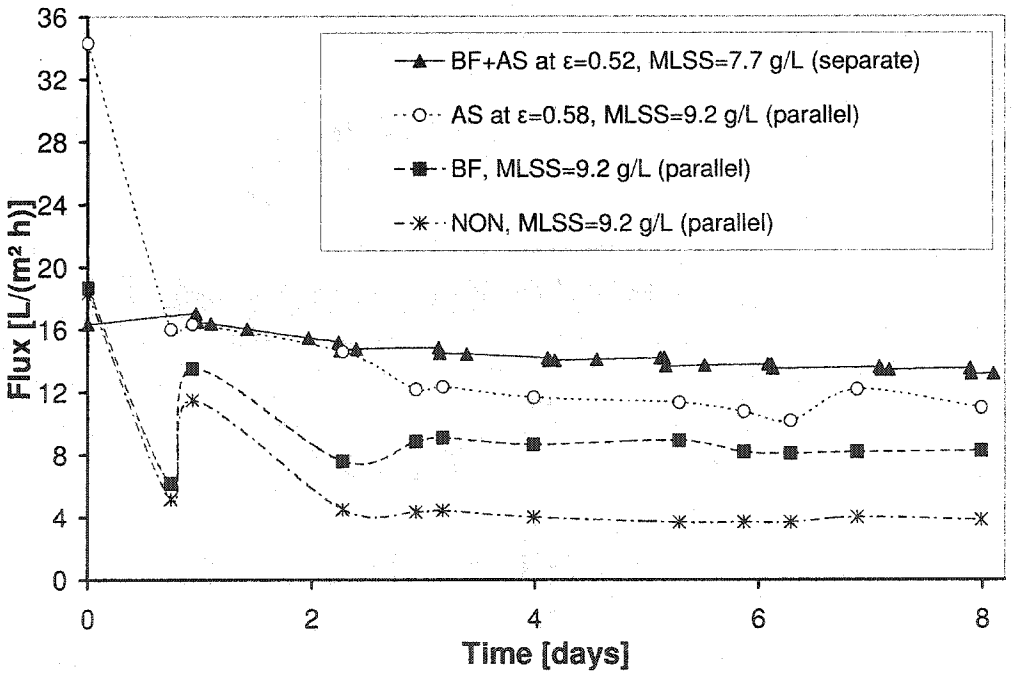

Fig. 4.8. Comparison of NON-enhanced flux to air sparging, backflushing and combination of backflushing and air sparging

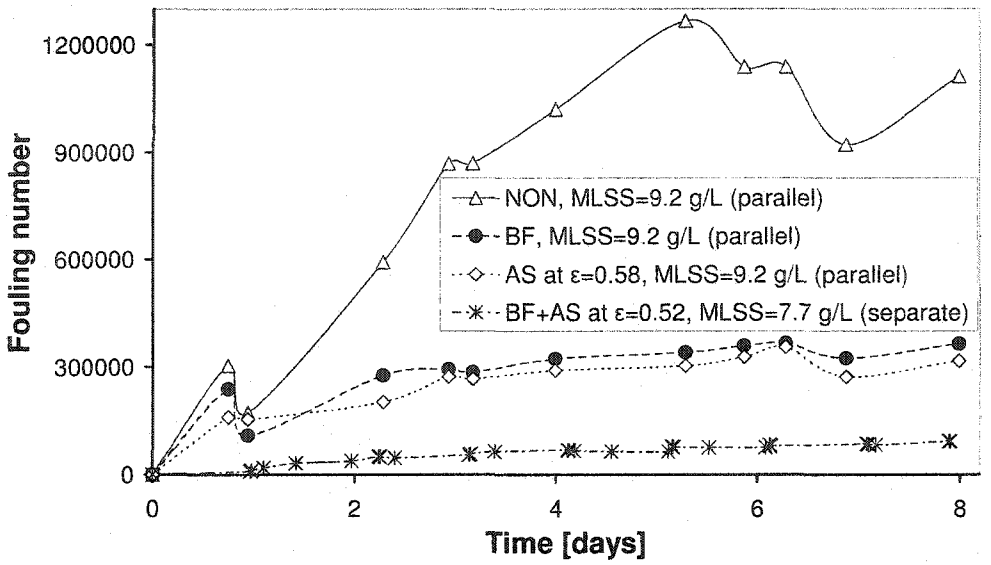

Fig. 4.9. Increase of Fouling number vs time for NON-enhanced filtration, AS filtration, BF filtration and a combination of AS and BF

Fig. 4.8 shows the flux decrease within 8 days for the last test series, which featured parallel operation of three modules (NON & AS & BF). Thus NON-enhanced, only AS, and only BF enhanced filtration could be compared under exactly the same conditions. In addition to these three, the results of an AS+BF combination are depicted that was most comparable to the high MLSS values from the parallel trials. The flux at day 8 was about double for BF compared to the NON series. This was achieved with minimal BF pressure and product loss of about 3%. AS improved the flux by a factor of about 3 at day 8. The strong flux decrease in the BF and NON curve after about 1 day is related to the malfunction of a pressure adjustment valve, which decreased the cross flow velocity down to 0.6 m/s (reduction by about 50%). The flux quickly recovered from this event. However, the combination of AS and BF

shows the strongest performance. A lower air injection rate, as for the AS only application, might be compensated by lower sludge concentration.

In Fig. 4.9 the same data sets as in Fig. 4.8 are compared. A gradual increase of the Fouling number over the period of 8 days can be observed. Without enhancement the Fouling number is about 3.5 times higher than the Fouling number of only AS or only BF. AS yields a little more favourable results than BF, but in a similar range. Nevertheless the combination of AS and BF shows again superior performance with Fouling numbers of less than 10% compared to the NON-enhanced filtration and only 25% of the value for only BF or only AS.

4.4 Conclusions

For the purpose of maintaining more sustainable fluxes, the combination of AS and BF shows very promising results in a membrane bioreactor for MLSS contents between 4 and 9.2 g/L over a time period of 8 days. The synergistic effects of AS to fight external fouling and BF to fight internal fouling are more emphasized at higher sludge concentrations. Within the slug flow regime higher air injection ratios of 0.58 show better results than lower air injection ratios of 0.44. BF can double the flux already with minimal BF pressures of 45 kPa and a product loss of only 3% due to BF.

Acknowledgements

Special gratitude to the Grundfos company which supported our study with two multistage pumps and further equipment and to the Microdyn-Nadir company which donated the membrane modules. We acknowledge funding of this project through a grant from the USGS/NIWR.

4.5 References

Al-Bastaki N. and Abbas A. (2001). Use of fluid instabilities to enhance membrane performance: a review. Desalination 136, 255-262

Bellara S., Cui Z. and Pepper D. (1996). Gas sparging to enhance permeate flux in ultrafiltration using hollow fiber membranes. J. Membr. Sci., 121, 175-184

Cabassud C., Ducom G. and Laborie S. (2003). Measurement and comparison of wall shear stresses in a gas/liquid two-phase flow for two module configurations. Conference proceedings IMSTEC'03 Sydney, paper 163 pp. 6

Cabassud C., Laborie S. and Laine J. M. (1997). How slug flow can improve ultrafiltration flux in organic hollow fibres. J. Membr. Sci. 128, 93-101

Chang I. and Judd S. (2002). Air sparging of a submerged MBR for municipal wastewater treatment. Process Biochemistry, 37, 915-920

Cheryan M. (1998). Ultrafiltration and Microfiltration Handbook. Technomic Publishing Co. Inc. Lancaster, Basel, ISBN: 1-56676-598-6

Cicek N., Winnen H., Makram T. S., Wrenn B. E., Urbain V. and Manem J. (1998). Effectiveness of the Membrane Bioreactor in the biodegradation of high molecular weight compounds. Water Research, Vol. 32, No. 5, 1553-1563

Flemming, H.-C. (1995). Biofouling be Membranprozessen. Springer Verlag Berlin/Heidelberg, ISBN: 3-540-58596-6

Ghosh R. and Cui Z. (1999). Mass transfer in gas-sparged ultrafiltration: upward slug flow in tubular membranes. J. Membr. Sci., 162, 91-102

Le-Clech P., Jefferson, B., Chang, I. and Judd, S. (2003). Critical flux determination by the flux-step method in a submerged membrane bioreactor. J. Memb. Sci. 227, 1-2, 81-93

Le-Clech P., Alvarez–Vazquez H., Jefferson B. and Judd S. (2003). Fluid hydrodynamics in submerged and sidestream membrane bioreactors. Wat. Sci. Tech. 48 (3) 113-119

Levy S. (1999). Two-Phase Flow in Complex Systems. Interscience Publication, John Wiley & Sons, Inc., New York, ISBN: 0471329673

Mulder M. (1996). Basic Principles of Membrane Technology. Kluwer Academic Publishers Dordrecht/Boston/London second edition, ISBN: 0-7923-4247-X

Psoch C. and Schiewer S. (2005). Synthetic wastewater treatment and fouling control in a temporary air sparged MBR. Water Research (in preparation)

Standard Methods for the Examination of Water and Wastewater, (1995) 19th edn, A P H A/American Water Works Association/Water Environment Fed., Washington DC, USA

Taha T. and Cui T. (2002). CFD modelling of gas-sparged ultrafiltration in tubular membranes. J. Membr. Sci., 210, 13 – 27

Vera L., Delgado S. and Elmaleh S. (2000). Gas sparged cross-flow microfiltration of biologically treated wastewater. Wat. Sci. Tech. 41(10), 173-180

Vera L., Delgado S. and Elmaleh S., (2000). Dimensionless numbers for the steady-state flux of cross-flow microfiltration and ultrafiltration with gas sparging. Chemical Engineering Science 55, 3419-3428

Vera L., Villarroel R., Delgado S. and Elmaleh S. (2000). Enhancing microfiltration through an inorganic tubular membrane by gas sparging. J. Membr. Sci., 165, 47-57

Verberk J., Hoogeveen P., Futselaar H. and van Dijk J. (2002). Hydraulic distribution of water and air over a membrane module using AirFlush. Wat. Sci. Tech.: Wat. Supply 2(2), 297-304

Wakemann R. and Williams C. (2002). Additional techniques to improve microfiltration. Separation and Purification Technology, 26, 3-18

5 Long term investigation of aeration and flux improvement by air sparging and backflushing for a membrane bioreactor[4]

C. Psoch and S. Schiewer*

Department of Civil & Environmental Engineering; Water & Environmental Research Center, University of Alaska Fairbanks, AK 99775; USA; email: ffsos@uaf.edu

Abstract

Fouling remains a major issue for all membrane applications. This study investigated anti-fouling applications for a side-stream membrane bioreactor (MBR) fed with glucose-based synthetic wastewater. Air sparging, backflushing and high cross flow velocity (CFV) were investigated as anti-fouling strategies. It has been shown that air sparging used as the sole means of MBR aeration does not impair degradation performance. For better comparison of longer test runs, an equation to model effects of MLSS and temperature on viscosity was developed. This study showed that for backflushing with a CFV of 5.2 m/s, the yield is about 3.2 times higher than that for for air sparging with CFV of 2 m/s. Long term investigations of combined air sparging and backflushing compared to conventional membrane filtration at equal CFVs of 2 m/s show 4.5 times higher yield. The long term enhanced permeability decline can be estimated by a $t^{-0.25}$ function.

[4] Water Research, Elsevier (to be submitted) 2005

Key words: water flux, viscosity, chemical cleaning, air sparging, backflushing

5.1 Introduction

Current legislation generally requires an activated sludge process as a major component of a wastewater treatment process. Demands for effluents to meet increasingly higher standards is driving optimization of the conventional activated sludge process, which is commonly comprised of a bioreactor and a subsequent clarification process (*Kraume et al.*, 2004). An alternative, intensified technology is available with the membrane bioreactor (MBR), which implants the sludge separation process into the bioreactor (*Le Clech*, 2002).

Due to more economical membrane production, use of and research about MBRs has grown since the early eighties (*Stephenson et al.*, 2000). The introduction of the submerged MBR configuration by *Yamamoto et al.* (1989) has led to a significant market penetration within the last 15 years. Nevertheless, utilization of membranes has its drawbacks and limitations; they are subject to declining flux with ongoing operation time due to fouling. The necessary measures to overcome fouling effects are expensive and only partially successful. In MBR fouling occurrence is especially relevant, since the membrane faces particularly hard conditions with high concentrations of biological suspensions, including colloids and extracellular polymeric substances (EPS) (*Judd,* 2004). The occurrence of EPS particularly is

widely recognized as a key foulant in membrane-related wastewater treatment (*Chang_et al.* 2002).

Major research efforts have been undertaken in the past to tackle the disadvantages that accompany membrane application. However, most studies have focused on the feasibility of improvement methods, but rarely investigated how these measures perform over longer time periods. Thus *Al-Bastaki and Abbas* (2001) pointed out that long-term investigations are necessary to verify findings indicated in short-term experiments.

For more than 10 years, researchers have recognized that air sparging offers an opportunity to enhance membrane flux for in-out and out-in filtration (*Cui and Wright,* 1994). Several authors have proved the efficacy of the technique in short term experiments (*Bellara et al.,* 1996; *Vera et al.,* 2000; *Pospisil et al.,* 2004). The aim of this project was to investigate the long-term behavior of air-sparged membrane filtration in an MBR and to compare the combination of air sparging and backflushing with non-enhanced filtration.

5.2 Materials and methods

For the experimental setup of the membrane bioreactor (MBR), an activated sludge tank with a capacity of 60 - 80 liters was used (see Fig. 1.). A multistage pump (Grundfos) moved the activated sludge through the membranes and back to the bioreactor. A thermostat maintained reactor temperature between 14 and 24°C.

The experiments were carried out with two vertical membrane modules, which were deployed in parallel. Each module (Microdyn-Nadir) consisted of three polypropylene capillary membranes (pore size 0.2 μm) in a plastic housing of 0.75 m length. The diameter of the tubes was 5.5 mm, yielding a membrane surface area of 0.036 m^2 per module.

One module (see Fig. 5.1., "membrane module") featured an air sparging system: On each end of the module, an acrylic rod, 15 cm in length, extended the membrane tube. On one side (the lower), three perpendicular drilled entries served for air supply to each tube. Each air supply included its own adjustable air valve. The total air volume stream was monitored by a volume flow meter, a mass flow meter, and a pressure gauge. The air pressure was 60 - 70 kPa above the transmembrane pressure (TMP) within the membrane to ensure enough air was pushed into the system. Fluctuation of airflow was prevented by the mass flow meter. On the other side (the upper), the acrylic rod served as a viewing area for flow pattern observation.

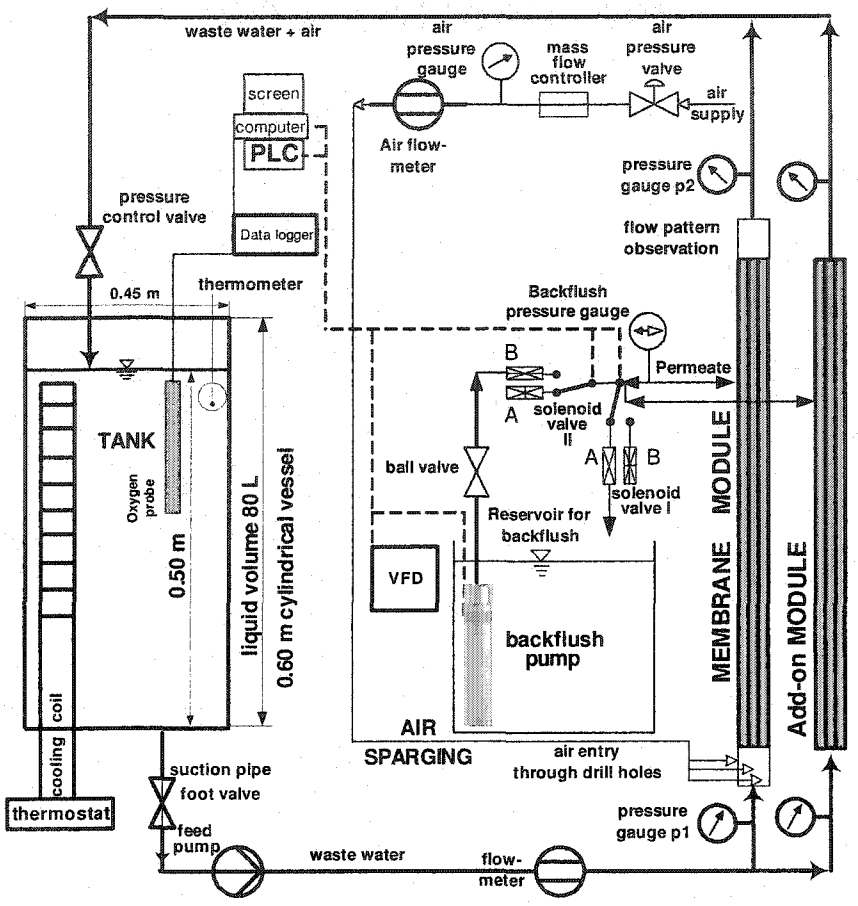

Fig. 5.1. Experimental setup of the membrane bioreactor (MBR).

If a two-phase flow is generated, several flow patterns may develop based on the liquid/gas volume flow ratio and the inclination of the pipe (*Levy,* 1999). The optimal flow regime as applied in these experiments, where the goal is to achieve the highest mass transfer rate, is the slug flow regime as depicted in Fig. 5.2, which shows the typical bubble train (*Cabassud et al.,* 1997).

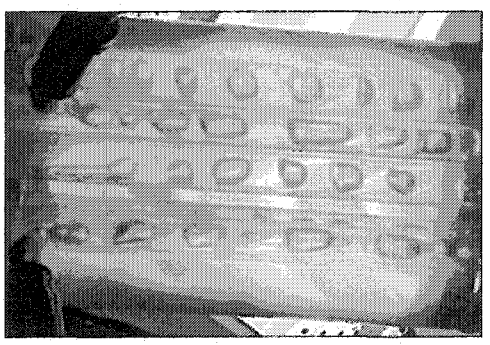

Fig. 5.2. Air sparging slug flow pattern during clear water test.

Both modules (as shown in Fig. 5.1) were equipped for backflushing. Applied TMP was between 98 and 200 kPa (1-2 bar) for each module. Cross flow velocities (CFV) of the water within the membrane tubes were between 2 and 5.2 m/s. For the module with acrylic extenders, the flow pattern was observed with a stroboscope; observations with the naked eye were impossible.

The pump speed -- and thus the pressure for the backflush pump (submerged pump, MP1, Grundfos) -- were regulated over a variable frequency drive. The experiments were carried out with a low backflush pressure of about 60 kPa (ca. 0.6 bar) above the transmembrane pressure (TMP), to minimize product loss.

With a programmable logic controller (PLC) connected to a personal computer, the backflush cycle was activated every 30 minutes for 15 seconds, and two solenoid valves (solenoid valves I and II in Fig. 5.1) were opened and shut alternatively to allow reversal of the normal flow direction within the membrane. When the membrane module was operated with air sparging and backflushing, the backflush procedure was superimposed over the continuously running air sparging.

Activated sludge was produced by inoculation of a feed solution with microbial cultures from the local wastewater treatment plant. Synthetic wastewater feed based on glucose was supplied for growth and maintenance of the microbial population in the membrane bioreactor. This feed contained high concentrations of the three major elements as Carbon (C), Nitrogen (N) and Phosphorus (P) and trace substances in minor concentrations. For more details on the recipe for the synthetic wastewater see *Psoch and Schiewer* (2005a).

The activated sludge content in the reactor, measured as mixed liquor suspended solids (MLSS), was regularly determined according to the *Standard Methods* (1995). The sludge retention time was maintained at 35 days by withdrawing about 2 liters of sludge every day.

Prior to each test run, chemical cleaning of the membranes was conducted to achieve similar initial conditions for each test series. The cleaning was accomplished by soaking the membranes, from the permeate side, in NaOH at about 60°C for an hour, followed by intensive flushing with de-ionized water for about 4 hours. However, one of the membranes had been used for a former test series; it was in service for up to 6 months, including multiple cleaning cycles. Due to very hard local tap water, which leads to scaling, the NaOH treatment was no longer sufficient after several cleaning cycles. Poor performance of the NaOH treatment for this membrane was indicated by a significant increase (factor 5-8) in the necessary soaking time for the NaOH and, further, by comparably low and decreasing initial fluxes. Because caustic cleaners fight mainly organic membrane foulants (*Cheryan,* 1998), a

combination of caustic and acid treatment was subsequently tested and brought remedy. When the NaOH application was preceded by treatment with a hot (about 60°C) blend of phosphoric and citric acid (ratio 1:4 at pH 1.4), very good cleaning results could be re-established.

The chemical composition of the feed and degradation performance of the reactor were monitored during startup and under stable operation conditions by means of HACH cuvette tests, using a HACH spectrophotometer (model DR/2010) and a HACH COD reactor.

5.3 Results and discussion

5.3.1 Chemical analysis and degradation performance

The original intention was to generate a feed fairly close to the average inlet concentration of American wastewater treatment plants as described by *Metcalf & Eddy* (1991). However, due to the low volumes of feed added daily to the reactor at startup, it was impossible to achieve the higher mixed liquor suspended solids (MLSS) concentrations typical for MBR reactors. Therefore higher feed concentrations were later used in order to supply sufficient substrate for the microbial biomass production. As Fig. 5.3 shows, the feed substrate concentration was doubled after 19 days. As a result of higher substrate concentration, the biomass production as expressed by the MLSS concentration was raised from about 2 g/L initially up to 16 g/L (data not shown) after 1 year of continuous operation of the MBR.

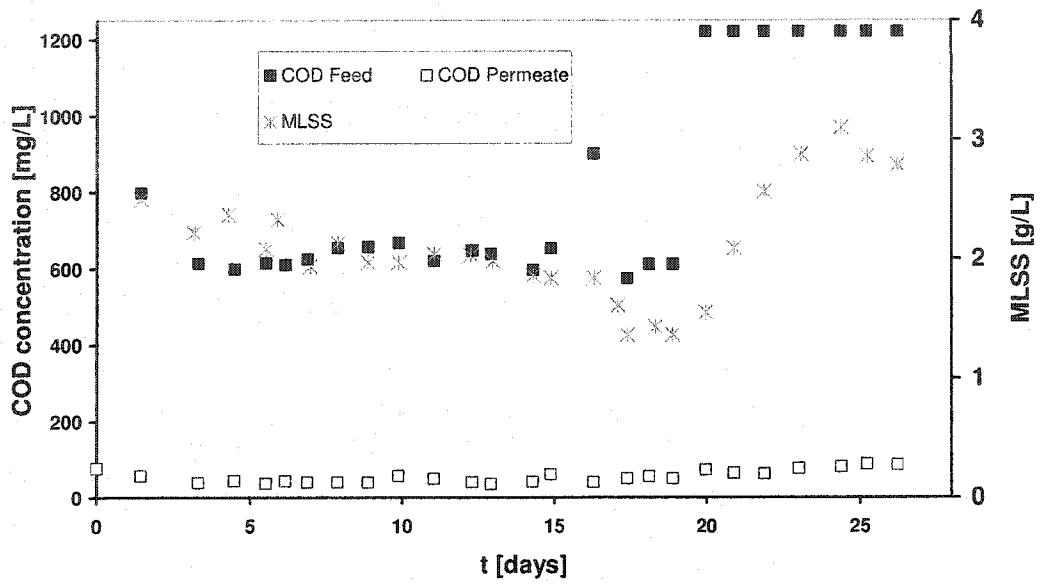

Fig. 5.3. Increasing COD feed and constant permeate concentration during MBR startup.

The permeate COD concentration remained on a constant low level of about 50-100 mg/L during the first 27 days, which proved a sufficient degradation performance of the microorganisms in the MBR. Even doubling the substrate load after 19 days of operation barely increased the permeate COD concentration.

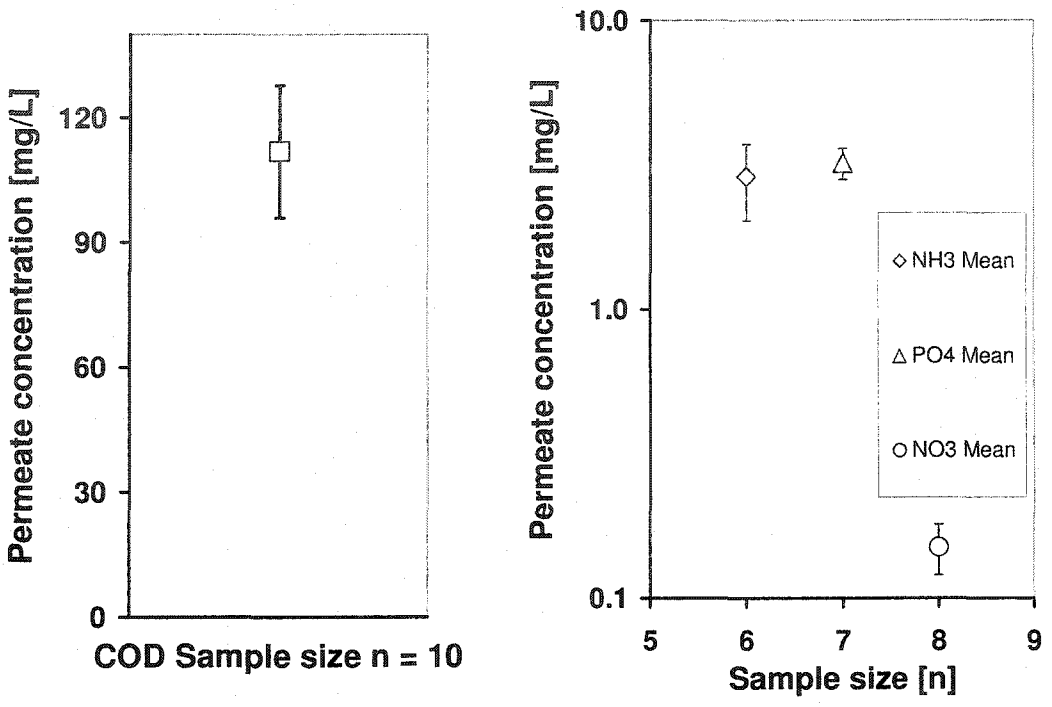

Fig. 5.4. Permeate mean concentration at stable bioreactor conditions, including standard errors.

Fig. 5.4 shows the permeate concentration of different macronutrients and the COD after about one year of stable operation, while the MLSS was around 12 g/L. Contrary to conventional MBR processes, aeration here was accomplished without any additional aeration beyond the air sparging system. This approach proves the feasibility of substituting conventional aeration by an air sparging system without impairing the degradation performance of the MBR. Thus air sparging can be very cost effective, requiring the same or even lower amounts of air supply than conventional aeration as shown below, with the added benefit of fouling reduction.

5.3.2 Long term observation of permeability – comparison AS+BF to NON enhanced filtration

5.3.2.1 General model

To introduce the topic, the simple but popular flux model as expressed in eq. 5.1 is given:

$$J = \frac{TMP}{\mu * R_t} = \frac{TMP}{\mu * (R_m + R_c + R_f)} \qquad \text{eq. 5.1}$$

For the resistance analysis, a resistance in series model is assumed, where J is the flux [m/s)], TMP is the applied transmembrane pressure [Pa], μ is the wastewater viscosity [Pas], and R_t is the total or overall resistance of the system [m^{-1}]. The total resistance can be divided into the intrinsic membrane resistance R_m, the cake resistance R_c and the fouling resistance R_f. R_c and R_f increase over time. The cake resistance R_c may be reversible with time due to changed process conditions; meanwhile the fouling resistance R_f is not reversible, but increases steadily over time due to irreversible adsorption and pore plugging.

R_m can be obtained by measuring the initial flux with the assumption that deposition on the membrane surface, pore plugging, or adsorption are negligible at filtration startup. Another common approach is to measure the clear water flux of the membrane to determine the membrane resistance based on eq. 5.1. However, as Fig. 5.5 shows, over time the clear water flux declines steadily and it remains unclear at what time the proper membrane resistance should be determined. It should be pointed out that the flux in Fig. 5 is depicted on a logarithmic scale and declines within the

first 12.5 hours by 90%. For the test as shown, a brand new activated polypropylene membrane (virgin) was used. Furthermore it is vital (but not easy) to assure that equal boundary conditions (temperature, CFV, TMP) are provided for comparison of water flux and process flux in order to determine the membrane resistance.

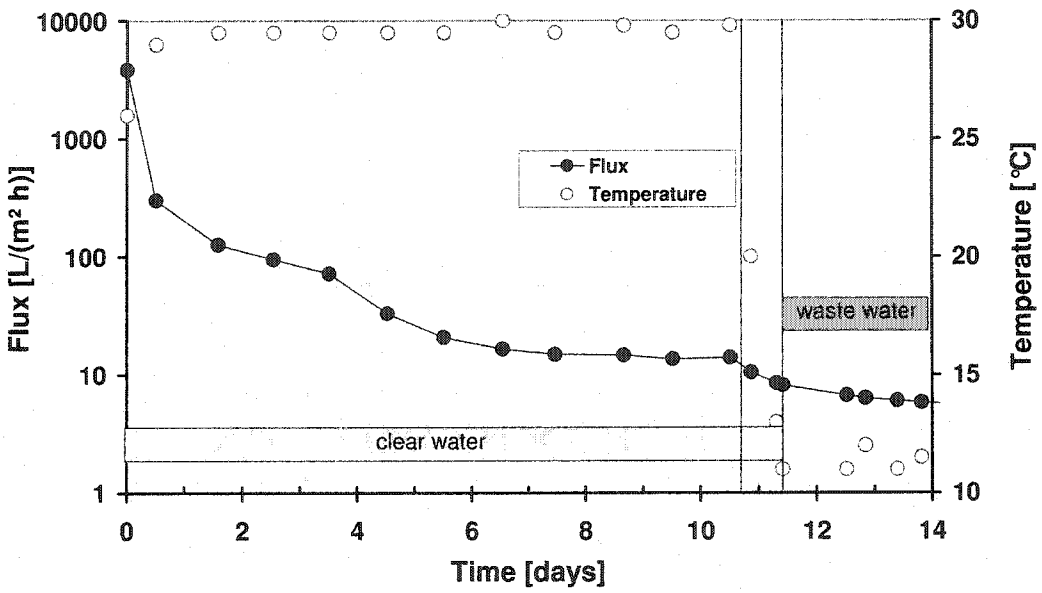

Fig. 5.5. Clear water flux development for an activated virgin polypropylene membrane.

5.3.2.2 Activated sludge viscosity

Fig. 5.5 shows a strong relationship between temperature and flux, a statement which holds for any membrane filtration. After about 10.5 days, the temperature of the clear water was decreased from ~30 to ~12°C, resulting in an obvious flux decline due to decreased dynamic water viscosity, which directly affects the flux according to

eq. 5.1. Over the past decades, several approaches have been made to describe the viscosity of activated sludge. It could be confirmed that the viscosity depends on several other parameters in addition to MLSS and temperature; for instance the extracellular polymeric substances (EPS), operating conditions, nutrient supply and so on (*Hoa et al.,* 2003). *Xing et al.* (2001) gave a simple but handy empirical estimate for activated sludge viscosities in side-stream MBR depending on MLSS values between 0 and 20 g/L, as shown in eq. 5.2.

$$\mu = 0.1488 * MLSS + 1.036 \qquad \text{eq. 5.2}$$

with:

μ= dynamic viscosity [mPas]

MLSS = mixed liquor suspended solids [g/L]

The results for eq. 5.2 were obtained at 30°C. In order to estimate the fluid viscosity of a side-stream MBR at any temperature, the authors suggest here linking eq. 5.2 to a ratio of the viscosities at actual temperature and at 30°C, as shown in eq. 5.3.

$$\mu = \left(\frac{\mu_{Temp}}{\mu_0} \right) * (0.1488 * MLSS + 1.036) \qquad \text{eq. 5.3}$$

with

μ0 = dynamic viscosity [mPas] = 0.8 at 30°C, MLSS = 0 (White, 1991), and

μ_{Temp}, the dynamic viscosity of water [mPas] at actual temperature for MLSS = 0, is calculated according to eq. 5.4:

$$\mu_{Temp} = \frac{1.78}{\left(1 + 0.0337 * T + 0.000221 * T^2\right)}$$ eq. 5.4 (*Busch et al.* 1993)

with:

T= actual temperature of the water or, alternatively, activated sludge [°C]

With the dynamic viscosity for 30°C and a re-arranged eq. 5.3, the following eq. 5.5 can be obtained to estimate the activated sludge viscosity μ [mPas] based on temperature T [°C] and MLSS [g/L].

$$\mu = \frac{0.33 * MLSS + 2.3}{\left(1 + 0.0337 * T + 0.000221 * T^2\right)}$$ eq. 5.5

Fig. 5.6 gives an overview of how the viscosity of activated sludge depends on the MLSS and the temperature, according to the proposed eq. 5.5. The graph on the bottom of the diagram (solid triangles) shows the temperature dependence of water on 0 g/L MLSS, according eq. 5.4. The graph just above (solid squares) shows the temperature dependence of water on 0 g/L MLSS according eq. 5.5, which results in a 29% over-prediction for 0 MLSS in the water. In general, with decreasing temperatures the influence of the MLSS on the activated sludge viscosity increases in absolute terms, while the relative effect is not affected by the temperature.

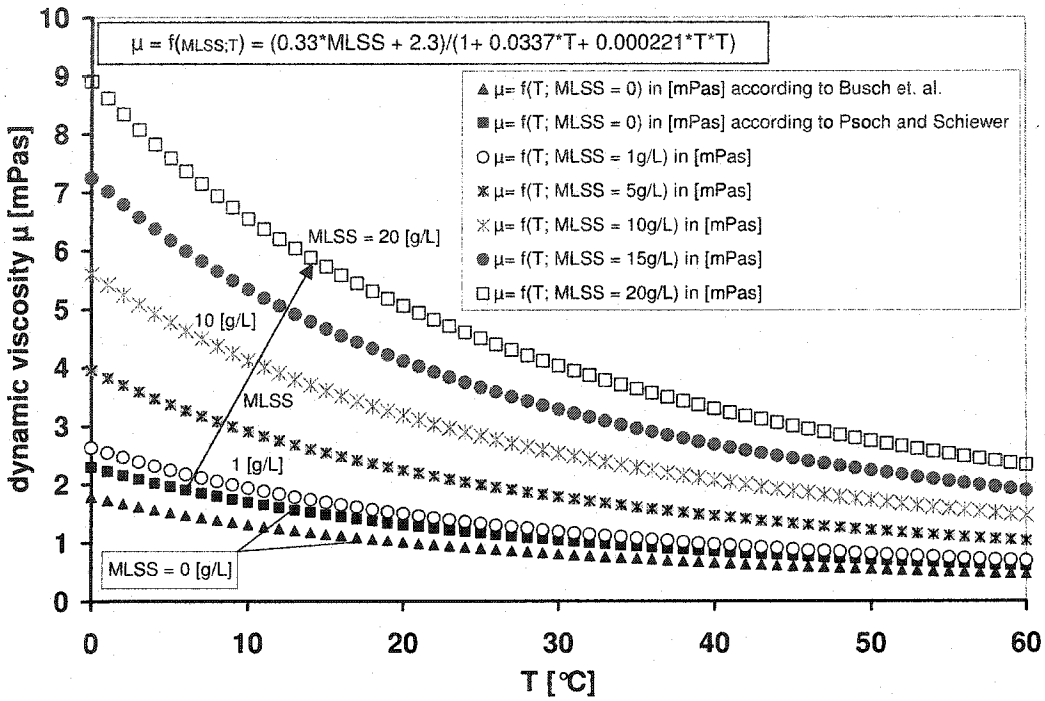

Fig. 5.6. Estimation for the impact of MLSS and Temperature on the viscosity of activated sludge in a sidestream MBR.

According to our own investigations (*Psoch and Schiewer,* 2005b), it is important to normalize flux results to temperatures or corresponding viscosities, especially for long term observations where temperature changes are more likely than in experiments of a few hours' duration. In order to overcome influences of changing temperatures, all data shown below were calibrated to the same temperature of 14.5°C by applying eq. 5.5. To increase the comparability of flux data, it is useful to compare the permeability rather than the flux to take varying TMP into account under otherwise equal operation conditions. The permeability is calculated by dividing eq.

5.1 by TMP, as shown in eq. 5.6. The common way to express the permeability is in terms of the non-SI unit bar:

$$P = \frac{J}{TMP} \qquad \text{eq. 5.6}$$

with:

P = permeability [L/(m²*d*bar)]

J = flux [L/(m²*d)]

TMP = transmembrane pressure [bar]

5.3.2.3 Permeability results

For evaluating enhancement technologies on MBR permeate flux, two test series were conducted. The first series compared the application of air sparging to backflushing. Because earlier results (*Psoch and Schiewer,* 2005c) under otherwise identical conditions showed similar results for both applications, this time backflushing was applied at more than 2.5 times higher CFV than for air sparging. The investigation lasted for about a week at MLSS values of about 10 g/L, and the results are shown in Fig. 5.7.

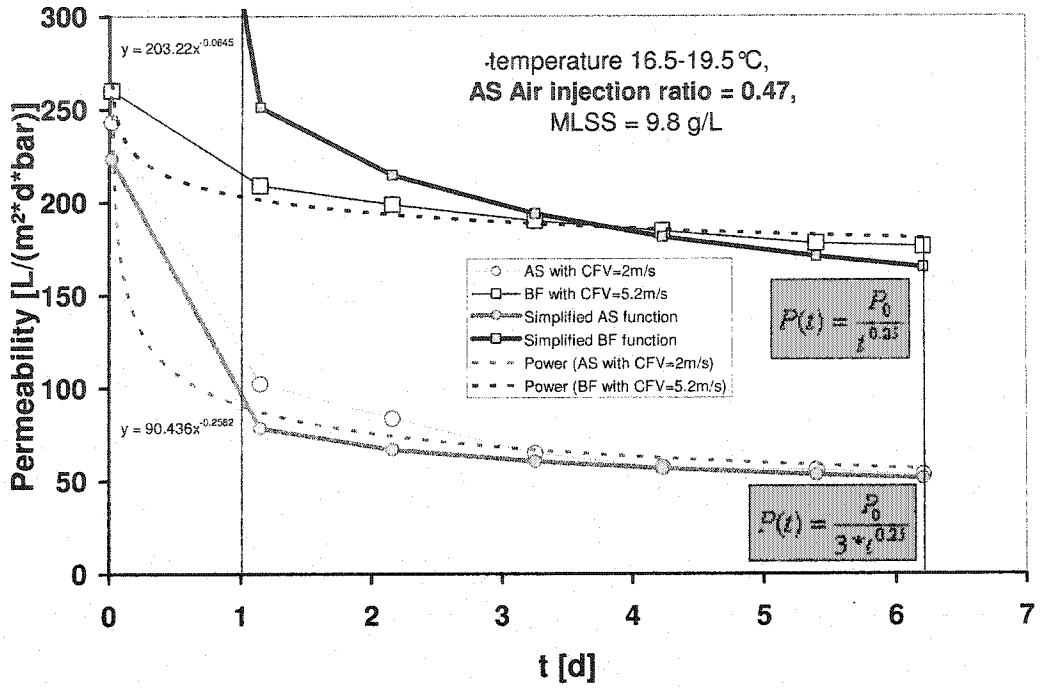

Fig. 5.7. Short term permeability for AS at 2 m/s CFV and BF at 5.2 m/s CFV with decline functions.

Both permeabilities start at about the same initial value, but the air sparging graph declines much faster than the graph for the velocity-supported backflush. This may be explained by the insufficient cleaning for the air sparging module, as discussed above in the Materials and Methods section. In addition, the less-than-optimal air injection ratio (comparatively low at 0.47) may have had some effect. The velocity-supported backflush shows over the course of the test only a 33% decline in permeability and sustains more than 2/3 of its initial value; meanwhile the air sparging system suffers a loss of 78% of its initial value. The resulting simplified permeability decline functions P ($t^{-0.25}$) are given at the right hand side (Fig. 5.7). The

main purpose was to generate what is often called a "1 dollar equation" reflecting the decline in its simplest way; this equation leaves Day One out of the modeling process because it is seldom characterized by stabilized conditions.

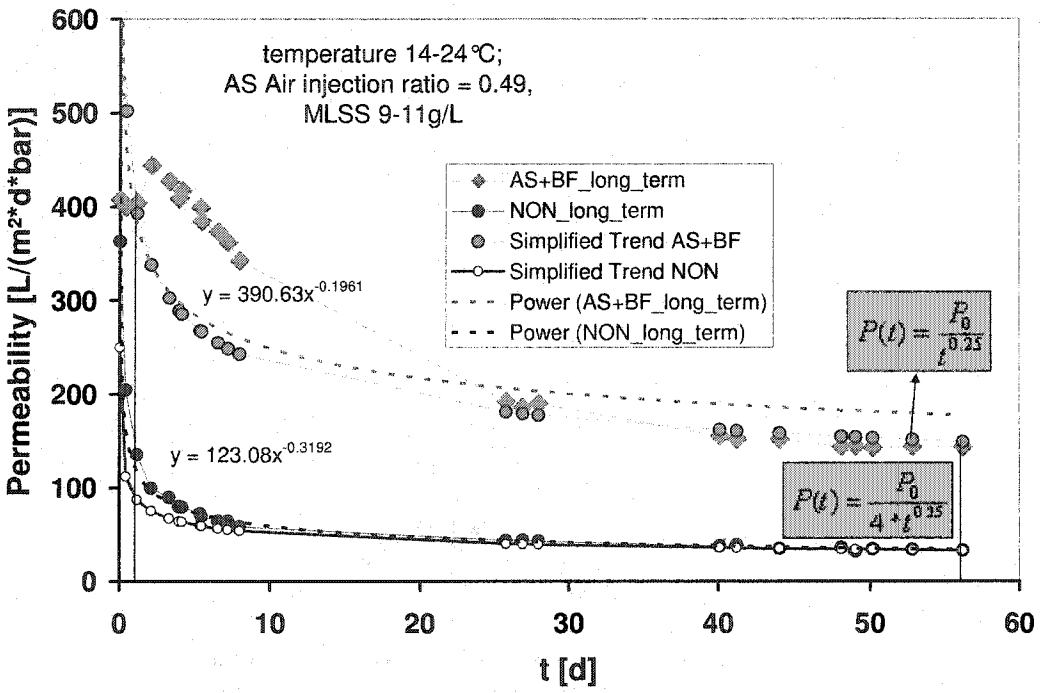

Fig. 5.8. Long term permeability of AS+BF and NON enhanced filtration at 2 m/s CFV in a MBR at about 18°C and 10 g/L MLSS.

The second test series compares a combined enhancement by means of air sparging and backflushing to conventional filtration without any improvement. This test series was studied for almost two months at the same CFV of 2 m/s, a common velocity for sidestream MBR. Results are depicted in Fig. 5.8. As a result of better cleaning procedures, higher initial permeabilities were obtained. An unexpected flux

rise for the combined enhancement technology can only be explained by the fact that initially some deposition was present on the membrane surface, and this was later removed due to turbulence of air sparging and efficacy of backflushing. However, after the second day, both fluxes declined, although the enhanced flux declined to a much lesser extent. The power functions for both graphs are depicted on the left hand side of Fig. 5.8. The simplified functions (or "1 dollar equations") are expressed in the colored frames on the right, again, with Day One omitted from the modeling observation since no stable conditions had been achieved yet. After 56 days of operation, the enhanced permeability is about 4 times higher than the conventional filtration approach. In both cases the simplified equations match the originally fitted power functions much better than was demonstrated in the investigations that lasted only one week.

To compare the achieved results, Table 5.1 lists the overall permeate yield over the whole duration of the experiment, except for the first day. The yield is obtained by integration of the simplified function within the limits of the first day (omitting Day One) and the last day, since none of the simplified functions fits the real curve before the end of Day One very well.

Table 5.1. Overview of applied techniques and yield.

Technique	t [d]	CFV [m/s]	Simple function	P_0 $\left[\frac{L}{m^2 * d * bar}\right]$	Overall permeate yield [$m^3/(m^2*bar)$]
AS+BF	56.16	2.0	$P(t) = P_0 * t^{-0.25}$	407.66	22806
NON	56.16	2.0	$P(t) = (P_0/4) * t^{-0.25}$	362.75	5073
BF	6.21	5.2	$P(t) = P_0 * t^{-0.25}$	260.01	12.3
AS	6.21	2.0	$P(t) = (P_0/3) * t^{-0.25}$	243.31	3.82

For the 56 day test, AS+BF improved the yield by a factor of 4.5, which is slightly under-predicted, because the simplified function for the AS+BF combination shows a substantial deficit within the first 20 days compared to the real graph. The under-prediction of the NON function is negligible. The 6 day test reveals a ratio of 3.2 in favor of the BF application.

5.4 Conclusions

1. For chemical membrane cleaning, a combination of acidic and caustic solutions is recommended.

2. Air sparging used to substitute aeration for MBR in side-stream has no adverse effect on the degradation performance of the bioreactor.

3. Pure water flux of freshly activated polypropylene membranes shows a flux decline of more than 99% within 10 days at temperatures of 30°C.

4. An equation is proposed to estimate the viscosity of activated sludge in a side-stream MBR in dependence on the MLSS and the temperature. It could be shown that with decreasing temperatures the biomass concentration will exert more influence on the overall viscosity.

5. Backflush application with 2.5 times higher CFV (up to 5.2 m/s) increases permeate yield over a 6 day period by a factor of 3.2, compared to air sparging alone at MLSS of 10 g/L.

6. For combined (simultaneous) deployment of air sparging and backflushing, the permeate yield is more than 4.5 times higher than for the conventional filtration in a 56 day period.

7. It is possible to estimate permeabilities of long term filtration processes with a $t^{-0.25}$ [d] function.

Acknowledgements

Special gratitude to the Grundfos company, which supported our study with a multistage pump and further equipment, and to the Microdyn-Nadir company which donated the membrane modules. We acknowledge funding of this project through a grant from the USGS/NIWR.

5.5 References

Al-Bastaki N. and Abbas A., 2001. Use of fluid instabilities to enhance membrane performance: a review. Desalination 136, pp. 255-262.

Bellara S., Cui Z. and Pepper D. (1996). Gas sparging to enhance permeate flux in ultrafiltration using hollow fiber membranes. J. Membr. Sci., 121, pp. 175-184.

Busch, K., Luckner, L. and Tiemer, K., (1993) Geohydraulik. Gebrueder Borntraeger, Berlin, 3rd edition, ISBN 3-443-01004-0.

Cabassud C., Laborie S. and Laine J. M. (1997) How slug flow can improve ultrafiltration flux in organic hollow fibres. J. Membr. Sci. 128, pp. 93-101.

Chang, I., Le Clech P., Jefferson, B. and Judd, S., (2002) Membrane fouling in membrane bioreactors for wastewater treatment. Journ. Environm. Eng. ASCE, 128, No 11, ISSN pp. 1018-1029.

Cheryan M., (1998) Ultrafiltration and Microfiltration Handbook. Technomic Publishing Co. Inc. Lancaster, Basel, ISBN: 1-56676-598-6.

Cui, Z., Wright, K., (1994) Gas-liquid two phase cross-flow ultrafiltration of BSA and dextran solutions. J. Membr. Sci. 90, pp. 183-189.

Hoa, P., Nair, L. and Visvanathan, C., (2003) The effect of nutrients on extracellular polymeric substance production and its influence on sludge properties, ISSN 0378-4738, Water SA, 29, No 4 October.

Judd, S., (2004) Keynote: Fouling control in submerged membrane bioreactors. IWA Special. Conference, WEMT 2004, June 7-10, Seoul, Korea.

Kraume, M., Bracklow, U., Drews, A., Vocks, M., (2004) Keynote: Nutrients removal in MBRs for municipal wastewater treatment. IWA Special. Conference, WEMT 2004, June 7-10, Seoul, Korea.

Le Clech, P., (2002) PhD thesis: Process configuration and fouling in membrane bioreactors, Cranfield University, UK.

Levy S., (1999) Two-Phase Flow in Complex Systems. Interscience Publication, John Wiley & Sons, Inc., New York, ISBN: 0471329673.

Metcalf & Eddy, edited by Tchobanoglous, G., and Burton, F., (1991) Wastewater Engineering, Treatment, Disposal and Reuse. McGraw-Hill Boston, 3rd edition, ISBN 0-07-041690-7.

Pospisil, P., Wakeman R., Hodgson, I. and Mikulasek, P., (2004) Shear stress-based modelling of steady permeate flux in microfiltration enhanced by two-phase flows. Chem. Eng. J., 97 pp. 257-263.

Psoch C. and Schiewer S. (2005a) Synthetic wastewater preparation and aeration via air sparging in a sidestream MBR. to be submitted to Water Research (in preparation).

Psoch, C. and Schiewer, S., (2005b) Resistance analysis for enhanced wastewater membrane filtration. to be submitted to J. Membr. Sci. (in preparation).

Psoch, C. and Schiewer, S., (2005c) Anti-fouling application of air sparging and backflushing for MBR. to be submitted to Water Research (in preparation)

Standard Methods for the Examination of Water and Wastewater, 1995 19th edn, A P H A/American Water Works Association/Water Environment Fed., Washington DC, USA.

Stephenson, T., Judd, S., Jefferson, B. and Brindle, K., (2000) Membrane bioreactors for wastewater treatment. IWA Publishing, London, UK.

Vera L., Delgado S. and Elmaleh S., (2000) Gas sparged cross-flow microfiltration of biologically treated wastewater. Wat. Sci. Tech. 41(10), pp. 173-180.

White, F., (1991) Viscous Fluid Flow. McGraw-Hill Boston, 2nd edition, ISBN 0-07-069712-4.

Xing, C., Qian, Y., Wen, X., Wu, W. and Sun, D., (2001) Physical and biological characteristics of a tangential-flow MBR for municipal wastewater treatment. J. Membr. Sci. 191, pp. 31-42.

Yamamoto, K., Hiasa, M., Mahmood, T. and Matsuo, T., (1989) Direct solid-liquid separation using hollow fiber membrane in an activated sludge aeration tank. Wat. Sci. Tech., 21, pp. 43-54.

6 Resistance analysis for enhanced wastewater membrane filtration[5]

C. Psoch and S. Schiewer*

Department of Civil & Environmental Engineering; Water & Environmental Research Center, University of Alaska Fairbanks, AK 99775; USA; email: ffsos@uaf.edu

Abstract

This study investigated enhancement techniques for wastewater filtration in a Membrane Bioreactor (MBR) at MLSS = 12-16 g/L. As improving methods, air sparging (AS), backflushing (BF) and a combined application of both (AS+BF) were compared to the conventional application (NON). In addition to the experimental analysis, a comparison of different models for determining cake resistance is given. Measurements of cake thickness served in evaluating flux results and as input data for some of the model calculations. Further findings revealed AS+BF showed the lowest overall resistance, and thus the highest yield, for about 2 weeks' observation. A split of the overall resistance was made, based on experimental data. Thus a comparison of the experimental cake resistance and the model resistances was possible, which helped to identify the best model approach. Other results showed that initial flux is linked to the cross flow velocity (CFV). The chemical cleaning of the membrane should be done with a combination of acid and caustic solutions rather than a caustic

[5] Journal of Membrane Science, Elsevier (to be submitted) 2005

treatment only, in order to compensate for the local water quality. Finally, a relationship between the backflush resistance and the permeate flow resistance is confirmed, suggesting that until a cake layer is built up, a relationship between CFV and backflush resistance exists.

Keywords: resistance, wastewater, cake thickness, initial flux, backflush resistance

6.1 Introduction

Major research efforts in recent years have been aimed at overcoming the drawbacks of membrane fouling. For microfiltration, a variety of operation techniques are available: changes in cross flow velocity (CFV), implantation of turbulence promoters, backflushing (BF) or backpulsing, pulsatile flow, rotation of flat sheet membranes, application of electrical and ultrasonic fields, and air sparging (AS) [1].

Flux enhancement through AS has been used since the late eighties and applied commercially for inside-out and outside-in filtration. Both variants have advantages and disadvantageous. For outside-in filtration, coarse air bubbling provides CFV and shear stress in membrane bioreactors for a row of products under different brand names. Advantages are easy use and low maintenance costs; its chief disadvantage is the limited effect the air bubbles have in preventing fouling development on top of the membranes. The application of AS inside of membrane channels for inside out

filtration is commercially less common due to membrane surface area restrictions for these module types. However, the advantage of this method lies in the direct accessibility of the membrane surface to the air bubbles which can suppress particle deposition [2]. If air is injected into a tube which already transports water, depending on the ratio of gas to liquid volume flow, the interface of this two-phase flow follows a variety of flow patterns. Through the air injection ratio r (r = superficial gas velocity/(superficial gas velocity + superficial liquid velocity)), sometimes called the "void fraction" of the pipe, the flow pattern can be predicted. The increase of air injection ratio r creates for vertical pipes bubble flow ($0 < r < 0.2$), slug flow ($0.2 < r < 0.9$) and, finally, annular flow ($0.9 < r < 1.0$) [3]. For flux enhancement, slug flow is the most effective at disrupting the concentration polarization layer and maintaining stable permeate fluxes over longer time periods [4].

The experimental setup for this paper provided both air sparging (AS) and the very common option of backflusing (BF) to minimize fouling. Both techniques were applied separately and simultaneously.

Air sparging is especially successful in fighting the build-up of cake layers. To overcome pore plugging, air sparging is less practical, but backflushing can partially tackle this problem of internal membrane fouling.

As Bowen et al. [5] described, four fouling mechanisms are usually distinguished in microfiltration. A) complete pore blocking; B) standard blocking; C) intermediate blocking; D) cake filtration. In practice usually all four mechanisms contribute to flux decline in different amounts.

For this study it is assumed (as in most microfiltration applications for wastewater) that the cake resistance is a major contributor to the overall fouling. The cake can act as an additional filter or secondary membrane, catching smaller particles and it undergoes a compaction process with ongoing time. Cake formation, together with other fouling mechanisms, can finally exceed the membrane resistance [6].

Several theoretical models for estimating cake resistance in wastewater microfiltration were evaluated by means of experimental data from conventional filtration. Those results served as comparison for the improvements with enhancement technologies as AS and/or BF discussed below.

6.2 Materials and methods

For experimental setup of the membrane bioreactor (MBR), an activated sludge tank with a capacity of 60 - 80 liters was used (see Fig. 6.1). A multistage pump (Grundfos) moved the activated sludge through braided hoses ½ inch (1.27 cm) in diameter to the membranes and back to the bioreactor. A thermostat maintained reactor temperature between 14 and 24°C.

The experiments were carried out with two vertical membrane modules, which were deployed in parallel. Each membrane module (Microdyn-Nadir) consisted of three polypropylene membrane tubes (pore size 0.2 µm) in a plastic housing of 0.75 m length. The diameter of the tubes was 5.5 mm, yielding a membrane surface area of 0.036 m^2 per module.

One module (see Fig. 6.1, "membrane module") featured an air sparging system: On each end of the module, an acrylic rod (15 cm long) extended the membrane tube. On one side (the lower), three perpendicular drilled entries served for air supply to each tube. Each air supply included its own adjustable air valve. The total air volume stream was monitored by a volume flow meter, a mass flow meter, and a pressure gauge. The air pressure was held at 60 - 70 kPa above the transmembrane pressure (TMP) within the membrane to ensure enough air was pushed into the system. Fluctuation of airflow was prevented by the mass flow meter. On the other side (the upper), the acrylic rod served as a viewing area for flow pattern observation.

Both modules were equipped for backflushing. Applied TMPs were between 100 and 200 kPa (1-2 bar). Cross flow velocities (CFV) of the water within the membrane tubes were between 1.3 and 3.5 m/s. For the module with acrylic extenders, the flow pattern was observed with a stroboscope; observations with the naked eye were impossible.

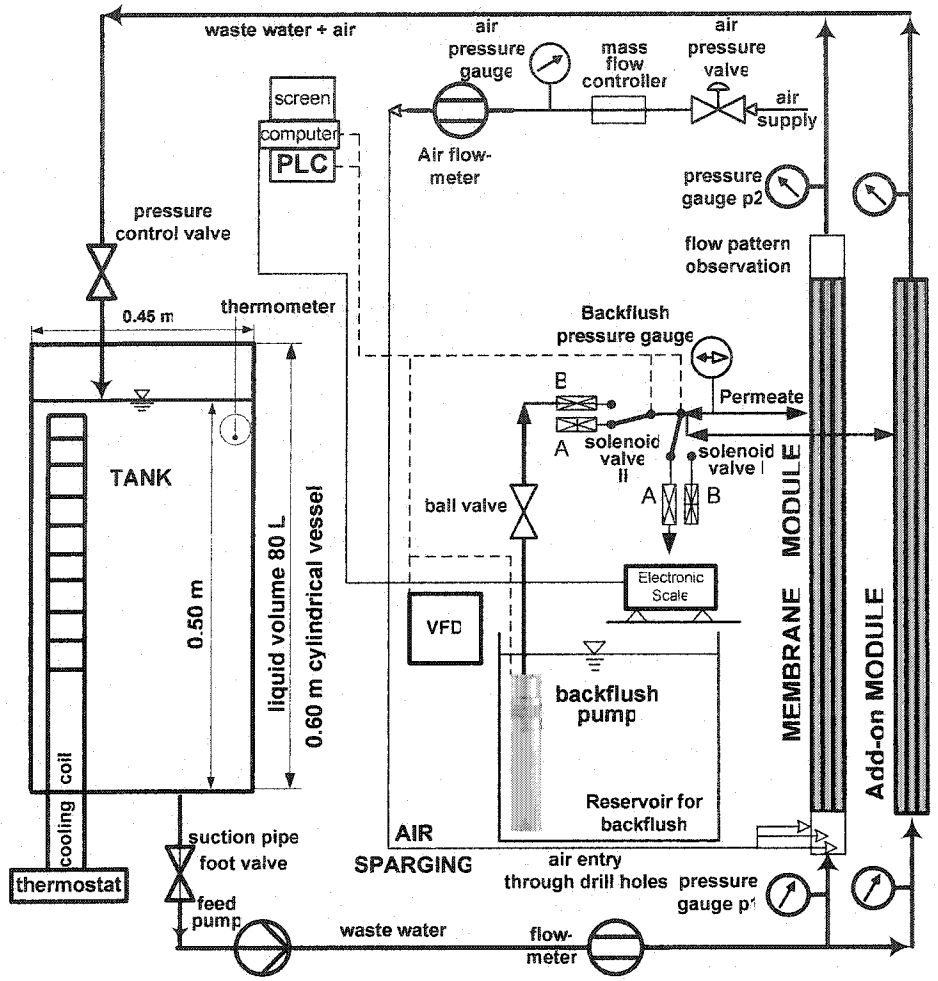

Fig. 6.1. Experimental setup schematic.

The pump speed, and thus the pressure for the backflush pump (submerged pump, MP1, Grundfos), were regulated over a variable frequency drive. The experiments were carried out with a low backflush pressure of about 60 kPa (ca. 0.6 bar) above the TMP, to minimize product loss.

With a programmable logic controller connected to a personal computer with additional software, the backflush cycle was regulated at every 30 minutes for 15

seconds, and two solenoid valves (solenoid valve I and II; see Fig. 6.1) were opened and shut alternatively to allow a reversal of the normal flow direction within the membrane. In case where the membrane module was operated with air sparging and backflushing, the backflush procedure was superimposed over the continuously running air sparging.

For this study, activated sludge was generated by synthetic wastewater. The synthetic wastewater feed was glucose-based and contained high concentrations of the three basic components as Carbon (C), Nitrogen (N) and Phosphorus (P) along with other compounds. For more details see Psoch and Schiewer [7].

Prior to all experiments a chemical cleaning of the membranes was conducted in order to achieve largely the same initial conditions at each test series. The cleaning was accomplished by pretreatment from the permeate side with a hot (about 60°C) blend of Phosphoric and citric acid (ratio 1:4 at pH 1.4), followed by soaking the membranes in hot NaOH (again about 60°C) for an hour. Subsequently an intensive flush with de-ionized water for about 4 hours was provided. However, one of the membranes had been used in an earlier test series; this module was "on duty" for up to 6 months and showed signs of membrane aging, indicated by comparably low initial flux.

The experiments included two test series, each of about 2 weeks' duration. The first series compared backflush (BF) and air sparged (AS) enhanced flux; the second series investigated a combination of AS+BF versus no enhancement (NON).

The main purpose of these test series was to study the flux decline for different techniques and to compare the results to the regular case, the NON enhanced flux. To achieve high accuracy in data collection and to back up manually obtained data, every day for about 5 hours the flux was electronically monitored by an automatic scale which recorded the permeate volume by weight once per minute. The data was stored on a personal computer; an example of the logged data is given in Fig. 6.2. Through examination of the electronically recorded data, it became clear that the influence of temperature is larger than assumed so far. Thus a temperature conversion which norms the received flux to a standard temperature was developed to interpret the data. For further details about temperature calibrations see Psoch and Schiewer [8].

As Fig. 6.2. shows, the flux declines during the observation time of 5 hours if the temperature in the reactor can be maintained at an ideal constant; otherwise, temperature fluctuations impaired the inclination of the flux decline. For every day a linear graph of the flux development for the five hours was obtained. All the linear graphs were put into one diagram to harvest a representative trend graph. For both test series, only one membrane could be monitored electronically. This methodology made it possible to compare the BF membrane from the first series and the AS+BF membrane from the second series using electronically recorded data in addition to the manually harvested results. Later, an average of electronically and manually collected data was generated.

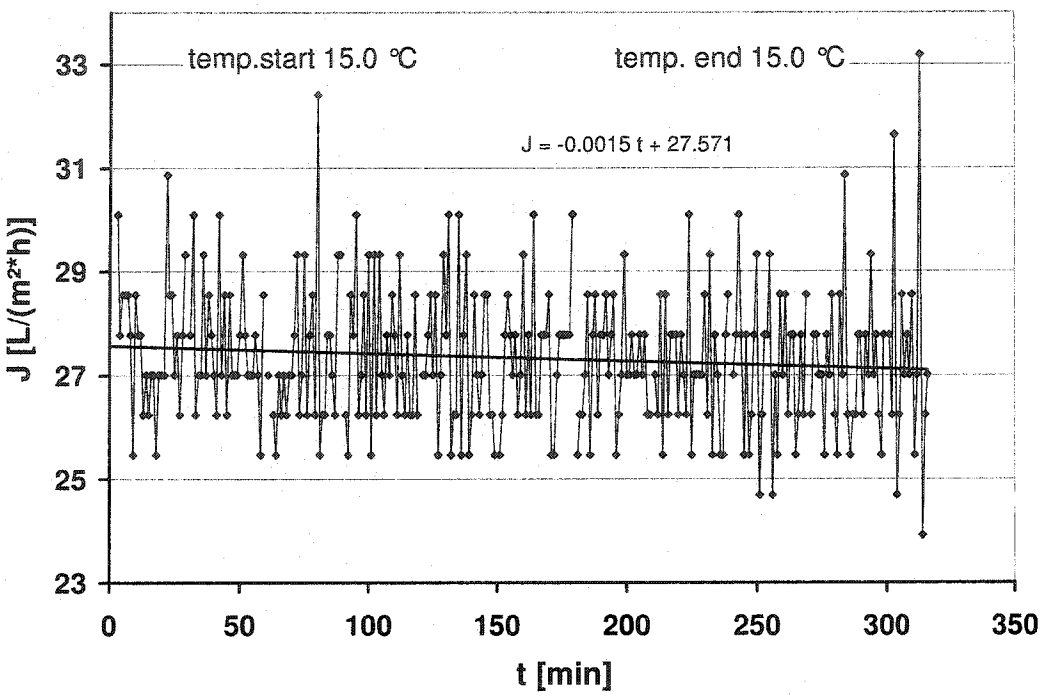

Fig. 6.2. Recorded data for AS+BF enhanced filtration of activated sludge under ideal temperature conditions on day 4 of the test series, at MLSS of 14.5 g/L.

Every 30 minutes, BF took place for 15 seconds, including the opening and closing of the two BF valves; this process resulted in regular flux decrease every 30 minutes.

The original plan included monitoring the electronically collected data to examine any differences in the flux decline before and immediately after backflush events. However, the resolution of scale was 0.5 g, which was not high enough to record more sensitive flux changes.

Parallel to the five hours when the process flux was recorded electronically, the used backflush volumes were monitored. For this purpose, the BF pump was taken

out of the reservoir and placed in a 2000 mL glass measurement cylinder. Our hypothesis was that there was a direct relationship between the process flux decline and the backflush volume.

One of the main objectives of the study was based on the resistance in series model, to distinguish between the single resistances and their values, as found by experimentation. Taking advantage of the tubular geometry, the application of 10 sponge ball passages through the membrane channels was supposed to remove all built-up membrane filter cake, by separating the inner (fouling) resistance from the outer (cake) resistance. Furthermore, three theoretical approaches taken from the literature are given, each based on different assumptions, to determine the specific cake resistance theoretically and with a combination of theory and empirical observation.

6.3 Theoretical resistance analysis

As is often found in the literature, in eq. 6.1 the resistance in series model is given:

$$J = \frac{TMP}{\mu * R_t} = \frac{TMP}{\mu * (R_m + R_c + R_f)} \qquad \text{eq. 6.1}$$

where J is the flux [L/(m²*h)], TMP is the applied transmembrane pressure [Pa], μ is the wastewater viscosity [Pas], and R_t is the total or overall resistance of the system

[m^{-1}]. The total resistance can be split into R_m, the intrinsic membrane resistance, R_c, the cake resistance, and R_f, the fouling resistance. R_c and R_f increase over time. The cake resistance, R_c, can be changed due to altered process conditions, backflushing or sponge ball applications. The fouling resistance, R_f, meanwhile is not changeable, but increases steadily over time due to irreversible adsorption and pore plugging.

R_m can be obtained by measuring the initial flux with the assumptions that neither significant deposition on the membrane surface occurs, nor is pore plugging or adsorption prevalent immediately after start up.

The cake resistance, R_c, can be obtained by measuring the total resistance and subsequently removing cake depositions. In tubular geometries sponge ball cleaning is a reliable technique. The remaining resistance after intensive surface cleaning with sponge balls, turbulence increase, and so on, is the sum of fouling resistance, R_f, and intrinsic membrane resistance, R_m, which finally reveals the cake resistance.

In order to predict membrane performance, a series of approaches exist to estimate the cake resistance of a membrane without direct measurements. Oftentimes model solutions are used for the calculations; this approach features the advantage of clearly defined particle size distributions, shape factors, surface areas, and so on. For real or synthetic wastewater, the case is more complex, and the suggested model approaches have only limited validity. To compensate for this limitation, an investigation and comparison of three models will be given.

Model A

The cake resistance Rc is related to the specific cake resistance α and the mass that accumulates on the membrane surface.

$$Rc = \alpha * V * Cb \qquad \text{eq. 6.2}$$

where α = specific cake resistance [m/kg]; V = permeate volume per unit area [m^3/m^2]; and C_b = bulk MLSS [kg/m^3].

With the following variation of the Carman-Kozeny equation we determine α_0 = specific cake resistance [m/kg] without any comppression:

$$\alpha_0 = \frac{k*(1-\varepsilon)*A_S^2}{\rho_S * \varepsilon^3} \qquad \text{eq. 6.3}$$

where ε is the porosity [-]; k = the Kozeny "constant", which depends on the particle shape and the porosity ε and is approximately 5 for $\varepsilon < 0.65$ [9; 10]. As = specific surface area [m-1] of the representative particle. As gives, in the case of spherical particles, As= A/V = 6/d, and ρs is the particle density [kg/m^3].

Wastewater particles which accumulate on top of a membrane are neither uniformly shaped nor have uniform (narrow) particle size distribution. Hence, here we consider a multi-grain layer deposit. We know that the porosity for an arbitrarily

formed bed of uniform, spherical particles can not be smaller than $\varepsilon = 0.36$. According to the literature [10], layers of multi-sized grains have porosities of $\varepsilon = 0.19 - 0.37$. Hermanowicz [11] pointed out that the connectivity threshold (threshold where less porosity does not admit pore connection and hence flow passage) for random spherical pores is 0.28 and smaller (up to 0.015) for other shapes.

Let us assume the ε value for the particle within the wastewater would be $\varepsilon = 0.3$. But that is not the real porosity, since the particles in the wastewater are surrounded by an extracellular polymeric substance [12]. According to the literature [11; 12] the extracellular polymeric substance (EPS) fills the void spaces between the biomass particles, which are deposited on top of the membrane. Hence the actual porosity is significantly decreased. Another possible approach, put forth by *Park et al.* [13] but not traced here, suggests, as a response to the decreased void fraction, the consideration of overlapping particles in spherical shape.

Flemming [14] investigated the specific resistance of model biofilms, which are, in terms of properties, reasonably close to the EPS of wastewater flocs; he found for agar a specific resistance of:

$\alpha = 1.3*10^{13}$ m/kg.

Let us assume a value of $\alpha = 10^{13}$ m/kg to respond to the fact that the wastewater flocs themselves are not absolutely impermeable grains. If we solve eq. 6.3 for ε (for instance with solver in MS Excel) with $\alpha = 10^{13}$ m/kg and use $\rho_s = 1300$ kg/m³ as suggested in *Metcalf and Eddy* [15], the Kozeny "konstant" $K = 5$ and $A_s =$

$4*10^7$ [m^{-1}] as found by Cicek et al. [16] under almost identical experimental conditions as those used by the authors of this paper, we receive $\varepsilon = \varepsilon_{EPS} \sim 0.62$. Now we can determine the real porosity of the cake:

$$\varepsilon_{real} = \varepsilon_{bed} * \varepsilon_{EPS} = 0.3*0.62 = 0.186 \qquad \text{eq. 6.4}$$

For further calculation according to eq. 6.3, take a closer look at the Kozeny "konstant" *k*.. After Happel [17], the following equation applies for the Kozeny "konstant" *k*, to express the dependence of *k* on the porosity ε:

$$k = \frac{1}{2} * \frac{\varepsilon^3}{1-\varepsilon} * \frac{1+\frac{2}{3}(1-\varepsilon)^{\frac{5}{3}}}{1-\frac{3}{2}(1-\varepsilon)^{\frac{1}{3}}+\frac{3}{2}(1-\varepsilon)^{\frac{5}{3}}-(1-\varepsilon)^2} \qquad \text{eq. 6.5}$$

With reasonable accuracy we can substitute the hard-to-utilize eq. 6.5 in the range of $0 \leq \varepsilon \leq 0.65$ by the approach shown in eq. 6.6, as suggested by *Brauer* [10].

$$k = 4.5 + \frac{\varepsilon^3}{2*(1-\varepsilon)^2} \qquad \text{eq. 6.6}$$

As return for *k* with ε = 0.186, we receive k = 4.505. Deploying eq. 6.3 we obtain:

$\alpha_0 = 7*10^{14}$ m/kg.

With indices zero expressed, we did not yet receive the final cake resistance. To respond to the compressibility of the cake resistance we apply eq. 6.7, which takes the increasing cake resistance at higher TMP due to compressibility into account:

$$\alpha = \alpha_0 * \left(1 + \frac{TMP_A}{TMP_T}\right)^n \qquad \text{eq. 6.7}$$

Where α is the final cake resistance; α_0 is the cake resistance according the Kozeny Equation (eq. 6.3); TMP_A = is the applied transmembrane pressure, TMP_T = is the threshold pressure below which no cake compression occurs, and the exponent n = cake compressibility. For this calculation the threshold pressure is estimated to be TMP_T = 30 kPa. The cake compressibility has, according to the literature, [14,18] values of n = 0.8 - 1.5 and here n = 1 is chosen. Eq. 6.7 according to *Flemming* [14] as well as *Lee and Wang* [19], seems to be the most accurate approach to respond to the cake compression; meanwhile several, more simple equations appear in the literature (see for instance [20]) or the compressibility is neglected. With eq. 6.7 and an applied pressure of about 150 kPa, we obtain finally

$\alpha = 4.21*10^{15}$ m/kg.

This value is in excellent agreement with results achieved by Kim, Lee and Chang [18] and by Parameshwaran, et al. [20]; and in good agreement with Flemming's results [14].

If the calculation for Model A are based on the generic approach of $\varepsilon = 0.36$ and the calculation of the specific surface area is based on As = 6/dp with dp = 3.5 µm according to *Cicek et al.* [16], we receive a not compressed specific cake resistance of $\alpha_0 = 1.41*10^{11}$ m/kg which gives after consideration of eq. 6.7 a final specific cake resistance of:

$$\alpha = 8.47*10^{11} \text{ m/kg}$$

Model B

For this model eq. 6.2 applies as well, but the calculation of the specific cake resistance is different. Several authors [13; 18; 21] stick to another variation of the Carman-Kozeny equation which appears in eq. 6.8:

$$\alpha = \frac{180*(1-\varepsilon)}{\rho_S * d_p^2 * \varepsilon^3} \qquad \text{eq. 6.8}$$

This equation incorporates the particle diameter dp; which is upon the believe of the authors of this paper not as handy as the use of the As = specific surface Area

[m^{-1}]. Because the Carman-Kozeny equation was originally developed to describe water flow through rigid particle layers such as soil or beds of carrier material, and activated sludge flocs are just not rigid (see discussion above), eq. 6.8 can only give a rough estimate. However, eq. 6.8 may serve if the surface area of the characteristic particle is not available, but the particle size is given with the further assumption of spherical dimensions. The failure of this approach may be pointed out by the fact that the specific surface area A_s for activated sludge particles (diameter = 3.5 μm) as measured by Cicek et al. [16] is A_s ca. $4*10^7$ [m^{-1}] but with spherical diameter approach $A_s = 1.7*10^6$ [m^{-1}].

If we use again the results of Cicek et al. [16], who found that for sidestream MBR the main particle size d_p is about 3.5 μm, we end up with the commonly used assumption of $\varepsilon = 0.36$ (closest possible packing of a mono-sized particle bed):

$\alpha = 2.3*10^{11}$ m/kg.

with the same porosity assumed ($\varepsilon = 0.186$) as in model A, we obtain a cake resistance of:

$\alpha = 1.4*1012$ m/kg.

For model B no cake compressibility is taken into account.

Model C

For model C, the appointment of the cake resistance R_c is not congruent with eq. 6.2, but follows eq. 6.9:

$$R_c = \alpha^* * \sigma \qquad \text{eq. 6.9}$$

α^* = specific cake resistance [m^{-2}] as in models A and B, but with another unit. To obtain the cake resistance Rc , α^* is multiplied by the cake thickness σ [m].

The specific cake resistance is calculated as another variation of the Carman-Kozeny equation. In contrast to model B, here the solid fraction of the percolated bed (1-ε) is raised to the 2nd power and the particle density is not taken into consideration. Equation 10 shows the approach as used by *Wiesner and Aptel in* Mallevialle et al. [6]:

$$\alpha^* = \frac{180*(1-\varepsilon)^2}{d_p^2 * \varepsilon^3} \qquad \text{eq. 6.10}$$

In this approach, an incompressible cake composed of uniform particles is assumed. With the same particle diameter as in model B and ε = 0.36 we obtain:

$\alpha^* = 1.28*10^{14}$ m^{-2}.

If ε = 0.186 the resistance is

$\alpha^* = 1.51*10^{15}$ m^{-2}.

6.4 Cake thicknesses comparison for different enhancement techniques by scanning electron microscopy (SEM)

To estimate the cake thickness in a real application, used membranes were cut at about half channel length to get a rough estimate for the thickness of the cake layer on top of the membrane. Even though only a limited number of cross sections can be examined by SEM, the thickness of the cake changes with every millimeter of channel length and with a reasonable time input only a local impression can be reflected by the SEM technique. The observed averages of different cake thicknesses for a variety of enhancement techniques and the regular (NON-enhanced) case appear in Table 6.1. Graphical data conversion is provided in Fig. 6.3.

The result for the NON case is essential input data for Model C calculation in the resistance analysis from Section 3. For the calculation, the predominant filter cake thickness was taken into account.

Table 6.1. Comparison of filter cake by visual observation using SEM.

Applied technique	Range of filter cake thickness [μm]	Predominant filter cake thickness [μm]	Visual cake impression, compared to NON cake
NON	20-70	50	
BF	5-20	12	rough surface, very fringed on feed water interface
AS+BF	8-20	10	rough surface, a little bit fringed on feed water interface
AS	4-10	7	smooth surface,

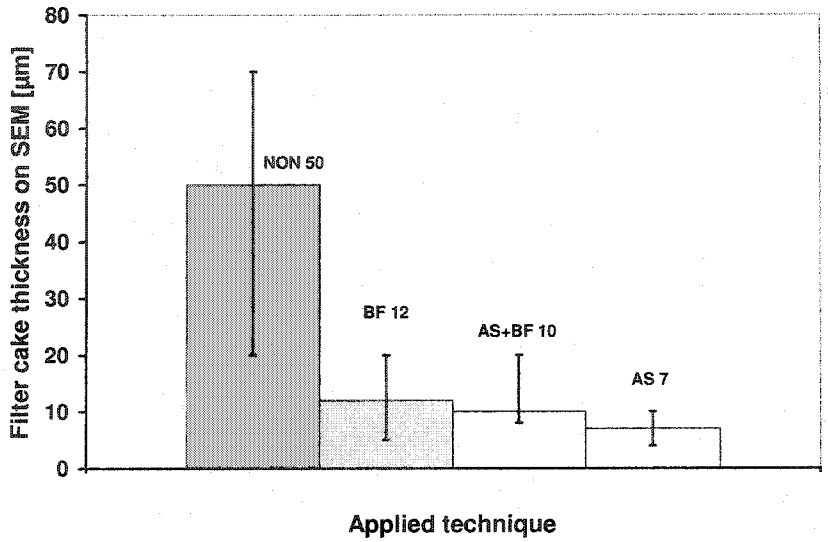

Fig. 6.3. Cake thickness average and range [µm] measurement results from SEM investigations.

6.5 Overview of theoretically determined cake resistances

Table 6.2. Combination of theoretically and empirically cake resistances.

Model	Governing Equation	Input for Gov. Eq.	Input for Gov. Eq.	R_c [m^{-1}]
A I	with eq. 6.3 in eq. 6.2	eq. 6.2: $\alpha = 4.21*10^{15}$ m/kg *) V = 1.605 m³/m² MLSS = 16.27 kg/m³	eq. 6.3: $\varepsilon = 0.186$; $k = 4.505$; n = 1 TMP_A=150 kPa TMP_T=30 kPa $A_s = 4*10^7$ m^{-1} (*measured*) ρ_s = 1300 kg/m³	$1.099*10^{17}$
A II	with eq. 6.3 in eq. 6.2	eq. 6.2: $\alpha = 8.47*10^{11}$ m/kg V = 1.605 m³/m² MLSS = 16.27 kg/m³	eq. 6.3: $\varepsilon = 0.36$; $k = 4.557$; n = 1 TMP_A=150 kPa TMP_T=30 kPa A_s = f(dp) =$1.714*10^6$ m^{-1} ρ_s = 1300 kg/m³	$2.214*10^{13}$
B I	with eq. 6.8 in eq. 6.2	eq. 6.2: $\alpha = 2.3*10^{11}$ m/kg V = 1.605 m³/m² MLSS = 16.27 kg/m³	eq. 6.8: $\varepsilon = 0.36$ dp = 3.5 µm ρ_s = 1300 kg/m³	$6.006*10^{12}$
B II	with eq. 6.8 in eq. 6.2	eq. 6.2: $\alpha = 1.4*10^{12}$ m/kg V = 1.605 m³/m² MLSS = 16.27 kg/m³	eq. 6.8: $\varepsilon = 0.186$ dp = 3.5 µm ρ_s = 1300 kg/m³	$3.656*10^{13}$
C I	with eq. 6.10 in eq. 6.9	eq. 6.9: $\alpha^* = 1.28*10^{14}$ m/kg σ = 50 µm (Fig. 3)	eq. 6.10: $\varepsilon = 0.36$ dp = 3.5 µm	$6.4*10^9$
C II	with eq. 6.10 in eq. 6.9	eq. 6.9: $\alpha^* = 1.51*10^{14}$ σ = 50 µm (Fig. 3.)	eq. 6.10: $\varepsilon = 0.186$ dp = 3.5 µm	$7.55*10^9$

*) V was based on the results from the NON graph in Fig. 6.6 until J_{t1}

6.6 Experimental determination of filter resistances

6.6.1 Electronically harvested flux data and concluded resistances

Fig. 6.4 shows the condensed results of the electronic data accumulation, as described earlier. Each of the two lines represents the average (representative) trend of a test series obtained between the Day 2 of operation and including Day 13. The first day was omitted since for each dataset some time was necessary to achieve stable operating conditions. Because the second test series ended after 13 days due to equipment failure, it seemed reasonable to compare the same time span for each test. The main point evident I Fig. 6.4 is that during 13 days of operation the combination of AS+BF is much more successful, even if the operating conditions were more to the advantage of the BF system (see Table 6.3, higher CFV, less viscosity). The AS+BF system shows about 20% higher initial permeability, and the slope for the AS+BF decline is about 3 times less as for the BF system.

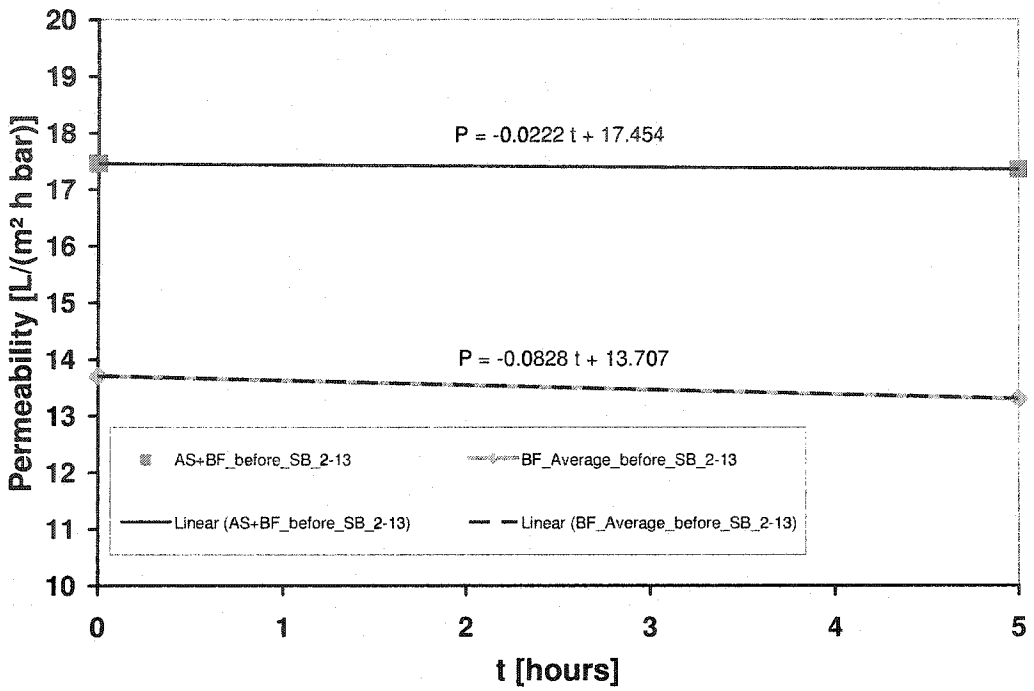

Fig. 6.4. Trend graphs for the permeability decline (MLSS= 12.2-16.3 g/L).

Based on eq. 6.1 and the data from Fig. 6.4, the calculation of the total resistance reveals the graphs presented in Fig. 6.5, which clearly shows less total fouling for the AS+BF combination.

The two more or less irregular data points in the curve of the BF system are due to different but clear, defined reasons. The resistance "jump" up to 10^{13} is based on a temperature calibration of approximately 14°C, which was applied for all data. However, the data was collected in mid-summer, and over one 5 day period, the room temperature adjustment failed, making it very difficult to maintain stable reactor temperature conditions (temperatures rose as high as 24°C. On Day 8, the average

temperature during the measurements was 23.8°C, about 5.5°C warmer than the average temperature. The temperature adjustment returned a very low viscosity. However, the flux increase was not appropriate. Obviously it is not possible to transfer temperature date directly and without any time delay toward flux data. The precipitous drop in resistance for the BF curve at the end of the curve is due to successful sponge ball application.

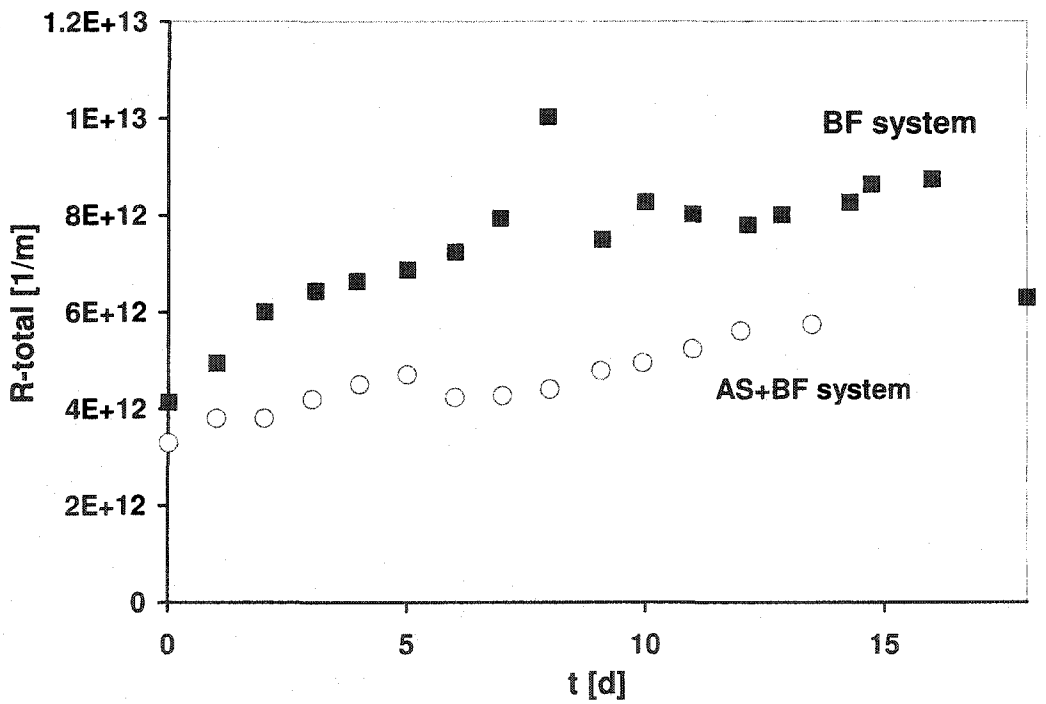

Fig. 6.5. Total resistance for combined AS+BF technique and BF application.

6.6.2 Manually obtained flux data

Fig. 6.6 shows the cumulative graphs of both test series. The initial fluxes for the first test series (BF vs AS) were almost 100% identical, perhaps due to the fact that both membranes were new. However, as *Cheryan* [22] points out in his handbook, the water flux (as an indicator for the initial flux) for brand new membranes may vary by ±25%, even under constant operating conditions. Both fluxes of the first test series declined within the first day by about 30%.

The comparison of AS and BF revealed some advantages of the BF system until Day 10, probably related to the higher CFV (see Table 6.3). Toward the end of the test series, at Day 17, the air sparging system was superior. The surprising flux increase of almost 30% over the course since Day 3 was presumably due to a CFV increase, from about 1.9 m/s up to 2.2 m/s and a consequent parallel increase of the fairly low TMP, from 110 kPa to about 130 kPa. The sponge ball application proves to be a successful cleaning procedure for both systems, as evidenced by the flux jump from J_{t1} to J_{t2}.

The second test series (AS+BF vs NON) was first operated at about 200 kPa and a CFV of 1.7 m/s. In the interest of better comparison of Test series I and II, both values were decreased after 4 hours by about 25%, which resulted in very quick flux decline, as is clear in Fig. 6.6 at the second data point. Hence, the decision was made to use flux values near the second data point as initial fluxes for further calculations (see Table 6.3).

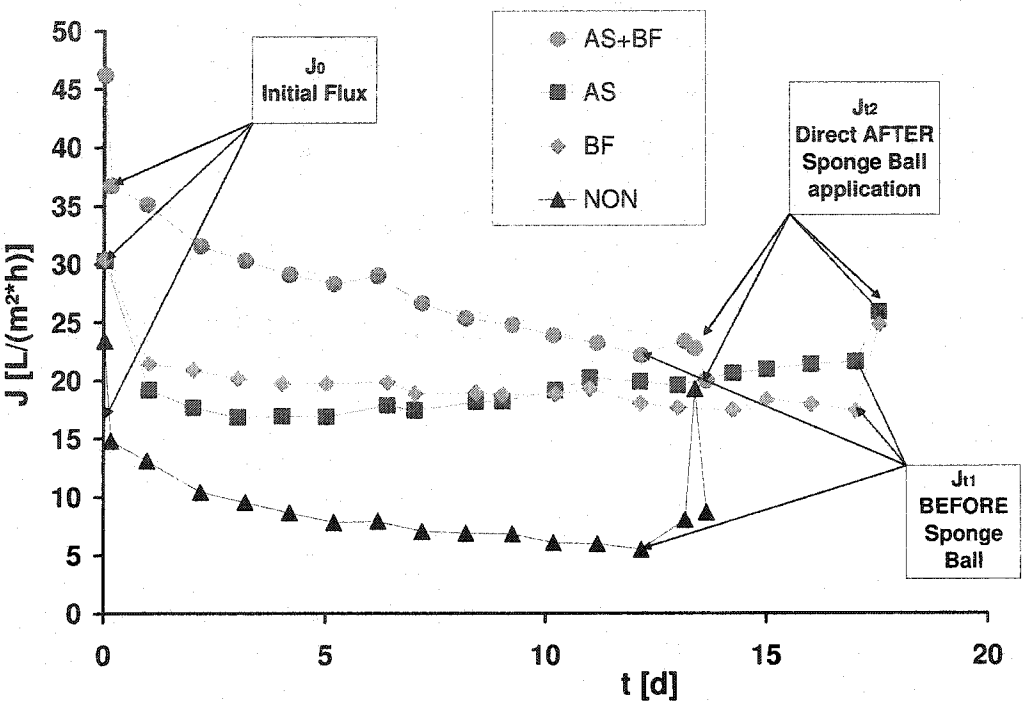

Fig. 6.6. Comprehensive depiction of flux date from both test series (operating conditions appear in Table 6.3).

In the second test series, the conventional system had by far the lowest initial flux (indicating residual fouling and a very quick loss of flux due to adsorption etc.) and showed a fairly steep decline. The AS+BF showed by far the highest initial flux based on superior cleaning technology. However, the flux declined similarly as the NON enhanced flux, possibly due to the increase of the MLSS during the test series, from MLSS = 12.5 g/L up to 18.1 g/L.

The differences in comparison between the AS+BF graphs in Figs. 6.4 and 6.6 are most likely based on how the data is collected. However the electronically

collected data seems more trustworthy. Referring to earlier experiments [8], it seems that the flux decline curve for long term applications of AS+BF systems can be divided in two sections, one with a steeper flux decline, as evident from Figs. 6.4 and 6.6, and another decline subsequent to 20-30 days of operation with a near zero flux decline.

At the end of the second test series, we investigated whether depressurization could raise the flux through cake/membrane decompression. As can be seen for both graphs, an interruption of the filtration procedure by exactly 30 minutes increases the flux without any further treatment, having an effect prior to the sponge ball cleaning. After the sponge ball application the combination of AS+BF does not show any further flux increase; rather, a decline indicates that there was almost no cake that could be swiped away with the help of the sponges.

The NON system shows the highest flux jump in the graph subsequent to the sponge passages, indicating that chemical cleaning is unable to overcome all mechanical membrane fouling impairing the surface properties.

6.6.3 Initial Flux observations

Fig. 6.6 indicates that from the initial flux something can already be derived about further flux development. It seems to be reasonable to implement observations regarding initial fluxes or alternative permeability. Fig. 6.7 shows the results of a row of initial fluxes obtained with the same experimental setup under similar operating

conditions, paying closer attention to the CFV. For the two different cleaning procedures prior to the test, it can be seen that the initial flux/permeability for wastewater filtration increases with the CFV. The observed relationship is almost proportional for the caustic/acid combined cleaning and less pronounced for cleaning exclusively with NaOH. Fig. 6.7 does not give any information about possible membrane aging. Thus Figs. 6.8 and 6.9 show the cleaning success of both procedures vs time. It can be concluded from Fig. 6.8 that the NaOH cleaning is not appropriate to maintain 100% equal startup conditions for test series, especially if longer test runs are the object. Even if the average graphs for CFV and P show the same trend, the velocity graph is almost horizontal and the decline for the permeability is 45 times steeper than that for the velocity. The last four data points in particular are recorded under higher CFV than points 2 and 3, but show a sturdy trend toward declining values.

Fig. 6.9 shows similar trends for permeability and CVF over time. The inclination of the velocity is about 10 times steeper than that of permeability, which essentially confirms the results presented in Fig. 6.7.

Finally, it can be stated that with chemical cleaning based solely on treatment with NaOH the cleaning result are not sufficient, revealing noticeable membrane aging. One indication of this in practice is substantially increased soaking times for NaOH for equal volume passages of the cleaning agent, eventually resulting in 8 times longer soaking times (up to 8 hours). The combined cleaning with caustic+acidic solutions otherwise shows acceptable results over longer times.

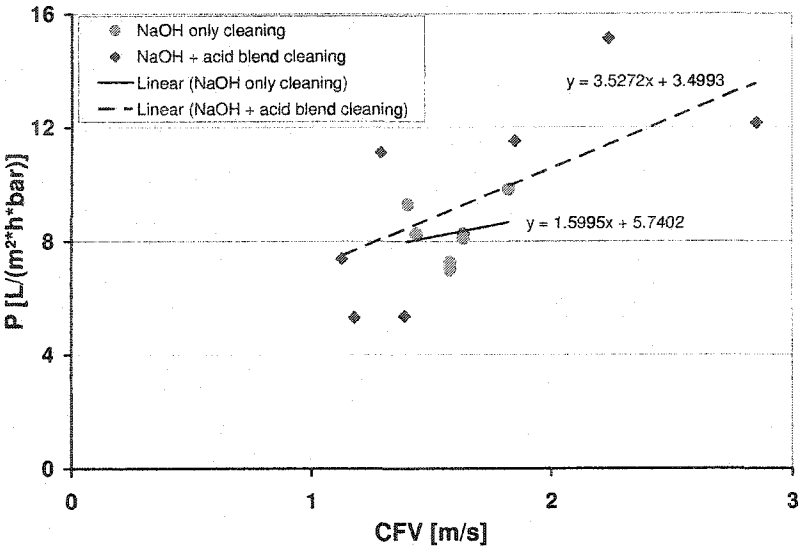

Fig. 6.7. Initial permeability and CFV for synthetic wastewater filtration of NaOH-only treated membranes and membranes cleaned with NaOH plus an acid blend (H_3PO_4 + citric acid)

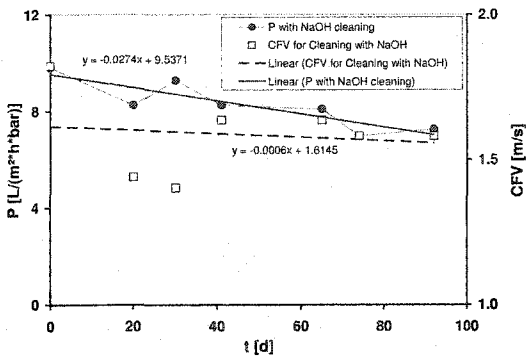

Fig. 6.8. Initial permeability of only NaOH treated membranes under consideration of CFV.

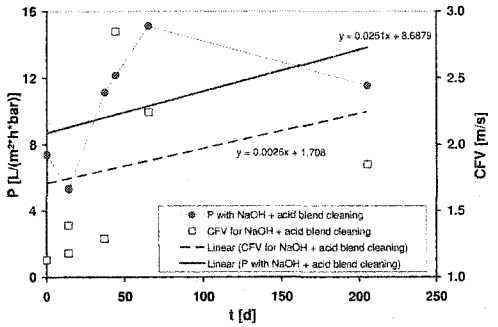

Fig. 6.9. Initial permeability of NaOH plus acid blend treated membranes under consideration of CFV.

6.6.4 Experimental resistance analysis

With the experimental results obtained as shown in Fig. 6.6, we can determine the single components of the total filtration resistance. Starting with a flux balance as shown in eq. 6.11:

$$J_0 - J_{t1} = \Delta J_{t1} \qquad \text{eq. 6.11}$$

with J_0 = initial Flux, J_{t1}= Flux at time t1 and delta J_{t1}= Flux difference at time t1. After substituting eq. 6.1 for J_{t1} and rearranging eq. 6.11 over eqs. 6.12 and 6.13, we are able to isolate the cake resistance R_c, as shown in eq. 6.14.

$$J_0 - \Delta J_{t1} = \frac{TMP_1}{\mu_1 * (R_m + R_c + R_f)} \qquad \text{eq. 6.12}$$

$$\frac{TMP_1}{\mu_1 * (J_0 - \Delta J_{t1})} = R_m + R_c + R_f \qquad \text{eq. 6.13}$$

$$R_c = \frac{TMP_1}{\mu_1 (J_0 - \Delta J_{t1})} - R_m - R_f \qquad \text{eq. 6.14}$$

With the assumption that after ten passages of oversized sponge balls (ca. 10% over tube diameter) no filter cake remains on the membrane surface, eq. 6.1 changes to eq. 6.15 for the case of flux J_{t2}:

$$J_{t2} = \frac{TMP_2}{\mu_2 * (R_m + R_f)} \qquad \text{eq. 6.15}$$

Rearranging eq. 6.15 yields the fouling resistance R_f, as shown in eq. 6.16:

$$R_f = \frac{TMP_2}{\mu_2 * J_{t2}} - R_m \qquad \text{eq. 6.16}$$

The membrane resistance was assumed to be the average initial resistance of the enhanced filtration tests. To determine the membrane resistance, the initial flux is measured, and it is assumed that neither cake nor fouling have accumulated yet. For NON enhanced filtration these circumstances are difficult to provide; thus, the initial flux does not match results with the assumption of no substance accumulation.

For the NON test, membrane aging takes its toll as shown in Fig. 6.8, which results in a negative fouling resistance. This "membrane aging" may be explained by the fact that any membrane cleaning before the sponge ball application was only provided by chemical cleaning, which presumably left some fouling material behind.

With the measured average membrane resistance, and substituting eq. 6.16 in eq. 6.14, we are able to obtain the cake resistance R_c. The final values for the singly resistance components based on measurement results are shown in Fig. 6.10. Data that was used for the calculation or might have influenced the results (CFV) is shown in Table 6.3, where electronically harvested data for AS+BF and BF was averaged with manually obtained data.

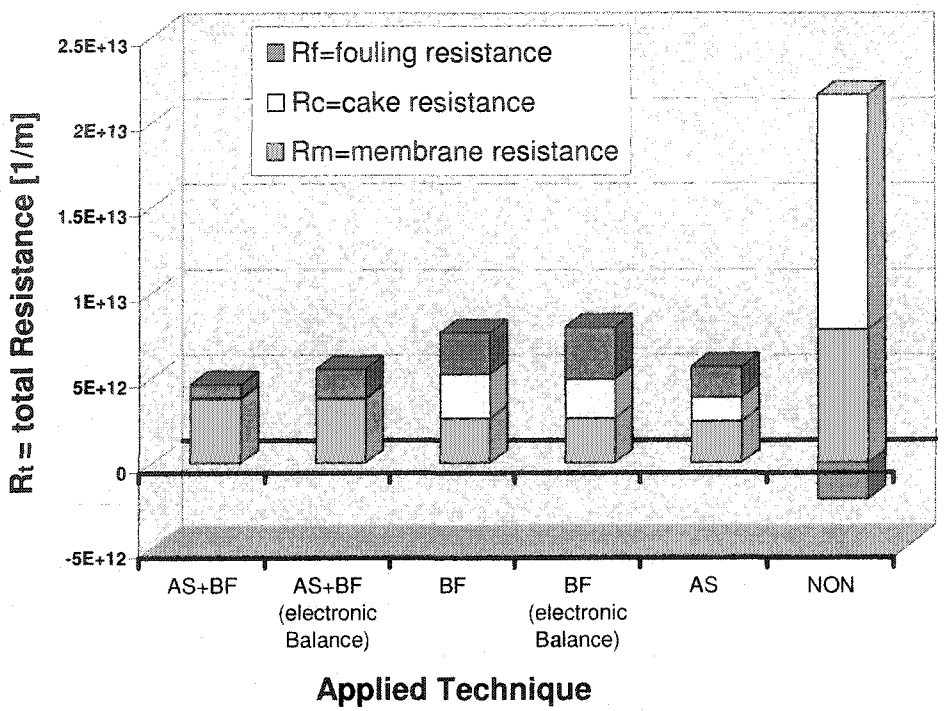

Fig. 6.10. Preliminary results for the single resistance analyses.

Table 6.3. Operation parameter as base for Figs. 6.6, Fig. 6.10. and Fig. 6.11.

	J_0	P_0*	CFV$_0$	μ_0	$Jt1$	P_1*	CFV1	μ1	$Jt2$	P_2*	CFV	μ2	Rt	Rc	Rf
	L/(m²h)	kPa	m/s	mPas	L/(m²h)	kPa	m/s	mPas	L/(m²h)	kPa	m/s	mPas	1/m	1/m	1/m
AS+BF	37.0	147	1.71	4.00	21.5	149	1.45	4.80	21.95	148	143	4.88	**$4.99*10^{12}$**	**$2.08*10^{10}$**	**$1.94*10^{12}$**
BF	30.4	117	3.00	5.30	17.4	144	2.87	3.84	24.38	139	2.46	3.83	**$7.36*10^{12}$**	**$2.02*10^{12}$**	**$2.31*10^{12}$**
AS	30.3	109	1.87	5.30	21.5	128	2.03	3.84	25.82	115	1.82	3.79	**$5.21*10^{12}$**	**$9.8*10^{11}$**	**$1.19*10^{12}$**
NON	17.0	152	1.85	4.00	5.5	152	1.38	4.98	19.25	152	1.36	5.00	**$1.96*10^{13}$**	**$1.39*10^{13}$**	**$2.65*10^{12}$**

* P = TMP

Fig. 6.11 shows the final results from the split of the total resistance (as shown in Fig. 6.5). For the value of the AS+BF systems, the manually and electronically harvested data was averaged. The membrane resistance Rm = $3.03*10^{12}$ [1/m].

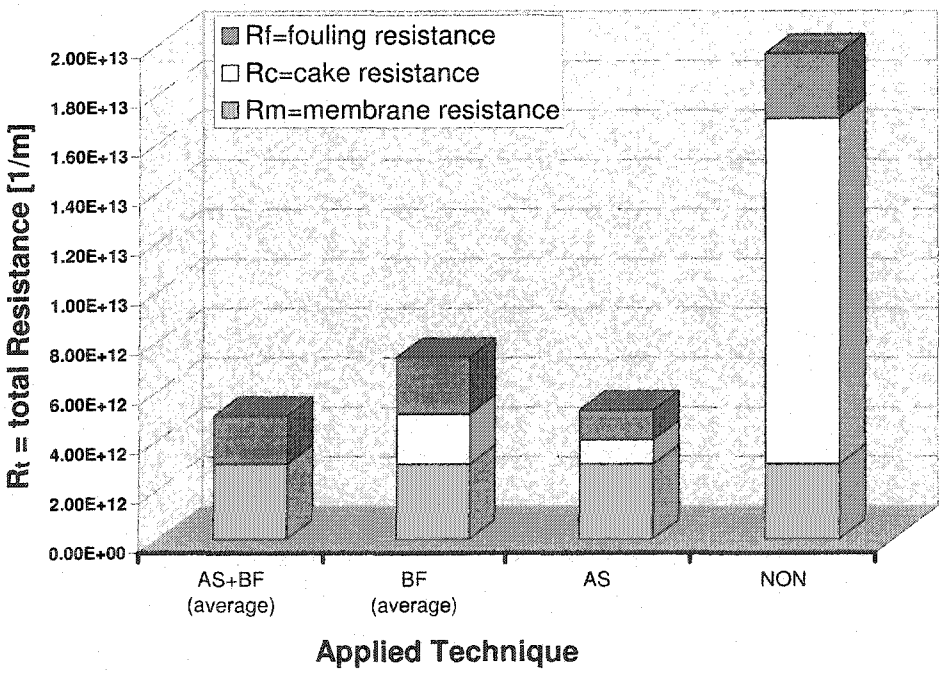

Fig. 6.11. Graphical conversion of experimentally determined single resistances.

The lowest overall resistance R_t was measured for the combination of AS+BF. The second lowest total resistance was observed for the AS system. If only BF was provided, the overall resistance was higher than the one for the systems which utilized air sparging, but still far less than the total resistance of the NON enhanced filtration. As discussed earlier, the intrinsic membrane resistance was assumed to be equal for all systems based on the average membrane resistance for the enhanced filtration.

The cake resistance R_c was (as expected) highest for the NON case. Backflushing was obviously unable to remove the cake sufficiently. Under consideration of comparably high CFV, a fairly dense and sturdy cake layer can be expected. The AS system showed remarkably less cake resistance than the NON case and the BF system, one of the major surprises of these investigations. Up to this point, reports available in the literature based on theoretical derivations for inorganic filter cake claim that the cake layer for AS systems is thicker than for applications without air sparging [23; 24]. It might be possible that this difference is related to the investigated solutions, since neither of these sources worked with wastewater; rather, both used nonliving model solutions. The cake resistance for the AS+BF was so low that it is not really visible in the scales of Figs. 10 and 11. However, Table 6.3 reveals the measured value for the AS+BF cake resistance, and it is at least about two orders of magnitude smaller than the R_c value for the other techniques.

The fouling resistance R_f did not vary much for the different types of membrane applications. All systems showed a fouling resistance between 1.2 -2.65*10^{12} [m^{-1}].

For the exact data, see Table 6.3. If the NON enhancement technique was provided, the fouling resistance was highest. If BF only was provided, the fouling resistance was second highest. The combination of AS+BF showed less (but still a considerable quantity of) fouling, but very close to the BF only application. The fouling resistance of the AS+BF system might suffer from continuous exposure of the membrane to the particles, since almost no shelter by an existing cake layer was available.

Fig. 6.12 presents data, obtained earlier from the described setup (at similar operation conditions), on how the evolution of a cake layer may influence flux development if different enhancement strategies are deployed. In this case, a noticeable cake development was arranged from Day 12 until Day 20. A backflush test (5 times at 120 kPa above TMP) was able to double the flux, which subsequently decreased in the typical manner. From Days 18 to 20, AS was provided, which was able to maintain the flux during this time with no noticeable decline. After additional deployment of BF, the flux increased by a factor of 5. This successful procedure (as shown in Fig. 6.12) is most likely based on the two step principle as presented by *Flemming* [14]:

1. Weakening of the matrix (it is assumed that AS generates higher film/cake porosity)
2. Removal of the film/cake

However, subsequent to stopping AS, the flux declines relatively fast, showing that if no cake covering is provided the fouling increases.

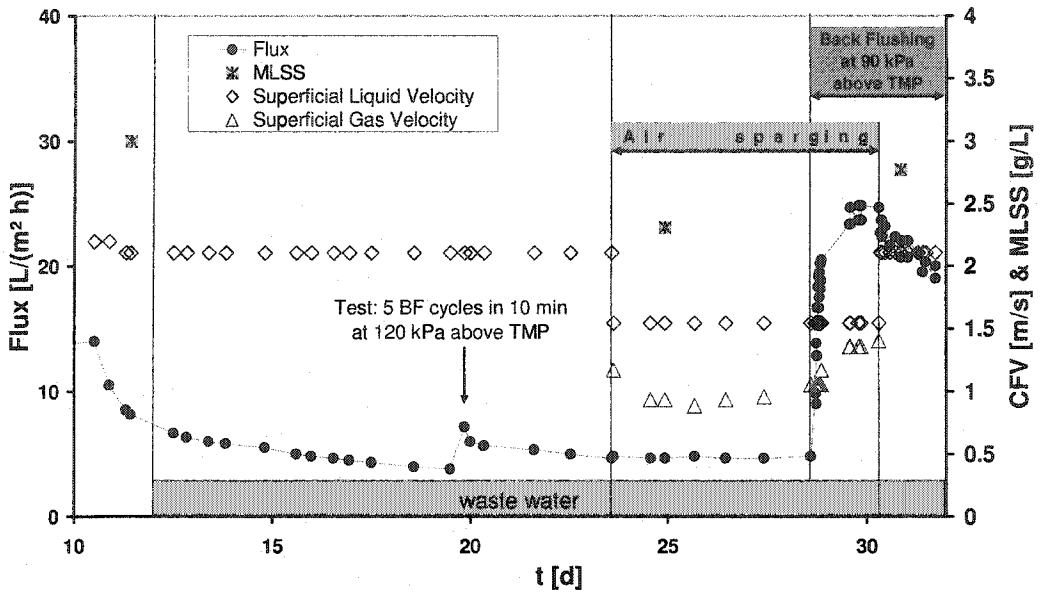

Fig. 6.12. Example of possible operation conditions which may impact flux development.

6.7 Evaluation of theoretically determined cake resistance values

The theoretically determined values for the cake resistance as derived in Section 6.3 (resistance analysis), partially calculated with the results from Section 6.4 (cake thickness), are numerical depicted in Section 6.5 (overview), Table 6.2. However, it is important to validate this model through comparison to the real cake resistance as measured in the NON case; see Table 6.3 and Fig. 6. 11. In a graphical conversion of the obtained data, Fig. 6.13 gives a comparison of the Rc values for the model data and actual measurements.

Model A I yields numbers too large by several orders of magnitude. Model A II and both B models yield findings acceptable for rough estimations. Model A II and

B I yield results that best fit the experimental measurements. Similar to Model A I, both C models yield results that are off (to small) by several orders of magnitude. For the calculation and the typical properties of these models see Section 6.3.

This investigation shows that oversimplified models such as C and too-elaborate models, such as A I, give not the expected returns. Using too-exact data for equations and estimating numbers can yield poor findings, perhaps because they contain safety factors which add up and lead to overestimation, as in Model A I.

Another explanation for the "failure" of the sophisticated Model A I might be that the wastewater flocs are more permeable than assumed. Even if it sounds plausible that the void fractions are filled with EPS, the assumption that the "solid" fraction is almost impermeable must be wrong!

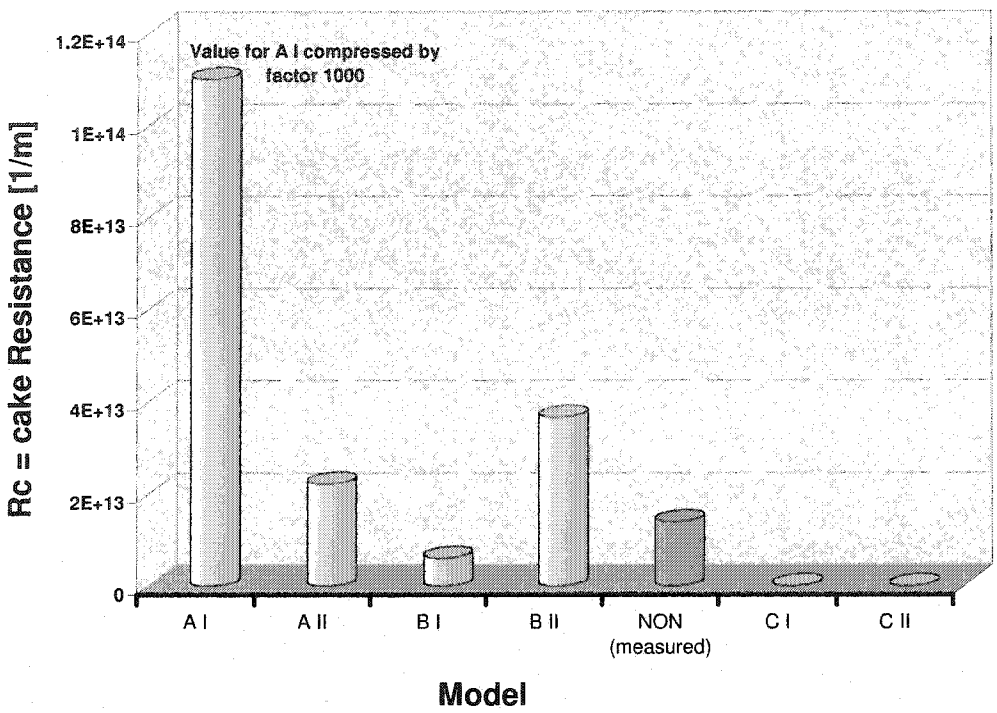

Fig. 6.13. Graphical comparison of theoretically obtained cake resistance values (light) based on Table 6.2 and experimentally obtained values (dark) based on Table 6.3 for NON.

6.8 Backflush resistance

Results from the backflush volume observations displayed as permeability vs time under consideration of the CFV are given in Fig. 6.14. Both graphs look similar to their respective flux graphs (since there was not much change in TMP, there is not much difference in the shapes of Flux and Permeability graphs) for the normal flow direction. The BF-only graph shows no significant trend, and the AS+BF graph shows a decline. It might be concluded from these graphs that the cross flow velocity has a considerable impact on the BF permeability. Both permeability graphs show

comparably high values (Day four AS+BF and Say 8 BF) near the time of the highest CFV measurements. However, at the end of the BF-only observations, the high CFV obviously does not impact the permeability anymore. Thus it might be concluded that subsequent to a threshold cake layer and fouling accumulation, the CFV has no impact on the BF permeability. Another strong relationship apparently exists between the temperature of the BF water and the BF permeability.

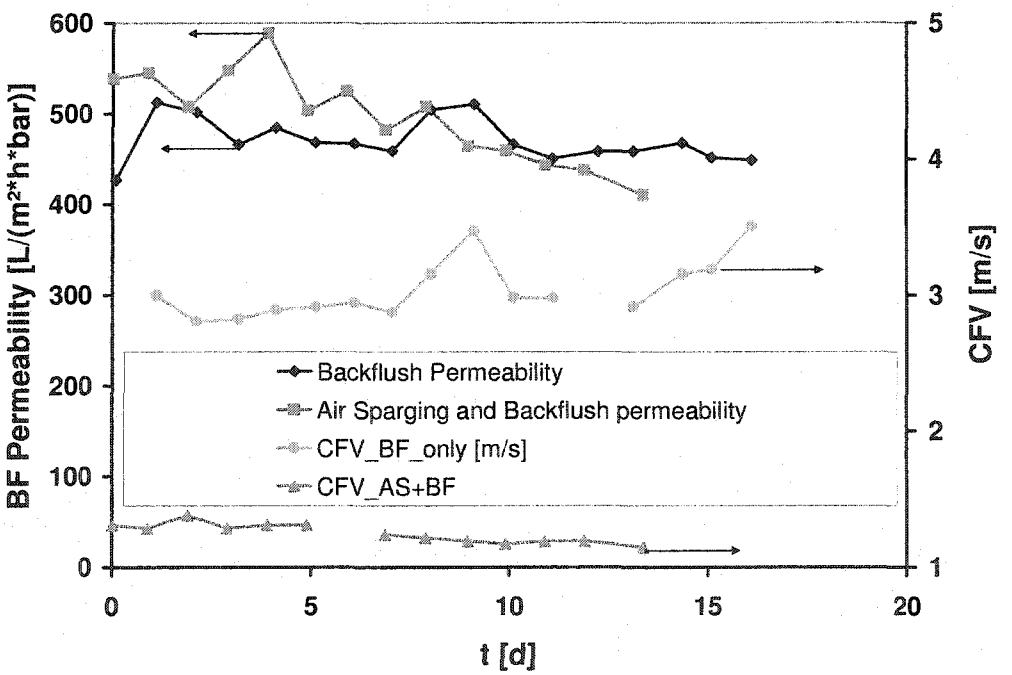

Fig. 6.14. Backflush permeability and CFV vs time.

Fig. 6.15 presents the total BF resistance R_t, calculated according to eq 6.1. The basis for the values given in Fig. 6.15 is the values shown in Fig. 6.14. The Backflush

resistance for the BF-only case shows a marginal incline, which basically confirms the flux observations with almost no flux decline subsequent to Day 1 of the observations. The permeability for the AS+BF combination reveals a steady increase in the overall resistance, confirming the flux data, crossing the graph of the BF-only resistance after 9 days. One advantage of overall BF resistance determination: it is not impacted by changes of the MLSS within the reactor and thus responds only to temperature and CFV in addition to fouling influences. Even if for the start of the setup a relatively strong relationship between CFV and overall Backflush resistance is assumed, this relationship should weaken after build up of a serious cake layer. After cake layer development, the speed at which the fouling is gaining ground should slow down considerably. This is not the case for the AS+BF system; the overall BF resistance increases continuously with time, whereas the overall Backflush resistance for the BF-only application rises only gently because a stable cake layer presumably prevents further fouling. It seems the overall BF resistance is more directly sensitive to the fouling resistance.

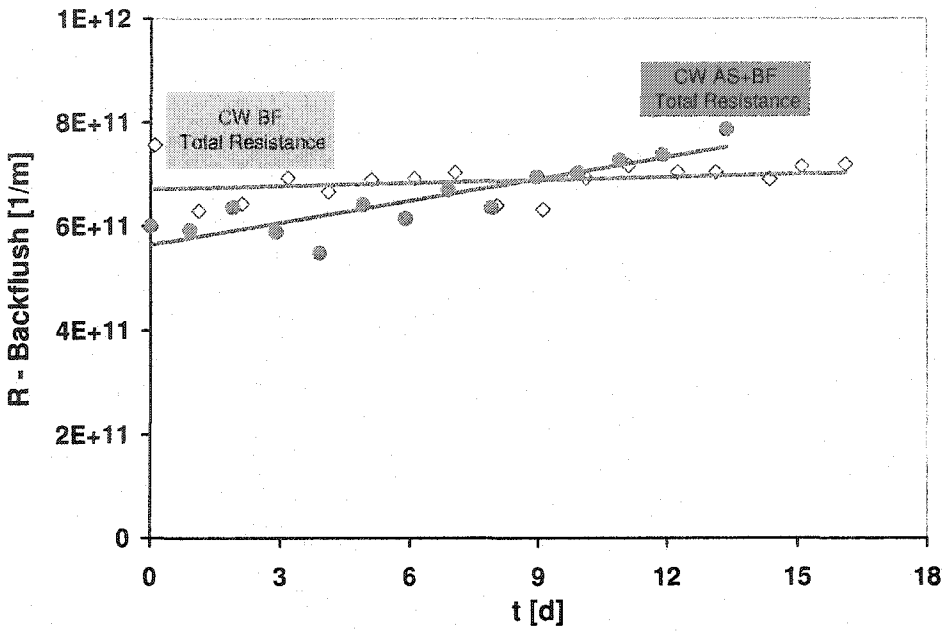

Fig. 6.15. Total resistance of the membrane against BF.

6.9 Conclusions

In this study different techniques for flux enhancement of synthetic wastewater filtration are investigated, and a resistance analysis that compares three different models for calculation of cake resistance arising in membrane filtration processes was made. Because one of the models requires cake thickness as input for the resistance analysis, the thickness was measured (via SEM) for the different enhancement techniques. From the non-enhanced system (NON) (about 50μm thickness) to back flushing only (BF), to air sparging combined with backflushing(AS+BF), and finally airsparging (AS) only, the cake thickness decreased, according to the findings revealed by the SEM technique. The differences between the cake thicknesses

measured for the enhancement techniques are not very pronounced (between 7 and 12 μm), and the measurement technique can only give a local estimate. However, removing the cake at the end of the filtration process essentially confirmed the SEM observations, yielding the lowest cake thickness for both the air sparging enhanced techniques. This result stands in opposition to literature about AS application for inorganic model solutions, which generally claim, based on theoretical proofs, that the cake thickness increases if AS is provided. The AS technique in combination with a cross flow velocity (CFV) of about 2 m/s shows the lowest fouling propensity; meanwhile the enhancement techniques which include BF show about equal fouling resistances. The highest fouling resistance is observed for the NON enhanced case. It seems to be confirmed that the cake build-up gives the membrane a "safety coating" that prevents more fouling. However, the highest flux yield for the time frame investigated shows, the combination of air sparging and backflushing performs best.

Furthermore, the findings show that there exists a relationship between the initial flux and the CFV. It was also found that for cleaning membranes used in synthetic wastewater applications, particularly with local tap water, cleaning with NaOH is not sufficient. The combination of acid and caustic cleaning methods performs best.

Comparing the results from several theoretical models for cake resistance with the experimental results for NON enhanced filtration revealed that models that are too sophisticated or oversimplified give less acceptable results. Testing the membrane resistance via backflushing revealed that there are analogies between the resistances

of both flow directions. It seems possible that before build up of a severe cake layer, a relationship between BF resistance and CFV exists.

Acknowledgements

Special gratitude to the Grundfos company which supported our study with a multistage pump and further equipment and to the Microdyn-Nadir company which donated the membrane modules. We acknowledge funding of this project through a grant from the USGS/NIWR. Moreover the authors thank Professor Mikulasek et al. from the University of Pardubice Czech Republic, for making recently published papers from their institute available.

6.10 References

[1] R. Wakemann and C. Williams, Additional techniques to improve microfiltration, Separation and Purification Technology, 26, 3-18. (2002).

[2] C. Cabassud, S. Laborie and J. M. Laine, How slug flow can improve ultrafiltration flux in organic hollow fibres, J. Membr. Sci. 128, 93-101, (1997).

[3] S. Levy, Two-Phase Flow in Complex Systems, Interscience, 1999. ISBN: 0471329673.

[4] R. Ghosh and Z. Cui, Mass transfer in gas-sparged ultrafiltration: upward slug flow in tubular membranes, J. Membr. Sci., 162, 91-102 (1999).

[5] W. Bowen, J. Calvo and A. Hernandez, Steps of membrane blocking in flux decline during protein microfiltration, J. Membr. Sci., 101, 153-165. (1995).

[6] J. Mallevialle, P. Odendaal and M. Wiesner, Water Treatment Membrane Processes, McGraw-Hill, New York, ISBN 0-07-001559-7. (1996).

[7] C. Psoch and S. Schiewer, Synthetic wastewater preparation and aeration via air sparging in a sidestream MBR. to be submitted to Water Research (in preparation), (2005).

[8] C. Psoch and S. Schiewer, Long term investigation of aeration and flux improvement by air sparging and backflushing for a membrane bioreactor. to be submitted to Water Research (in preparation), (2005).

[9] C. Orr, Filtration: principles and practices, Part I, Marcel Dekker, New York, ISBN 0824762835, (1977).

[10] H. Brauer, Grundlagen der Einphasen- und Mehrphasenströmung, Verlag Sauerländer, Aarau (Swiss) and Frankfurt am Main (Germany), (1971).

[11] S. Hermanowicz, Membrane Filtration of biological solids: A unified framework and its applications to membrane bioreactors, IWA Special. Conference, WEMT 2004, June 7-10, Seoul, Korea, paper M-2-12, (2004).

[12] J. Kim, C. Lee and H. Chun, Comparison of ultrafiltration characteristic between activated sludge and BAC sludge, Water Research, Vo. 32, No. 11, pp. 3443-3451, (1998).

[13] P. Park, S. Lee and C. Lee, Permeability of cake layers formed by chemical flocs in coagulation-membrane processes, IWA Special. Conference, WEMT 2004, June 7-10, Seoul, Korea, paper W-1-1, (2004).

[14] H. Flemming, Biofouling bei Membranprozessen, Springer Verlag Berlin, ISBN 3-540-58596-6, (1995).

[15] Metcalf & Eddy, edited by G. Tchobanoglous, and F. Burton, Wastewater Engineering, Treatment, Disposal and Reuse. McGraw-Hill Boston, 3rd edition, ISBN 0-07-041690-7, (1991).

[16] N. Cicek, J. Franco, M. Suidan, V. Urbain and J. Manem, Characterization and comparison of a membrane bioreactor and a conventional activated-sludge system in the treatment of wastewater containing high-molecular-weight compounds, Water Environment Research, Vol. 71, No.1, (1999).

[17] J. Happel, Viscous flow in multiparticle systems; Slow motion of fluids relative to beds of spherical particles, AICHE 4, , 2, pp. 197-201, (1958).

[18] J. Kim, C. Lee and I. Chang, Effect of pump shear on the performance of a crossflow membrane bioreactor, Water Research, Vol. 35, No. 9, pp. 2137-2144, (2001).

[19] D. Lee and C. Wang, Review paper: Theories of cake filtration and consolidation and implications to sludge dewatering, Water Research, Vol. 34, No. 1, pp. 1-20, (2000).

[20] K. Parameshwaran, A. Fane, B. Cho and K. Kim, Analysis of microfiltration performance with constant flux processing of secondary effluent, Water Research, Vol. 35, No. 18, pp. 4349-4358, (2001).

[21] I. Chang, P. Le-Clech, B. Jefferson and S. Judd, Membrane fouling in membrane bioreactors for wastewater treatment, Journal of Environmental Engineering, Vol. 128, No. 11, pp. 1018-1029, Nov. (2002).

[22] Cheryan M., Ultrafiltration and Microfiltration Handbook. Technomic Publishing Co. Inc. Lancaster, Basel, ISBN: 1-56676-598-6, (1998).

[23] S. Laborie, C. Cabassud, L. Durand-Bourlier and J. Laine, Flux enhancement by a continuous tangenial gas flow in ultrafiltration hollow fibers for drinking water production: effects of slug flow on cake structure, Filtration & Separation, pp. 887-891, October (1997).

[24] P. Mikulasek and P. Pospisil, Influence of two-phase gas-liquid flow on permeate flux and cake characteristics in ceramic membrane crossflow microfiltration, scientific papers of the Univ. of Pardubice, Series A, Faculty of Chemical Technology 6, pp. 79-94, (2000).

7 Critical flux aspect of air sparging and backflushing on membrane bioreactors[6]

C. Psoch and S. Schiewer*

Department of Civil & Environmental Engineering; Water & Environmental Research Center, University of Alaska Fairbanks, AK 99775; USA

Abstract

Membrane bioreactors (MBR) combine biological processes with membrane filtration. The main obstacle to efficient operation remains the deterioration of membrane permeability with time. One possible approach to the fouling issue is sub-critical flux operation. Other options are air sparging and backflushing. This study investigated the impact of air sparging and backflushing on flux enhancement, as well as exploring the relationship between use of these strategies and critical flux. The research was accomplished in pilot plant scale using a 70 L reactor fed with glucose-based synthetic wastewater at temperatures around 20°C and MLSS of approximately 10 g/L. Results showed that air sparging and backflushing each increased the flux in the MBR. Using both strategies at low transmembrane pressures (TMP) yielded the most substantial flux enhancement (factor 2) at sub-critical conditions. Without enhancement, no critical flux could be identified for permeate flow rates of less than 2/3 of the limiting flux, and the flux dropped to 20% of the limiting flux after 8 days in pseudo-steady state. With a combination of air sparging and backflushing at low

[6] Desalination, Elsevier (in press) 2005

TMP (38 kPa), it was possible to maintain flux for the same time frame at about 40% of the limiting flux. The fact that no fouling occurred indicates (by definition) sub-critical flux.

Keywords: membrane bioreactor, fouling, critical flux, limiting flux, pseudo-steady state flux, air sparging, backflushing, synthetic wastewater

* Corresponding author: Tel.: ++1 (907) 474-2620; fax: ++1 (907) 474-6087, E-mail address: ffsos@uaf.edu

7.1 Introduction

To handle the annoyance of fouling is one of the main challenges of membrane technology. One approach to the fouling problem is operation below what is often termed "critical flux". According to one of the first papers on this topic, published by *R. Field et al.* [1], no flux decline over time periods of several hours occurs if the flux, defined as a combination of driving force (TMP) and hydrodynamics, does not exceed a certain threshold value. This "critical flux" is by definition the flux below which no particle accumulation on the membrane surface occurs.

According to *J. Howell* [2], critical flux must be distinguished from the limiting flux, which is the maximum flux possible by incrementally increasing the transmembrane pressure. *Bacchin* [3] suggested that under certain conditions the critical flux is about 2/3 of the limiting flux. Since the limiting flux increases at higher crossflow velocities (CFV) according to the film theory model (see for instance *Mulder* [4] and *Cheryan* [5]), the CFV significantly impacts the level of critical flux as well. Subseq.uently, higher transmembrane pressures can be applied with less particle deposition, which results in higher critical fluxes ([6], [7]). Sufficient shear stress, achieved at sub-turbulent or turbulent flow conditions and indicated by dimensionless parameters such as Reynolds, Shear Stress or Fouling numbers, prevents particle deposition on the membrane surface and, ultimately, external fouling [8].

In tubular membranes, one way to deliver shear stress is to inject air (air sparging = AS) into the system to generate a two-phase flow. If liquid and gas flow together in a tube, several flow patterns develop, depending on air injection ratio, pipe diameter, interfacial tension and inclination. For air-sparging, slug flow is the most successful flow regime, because it enhances the cross flow hydrodynamics near the membrane surface, which helps maintain stable permeate fluxes over longer time periods [9-11]. In addition to water and air slugs, which strongly influence the concentration polarization layer, a parallel water film flows in countercurrent to the rising gas slugs [12-14]. The most severe turbulence phenomena occur within the wake zone of the gas slugs, where, in tubular membranes, smaller gas bubbles move after the gas slugs in heavily turbulent movements [15]. These turbulent movements, associated with small gas bubbles, are to some extent able to dislocate and remove cell debris and particles, which otherwise would accumulate and partially clog the pore channels [16].

However, according to *A. Marshall et al.* [17] severe pore plugging occurs in microfiltration of proteins, such as those found in waste water. *G. Belfort et al.* [18] corroborate this statement and emphasize that the intrusion of macromolecules, colloids and particles limits microfiltration. Similarly, *P. Bacchin et al* [19] state that pressure-driven membrane filtration is impossible without mass accumulation. Our own prior experiments have shown [20] that solely the allocation of ample hydrodynamics, proven with appropriate dimensionless numbers, is not sufficient to prevent flux declines over longer time periods due to internal fouling.

One technique for reducing internal fouling is backflushing (BF). Backflushing pushes clear water (for instance permeate), back into the feed stream and it minimizes pore blockage (internal fouling) in the deeper layers of the membrane and channel clogging near the membrane surface. Backflushing's effectiveness decreases with growing deposited layer thickness, as pressure and velocity decrease along the flow passage according to Darcy's law. One disadvantage of backflushing is the energy req.uired to achieve a pressure suitable for flow reversion; another is the unavoidable product loss, which can severely decrease the recovery rate at higher flow volumes. The objective of this study was to examine these antifouling technologies individually and in combination, and to identify a critical flux where no fouling occurs, even over several days.

7.2 Materials and methods

For the experimental setup (see Fig. 7.1), an activated sludge tank with a capacity of 60 - 80 liters was used. A multistage pump (Grundfos) moved the activated sludge through braided hoses ½ inch diameter to the membranes and back to the bioreactor. A thermostat maintained reactor temperature at around 20°C.

The experiments were carried out with three vertical membrane modules, which were deployed in parallel. Each membrane module (Microdyn-Nadir) consisted of three polypropylene membrane tubes (pore size 0.2 μm) in a plastic housing of 0.75

m length. The diameter of the tubes was 5.5 mm, yielding a membrane surface area of 0.036 m^2 per module.

One module (see Fig. 7.1, "membrane module") featured an air sparging system: On each end of the module, a 15 cm long acrylic rod extended the membrane tube. On one side (the lower), three perpendicular drilled entries served for air supply to each tube. Each air supply included its own adjustable air valve. The total air volume stream was monitored by a volume flow meter, a mass flow meter, and a pressure gauge. The air pressure was between 60 kPa at an aeration rate of 3.5 L/min and 125 kPa at an aeration rate of 8 L/min. Fluctuation of airflow was prevented by the mass flow meter. On the other side (the upper), the acrylic rod served as a viewing area for flow pattern observation.

Two modules (the membrane module and add-on module II; see Fig. 7.1) were eq.uipped for backflushing. Cross flow velocities (CFV) of the water (for all three modules) within the membrane tubes were between 1.08 and 2.85 m/s. For the module with acrylic extenders, the flow pattern was observed with a stroboscope; observations with the naked eye were impossible. With flow velocities exceeding 1 m/s, monitoring the flow pattern in the system was a challenge. The application of a stroboscope brought some remedy, but still the flow patterns varied too rapidly to obtain good photographs with a conventional camera.

The pump speed and thus the pressure for the backflush pump (submerged pump, MP1, Grundfos) were regulated over a variable freq.uency drive. The experiments

were carried out with a low backflush pressure of about 60 kPa (ca. 0.6 bar) above the transmembrane pressure (TMP), to minimize the product loss.

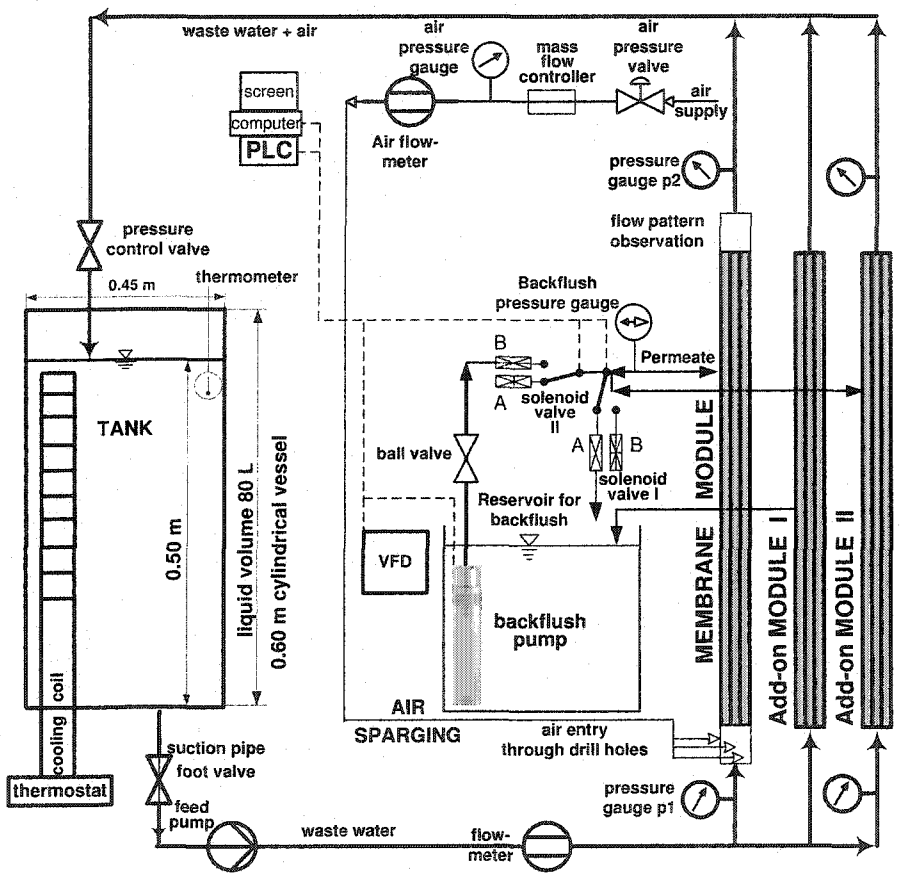

Fig. 7.1. Experimental setup scheme with activated sludge tank and the three membranes in parallel

With a programmable logic controller connected to a personal computer with additional software, the backflush cycle was regulated at every 30 minutes for 15 seconds, and two solenoid valves (solenoid valve I and II) were opened and shut alternatively to allow a reversal of the normal flow direction within the membrane. In

case the "membrane module" was operated with air sparging and backflushing, the backflush procedure was superimposed over the continuously running air sparging. Synthetic wastewater was prepared as described in *C. Psoch and S. Schiewer* [21]. The main carbon source for the reactor microbes was supplied by a dosage of 60 g glucose per day. In addition, a supplement of trace elements and different sources of carbon, nitrogen and phosphorus was added daily for sustainable microbial growth. The mixed liquor suspended solids (MLSS) content in the reactor was determined according to the *Standard Methods* [22].

In this study at first the limiting flux for the used membrane type was determined by stepwise increasing the transmembrane pressure (TMP). Subseq.uently tree data sets were performed based on operating all three modules for about a week.

Prior to all experimental runs, a chemical cleaning of the membranes was conducted to achieve largely the same initial conditions at each test series. The cleaning was accomplished by soaking the membranes in hot NaOH at about 60°C from the permeate side for an hour, followed by an intensive flush with de-ionized water for about 4 hours.

The first test series was performed with increasing transmembrane pressure (TMP) and moderate cross flow velocity (CFV), pursuing nearly constant flux. Air sparging ("MEMBRANE MODULE"), NON-enhanced flux ("Add-on MODULE I"), and backflushing ("Add-on MODULE II") were compared at MLSS between 9.8 and 11.5 g/L.

During the second test series, the combination of air sparging and backflushing installed at the "MEMBRANE MODULE" was compared to NON-enhanced flux at both Add-on MODULES. At constant TMP of 88 kPa the AS+BF module was operated at ca. 1.35 m/s CFV and the NON modules at similar velocities.

Finally a third test series was performed with identical setup as in the second series but at lower CFV (ca. 1.15 m/s) and lower constant TMP (38 kPa) for the AS+BF module. For an overview of all experiments, see Table 1, in Results and Discussions.

7.3 Results and discussion

Fig. 7.2 documents flux development for conventional filtration at increasing transmembrane pressure. According to the classical approach for determining the limiting flux [4], which is defined as the maximum steady state flux obtained when increasing the pressure, Fig. 7.2 indicates a limiting flux of approximately 20 L/(m²h) for synthetic wastewater (MLSS=10.3 g/L, temperature 15.5°C and CFV=1.35 m/s). Based on *Bacchin's* approach [3], which specifies that under certain assumptions the critical flux is eq.ual to 2/3 of the limiting flux, a critical flux of approximately 13 L/(m² h) should be expected. An initial flux of about 11.5 L/(m² h) was chosen and TMP and CFV were varied. However, no sub-critical conditions were observed, since fouling occurred in all cases. This implies that the flux exceeded the critical flux (defined as the flux below which no fouling occurs).

Fig. 7.3 shows the permeate flux evolution over time for conventional filtration until a pseudo-steady state is achieved. The results were obtained as byproducts from the enhanced filtration and assure comparability of enhanced and conventional filtration. Tests for which no air sparging (AS) or backflushing (BF) was supplied are subseq.uently called the *NON*-case. One data set (IA and IB) was obtained at low liquid cross flow velocities (CFV) and high TMP, and one (IIA and IIB) at high liquid velocities and fairly low TMP. Cases IIA and IIB conducted under the similar conditions as the first data set and show the reproducibility of the experimental results. MLSS values ranged from 8.3 to 10.8 g/L in all cases. The higher flux for case IA compared to case IB was due to higher CFV's. Since a sharp flux decline was observed within the first two days at different filtration conditions, it can be assumed that the critical flux must be far below the chosen 11.5 L/(m² h). It may rather be close to the pseudo-steady state flux, which was 4-5 L/(m² h) after a time period of 8 days.

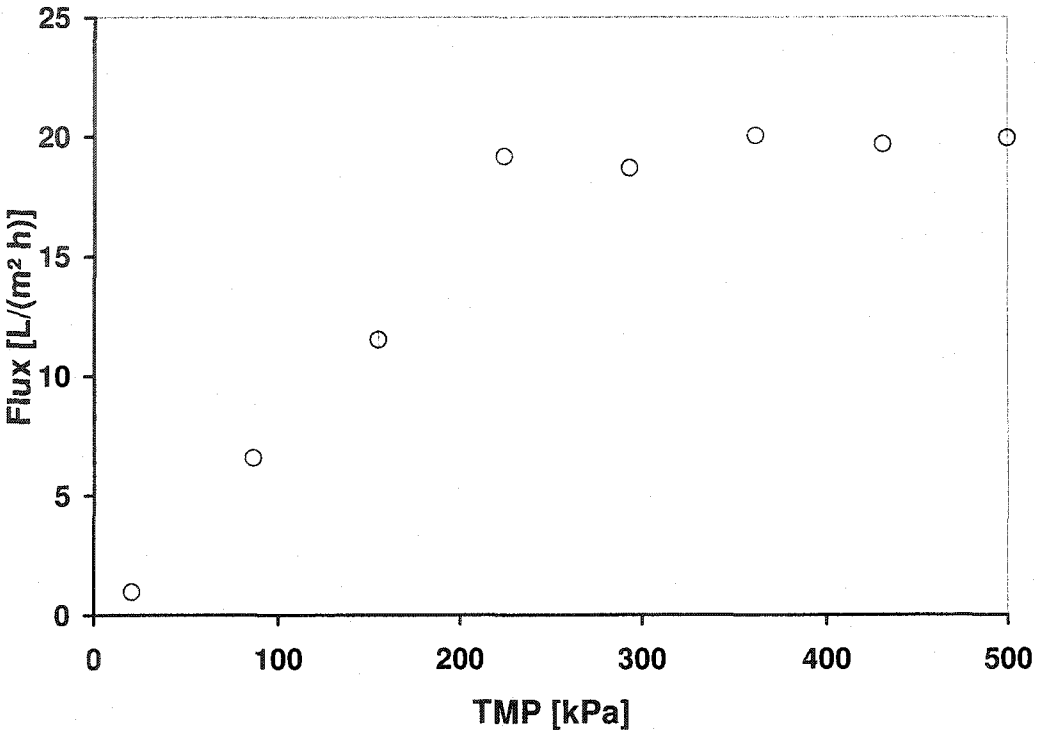

Fig. 7.2. Determination of the limiting flux of about 20 L/(m² h) for MLSS approx. 10 g/L, CFV approx. 1.35 m/s and approx. 15.5°C wastewater temperature.

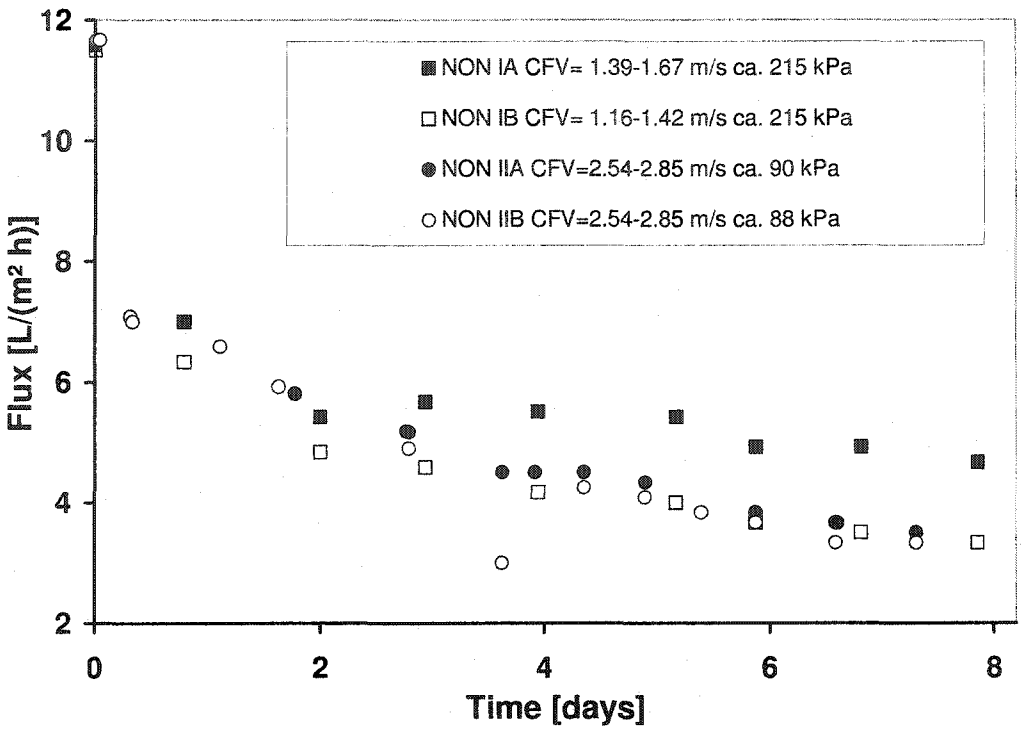

Fig. 7.3. Flux decline for NON-enhanced filtration to pseudo steady state at comparable conditions. wastewater temperatures about 17°C.

Fig. 7.4 depicts the permeability against time. The permeability is the quotient of flux and applied pressure. Three different cases are shown at almost identical conditions in terms of CFV, MLSS, and temperature: air sparged (AS) filtration, filtration with BF, and NON-enhanced filtration. In all three cases the permeability decreases significantly within the first 6 hours. For the AS filtration, a combination of a small, gradual increase of the air injection ratio (see eq. 7.1) from 0.4 to 0.59 and doubling the TMP from about 40 to 98 kPa (after 7 hours) could stabilize the permeability at a comparably high level after the initial decline. The permeability never dropped below 10 L/(m² h bar) and the flux was maintained at levels of

approximately 10-12 L/(m²h) up to the end of the trial, at about 5 days. No further increase of the TMP was necessary. The overall permeability decrease for AS within the investigated time frame was about 50%. Maintaining the flux with AS was unintentionally supported by a temperature rise within the reactor from about 23°C (after 1.6 days) to 28°C at the trial end, since the cooling capacity of the thermostat was exceeded.

The air injection ratio ε is defined according to *Vera et al.* [16] as

$$\varepsilon = \frac{u_{Gas}}{(u_{Gas} + u_{Liquid})} \qquad \text{eq. 7.1}$$

with:

u_{Gas} = superficial gas velocity, i.e. velocity if only gas was in the channel [m/s]

u_{Liquid} = superficial liquid velocity, i.e. velocity if only liquid was in the channel [m/s]

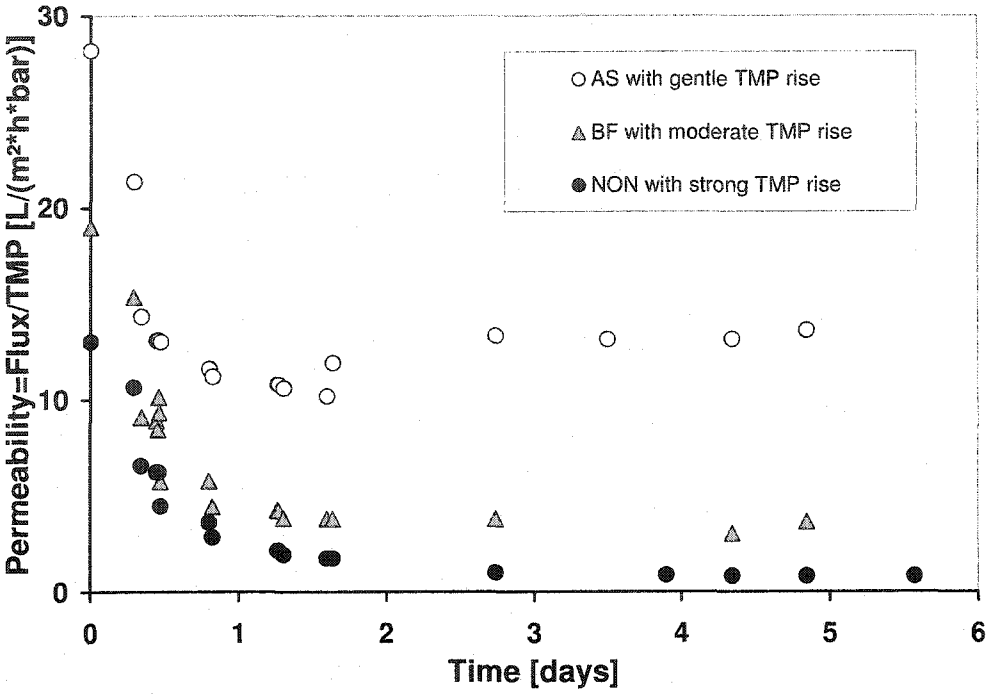

Fig. 7.4. Permeability= flux/TMP vs. time for AS, BF and NON-enhanced filtration at stepwise TMP increase. CFV are about 1.3 m/s for all cases and MLSS range between 9.8 and 11.5 g/L

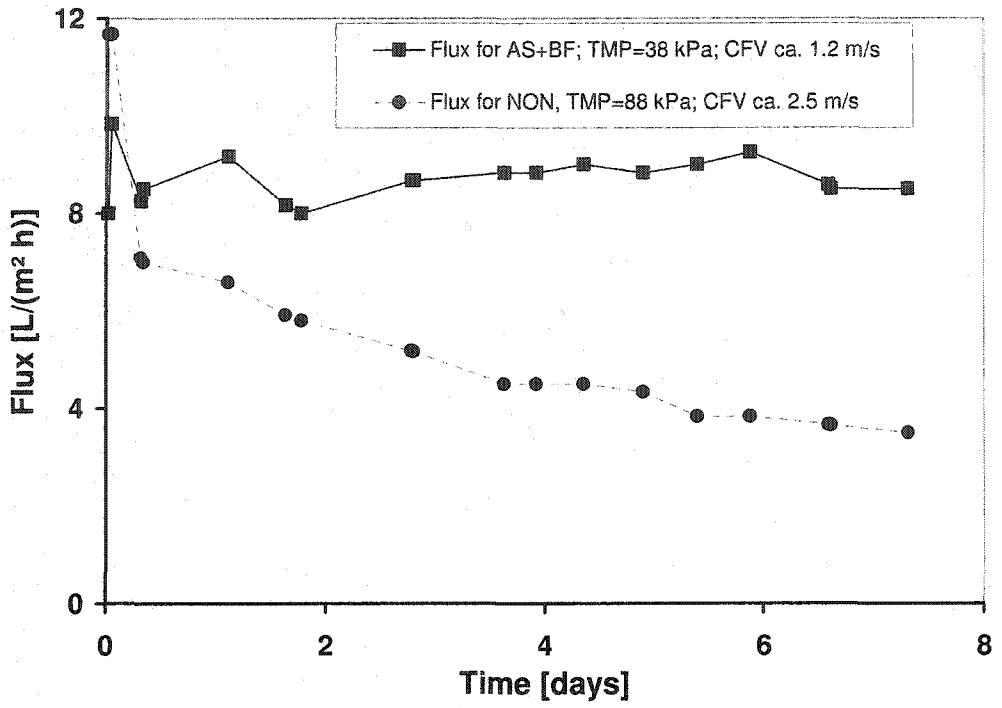

Fig. 7.5. Combination of AS+BF vs. NON-enhanced flux. MLSS between 8.3 and 9.1 g/L.

For the BF experiment, the permeability further decreased after the initial decline, but could be stabilized with a pressure increase from 80 to 350 kPa. Thus a permeability of about 3.5 [L/(m² h bar)] was obtained after approximately 5 days operation with the backflush technique, and the flux was maintained close to the initial value (data not shown). Throughout the test, the flux was comparable to that obtained for AS, whereby for AS filtration a much lower TMP was req.uired to maintain the flux at approximately 11 L/(m² h) (data not shown). The overall permeability decrease for BF within the investigated time frame was about 80%.

For the NON-enhanced filtration, which started at an already higher TMP of about 80 kPa, an increase of the TMP could not stabilize the permeate flux. The flux declined severely -- down to 2.7 L/(m² h) within less than 6 days -- in spite of incrementally increasing the TMP up to 350 kPa within 1.5 days. That resulted in a permeability decrease to about 3.5 [L/(m² h bar)] after 20 hours, with further decline to about 0.8 [L/(m² h bar)] at the end of the investigation cycle of 5 days. The overall permeability decrease for NON-enhanced filtration within the investigated time frame was about 94%.

Fig. 7.5 shows the flux evolution at constant TMP for enhanced flux by means of a combination of air sparging and backflushing (AS+BF) and NON-enhanced flux. The NON-enhanced test shows, after less than 6 hours, the typical flux decrease of filtration operated at super-critical flux, which later approaches pseudo-steady state filtration as described for Fig. 7.3. The NON-filtration cannot compete with the superior performance of the AS+BF enhanced filtration, even at about twice the TMP (approximately 88 kPa) and more than doubled CFV. The AS+BF enhanced filtration shows no signs of flux decrease over 7 days, even though by the end the velocity decreases slightly. That and choosing the highest flux (after 6 hours) during this test series as base value causes a permeability decline of 3.5% as in Table 1 expressed.

Sub-critical flux by definition does not decrease under constant boundary conditions. The flux for the combined enhanced filtration remains slightly above 8 L/(m² h) for the whole test period and so the critical flux for the combination of air sparging and backflushing must be above 8 L/(m² h). For the NON-case it was

impossible to identify any critical flux at different operating conditions. The flux sharply declined within 2 days to values of about 6 L/(m² h), as shown in Fig. 3, and declined further into a pseudo-steady state flux of about 4 L/(m² h) after 8 days. The critical flux must therefore be less than 4 L/(m² h) and thus definitely lower than that for the enhanced applications.

The combination of air sparging and backflushing operates at only 38 kPa pressure compared to 88 kPa for NON, and the CFV is less than half of that of the NON-case. In terms of energy req.uirements for filtration a combination of AS and BF is conseq.uently a more efficient technology.

The clearly different flux results in spite of similar shear stress numbers (data not shown) indicate that shear on the membrane surface alone is unable to prevent internal fouling due to the intrusion of particles over longer time periods. Only the application of backflushing, which overcomes a substantial part of the internal fouling, can provide flux maintenance over time frames of about a week.

Fig. 7.6 shows the comparison of combined applications of AS and BF at different TMP. In both cases the air injection ratios are basically between 0.5 and 0.6. The reactor temperatures of 17°C are comparable and so are the liquid velocities, which vary between 1.08 and 1.4 m/s. Moreover the MLSS are in similar ranges of about 8.3 and 10.8 g/L. The noticeable decrease of CFV for the low pressure application was most likely due to MLSS increase which reduced the pumpage; meanwhile all other parameters remained constant. The main value that varies is the TMP (compare 38 to 212 kPa). More than 5 times higher TMP leads to about doubled

fluxes throughout the tests. However, at the end of the tests, after about one week, the high pressure application shows a noticeable flux decrease compared to the measurements from the first days. This decrease indicates that with higher TMP the combined application of AS and BF cannot eliminate all fouling, but suggests favorable operation conditions with higher recovery rates. That might be termed "sustainable conditions", (i.e., conditions with no residual fouling after chemical cleaning). Table 7.1 gives a summary of the sustainability of the different operating conditions.

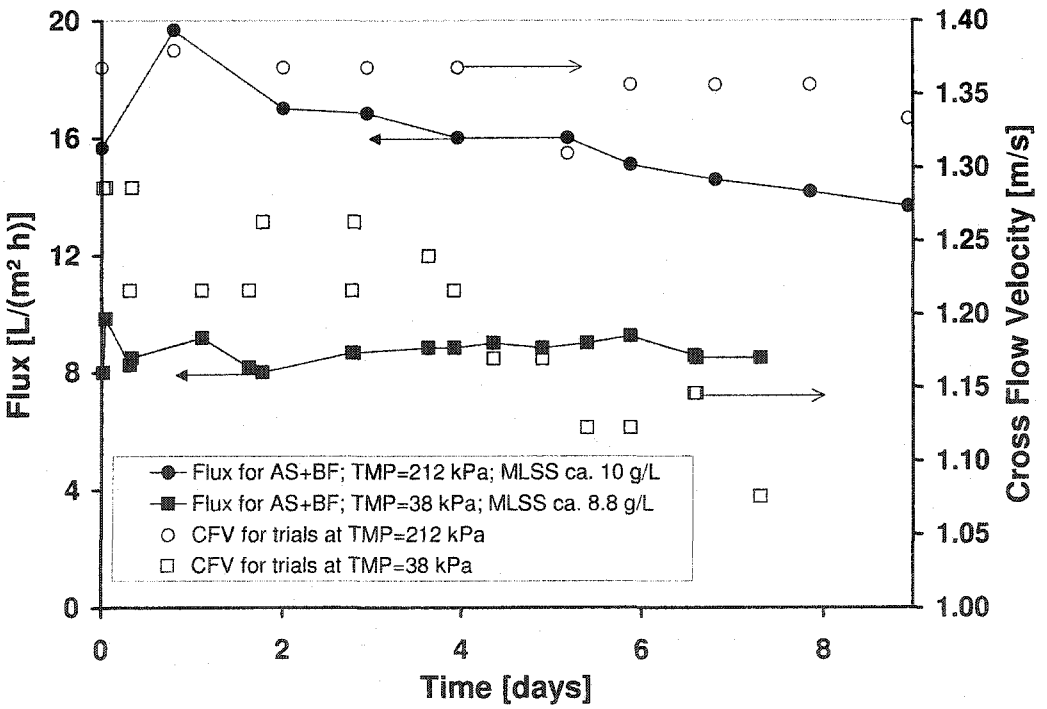

Fig. 7.6. Comparison of combined application of air sparging and backflushing at different pressures. CFV vary slightly from 1.1-1.4 m/s and MLSS are between 8.3 and 10.8 g/L. Applied TMP are 212 kPa, respectively 38 kPa.

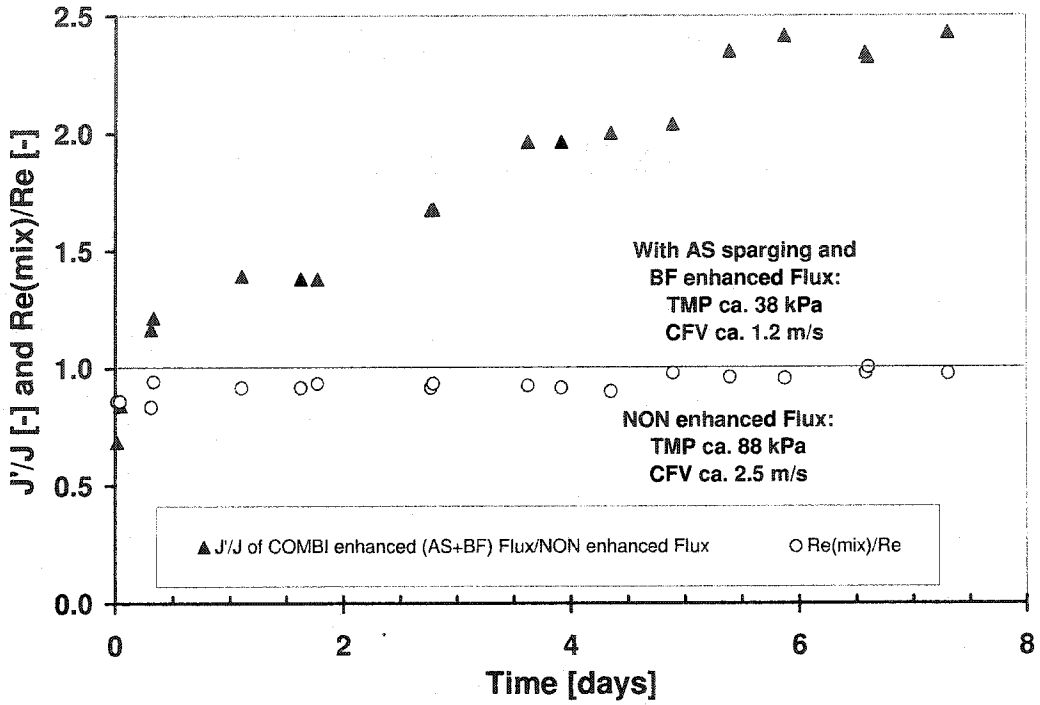

Fig. 7.7. Evolution of Flux ratios i.e. ratio of enhanced flux J' to NON enhanced flux J for a combination of air sparging and backflushing and NON enhanced flux. Re number ratio, i.e. ratio of mixture Re number and conventional Re number.

Table 7.1. Comparison of sustainability for different conditions

Filtration Type	Time [d]	TMP [kPa]	CFV [m/s]	Temp. [°C]	MLSS [g/L]	Final permeability [L/(m² h bar)]	Sustainability = Final/Start permeability [%]
NON	8.94	212-218	1.39-1.67	15-19	9.3-10.8	2.12	39
NON	8.94	212-218	1.16-1.42	15-19	9.3-10.8	1.41	26
NON	4.84	85-333	1.24-1.30	21-28	8.3-10.8	0.8	6
AS	4.84	40-98	1.22-1.31	21-28	9.8-11.5	13.59	48
BF	4.84	79-348	1.24-1.30	21-28	9.8-11.5	3.64	19
AS+BF	8.94	88	1.31-1.38	15-19	9.3-10.8	6.45	87
AS+BF	7.31	38	1.08-1.20	12-17	8.3-9.1	23.94	96.5

Fig. 7.7 shows the evolution of the flux ratios of enhanced flux = J' and NON-enhanced flux = J for the combination of AS+BF (at 38 kPa) and NON-enhanced flux. Moreover, the ratios of mixture Reynolds number and conventional Reynolds number are shown. The calculation of these two dimensionless numbers is done according to eq. 7.2 and 7.3. For the single phase flow the conventional Re number applies:

$$\mathrm{Re} = \frac{\rho^* u_{Liquid}{}^* L}{\mu} \qquad \text{eq. 7.2}$$

with:

ρ = density [kg/m³]

u_{Liquid} = liquid velocity [m/s]

L = characteristic length, here channel diameter [m]

μ = dynamic viscosity [Pas]

For the two-phase flow, the calculation of the mixture Reynolds number applies, according to J. Verberk and J. van Dijk [23]:

$$Re_{mixture} = \frac{\rho_{Liquid} * (u_{Liquid} + u_{Gas}) * L}{\mu_{Liquid}} \qquad \text{eq. 7.3}$$

with:

$Re_{(mixture)}$ = two phase Reynolds number [-]

For the comparison of the flux, the data from Fig. 5 was utilized. Even though the higher velocity and TMP for NON give a slight advantage within the first hour, this advantage is overcome after 6 hours, when the AS+BF enhancement leads to higher flux in spite of lower TMP and CFV. Throughout the test a steady increase of the flux ratio is observed, which reaches a value of 2.4 at the end of the week. Surprisingly throughout the whole time the mixture Reynolds number is smaller than the conventional Reynolds number; however both Reynolds numbers are very close to each other with differences generally less than 10%.

In Fig. 7.8 the Fouling number is depicted, calculated according *Vera et al.* [12] as described in eq. 7.4.

$$N_F = u_{Liquid} * \left(\frac{1}{J} - \frac{1}{J_0} \right) \qquad \text{eq. 7.4}$$

with:

J = flux at any time larger than zero [m/s]

J_0 = initial flux at time t = zero [m/s]

N_F = Fouling number [-]

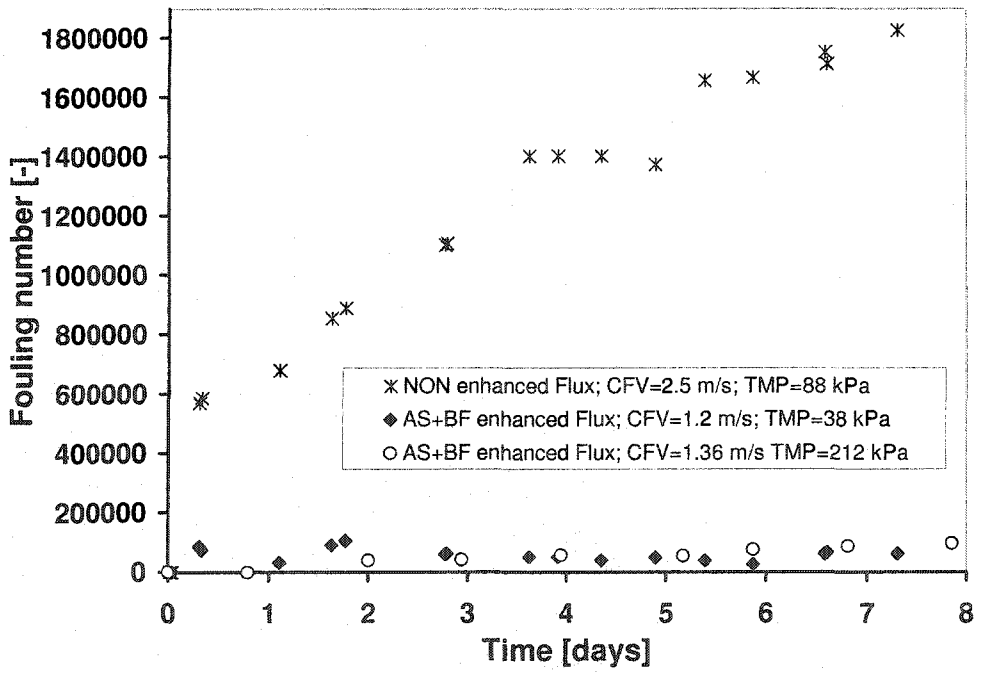

Fig. 7.8. Comparison of Fouling number for NON-enhanced flux and enhanced application with a combination of AS + BF. NON-enhanced flux had a substantially higher CFV. AS+BF enhancement featured high or low TMP. MLSS ranged between 8.3 – 10.8 g/L.

It is clear from Fig. 7.8 that the NON-enhanced flux shows Fouling numbers about 10 times as high as the enhanced filtration after 7 days. Due to the depiction scale, it is hard to distinguish between the high pressure and low pressure BF+AS enhanced filtration. However the low pressure application shows a lower tendency for increase of the Fouling number; meanwhile the high pressure application shows the recognizable trend to increase vs. time.

7.4 Conclusion

1. The limiting flux for the experimental setup was determined to be about 20 L/(m^2 h) when no enhancement techniques were applied.

2. It was impossible to identify critical flux for conventional filtration (NON) of the chosen synthetic wastewater at about 2/3 of the limiting flux at various operation conditions.

3. It is assumed that, if a critical flux for conventional filtration (NON) exist, it must be close to the pseudo-steady state flux, which is 4 L/(m^2 h) after about 8 days.

4. Stepwise pressure increase for NON-enhanced filtration of synthetic wastewater can not overcome the flux decline at MLSS of ca. 10 g/L and CFV of ca. 1.3 m/s. The permeability decreases by about 94% within 5 days. For NON-enhanced constant pressure filtration the permeability decreases by at least 60% within ca. 9 days. With BF enhancement and TMP rise, it is possible to stabilize the flux for roughly over 7 days. However, the permeability of only BF-enhanced operation

decreases by about 80% within 5 days at the chosen conditions. Air sparging enhanced filtration sustains the permeability at about 50% from the initial value after 5 days. With gentle TMP increase from 40 to 98 kPa AS can provide stable flux over 5 days.

5. At very low TMP of about 38 kPa and CFV of ca. 1.2 m/s the combination of AS+BF shows no flux decline and can maintain twice the value of the pseudo-steady state flux for NON-enhanced filtration for more than one week and thus indicates sub-critical flux behavior.

6. At higher TMP of 212 kPa even the combination of AS+BF shows gentle flux decline and steadily increasing fouling, but promises the highest recovery rate at sustainable conditions.

7. Rising the CFV from approximately 1.2 m/s to more than 2.5 m/s bears almost no change of flux behavior for conventional filtration of synthetic wastewater at MLSS close to 10 g/L.

8. At low TMP the combination of AS+BF shows the highest sustainability as shown in Table 1.

Acknowledgements

The authors would like to thank the Microdyn-Nadir Company for donating the membrane modules and for their valuable suggestions. Moreover, we are especially thankful to the GRUNDFOS Company, which served our research with high quality

equipment and excellent technical advice. We would also like to acknowledge a USGS NIWR grant for funding this research.

7.5 References

[1] R. Field, D. Wu, J. Howell and B. Gupta, Critical flux concept for microfiltration fouling, J. Membr. Sci., 100 (1995), 259-272

[2] J. Howell, Sub-critical flux operation of microfiltration, J. Membr. Sci. 107 (1995) 165-171

[3] P. Bacchin, A possible link between critical and limiting flux for colloidal systems: consideration of critical deposit formation along a membrane, J. Membr. Sci., 228 (2004), 237-2241

[4] M. Mulder, Basic Principles of Membrane Technology, Kluwer Academic Publishers, Dordrecht/Boston/London (1996), second edition, ISBN: 0-7923-4247-X.

[5] M. Cheryan, Ultrafiltration and Microfiltration Handbook, Technomic Publishing Co., Inc. Lancaster, Basel (1998), ISBN: 1-56676-598-6.

[6] H. Li, A. Fane, H. Coster and S. Vigneswaran, Direct observation of particle deposition on the membrane surface during crossflow microfiltration, J. Membr. Sci. 149, (1998), 83-97

[7] H. Li, A. Fane, H. Coster and S. Vigneswaran, An assessment of depolarization models of crossflow microfiltration by direct observation through the membrane, J. Membr. Sci. 172 (2000) 135-148.

[8] D. Wu, J. Howell and R. Field, Critical flux measurements for model colloids, J. Membr. Sci. 152 (1999), 89-98

[9] C. Cabassud, S. Laborie, and J. M. Laine, How slug flow can improve ultrafiltration flux in organic hollow fibres, J. Membr. Sci. 128 (1997) 93-101.

[10] C. Cabassud, G. Ducom and S. Laborie, Measurement and comparison of wall shear stresses in a gas/liquid two-phase flow for two module configurations, Conference proceedings IMSTEC Sydney, paper 163 (2003) 6 pages.

[11] S. Levy, Two-Phase Flow in Complex Systems, John Wiley& Sons, Wiley-Interscience publication, New York (1999), ISBN: 0471329673.

[12] S. Bellara, Z. Cui, and D. Pepper, Gas sparging to enhance permeate flux in ultrafiltration using hollow fiber membranes J. Membr. Sci., 121 (1996) 175-184.

[13] G. Ducom, and C. Cabassud, "Possible effects of air sparging for nanofiltration of salted solutions"; Desalination 156 (2003) 267-274.

[14] K. Majewska-Nowak, M. Kabsch-Korbutowicz, and T. Winnicki, "The effect of gas bubble flow on ultrafiltration efficiency, Desalination 126 (1999) 187-192.

[15] T. Cheng, Influence of inclination on gas-sparged cross-flow ultrafiltration through an inorganic tubular membrane, J. Membr. Sci., 196 (2002) 103-110.

[16] L. Vera, S. Delgado, and D. Elmaleh, Gas sparged cross-flow microfiltration of biologically treated wastewater, Water Science and Technology, 41, 10 (2000) 173-180.

[17] A. Marshall, P. Munro and G. Träghardh, The effect of protein fouling in microfiltration and ultrafiltration on permeate flux, protein retention and selectivity: A literature review., Desalination 91, 1, (March 1993) 65-108

[18] G. Belfort, R. Davis, A. Zydney, The behavior of suspensions and macromolecular solutions in crossflow microfiltration, J. Membr. Sci., 96, 1, (1994) 1-58

[19] P. Bacchin, D. Si-Hassen, V. Starov, M. Clifton, P. Aimar, A unifying model for concentration polarization, gel-layer formation and particle deposition in cross-flow membrane filtration of colloidal suspensions, Chem. Eng. Sci., 57 (2002) 77-91

[20] C. Psoch and S. Schiewer, Dimensionless numbers for the analysis of air sparging aimed to reduce fouling in tubular membranes of a Membrane Bioreactor, Desalination 2004, submitted for publication

[21] C. Psoch and S. Schiewer, Flux improvement in a MBR by air sparging in sidestream, Water Research, in preparation.

[22] Standard Methods for the Examination of Water and Wastewater, (1995) 19th edn, A P H A/American Water Works Association/Water Environment Fed., Washington DC, USA

[23] J. Verberk, H. van Dijk, Research on AirFlush: distribution of water and air in tubular and capillary membrane modules, Berichte aus dem IWW Rheinisch-Westfälisches Institut für Wasserforschung, Band 37a, 2002, ISSN 0941-0961

8 Direct filtration of natural and simulated river water with air sparging and sponge ball application[7]

C. Psoch and S. Schiewer*

Dept. of Civil & Environmental Engineering, Water & Environmental Research Center, University of Alaska Fairbanks, AK 99775; USA, Tel. 1-907 474-2620, E-mail: ffsos@uaf.edu

Abstract

Membrane filtration is increasingly used for converting surface water to drinking water. This study investigated the effectiveness of air sparging in reducing fouling during direct membrane filtration of river water. Air sparging via side-stream filtration in tubular membranes at crossflow velocities (CFV) between 0.5-1.0 m/s enhanced the permeability by a factor of 4.6, given that the water used showed a high propensity of fouling. Sponge ball application to remove fouling proved, for model solutions with silt and clay, that chemical cleaning with NaOCL cannot erase mineral fouling on the membrane surface by 100%. Residual fouling, indicated by flux increase above the initial flux observed after sponge ball cleaning, remains. Repeated sponge ball application appears to reduce the residual fouling. In terms of seasonal water sampling, the fouling potential declined from spring to fall due to a decrease of Natural Organic Matter (NOM), colloids and mineral load (indicated by total organic carbon and turbidity). Air sparging (AS) effectiveness, measured by the permeability

[7] Desalination, Elsevier, (to be submitted) 2005

ratio of AS-enhanced and non-enhanced filtration, decreased with the dwindling fouling potential of the raw water. When model solutions were investigated (silt 5 g/L and clay 10 g/L), the enhancement factor for the silt slurry was less than that for the clay.

Keywords: air sparging, cake compression, chemical cleaning, residual fouling, sponge ball, surface water quality

8.1 Introduction

In recent years, producing drinking water from surface water is increasingly accomplished by membrane filtration. Declining membrane costs in combination with more stringent water quality requirements have led to an exponential growth in production capacity and numbers of operated membrane units. Membrane filtration reduces the need for elaborate chemical treatment processes prior to filtration, resulting in a shorter, simplified process flow. A screen followed by a sedimentation tank is often sufficient for pretreatment; in some cases gravitational settling may even be omitted as well [1].

This study's objective was to determine to what extent it is possible to process surface water from an Alaskan river with membrane direct filtration at different times of the year. The chosen test equipment was a tubular microfiltration system (filtration direction was from the inside out). Since the river water quality undergoes significant changes during the ice-free months, some variation in filterability and fouling potential was expected. Moreover several approaches were developed to mitigate unavoidable fouling. One of the applied methods was continuous air sparging (AS), which generates a two phase flow to overcome external fouling in the first place, by reducing the amount of caking layered in the tubes. Depending on the superficial liquid and air velocities, several flow patterns are possible. According to the literature [2] and our own investigations [3], slug flow is the most effective regime to enhance mass flow; and this regime was applied. To evaluate the effect of air sparging as a

method for fighting external fouling, tests with sponge balls were conducted. These tests allowed comparing air sparging results with a recognized and commercially available surface cleaning technology in tubular systems [4-5].

8.2 Material and methods

With a multistage pump (Grundfos) the water was forced through two polymer membrane modules (PCI Membranes Inc.) with a pore size of 0.2 μm (each 0.1 m^2 surface area), installed in parallel (see Fig. 8.1). At one of the two membranes the membrane module 1, air sparging (AS) was supplied to enhance the mass flow through the membrane with air injection ratios $\varepsilon \sim 0.6$ [ε = gas velocity/(gas velocity + liquid velocity)]. The conventionally operated membrane (module 2) with no enhancement will hence be called "NON". Applied transmembrane pressures (TMP) were between 48 and 276 kPa, and the cross flow velocities (CFV) between 0.46 and 2.12 m/s. The permeate from both modules was recycled into the 20 L feed tank, except for sampling, as shown in Fig. 8.1. The bulk stream was well mixed by the discharge of the two membranes and by a magnetic stirrer in order to maintain a constant concentration of suspended solids and colloids. The heat generated by the multistage pump was balanced with a thermostat and cooling coil, and the temperatures were held between 11.7-13.3°C on average.

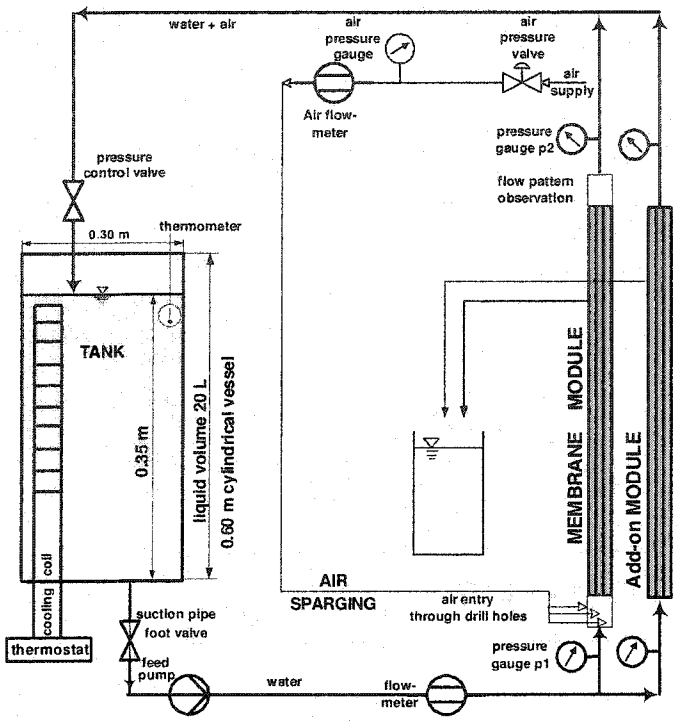

Fig. 8.1. Experimental setup.

Seven different batches of raw water or model solution were investigated. After each batch, a chemical cleaning (c.c.) of the membranes was carried out, except prior to the last batch, and different cleaning solutions were tested. Water used for this study was obtained from the Tanana, one of the major rivers in central Alaska. First samples were taken in late May, at a time when the river possesses a high load of fine suspended solids and NOM, yielding high turbidity. It was not possible to reduce the water turbidity significantly (based on visual inspection) by passing it through a 0.7 μm filter. The first water batch was processed with two virgin membranes for seven weeks. To create the second batch, 5 g of silt per liter was added to the water from

batch one, which was previously treated for seven weeks with permeate recycling to maintain a constant concentration of solids. The silt was obtained by sieving sediments from the river banks through a 50 µm sieve. The second test lasted for over three weeks. After twelve days, only the NON (air-sparged) membrane was cleaned with commercially available sponge balls (PCI Membranes and Taprogge). This procedure was done by manually inserting the sponge balls (which had a diameter approximately 10% larger than the membrane tubes; tube diameter = 6.35 mm) into the module and running the pump afterwards for a short time. This procedure was repeated three times. Subsequently, river water collected in the months of August, September and October was investigated for several days. After filtration of the October batch, no chemical cleaning was performed, since the turbidity in the water disappeared after one day of operation and the flux appeared very close to the clear water flux. For the last batch, 10g AMACO American Art Clay No. X-11 were added to each liter of water from the October batch.

8.3 Results and discussion

For the following considerations the permeability ratio was used as an indicator of flux enhancement through AS. The permeability is calculated according to eq. 8.1:

$$P = \frac{J}{TMP} \qquad [\mathrm{L/(m^2\ h\ bar)}] \qquad \text{eq. 8.1}$$

with J as the measured flux and TMP, the applied transmembrane pressure.

The permeability ratio is the quotient of AS permeability and NON permeability:

AS permeability/NON permeability = P'/P

The first batch (Test I) sampled in late May showed excellent results, as is obvious from Fig. 8.2. Already, after one day, flux was enhanced by a factor of 2.

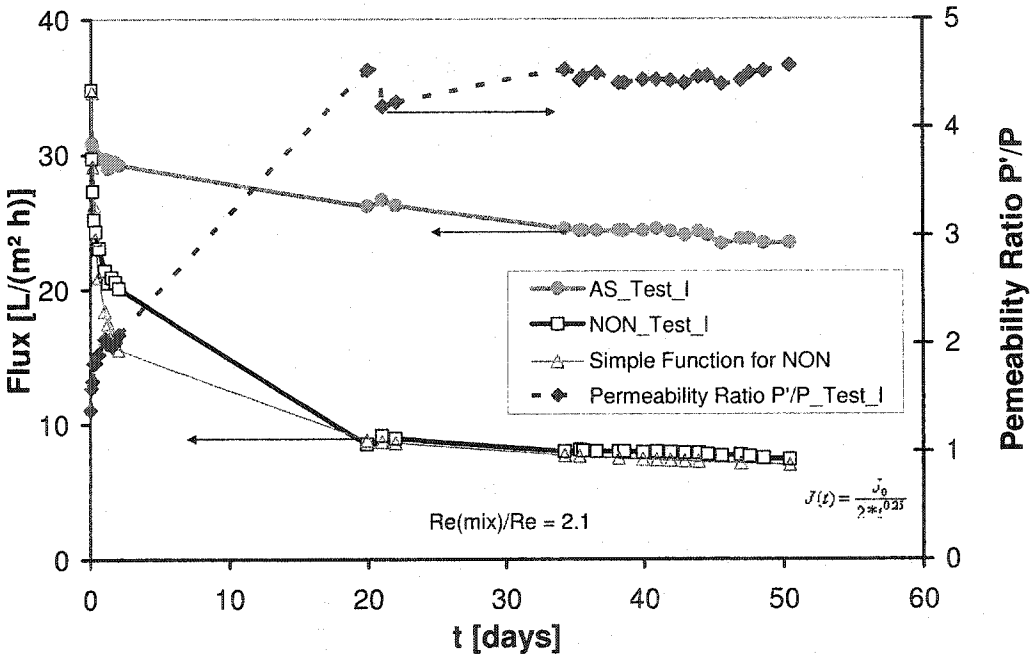

Fig. 8.2. Test I used untreated river water collected in May, with high fouling potential in a 7 week investigation of AS vs NON.

The divergence of the NON and AS enhanced flux continued beyond the first days since the NON enhanced flux declined more strongly than the enhanced flux.

This test continued for more than 50 days, revealing a permeability enhancement by a factor of 4.6. The flux decline J (t) for the NON case was close to a $J(t) = k*t^n$ function with k=2 and n= 0.25, which is similar to concentrated wastewater sludge (in

this case k is ~ 4), according to *Psoch and Schiewer* [6]. The ratio of the Reynolds numbers (mixture Reynolds number for AS divided by regular Re number from NON) was about 2.1, giving only a small hydrodynamic advantage to the enhanced filtration. The liquid velocity for the NON enhanced case was, at 0.90 m/s, even higher than for the AS case (0.74 m/s), while the TMP was 33 kPa for the AS system and 48 kPa for the NON system.

The first chemical cleaning was performed according to the recommended procedures of PCI membranes Inc. with a solution of distilled (DI) water and CLOROX ULTRA, a household bleaching agent (contains 6% Sodium Hypochlorite = NaOCl).

At first, a pretreatment of the membranes was performed by pumping a mild caustic solution (achieved by adding NaOH to DI water until pH = 10.5) at about 50°C for 15 minutes through the system.

Another 17 liters of DI water were made mildly caustic with NaOH (pH ~ 10.5). To this warm (50°C) solution, about 60 mL of CLOROX were added; then the mixture was pumped through the system for 30-40 minutes. Finally, a rinsing with DI water for 30 min was performed.

For Test II, the water from the first batch (Test I water) was taken and 5 g silt per liter were added to obtain a model solution. Although and even more pronounced divergence of the AS vs NON Flux was expected, contrary to these expectations, the flux enhancement was considerably less emphasized, as is apparent in Fig. 8.3. The permeability ratio was less than 2 (in Test I it was above 4), even though the

operation conditions were almost identical to those of Test I (34 kPa TMP and 0.77 m/s CFV for AS; 48 kPa TMP and 0.91 m/s CFV for NON). A Reynolds number ratio of about 2.15, again close to that of Test I, pointed out similar operation conditions.

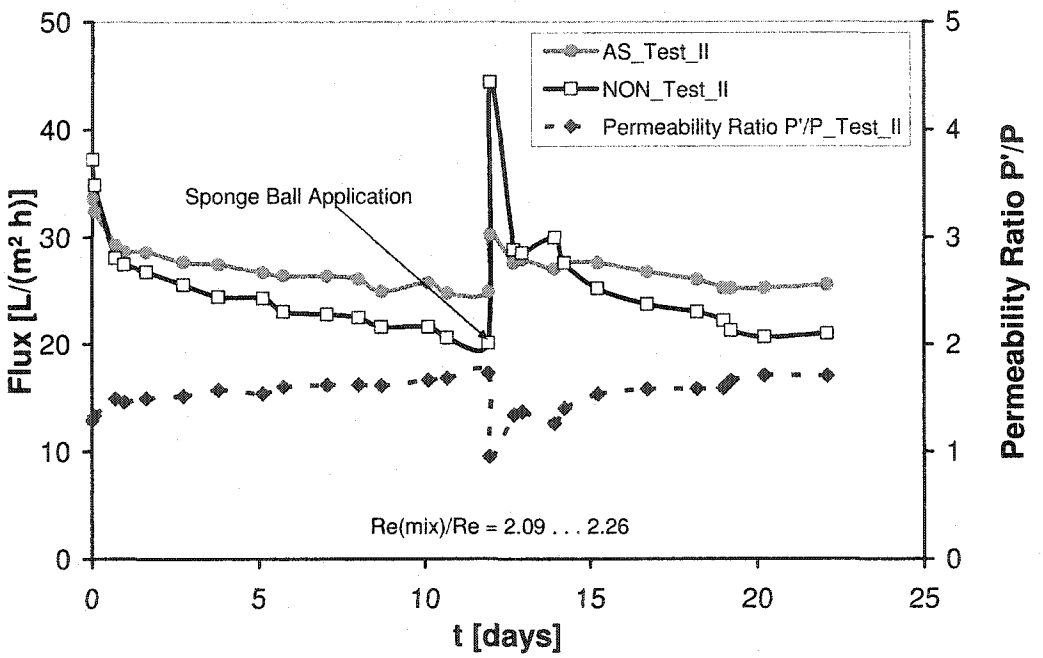

Fig. 8.3. Test II; river water collected in May after undergoing 7 weeks' treatment + 5 g/L silt (model solution), flux for AS vs NON.

A possible explanation might be that processing the first batch for 7 weeks with continuous aeration via air sparging and mixing degraded parts of the organic compounds in the water. Furthermore the membrane properties of the virgin membrane are most likely not identical to those properties after chemical cleaning

(c.c.). Finally, parts of the sediments were not held in suspension anymore due to insufficient turbulence in the tank.

As indicated in Fig. 8.3, sponge ball application in the NON membrane after 12 days showed that a substantial cake layer definitely existed on top of the membrane. With removal of this cake layer, the NON permeability approached the AS permeability, reducing the permeability ratio from 1.5 to 1. Subsequently, the permeability ratio quickly rose again until values around 1.5 were achieved after approximately 3 weeks.

As Fig. 8.4, based on the same data, further suggests, the permeability of the NON system increased by almost 20% beyond its initial permeability after the sponge ball cleaning, (even exceeding the AS permeability), then dropped again very quickly soon after. The rise above the initial permeability can only be interpreted as residual surface fouling that was not erased by chemical treatment via caustic and chlorine solutions. Though a time lag during which some initial fouling may have occurred exists between starting the operation and recording the actual first measurement, this is also the case for the first measurement after sponge ball cleaning, and can thus be neglected.

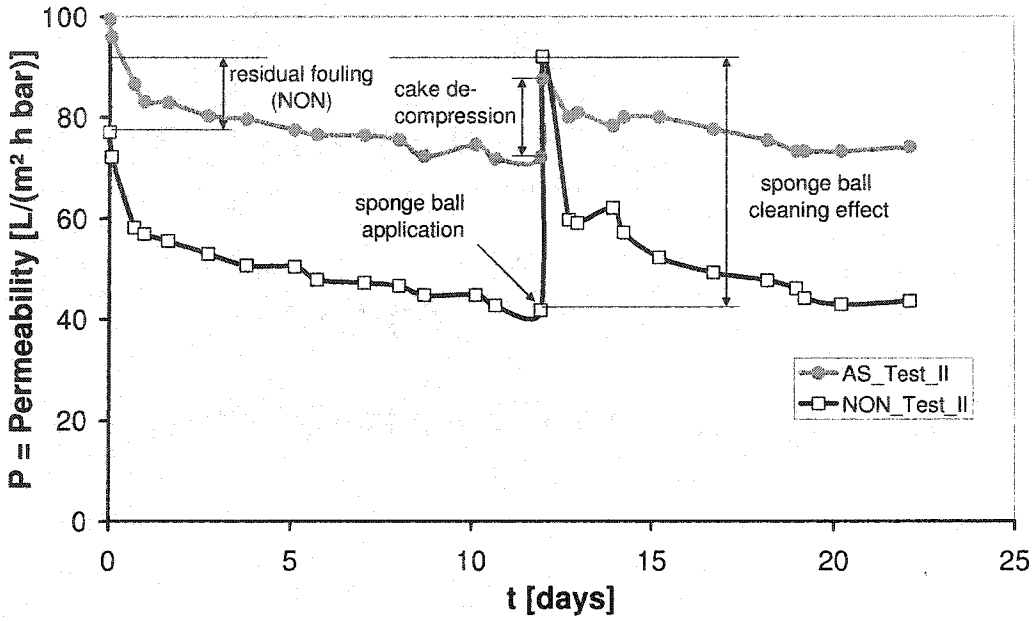

Fig. 8.4. Test II river water (May collection after 7 weeks treatment + 5 g/L silt for a model solution), permeability for AS vs NON

Another interesting observation was that the permeability for the AS system also increased by 18%, though no sponge balls were applied for this module; this increase is obviously due to decompression of the filter cake of silt. The permeability for the NON filtration increased by 125% after three sponge ball passages, but suffered a sharp decline afterwards. Surprisingly, the permeability increase due to decompression for the AS filtration lasted at least as long as the flux enhancement in the NON achieved due to sponge ball cleaning, even though the mass transfer improvement immediately after the decompression was relatively small.

The considerably lower enhancement effect in Test II compared to Test I may be caused by organic degradation in the water. Thus, in August new river water samples

were obtained and after a c.c. as describe above, new tests were undertaken. Fig. 8.5 shows the results of Test III.

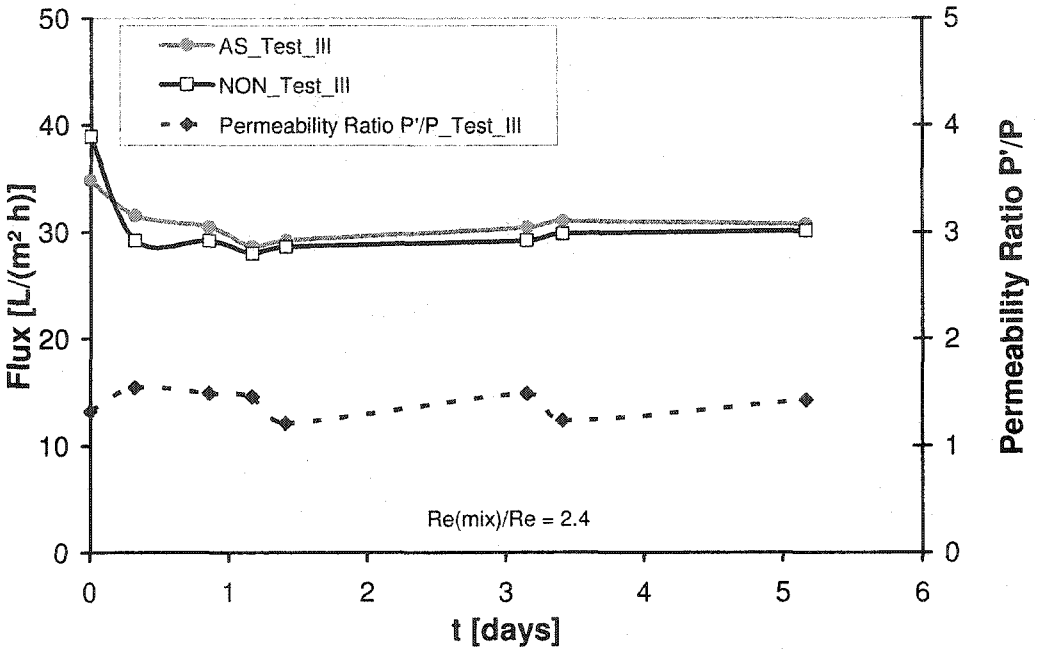

Fig 8.5. Test III, straight river water collected in August, AS vs NON.

The results were again not as convincing as in Test I; the permeability ratio was even lower than in Test II, but, with 35 kPa TMP and 0.80 m/s CFV for AS and 48 kPa TMP and 0.83 m/s CFV for NON, the operating conditions were almost identical to those of Tests I and II. A Reynolds number ratio of 2.4, close to that of Test I (2.1), confirmed that there was little change in operating conditions, and the turbidity, based on visual observation, was unchanged.

For Test IV, in September, new river water samples were used and the c.c. performed as described above. At this time significantly lower water turbidity was noticeable under visual inspection, as well as less sediment settling after a few hours, compared to the first samples from May and August. It was concluded that letting the water from Test III rest for 7 days in the laboratory, under conditions favorable to microbial activity (28°C) before treatment might have impacted the outcome by allowing microbial degradation. Fig. 8.6 shows the results from Test IV.

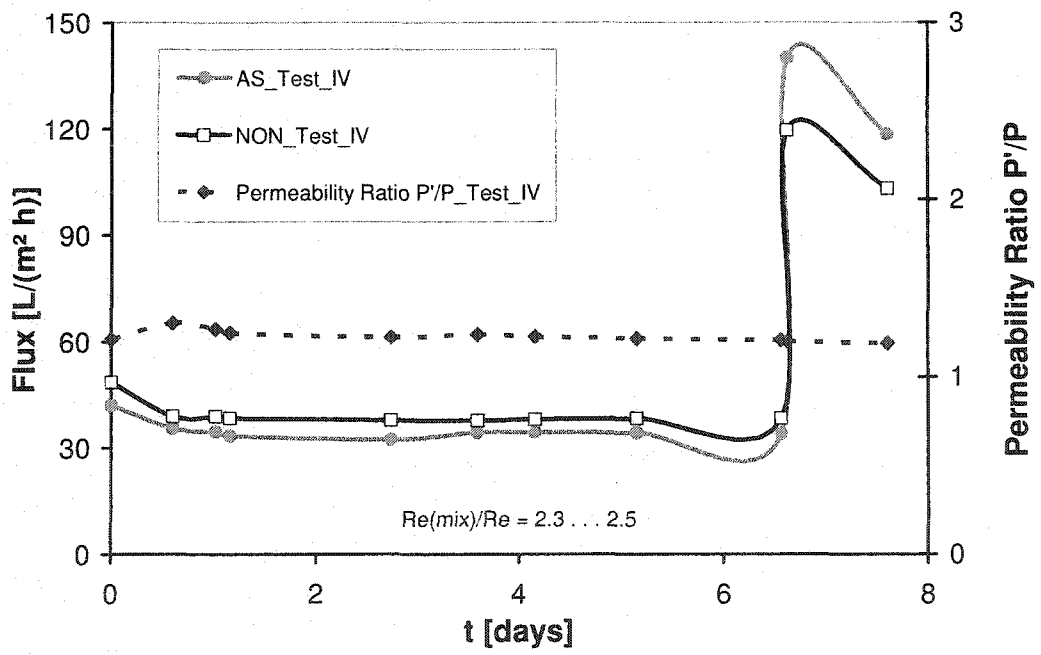

Fig 8.6. Test IV, straight river water collected in September, AS vs NON.

Because the results did not show such a significant permeability enhancement by air sparging as those of Test I, for the last 36 hours the TMP was raised. The pressure

was increased from the constant 48 kPa (NON) and 34 kPa (AS) to about 150 kPa for both, in hopes that these conditions would be more favorable to the AS system. However, no significant improvement was accomplished. With an average of 55 kPa TMP and 0.79 m/s CFV for AS, and 67 kPa TMP and 0.80 m/s CFV for NON, the operation conditions until the TMP rise were almost identical to Tests I-III. A Reynolds number ratio of 2.4, again close to that of the other tests confirmed a similar flow regime.

Another possible explanation for the unsatisfactory results of the AS application was that the chemical membrane cleaning procedure might not have been thorough enough to restore the membrane to a state similar to that of the virgin membranes. Thus another chemical cleaning procedure was performed prior to test V. Instead of pretreatment using the chlorine solution, a stronger caustic NaOH solution (50°C) was pumped through the system for 30 minutes.

The operation conditions were altered too, with a much higher CFV for the NON case of 2.10 m/s compared to about 0.65 m/s for the AS case. The Reynolds number ratio was initially 0.7;it returned to over 1.14, then up to 2.3 after the CFV was reduced for the NON down to 1.4 m/s (after 2.07 days) and finally to about 0.7 m/s, (after 2.64 days). At these points the TMP for NON was raised from 98 kPa to 138 (2.07 days) and later until 155 kPa. For the AS module, the TMP was raised from 134 kPa (2.07 days) to 145 (2.64 days) and later up to 155 kPa.

With about equal average TMP (144 kPa for AS and 131 kPa for NON), this time the permeability ratio was even in favor of the NON application. These results prove

that regular flow conditions can under favorable circumstances (high CFV) even outperform AS (see Fig. 8.7).

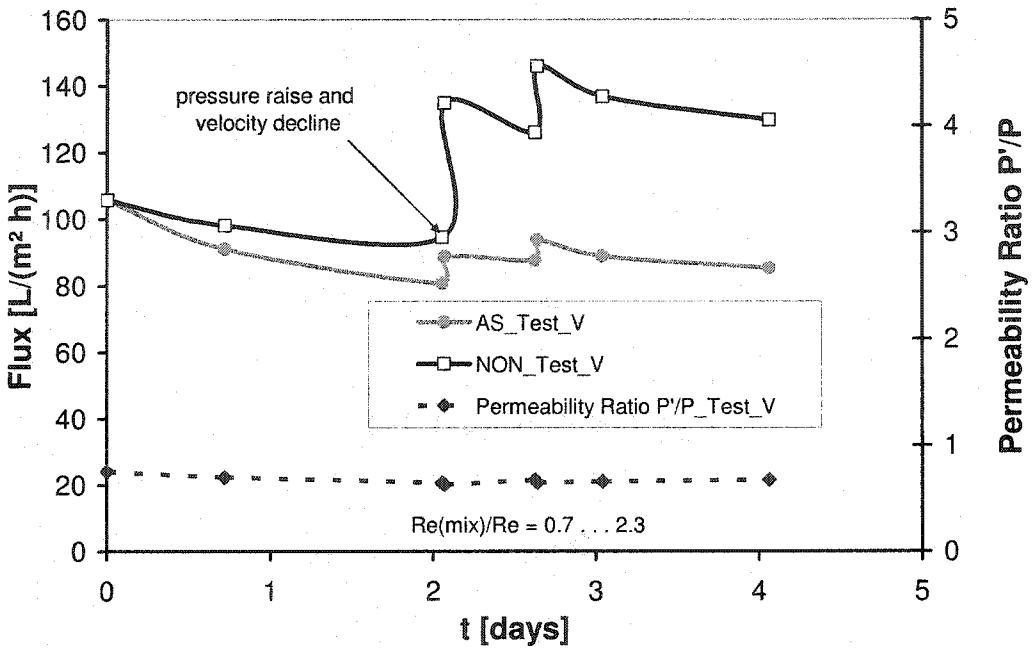

Fig. 8.7. Test V, straight river water (September collection) and changed c. c. procedure, AS vs NON.

Prior to Test VI, new water was sampled from the Tanana River and the chemical cleaning procedure was changed again, in hopes of overcoming the rather poor performance of the AS system. This time, instead of a chlorine solution, a blend of citric and phosphoric acid was used after the pretreatment with NaOH and thorough rinsing. But, as Fig. 8.8 shows, even increasing TMP up to 276 kPa and operating at high air injection ratios (up to 0.7 and CFV of 0.63 m/s vs 0.53) favorable to the AS system, no significant advantage toward the AS system could be demonstrated.

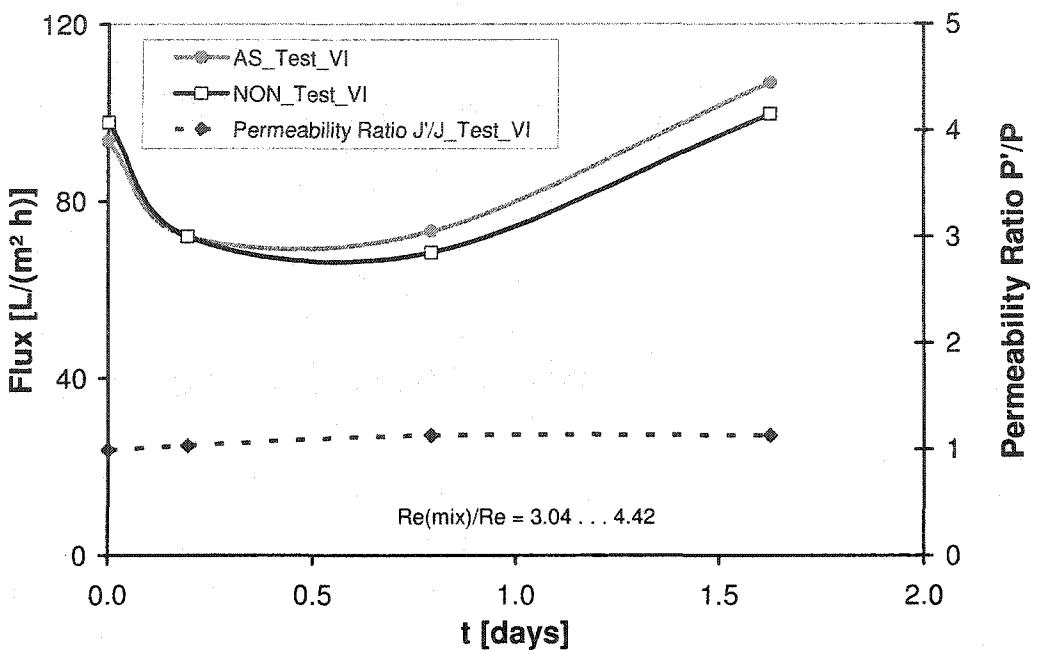

Fig. 8.8. Test VI, straight river water (October collection), membrane pretreatment with NaOH and acid blend, AS vs NON.

The very low turbidity observed during Test VI, which allowed process fluxes close to the corresponding clear water flux and the obviously low impact of the cleaning procedure on the outcome of the filtration process lead to the decision to interrupt the test after little more than 1.5 days.

Prior to the last test (Test VII) no cleaning was performed except rinsing with clear water. Subsequently a model solution was generated by supplementing the batch water from Test VI with 10 g/L of clay. The clay model solution was hard to keep in suspension, and it appeared that it is not feasible to achieve much higher suspended clay concentrations. The results for the clay solution at CFV = 0.67 m/s and TMP =

261 kPa for AS, and 0.79 m/s CFV and 265 kPa for NON, are shown in Fig. 8.9. The Reynolds number ratio was with 1.8-2.8, similar to the other tests.

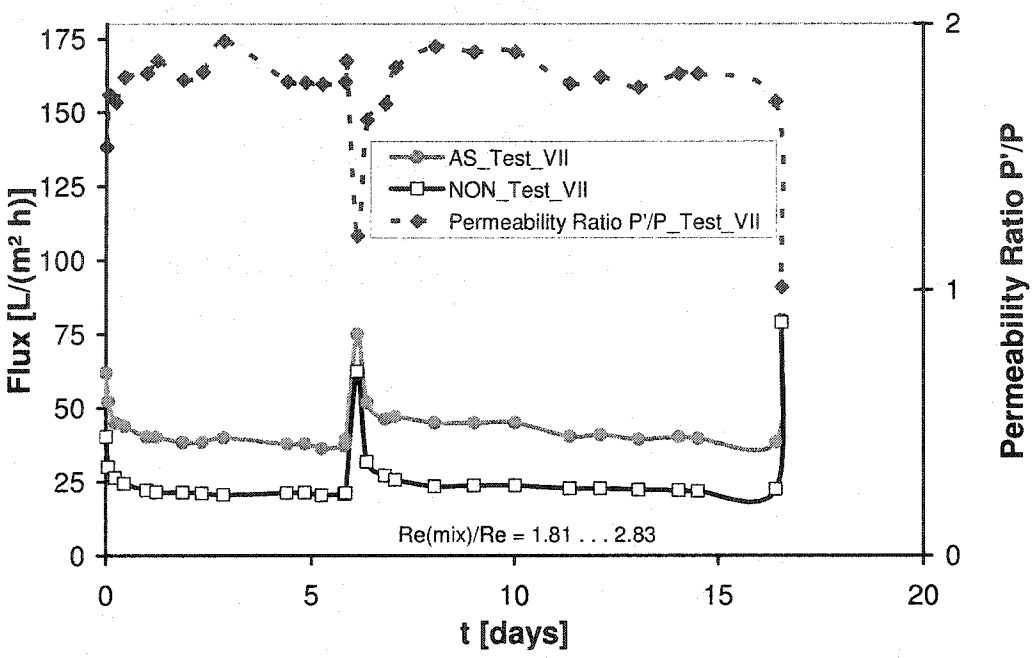

Fig. 8.9. Test VII (model solution), October river water with 10 g/L clay, AS vs NON.

With the added clay, the advantages of the AS system came to the front again, with a permeability ratio around 1.8. Application of sponge balls in NON and AS membranes increased permeability in both cases, indicating some caking, even on the AS membrane surface. However the flux increase at the AS module was less than that for the NON module, which could suggest that AS does generate a thinner cake layer. This assumption was supported by the fact that -- due to the cumbersome manual sponge ball cleaning procedure -- considerably more time was necessary for passing

the sponge balls through the membrane channels of the NON system with its notably thicker filter cake.

The permeability ratio was reduced after sponge ball cleaning of both modules (3 passages each); however the reduction was not as strong as in the case when sponge balls were applied only to the NON membrane (see Figs. 8.3. and 8.4). As Fig. 8.10 further suggests, there was again, as observed during Test II, residual fouling on the membrane surface which could be overcome by sponge ball cleaning. After the sponge ball application, the flux for both systems jumped

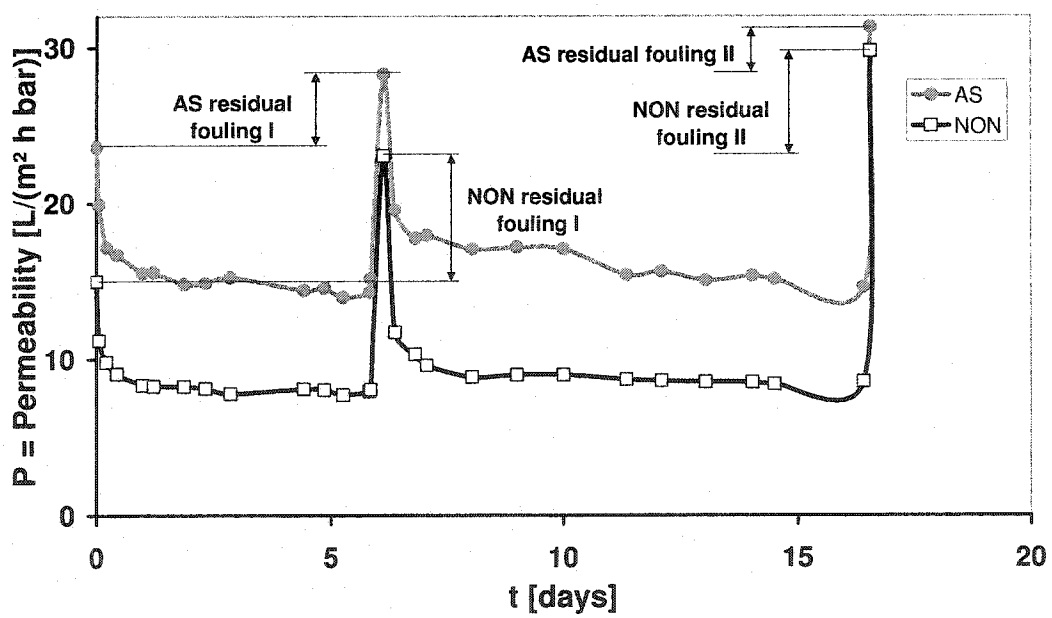

Fig. 8.10. Test VII, October river water with 10 g/L clay, AS vs NON, residual fouling analysis.

above the initial flux, showing that substantial membrane surface fouling was inherited from Test VI. However, the differences between the maximal levels were

less for the AS module (see Fig. 8.10). Another observation was that the flux for the NON system dropped immediately after the sponge cleaning procedure, whereas the AS system maintained a more significant flux improvement for a longer time.

In Fig. 8.11 all non-enhanced permeabilities are depicted. It can be concluded, since most of the tests were performed under similar conditions, that as the seasonal year progressed, the permeability increased, indicating a decreasing membrane fouling tendency from spring to fall. However, the influence of the CFV cannot be neglected, which explains the low permeability in October.

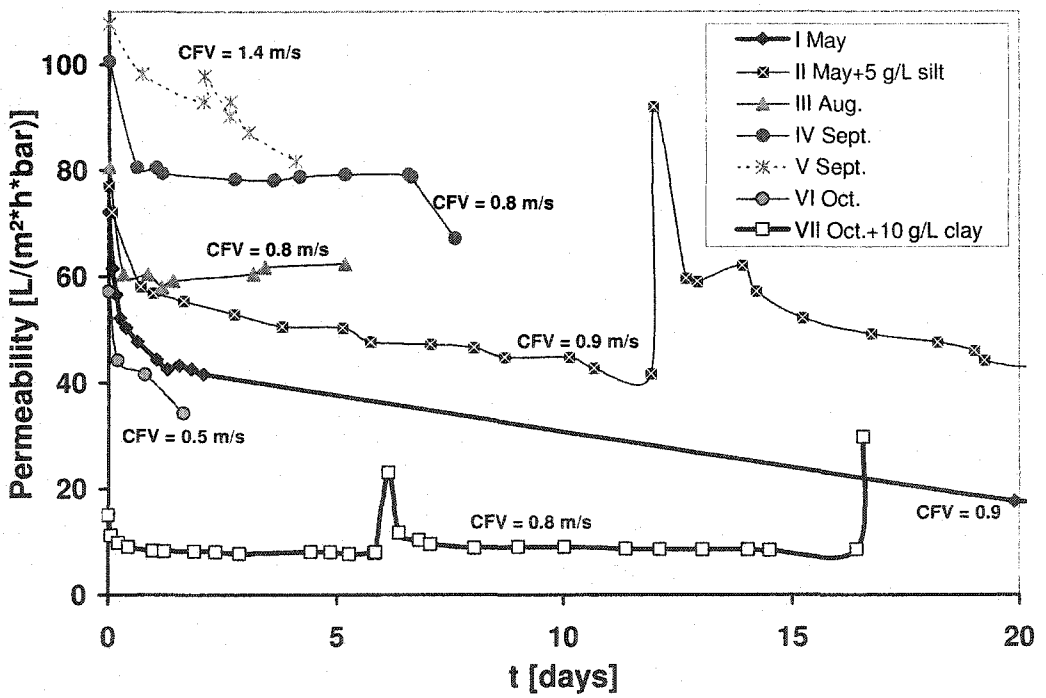

Fig. 8.11. All investigated NON permeabilities (without enhancement).

This conclusion could be confirmed based on total organic carbon (TOC) measurements of different samples. Less NOM and colloids occur during low water phases in contrast to the higher loads seen in the spring, as shown in Fig. 8.12. The water from Test I, Test II and III was investigated, measuring the TOC as an indicator for NOM in the water. The highest amount of NOM was found in the first batch, which together with inorganic colloids (not measured) caused a much higher membrane fouling potential. Further, assuming partial degradation of NOM by mixing and aeration seems supported; however, the TOC decline is not very significant. The lowest TOC (NOM) was measured in late August, confirming the results of visual inspection, that there was less fouling potential due to clearer water in fall than in spring.

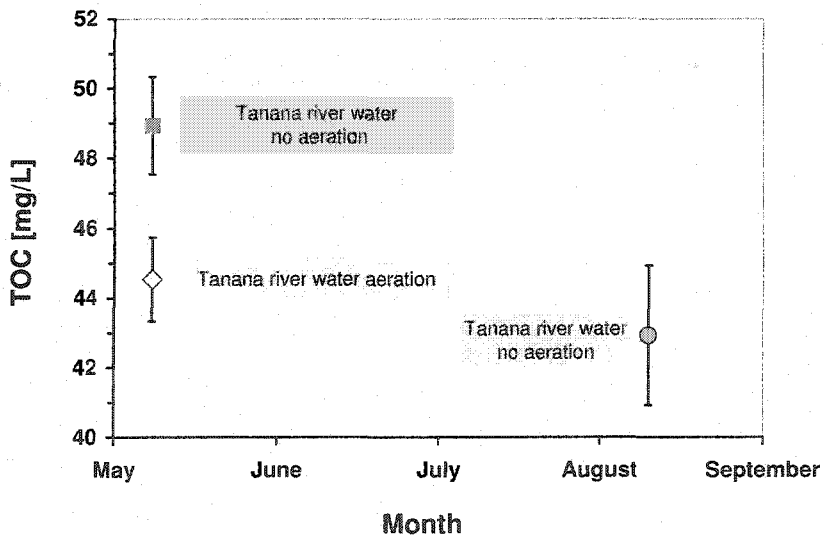

Fig. 8.12. Change of river NOM, indicated by TOC, over the course of the year.

Fig. 8.13 gives an overview of all but one permeability ratio for similar operation conditions. It can be seen that for natural river water collected in October and May, the permeability ratio increased within the first day from about 1.1 up to 2. The silt and clay enriched solutions fall mixed in between. The clay suspension shows surprisingly less fouling potential than the pure river water from May. The suspension with silt shows a similar fouling propensity to that of as straight river water from August.

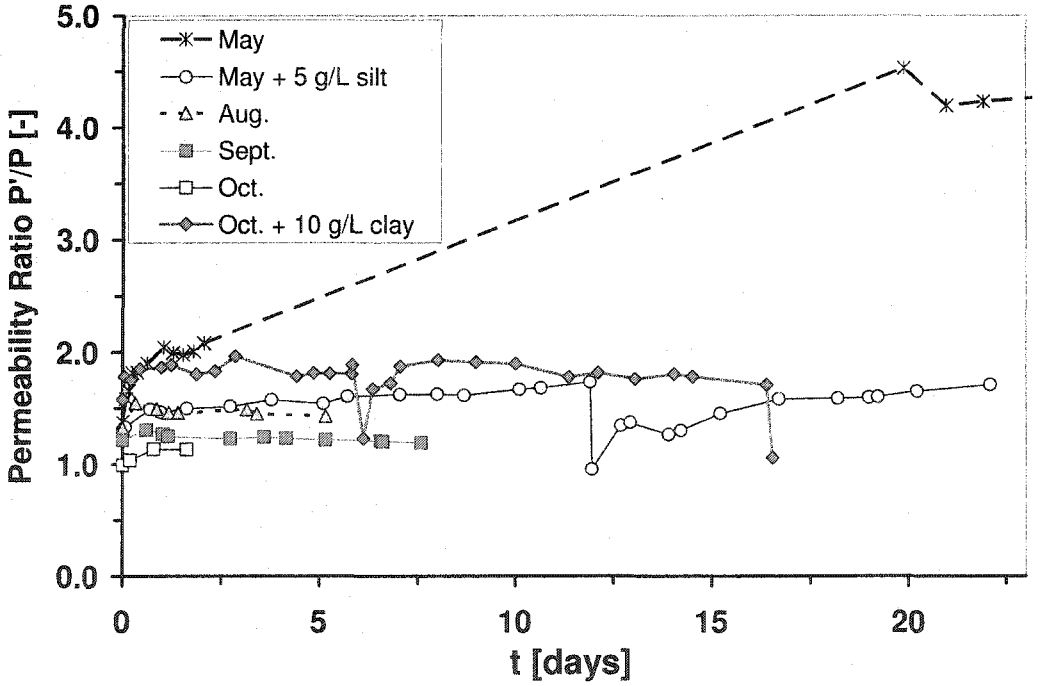

Fig. 8.13. Permeability ratio AS vs NON- at different month and with addition of silt and clay.

8.4 Conclusions

- Mineral residual fouling remains after chemical cleaning with chlorine solution only.
- Chemical cleaning is obviously insufficient in the case of highly loaded river water filtration.
- The type/procedure of chemical cleaning does not significantly change the filtration results.
- The failure to show repeatable success with AS was inherent in the water properties; later batches showed significantly less fouling potential due to seasonal changes in the river water properties. These conditions led to no substantial increase ($P'/P \geq 1.4$) in permeability less successful AS application, as compared to the NON enhanced filtration.
- The total organic carbon (TOC) level in the river water is decreased by intensive aeration and mixing.
- The TOC level in the river water declines between spring melt and midsummer.
- For river water direct filtration, a membrane system with backflushing is suggested, since after sponge ball application the flux almost immediately collapses again.
- Direct river water filtration cannot be recommended.

- It seems definitely worthwhile to consider pretreatment of the river water, or consider a riparian filtration gallery to equalize the significant fluctuations in the river water quality; under certain circumstances (for instance by using horizontal filter wells underneath the river bed) this approach would even allow running the system the whole year around.
- The advantages of air sparging come to the fore only if fouling propensity is significantly high, due to NOM, colloids, and/or mineral particles.
- Air sparging can raise the permeability of virgin membranes for filtration of surface waters with high fouling potential up to 400% after more than 3 weeks of deployment.
- Air sparging can increase the permeability of polymer membranes, fouled by a concentrated clay slurry of 10g/L, in tubular applications by 80% after 16 days of deployment
- Cake layer mainly built of silt and treated with air sparging (ε =0.6) shows a permeability decrease of 18% at operation pressures of about 34kPa due to cake compaction (permeability increase from 72.1 to 87.6 [L/(m²*h*bar)] due to depressurization) after 12 days.
- Based on the sponge ball cleaning procedures, it can be concluded that there is less cake thickness with AS, as the ball passage was significantly easier in the AS enhanced membrane.

Acknowledgements

The authors would like to thank PCI Membrane Incorporated for the donation of the membrane module and valuable suggestions. Moreover, we are especially thankful to the GRUNDFOS Company, which served our research with high quality equipment and excellent technical advice.

8.5 References

[1] Lerch, A.; Panglisch, S. and Gimbel, R., "Research Experiences in Direct Potable Water Treatment using Coagulation/Ultrafiltration", Proceedings of WEMT, (2004), No. M-1-8.

[2] Pospisil, P.; Wakeman, R.J.; Hodgson, I.O.A. and Mikulasek, P., "Shear stress-based modelling of steady state permeate flux in microfiltration enhanced two phase flows", Chemical Engineering Journal 97 (2004) 257-263.

[3] Psoch, C. and Schiewer, S., "Long-term trial of intermittent air sparging for fouling reduction in a MBR", (2005a) submitted for publication to Journal of Membrane Science.

[4] Gillighan, A., Judd. S.J. and Eyres, R., "Membrane thickening of water works sludge", Water Science and Technology: Water Supply Vol. 1 No 5/6 (2001) 215-220.

[5] Al-Bakeri, F. and El Hares, H., Optimization of sponge ball cleaning system operation and design in MSF plants, Desalination, 92 (1993), pp. 353-375.

[6] C. Psoch and S. Schiewer, Long term investigation of aeration and flux improvement by air sparging and backflushing for a membrane bioreactor, (2005b) to be submitted to Water Research (in preparation).

9 Overall conclusions

9.1 Conclusions wastewater membrane filtration

Air sparging (AS) was able to increase the flux in a membrane bioreactor fed with synthetic wastewater over several weeks.

Supplying oxygenation with air sparging as a substitute for conventional aeration had no adverse effect on the treatment performance of the bioreactor. Therefore air sparging could eliminate the need for conventional aeration in MBR.

It can be shown that Shear Stress Numbers between 0.004 and 0.007, which resulted either from air sparging or increased liquid velocity, lead to significantly lower Fouling numbers than those obtained after a period with lower Shear Stress numbers. The dimensionless Fouling number seems to be a good tool to reflect the flux decrease in the system used.

A new dimensionless number, the viscous fouling number (VFN) is proposed. It is calculated by dividing the Fouling number by the ordinary Reynolds and a substantially smaller, more manageable dimensionless number is obtained. In case the liquid viscosity remains constant, the VFN shows similar behavior as the conventional Fouling number. If the viscosity changes, the VFN reacts differently, exhibiting more sensitivity to the altered viscosity. This is especially advantageous for MBR, when changes in MLSS can lead to changed viscosity.

The one-phase and two-phase Mixture Reynolds number gives only limited information about the fouling tendency of the system. For the two-phase Mixture

Reynolds number the highest fluxes where obtained in the moderate turbulent range (below Re = 4000) in combination with optimized air injection ratio.

When deploying air sparging, a lag time (from several hours up to days) existed before the advantages of scouring air bubbles became apparent, which emphasized the importance of long-term studies.

For the purpose of maintaining more sustainable fluxes, the combination of AS and BF showed very promising results in MBR for MLSS contents between 4 and 9.2 g/L over a time period of 8 days. The synergistic effects of AS to fight external fouling and BF to fight internal fouling were more emphasized at higher sludge concentrations.

Within the slug flow regime, higher air injection ratios of 0.58 showed better results than lower air injection ratios of 0.44.

BF doubled the flux with minimal BF pressures of 45 kPa and a product loss of only 3% due to BF.

The limiting flux for the experimental setup was determined to be about 20 L/(m^2 h) when no enhancement techniques were applied.

It was impossible to identify critical flux for conventional filtration (NON) of the chosen synthetic wastewater at about 2/3 of the limiting flux for various operation conditions. It is assumed that if a critical flux for NON exists, it must be close to the pseudo-steady state flux, which was 4 L/(m^2 h) after about 8 days.

Stepwise pressure increase for NON-enhanced filtration of synthetic wastewater could not overcome the flux decline at MLSS of ca. 10 g/L and CFV of ca. 1.3 m/s,

and so the permeability decreased by about 94% within 5 days. For NON-enhanced constant pressure filtration, the permeability decreased by at least 60% within ca. 9 days.

With BF enhancement and TMP rise, it was possible to stabilize the flux for roughly 7 days. However, the permeability of only BF-enhanced operation decreased by about 80% within 5 days at the chosen conditions.

Air sparging enhanced filtration sustained the permeability at about 50% from the initial value after 5 days. With gentle TMP increased from 40 to 98 kPa, AS provided a stable flux over 5 days.

At very low TMP of about 38 kPa and CFV of ca. 1.2 m/s, the combination of AS+BF showed no flux decline and maintained twice the value of the pseudo-steady state flux for NON-enhanced filtration for more than one week, thus indicating sub-critical flux behavior.

At higher TMP of 212 kPa, even the combination of AS+BF showed gentle flux decline and steadily increased fouling, but promised the highest recovery rate at sustainable conditions. Raising the CFV from approximately 1.2 m/s to more than 2.5 m/s bore almost no change of flux behavior for conventional filtration.

Pure water flux of freshly activated polypropylene membranes showed a flux decline of more than 99 % within 10 days at temperatures of 30°C.

An equation was proposed to estimate the viscosity of activated sludge in a sidestream MBR, with dependence on the MLSS and temperature. It was shown that

with decreasing temperatures a higher influence of the biomass concentration on the overall viscosity could be expected.

Backflush application with 2.5 times higher CFV (up to 5.2 m/s) increased permeate yield over a 6 day period by a factor of 3.2 compared to air sparging application at MLSS of 10 g/L.

For combined (simultaneous) deployment of air sparging and backflushing, the permeate yield was more than 4.5 times higher than for the conventional filtration in a 56 day period. It was possible to estimate permeabilities of long term filtration processes with a $t^{-0.25}$ [d] function.

A resistance analysis that compared three different models for the calculation of the cake resistance arising in membrane filtration processes was made. The cake thickness was measured (via SEM) for the different enhancement techniques. From NON (about 50μm thickness) to BF to AS+BF and finally to AS, the cake thickness decreased according to the SEM technique. The measured differences between the cake thicknesses for the enhancement techniques were not very pronounced (between 7 and 12 μm) and the measurement technique could only give a local estimate. However, removing the cake via sponge balls at the end of the filtration process confirmed the SEM observations with the lowest cake thickness belonging to both AS enhanced techniques. This result stands in the opposition to theoretical calculated publications about AS application for model solutions.

The AS technique in combination with CFV of about 2 m/s showed the lowest fouling propensity, while the enhancement techniques which include BF had about

equal fouling resistances. Highest fouling resistance was observed for the NON enhanced case.

It seemed to be confirmed that some cake build up gives the membrane a "safety coating", which prevented more fouling. However, the combination of AS+BF yielded the most permeate for the investigated time frame.

Furthermore, the findings show that there exists a relationship between the initial flux and the CFV.

It was also found that for the cleaning of membranes in wastewater applications with local tap water, a cleaning with NaOH was not sufficient. It was necessary to combine acid and caustic methods for sufficient cleaning.

Comparing the results from theoretical models for the cake resistance with the NON enhanced case revealed that either too sophisticated or oversimplified models gave unacceptable results.

Comparisons of the regular permeate flow to the backflush flow showed that there was a relationship between the resistances in both flow directions.

It seems to be possible, that before the build up of a severe cake layer a relationship between BF resistance and CFV exists.

9.2 Conclusions river water membrane filtration

Mineral residual fouling remained after a chemical cleaning with chlorine solution only. Chemical cleaning was obviously not sufficient in the case of highly

loaded river water filtration. The type/procedure of chemical cleaning did not really change the filtration results.

The reason for the inconsistent results with AS was due to the water properties, which showed, that in later batches there was significantly less fouling potential. The TOC level in the river water decreased during the experiment due to intensive aeration and mixing. Additionally the TOC level in the river water also declined between spring melt and midsummer.

For direct filtration of river water, a membrane system with backflushing was suggested. This is because after sponge ball application, the flux almost immediately collapsed again.

Direct river water filtration could not be recommended as the best choice. It seems definitely worthwhile to consider a pretreatment of the river water or for example a riparian filtration gallery to equalize the significant fluctuations in the river water quality. Under certain circumstances riparian filtration would even allow (for instance by horizontal filter wells underneath the river bed) the system to be run year-round.

Air sparging was only advantageous if significant fouling propensity was given by NOM, colloids, and/or mineral particles. Air sparging was able to raise the permeability of virgin membranes for surface water filtration of high fouling potential up to 400% after more than 3 weeks of deployment.

For clay slurry filtration (10g/L), AS in tubular polymer membranes was able to maintain its permeability at an 80 % higher rate than for a NON-enhanced parallel filtration experiment (after 16 days).

The cake layer, mainly built of silt and treated with air sparging (ε =0.6), showed a decrease in permeability at operation pressures of about 34kPa. This was due to cake compaction (permeability raise from 72.1 to 87.6 [L/(m^2*h*bar)] due to depressurization) after 12 days.

From the sponge ball cleaning procedures it was concluded that there was less cake thickness with AS because the ball passage was significantly easier in the AS enhanced membrane.

10 Recommendations for future work

It is recommended that subsequent work following this thesis utilize the available equipment as far as possible. In addition to the connections already established with the membrane filtration industry, it is recommended to activate further contacts and collaborations with other universities and the industry.

Future investigations in the laboratory should be evaluated under field conditions. The focus should be on long term investigations with low maintenance and very few chemical cleaning cycles.

For work in the laboratory the following suggestions are made to continue with the recent research:

- Determine oxygen consumption in the bioreactor at high MLSS.
- Conduct measurements of heat transfer in the reactor.
- Modify the synthetic wastewater composition to obtain different wastewater properties according to changes in the recipe.
- Measure viscosity to evaluate the suggested equation
- Vary and optimize BF times and frequencies, change BF amounts and pressures, and investigate different BF solutions (only under certain circumstances, e.g. long BF cycles)
- Conduct more thorough membrane autopsy, with SEM and AFM

- Investigate more chemical cleaning solutions/temperatures and develop an optimized cleaning protocol.
- Study the impact of the air slug length and frequency when applying AS for flux enhancement.
- Find a relationship between limiting and critical flux and a dependency to the used filter solution.

Additional questions future work may seek to answer are:

- Does MLSS have a significant impact on the maintenance level of mechanical equipment in MBR and does an optimum MLSS content exist?
- Is intermittent AS sufficient for high MLSS?
- Does intermittent AS have an impact on membrane fouling compared to continuous operation and if so, what can be done to prevent this?

Appendix A

SEM analysis

A1 Optical surface investigation with the scanning electron microscope (SEM)

The SEM is utilized in medical science, biology, and material development. The application in membrane science is very common since magnifications up to 20000 times are possible. Especially for membrane autopsy, SEM is very helpful to investigate the membrane surface prior and subsequent to the use and for failure identification. The disadvantage for the specific model (ISI-40 SEM, UAF Geology Department), which was used for this study, is that the samples have to be precoated and the membrane can no longer be used for filtration processes.

A2 Basic principle

As opposed to a transmission electron microscope, the lenses of the SEM are used to generate a demagnified, focused spot of electrons scanned over the specimen that is electronically conductive. If these impinging electrons strike the specimen, they give rise to low energy secondary electrons from the top layers of the specimen. Some of the electrons are collected, processed, and eventually translated as a series of picture elements (pixels) on a monitor. The brightness of the pixel is directly related to the number of secondary electrons generated from the specimen surface. Because

the electron beam is scanned rapidly over the specimen, the many points appear to be one continuous-tone image composed of many density levels or gray shades, similar to black and white photography.

A3 SEM application in the context of this thesis

The SEM technique is one of the basic tools for the investigation of membranes. It was considered as major assignment during this thesis to gain a reasonable proficiency in handling this device to contribute to a competitive education in membrane science at UAF. With the help of the SEM technology, estimation of the internal membrane fouling, were possible. Furthermore, valuable cake thickness analysis, used as an estimate for cake resistance calculations and backup values for quantitative contribution of cake fouling to the overall fouling, were possible. This is shown in Chapter 6: "Resistance analysis for enhanced wastewater membrane filtration". Fig. A1.1. and Fig. A1.2. show two images as examples for different resolution/magnification. Fig. A1.1. depicts a virgin membrane without any particle deposition onto the surface. Fig. A1.2. shows the inside edge of a used membrane after treatment with air sparging at high magnification (bar length 1μm). It can be seen that the thickness of the cake layer does not exceed the bar length by much more than one order of magnitude.

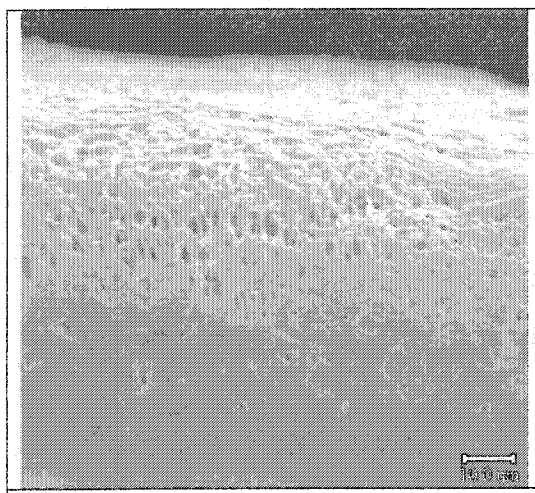

Fig. A-1. Virgin membrane.

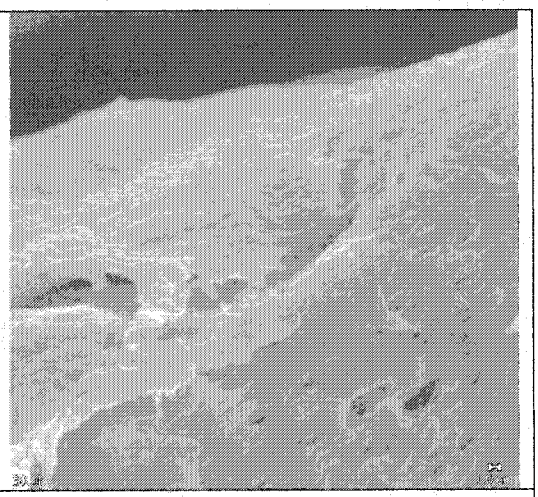

Fig. A-2. Dirty membrane

Appendix B

Cost analysis

B1 Calculation

As emphasized in this thesis, air sparging (AS) is an efficient technique to enhance flux for microfiltration processes in water and wastewater filtration. A cost comparison between the sponge ball method and the AS technique is presented below.

As investigations in this thesis showed (Chapter 6), operating membranes with AS generates the least amount of fouling. This is owed to the fact that a thin filter cake preserves the surface of the membrane, resulting in a longer lifetime than the conventional membrane filtration. Another advantage of the AS application is that there are no moving parts resulting in lower maintenance costs.

For the sponge ball application, a set of sponge balls is pushed through the system once every hour to scour the membrane surface. Passage of these balls leads to an almost permanent exposure of the membrane surface to particle intrusion. As a result, serious internal membrane fouling can occur, which can only be treated with more chemical cleaning, leading to faster aging of the membrane. Thus, in the long run, AS prevents premature membrane aging, yielding a return on investment as Table A2.1 shows.

Table B-1. Cost comparison of NON vs AS

	NON	AS
Initial costs [$]		
1300 modules	260,000	260,000
Sponge balls + baskets	2,000	0
Valves + piping + PLC	3,000	3,000
AS system	0	5,000
Air blower	0	6,000
Air compressor	0	50,000
Air flow meter, pressure gauges		8,000
Total initial costs [$]	265,000	332,000
Life expectancy =n [years]	5	10
Interest rate = I [6%]		
Capital recovery factor CRF=I/(1-(1+I)^n)	0.24	0.14
Annualized initial costs [$]	**63,600**	**46,480**
Operational costs per year [$]		
Air blower	0	2,000
Compressor	0	22,000
Chemicals	13,000	6,500
Annualized operation costs [$]	**13,000**	**30,500**
Total annualized costs [$]	**76,600**	**76,980**

The above data were based on industry information from PCI Membrane Systems Inc. [1] and experience from plant operation provided by US Filter [2]. Cost estimates for equipment were obtained from the McMaster-Carr Company [3]. For the calculation of Table A2.1 the following assumptions were made:

- Plant size with an output of 2.5 m^3/h
- 1300 membrane modules (0.1 m^2 each),
- 5 tubes (6.3 mm diameter each)
- Flux 20 (L/m^2 h)
- Cross-flow velocity (CFV) of approximately 1 m/s
- Twice the necessary cleaning for sponge ball applications (26 times per year vs. 13 times per year) compared to the AS system
- Chemical costs of $ 500 per cleaning
- Minimum of approximately 10 L of cleaning solution necessary per module
- Cleaning with acid for 0.5 hours and subsequent 0.5 hours (after rinsing) cleaning with caustic solution
- Costs per kWh = $ 0.065
- Life expectancy for the AS system twice as long as for sponge ball system

If a lower CFV would be chosen, cost advantages for the AS system would be expected, according to investigations by *Labourie et al.* [4].

For the application of AS in the context of membrane bioreactors (MBR), where an aeration of the wastewater is necessary, definite cost advantages are foreseeable.

B2 References

[1] L. Pain, PCI Membrane Systems, personal information March 2005.

[2] USFilter information regarding operation costs for membrane plants 2005

[3] McMaster Carr supply Company, Catalog 1996.

[4] S. Laborie, C. Cabassud, L Durand-Bourlier and J. Laine, Fouling control by air sparging inside hollow fibre membranes – effects on energy consumption, Desal., 118, (1998), pp. 189-196.

Appendix C

Error Analysis

C1 Introduction

C1.1 Overview

It is well established in science that if an experiment is performed for the first time, the results reflect the truth only to a certain extent. With repetition of the experiments and better equipment and methods, the results begin to approach the "true" description of nature within an acceptable range [1].

The simpler the experiments and the older the field of science, the more rules are established for conducting those experiments, and thus the easier it is to repeat measurements/observations and compare results. For the rather new field of membrane science, there is still a lot of work to be done when it comes to standardizing and establishing accepted cleaning protocols and measures for membrane comparison. Almost every month, new membranes appear on the market with new properties, made out of new materials. Hence, it is not easy to catch up with recent developments to normalize procedures for a fair membrane assessment. This rapid development of the market is based on furious research activities. The expectations of a quick return on investments in research and development are reflected in increasing market shares and larger profit margins. Thus, it is rare that the researchers incorporated long term data analysis. Instead, they choose to quickly investigate new combinations of membranes and fluids.

Most important, research results reflect material properties, which have to be evaluated in a time-dependent context. So it is not very common to repeat flux measurements in small time frames because the larger picture is of interest, and the achieved trends give a reasonable and sufficient amount of certainty. Although automated devices can record data at small time intervals, investigations are still relatively short lived.

This dissertation reports on a complex experimental setup, investigating multiphase-flow separation techniques on fluids with changing properties due to microbial activity and segregation for long term studies up to 190 days. To provide for more data transparency, the investigated enhanced filtration was operated in parallel to conventional filtration at advanced stages of the research (subsequent to chapter 3). This is a novelty since most of the research found throughout the literature (see references Chapter 1-8) reflects research within 3-5 hour time frames, when the experiments are easily repeated without measurable changes in fluid and membrane properties. The parallel observation of enhanced and non enhanced membranes served as a simple but powerful technique to identify wrong data collection and prevent improper result interpretation.

C1.2 Introduction to error analysis and error propagation

An error is the difference between an obtained value, either by observation or calculation, and the true value. The real or true value is not known, but usually an estimate exists of what the real value should be. The estimate is obtained from previous experiments. In fact, every measurement is inherently error afflicted.

We can express differences in measurements as a discrepancy between two results. The discrepancy arises because we can determine our results only up to a given uncertainty. According to *ISO* [2], the term uncertainty is preferred over measurement error since the latter can never be known. However, throughout this appendix the term uncertainty has the same meaning as measurement error.

In the context of error analysis, it is important to clarify the often confused difference between the terms *Accuracy* and *Precision.*

Accuracy is the nearness of the measured result to the true value. Accuracy is often reported as relative error [3]:

relative error = (measured value – expected value)/expected value

Precision means how good repeated measurements agree with each other [4]. Precision is often reported quantitatively by using relative or fractional uncertainty:

relative uncertainty = absolute uncertainty/measured value

The absolute uncertainty is the amount (often stated as $\pm$ δx) that along with the measured value indicates the range in what the true value most likely is [3].

To simplify the statements above, we can pick the following analogy: "Accuracy is telling the truth, precision is telling the same story over and over again" [5].

In regards to those definitions, emphasis in this PhD work was given primarily to the term accuracy. The term precision assumes that the repetition of experiments is performed under the exact same conditions, which is almost completely precluded by the character of the investigations. Thus, the main objective during this work was to eliminate or reduce errors, which influence the accuracy of the result. In general three classes of errors are distinguished [1]:

- illegitimate errors
- systematic errors
- statistical errors

The sum of systematic and statistical errors gives the total error for a reasonable estimate (illegitimate errors should be excluded in general).

If results significantly diverge from the estimate and we know what caused the problem than we can immediately identify them as mistakes. Such blunders are called *illegitimate errors* and can be corrected by repetition of the erroneous operation or changing the adjustments (for instance air injection ratio to low or cross-flow velocity (CFV) to high).

The class of *systematic errors* is not easy to identify because they produce repeatable wrong results based on an erroneous pre adjustment of devices or faulty calibration. The systematic errors must be estimated via analysis of experimental

conditions and techniques or by looking at the quality of measurement devices [1]. Systematic errors make our results deviate from the true value and how well we can control them influences the accuracy of our results. To work with more sensitive, but well calibrated equipment is one way to reduce systematic errors.

How well we can control *statistical errors* (sometime called random errors) has a significant influence on the precision of our experiments. Statistical errors are the fluctuations in observations, which yield results that differ from experiment to experiment and require repeated experimentation to obtain precise results. It is possible to reduce statistical errors by improving the experiment, refining the techniques, as well as simply repeating the experiment.

If measurements of the same value are repeated, statistical analysis can be applied for the evaluation of uncertainty. Statistical descriptions of the data are expressed as the mean, the standard deviation and the standard error.

The mean $\bar{x}$ (also called average) gives the best estimate of a measured quantity from N measurements and is calculated by:

$$\bar{x} = \frac{\sum_{i=1}^{N} x_i}{N} \qquad \text{eq. C1}$$

The standard deviation σ reflects the scatter of measurements about the average and is given with eq. C2

$$\sigma = \sqrt{\frac{\sum_{i=1}^{N} \left(x_i - \bar{x}\right)^2}{N-1}} \qquad \text{eq. C2}$$

The standard deviation determines the sector, if the values follow a normal Gaussian distribution (bell shape), in which about 68 % of the quantities lay [6]:

$\bar{x} \pm \sigma$. In case that expanded uncertainty is given as follows

$\bar{x} \pm 2\sigma$ about 95% of the quantities are within the confidence interval, or

$\bar{x} \pm 3\sigma$ than about 99% of the quantities lay in the confidence interval.

The standard error δ is calculated according to eq. C3

$$\delta = \frac{\sigma}{\sqrt{N}} \qquad \text{eq. C3}$$

This quantity is also known as the standard deviation of the mean. It estimates the standard deviation of the distribution of means that would be obtained if the mean would be measured many times [7].

Often the value that we wish to determine is derived from other measured quantities. If the quantities $x \pm \Delta x$ and $y \pm \Delta y$ result in the new quantity $z \pm \Delta z$, the uncertainty $\pm \Delta z$ will be calculated according to the rules of ***Error Propagation***.

In the frame of this error analysis the guiding principle will be the most pessimistic situation or the worst case propagation of uncertainty. For a more sophisticated statistical treatment, the standard deviation would be an appropriate treatment. However, the data collected in this work (see section C3) does not really provide the necessary variety for the calculation of standard deviations and standard errors. Moreover, the standard deviation gives always smaller quantities than the most pessimistic approach.

Following are explanations of the different laws of error propagation.

If the uncertainty is based on a sum or difference of measurement results, the uncertainty of the final calculation is determined according to eq. C4 [8]:

$$\Delta z = |\Delta x| + |\Delta y| + \ldots \qquad \text{eq. C4}$$

If the determined value is obtained by a product or quotient of measured quantities, the following eq. C5 applies:

$$\frac{\Delta z}{z} = \frac{\Delta x}{x} + \frac{\Delta y}{y} + \ldots \qquad \text{eq. C5}$$

Another way to express eq. C5 is shown in eq. C6 with the total derivative

$$dz = \left(\frac{\partial f}{\partial x}\right) dx + \left(\frac{\partial f}{\partial y}\right) dy + \ldots \qquad \text{eq. C6}$$

where $dz = \Delta z$ etc.:

Applying the total derivative of eq. C6 to the rearranged eq. 1.2 (Chapter 1):

$$R_t = \frac{TMP}{\mu * J} \qquad \text{eq. 1.2a}$$

we obtain the following expression of eq. C6:

$$dR_t = \left(\frac{\partial f}{\partial TMP}\right) * dTMP + \left(\frac{\partial f}{\partial \mu}\right) * d\mu + \left(\frac{\partial f}{\partial J}\right) * dJ \qquad \text{eq. C6a}$$

If we want to have the maximum error possible, using absolute values and with dx = Δx, we receive eq. C6b:

$$dR_t = \left|\frac{\partial R_t}{\partial TMP} * \Delta TMP\right| + \left|\frac{\partial R_t}{\partial \mu} * \Delta\mu\right| + \left|\frac{\partial R_t}{\partial J} * \Delta J\right| \qquad \text{eq. C6b}$$

The above total derivative gives:

$$dR_t = \left|\frac{1}{\mu * J} * \Delta TMP\right| + \left|-\frac{TMP}{\mu^2 * J} * \Delta\mu\right| + \left|-\frac{TMP}{\mu * J^2}\Delta J\right| \qquad \text{eq. C6c}$$

Multiplying with advantageous terms to substitute three components for Rt in each of the absolute values gives:

$$dR_t = \left|\frac{1}{\mu * J} * \frac{TMP}{TMP} * \Delta TMP\right| + \left|-\frac{TMP}{\mu^2 * J} * \frac{\mu}{\mu} * \Delta\mu\right| + \left|-\frac{TMP}{\mu * J^2} * \frac{J}{J} * \Delta J\right| \qquad \text{eq. C6d}$$

Each expression of the absolute values on the right hand side contains eq. 1.2a (Rt). Dividing by Rt we obtain the following expression:

$$\frac{dR_t}{R_t} = \left|\frac{\Delta TMP}{TMP}\right| + \left|\frac{\Delta \mu}{\mu}\right| + \left|\frac{\Delta J}{J}\right| \qquad \text{eq. C5a}$$

This equation (eq. C5a) brings us back to equation C5.

In case the formula which delivers the wanted information is a product of powers, i. e. $z = x^m * y^n$, the error propagation is calculated according to eq. C7 [9]:

$$\frac{\Delta z}{z} = |m|\frac{\Delta x}{x} + |n|\frac{\Delta y}{y} \qquad \text{eq. C7}$$

C2 Utilized equipment and tolerances

For the determination of the systematic errors, the given or estimated uncertainty ranges of the measurement device were used. An overview of the used measurement devices, their tolerances, and in which section they are applied is given in table C-1.

Table C-1. Measurement devices and tolerances

Measurement device	Type	tolerance	used in section
pressure gauge	100 PSI WIKA 232.34	± 1 PSI	C3.1
pressure gauge gas	100 PSI Campbell PG1T	± 2 PSI	C3.1 (indirect)
scale	80 g Mettler Toledo AE 160	± 0.0002 g	C3.1
automatic balance Ohaus	4 kg Navigator NOH 110	± 0.5 g	C3.1
thermometer VW 60°C	Cat.-No. 61019-010	± 1 °C	C3.1
Quarz Chronograph	Pulsar V041	± 0.1 s	C3.1/2/3 (indirect)
gas flow meter Gilmont	100 L/min No. 54331-54390	± 2 L/min	C3.1 (indirect)
mass flow meter OMEGA	15 L/min gas FMA 5522	± 0.2 L/min	C3.1 (indirect)
glas cylinder 4L	4L metric Pyrex 3022	± 29 mL	C3.2
glas cylinder 10 mL	10 mL metric Pyrex 3022	± 0.2 mL	C3.1

C3 Evaluation of results based on error analysis and error propagation

C3.1 Determination of uncertainty for the membrane resistance

First, the equation has to be determined for calculating the desired result. Then, depending on how the variables in the equation are related to each other, the error propagation can be determined. The most significant equation in the context of this thesis is eq. 1.2, which is cited, in some form, in every chapter of this work.

$$J = \frac{TMP}{\mu * R_t} \qquad \text{eq. 1.2}$$

In a rearranged form, suitable for the calculation of the total resistance, Rt, we obtain eq. 1.2a, which will serve as the base equation for the error propagation.

$$R_t = \frac{TMP}{\mu * J} \qquad \text{eq. 1.2a}$$

According to eq. 1.2a, the governing law for the error propagation is going to be a multiplication and division in the first step, requiring the application of eq. C5/6.

In the frame of this work, there are only 6 data sets available, which allow a statistical data analysis, in addition to the analysis of systematic errors. The data sets, three each from backflushing (BF) and air sparging and backflushing (AS+BF), will further be investigated for the error analysis.

The 6 data sets qualified because it was possible during the automatic data collection to hold the temperature constant over about 5 hours. During this time repeated measurements under 99.9% identical conditions were possible.

C3.1.1 Determination of Δ TMP

For application of eq. 1.2a on the transmembrane pressure (TMP), only systematic errors can be determined. According to Table C-1, the systematic error is 1 PSI. For the calculated values see Table C-2.

C3.1.2 Determination of $\Delta\,\mu$

For applying eq. 1.2a for the dynamic viscosity, eq. 5.5 (Chapter 5) has to be used in order to calculate the viscosity as suggested by *Psoch and Schiewer* in Chapter 5:

$$\mu = \frac{0.33 * MLSS + 2.3}{\left(1 + 0.0337 * T + 0.000221 * T^2\right)} \qquad \text{eq. 5.5}$$

C3.1.2.1 Determination of Δ MLSS and the numerator of eq. 5.5

The mixed liquor suspended solids (MLSS) have to be determined according to the following equation

$$MLSS = \frac{m_2 - m_1 * 1000}{V} \qquad \text{eq. C8}$$

where m_2 and m_1 are the measured masses of the filter paper, and V is the filtered volume of sample. According to Table C-1, the systematic error for the scale is 0.0002 g and for the measurement cylinder (10 mL), $\pm$ 0.2mL. For the error propagation, eq. C5 applies as well as the rule for multiplication with a constant value. For the calculated results see Table C-2.

Table C-2. Error analysis based on error propagation

BF

	TMP [Pa]	Δ TMP [Pa]	ratio TMP	μ [Pas]	Δ μ [Pas]	ratio μ	J [L/(m²h)]	Δ J syst [L/(m²h)]	Δ J stat. [L/(m²h)]	ratio J	Rt [1/m]	Δ Rt [1/m]	ratio Rt	CFV [m/s]	Δ CFV [m/s]	ratio CFV
Aug. 16	129277	7000	0.054	0.0037	0.0003	0.070	20.06	0.32	0.20	0.016	6.6E+12	9.3E+11	0.140	2.89	0.030	0.010
Aug. 19	143066	7000	0.049	0.0036	0.0002	0.0668	20.23	0.32	0.14	0.016	7.9E+12	1.0E+12	0.132	2.88	0.030	0.010
Aug. 22	144790	7000	0.048	0.0037	0.0002	0.0653	18.63	0.32	0.19	0.017	8.3E+12	1.1E+12	0.131	2.98	0.030	0.010

AS+BF

	TMP [Pa]	Δ TMP [Pa]	ratio TMP	μ [Pas]	Δ μ [Pas]	ratio μ	J [L/(m²h)]	Δ J syst [L/(m²h)]	Δ J stat. [L/(m²h)]	ratio J	Rt [1/m]	Δ Rt [1/m]	ratio Rt	CFV [m/s]	Δ CFV [m/s]	ratio CFV
Oct. 17	146514	7000	0.048	0.0045	0.0003	0.0682	27.29	0.32	0.37	0.014	4.2E+12	5.4E+11	0.130	1.29	0.018	0.014
Oct. 19	148237	7000	0.047	0.0045	0.0003	0.0682	26.12	0.32	0.18	0.012	4.5E+12	5.7E+11	0.128	1.31	0.018	0.014
Oct. 20	143928	7000	0.049	0.0046	0.0003	0.0685	26.08	0.32	0.14	0.012	4.2E+12	5.5E+11	0.129	1.31	0.018	0.014

C3.1.2.2 Determination of Δ T and the denominator of eq. 5.5

According to Table C-1, the systematic error for the scale is ± 1°C. For the error propagation, eq. C4 and eq. C7 apply. For the calculated values see Table C-2.

C3.1.2.3 Calculation of Δ μ

For the calculation of the uncertainty of the viscosity, eq. C5 is used, which works with the above obtained results for the denominator and numerator of eq. 5.5. For the calculated results see Table C-2.

C3.1.3.1 Determination of Δ J based on systematical errors

According to Table C-1, the systematic error for the flux determination is ± 0.2 mL. For the calculated values see Table C-2.

C3.1.3.2 Determination of Δ J based on statistical errors

For the statistical error analysis, the standard error eq. C3 was used. From each of the 6 days, the standard error was calculated based on the mean out of 10 independent standard errors with 10 data points each. The single independent standard errors were calculated from balance data the last 10 min before a BF within one BF-cycle, which provides almost identical conditions for each set of data. For the calculated results see Table C-2.

C3.2 Determination of uncertainty for the cross-flow velocity

The cross-flow velocity was determined according to the relationship v=Q/A. A was the cross-section of the membrane and Q was determined by the relationship Q=V/t. According to Table C-1, the uncertainty for the volume determination was given with $\pm$ 29 mL and for the time measurement with $\pm$ 0.1 s. For the calculated results see Table C-2.

C4 Conclusions of error analysis and error propagation

The running of parallel experiments over a given period of time allowed comparable results, although different techniques were applied.

Therefore a reduction of illegitimate and systematic errors was possible. In Table C-2 all performed calculations were summarized. Based on eq. 1.2a, the largest impact on the total membrane resistance was the calculation of the viscosity. With

about 7% deviation from the best guess (measurand), the uncertainty of the viscosity had an even greater impact on the total uncertainty than the pressure, which contributed about 5% deviation from the measured. The flux measurement was obviously the most reliable influence variable on the total deviation when calculating total membrane resistance. In all cases but one (Oct. 17th) the statistical error was smaller than the systematical error. To determine the error for calculation of total membrane resistance, the largest flux error was used (5 times systematic error and one time statistical error). The calculation of the overall system resistance shows a deviation of about $\pm$ 13 - 14%. This is considered to be reasonably accurate with the equipment used. The calculation of the CFV showed that there is deviation of $\pm$ 1 - 1.4%, which is considered to be very good.

C5 References

[1] P. Bevington, Data reduction and error analysis for the physical sciences, McCraw-Hill, New York (1969)

[2] ISO. Guide to the Expression of Uncertainty in Measurement. International Organization for Standardization (ISO) and International Committee on Weights and Measures (CIPM): Switzerland, 1993

[3] University of North Carolina, Department of Physics and Astronomy: //www.physics.unc.edu/~deardorf/uncertainty/UNCguide.html

[4] Hach Company, DR/2010 Spectrophotometer Handbook

[5] Flatirons Surveying Inc.: //www.flatsurv.com/accuprec.htm

[6] NIST Essentials of Expressing Measurement Uncertainty.
//physics.nist.gov/cuu/Uncertainty/basic.html

[7] Case Western Reserve University, Physics department:
//physicslabs.phys.cwru.edu/EM/Manual/pdf_version/Appendix_V_Error%20Prop.pdf

[8] Rochester Institute of Technology, Physics department:
//www.rit.edu/~uphysics/uncertainties/Uncertaintiespart1.html

[9] Purdue University, Physics department:
//www.physics.purdue.edu/Zope/courses/phys152L/MeasurementAnalysis.pdf

Appendix D

Synthetic wastewater composition

D1 Mixture evolution

In the frame of this work, activated sludge was produced by inoculation with microbial cultures from the local wastewater treatment plant. Synthetic wastewater was supplied for growth and maintenance of the microbial population in the membrane bioreactor. The feed contained high concentrations of the three major elements as Carbon (C), Nitrogen (N) and Phosphorus (P) and other compounds. Next to the so called macronutrients, trace substances in minor concentrations were necessary in order to sustain microbial growth.

After evaluating the literature (review Table A4.1), first tests were made with dry milk powder as the main component. A milk powder based medium was chosen as the simplest option. However, injecting air into a milk powder/water blend generated high foam production. Anti foam substances, that were applied to reduce foam production, degraded fast and may have adversely affected the membrane permeability. Thus dry milk powder was abandoned as a feed for air sparging tests and other microbial food sources were investigated. The feed of the MBR was finally generated from 10 components. Glucose with increasing concentrations (up to 60 g/day) [1, 2] with ongoing test duration and slowly increasing biomass concentration served as the main carbon source following a recipe suggested by *Shim et. al.* [3].

As pointed out by *LeClech* [4], the most commonly used synthetic wastewater composition in the last decade is that of *Chang et al.* [5]. Shims recipe is fairly close to that in regards of its major components.

Shim's original composition caused problems due to high pH values. A variation of Shim's recipe to suit own needs (for instance decreased $NaHCO_3$ concentration for pH adjustment) resulted in change a in composition [2].

The feed was generated as a concentrate and stored at 2°C in a 4.5 L batch which served for about 9 days. Every day 500 mL of this stock solution was diluted with 2 L of tap water to feed the reactor. Even at such low temperatures and thorough disinfection of all surfaces that came in contact with the medium, a COD decrease of the feed solution (within 9 days storage) by 30 % due to microbial activities could not be prevented. In order to overcome this issue, glucose and glutamic acid as the main carbon sources were no longer added to the feed solution mixture but supplied separately every day in the appropriate amounts.

The activated sludge content in the reactor, measured as mixed liquor suspended solids (MLSS), was regularly determined according to the *Standard Methods* [6]. The sludge retention time was maintained at 35 days by withdrawing every day about 2 L of sludge.

Table D-1. Synthetic wastewater compositions [2; 3; 5; 7-16]

Substance	Mol weight [g/mol]	First Author	Main Compound	Cicek mg/L	Saby mg/L	Kiso mg/L	Kiso mg/L	Ghyoot mg/L	Ghyoot mg/L	Ghyoot mg/L	Ghyoot mg/L	Yamagishi mg/L	Yamagishi mg/L	Seo mg/L	LaPara mg/L	Holler mg/L	Shim mg/L	Lee mg/L	Kim mg/L	Chang mg/L	pspch mg/L
skim milk powder			Milk					400	600	800	1200										
antifoam			Additive					0.00005	0.00005	0.00005	0.00005										
Skim Milk			Milk			333	333														
beef extract			Mixture											1.802		220					
C5H8NNaO4H2O (Glutamat)			Mixture															48.7			
glucose [C6H12O6]	180	C															875	114	9000	16000	24000
alpha-lactose		C													1500						
Tannic acid		C												4.175							
arabic gum powder		C												4.695							
Starch in COD/L		C		90																	
C3H5(OH)3	92	C		15																	
H3C-(CH2)8-COOH		C		30																	
Casein in COD/L		C/N		175																	
Ammoniumacetat CH3COONH4		C/N															285	37.7			0.512
glutamic acid		C/N															370				1200
Sodium lignin sulfonate		C/Macronutrient*												2.427							
Sodium lauryl sulphate		C/Macronutrient												0.942							
Urea		N														60					
Peptone (bacto)		N			75									2.703		320			6000	12000	
gelantine	(Aldrich)	N													1500						
yeast extract		N			150										50				90	1600	
H3C-CNOONa		N		15																	
NH4HCO3	79	N												19.8							
NaOH	40	Macronutrient		175																	
NH4Cl	53.5	Macronutrient			126.6	120	120							55	500		43	5.67			0.1375
(NH4)2SO4		Macronutrient		38										7.1				56.7	64	12800	
KH2PO4 (Phasbuff	136.1	Macronutrient			68												62	5	1280	2560	0.045
K2HPO4	(P - buffer)	Macronutrient		6.5	174	13.4	13.4							7		50	90	7			0.054
CaCl2 * nH2O	111	Macronutrient		22.5	54.28							40	20		0.6		20	0.6	160	320	0.054
MgSO4*nH2O	120.3	Macronutrient		66.6	22.5							140	70	0.71	50	4	93	9.02	1600	3200	0.1058
Na2HPO4	(P - buffer)	Macronutrient										384	194		576						
NaH2PO4		Macronutrient													830						
NaHCO3		Macronutrient				583	583					1200	1200				1875	150	1000	2000	2
NaCl		Macronutrient														14	25	6.27			0.06
KCl		Macronutrient										80	40		2	8					
COD [mg/L]				323	330			360	562	764	1033			17.3	3100	1500	1250	250	24400		
BOD [mg/L]						200	200														
Total N [mg/L]				46.8	58	50	50												1550		
NH4-N [mg/L]					36	32	32					~200	~200								
NO3-N [mg/L]				20.2	2 -	-															
PO4-P [mg/L]				< 0.6	10	5.7	5.7														
Carbohydrat [mg/L]															1350						
Protein [mg/L]															950						
Temperature feed [°C]				4				4	4	4	4	4	4								2
Feed tank volume [L]				220*2												1000					4.5
DOC [mg/L]				36																	
DO [mg/L]					7			2.1	2.1	2.1	2.1				4			6.1	3.5		4-9
Reactor volume [L]				40	10	17	25	4.6	4.6	4.6	4.6	0.5	1	21.3	0.58	14	21	5	5		70
HRT [d]				0.25	0.25	0.021	0.029								1.54-0.33	0.067		0.3333	0.3333		
MLSS [g/L]				11		7	5.75					8.3				16	8-16	3	6.5	3.5	8-15
Temperature reactor [°C]				18	20 -	-	-	~ 24	~ 24	~ 24	~ 24	25	25	15	55	24		25	-		17
Sludge age [d]				30	4	8	4					900	1000				25		30		35
pH				7.5	7.7			7.15	7.15	7.15	7.15	7.4	7.4			7.05		7			8
Organic loading [kg/(m³*d)]												0.23	0.23			9.5					

*Macronutrients are: C & N and P, S, K, Mg, Ca, Na

**Trace substances are: Cr, Co, Cu, Mn, MO, Ni, Se, W, V, Zn, Fe

D2 References

[1] C. Psoch and S. Schiewer, Long-term study of an intermittent air sparged MBR for synthetic wastewater treatment. J. Membr. Sci, (2005) in press.

[2] C. Psoch and S. Schiewer, Synthetic wastewater preparation and aeration via air sparging in a sidestream MBR. to be submitted to Water Research (in preparation), (2005).

[3] J. Shim, I. Yoo, Y. Lee, Design and operation considerations for wastewater treatment using a flat submerged membrane bioreactor, Process Biochemistry, 38 (2002) 279-285.

[4] Le Clech, P., PhD thesis: Process configuration and fouling in membrane bioreactors. Cranfield University UK, (2002).

[5] I. Chang, C. Lee and K. Ahn, Membrane filtration characteristics in membrane-coupled activated sludge system: the effect of floc structure on membrane fouling. Sep. Sci. Techn., 34, 9, (1999), pp. 1743-1758.

[6] APHA-AWWA-WEF, Standard Methods for the Examination of Water and Wastewater, A. Eaton, L. Clesceri, A. Greenberg, (Eds.), 19th ed. (1995) Washington DC.

[7] N. Cicek, et. al., Effectiveness of the membrane bioreactor in the biodegradation of high molecular weight compounds, Water Research, 32, 5 (1998) 1553-1563.

[8] S. Saby, M. Djafer and G. Chen, Feasibility of using a chlorination step to reduce excess sludge in activated sludge process. Wat. Res. 36, (2002), pp. 656-666.

[9] Y. Kiso et. al., Wastewater treatment performance of a filtration bio-reactor equipped with a mesh as a filter material. Wat. Res. 34, 17, (2000), pp. 4143-4150.

[10] W. Ghyoot and W. Verstraete, Reduced sludge production in a two-stage membrane-assisted bioreactor. Wat. Res. 34, 1, (1999), pp. 205-215.

[11] T. Yamagishi, J. Leite, S. Ueda, F. Yamaguchi and Y. Suwa, Simultaneous removal of phenol and ammonia by an activated sludge process with cross-flow filtration. Wat. Res., 35, 13, (2001), pp. 3089-3096.

[12] G. Seo, Y. Suzuki and S. Ohgaki, Biological powdered activated carbon (BPAC) microfiltration for wastewater reclamation and reuse. Desal., 106, (1996), pp. 39-45.

[13] T. LaPara, A. Konopka, C. Hakatsu and J. Alleman, Thermophilic aerobic treatment of a synthetic wastewater in a membrane-coupled bioreactor, Journal of Industrial Microbiology & Biotechnology 26, (2001), pp. 203-209.

[14] S. Holler and Walter Trösch, Treatment of urban wastewater in a membrane bioreactor at high organic loading rates. Journal of Biotechnology, 92, (2001), pp. 95-101.

[15] J. Lee, W. Ahn and C. Lee, Comparison of the filtration characteristics between attached and suspended growth microorganisms in submerged membrane bioreactor. Wat. Res. 35, 10, (2001), pp. 2435-2445.

[16] J. Kim, C. Lee and I. Chang, Effect of pump shear on the performance of a crossflow membrane bioreactor. Wat. Res., 35, 9, (2001), pp. 2137-2144.

Appendix E

Oxygenation

E1 Aeration tests in clear water

As already described throughout the Chapters 2 - 8 and shown in Fig. 2.2 and Fig. 5.2 air was pushed into the system via separate channels which were extensions of the membrane tubes generating a two-phase flow. The optimal flow pattern in order to achieve the highest mass transfer rate was the slug flow regime with bullet like air bubbles. The wake of those air slugs contained numerous bubbles whose size is only a fraction of a millimeter [1]. The very high specific surface area of such tiny air bubbles in combination with the larger air slugs and the sidestream (see section 1.1.3.2) specific long contact time while "traveling" through the loop lead to optimal oxygen mass transfer conditions.

Fig. E-1 provides a comparison of air sparging and conventional aeration under equal conditions in clear water. The conventional aeration was simulated by a diffuser hose with drill holes of about 1 mm located at the bottom of the reactor vessel. Clear water tests were performed to exclude any outer effects such as microbial activity. As evident from Fig. E-1, the conventional aeration is unable to raise the oxygen content significantly above 93%. However, air sparging at the same air mass flow rate raises the oxygen content well above 100% saturation and serves as a more than sufficient oxygen supply.

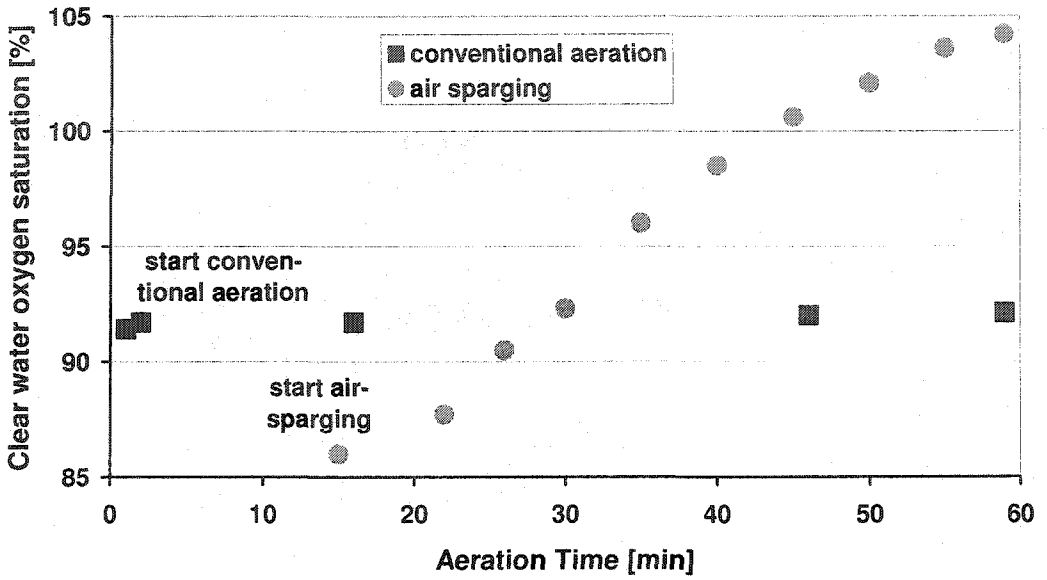

Fig. E-1. Comparison of air sparging aeration and conventional aeration

E2 Aeration tests in wastewater

After obtaining very good aeration results with air sparging in clear water, tests in the MBR were launched. For the first 14 days (section A in Fig. E-2) air sparging served as the sole means of aeration, being provided only every other 30 minutes. As obvious from Fig. E-2, the dissolved oxygen (DO) content in the reactor almost never fell below 2 mg/L, which is a typical value for municipal wastewater treatment plants [3]. Averaging 7 mg/L, air sparging served well even under challenging conditions. For the days 13 to 33 (section B in Fig. E-2) conventional aeration was provided continuously. However, the oxygen content is barely higher than for the air sparging system and no substantial advantage can be recognized.

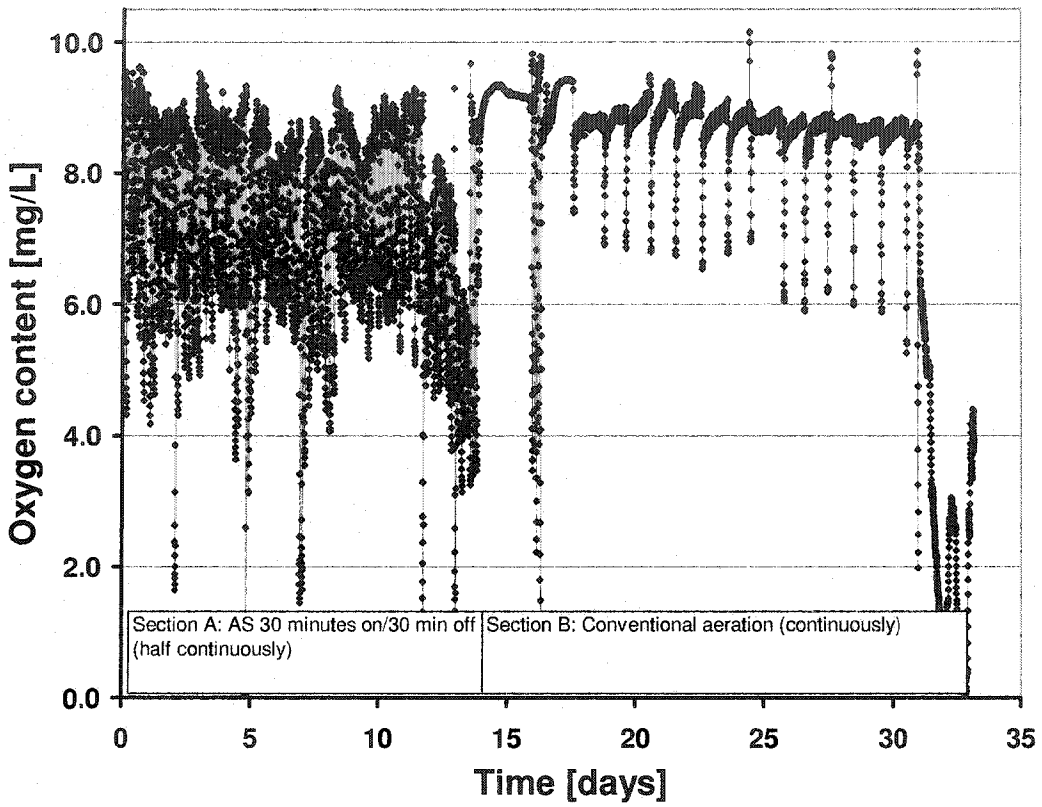

Fig. E-2. Oxygen content in MBR, Section A: 30 min air sparging alternating with 30 min without aeration (day 0-14). Section B: continuous conventional aeration (day 14-33). MLSS 3 g/L, temperature 18°C.

E3 Determination of the mass transfer coefficient in the air sparged system

Finally the aeration capacity of the air sparging system was evaluated using accepted procedures such as the ASCE Standard [2].

According to Metcalf & Eddy [3] the commonly used equation for determination of the mass transfer coefficient is based on the following expression (eq. E1):

$$r_C = \frac{dC}{dt} = K_L a * (C_S - C) \qquad \text{eq. E1}$$

with:

r_C = rate of change in concentration [mg/(L*s)]

C = concentration of gas (oxygen) in solution [mg/L]

t = time [s]

$K_L a$ = overall mass transfer coefficient [s^{-1}]

C_S = saturation concentration of gas in solution [mg/L]

Eq. E1 is integrated with the boundary conditions $C = C_0 = 0$ at $t = 0$ and $C = C_t$ at $t = t$ as shown in eq. E2:

$$\int_{C_0}^{C_t} \frac{dC}{C_S - C} = K_L a \int_0^t dt \qquad \text{eq. E2}$$

The solution of this expression is shown in eq. E3, which is the working equation for the oxygen transfer calculations:

$$\frac{C_S - C_t}{C_S - C_0} = e^{-(K_L a)*t} \qquad \text{eq. E3}$$

The rewritten eq. E3, linearized and expressed applying the decadic logarithm is shown below as eq. E4. The $K_L a$ value can be obtained from the slope of a plot of (C_S-C_t) versus t:

$$\log(C_S - C_t) = \log(C_S - C_0) - \frac{K_L a}{2.303} * t \qquad \text{eq. E4}$$

Following the procedures of the *ASCE Standards* [2] for the determination of an approximate $K_L a$ value of an aeration device, at first all oxygen in the vessel has to be eliminated by adding chemicals. Cobalt-free sodium sulfite (Na_2SO_3) serves as the deoxygenation substance. The theoretical sodium sulfite requirement for deoxygenation is 7.88 mg/L per 1.0 mg/L Dissolved Oxygen (DO). Cobalt chlorite hydrate ($CoCl_2*6H_2O$) or cobalt sulfate ($CoSO_4$) is used to catalyze the deoxygenation reaction. The cobalt concentration should be between 0.1 and 0.50 mg/L in the test water. After the oxygen content in the test vessel dropped below 0.50 mg/L at all points, water re-aeration was started, while monitoring the time and the

DO concentration at constant temperature. To eliminate the temperature dependence of the K_La value, all tests had to be calibrated to 20°C using an exponential function to appropriate the van't Hoff-Arrhenius relationship (eq. E5):

$$K_L a_{(T)} = K_L a_{(20°C)} * \theta^{T-20} \qquad \text{eq. E5}$$

with:

$K_La_{(T)}$ = oxygen mass-transfer coefficient at temperature T, [s^{-1}]

$K_La_{(20°C)}$ = oxygen mass-transfer coefficient at 20°C, [s^{-1}]

θ = constant in the range of 1.015-1.040; 1.024 applies for diffused and mechanical aeration devices [3]

The tests results shown below were obtained at a temperature of 20°C in order to simplify the test evaluation. Fig. E-3 shows the development of the oxygen concentration in the aeration vessel for the conventional and air sparged aeration after oxygen depletion down to zero and subsequent re-aeration. It is obvious from the graph that with the air sparged aeration the oxygen concentration in the tank after 120 min asymptotically approaches the saturation concentration of 9.1 mg/L, meanwhile the conventional aeration did not achieve this point during the test duration of 200 min.

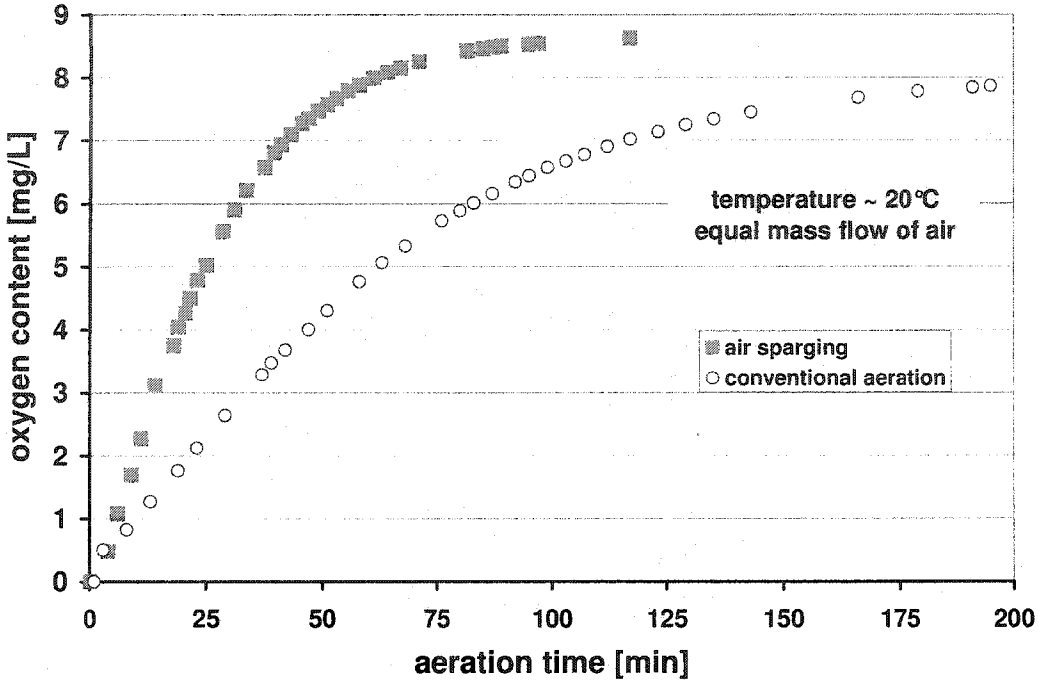

Fig. E-3. Oxygen content development in 70 L tank filled with clear water for two types of aeration

Plotting the results according to eq. E4, the K_La value is obtained from the slope by the linear regression analysis as shown in Fig. E-4. The K_La value for the air sparging system exceeds that for conventional aeration by a factor of 1.5 and is thus clearly superior. That means that for air sparged MBR in tubular sidestream systems, where filtration occurs from the inside out, conventional aeration can be omitted. Thus the air sparging serves a dual purpose: First, it increases the mass transfer through the membrane (original intention of air sparging) by enhancing turbulence and providing shear stress. Second, it takes excellent care of the necessary aeration for aerobic microbial degradation processes. Thus it is even possible to save energy

because the air sparging process is more efficient than the conventional aeration. Moreover, higher DO values yield in larger floc size and better settling [4].

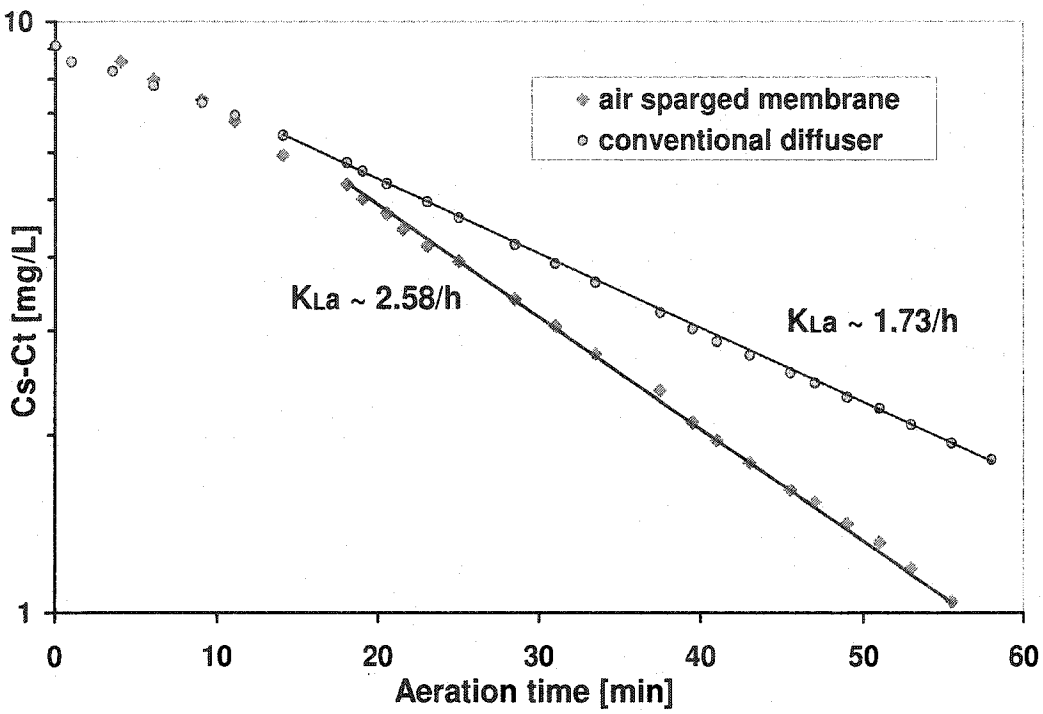

Fig. E-4. Determination of the mass transfer coefficient for clear water for two different types of aeration based on results shown in Fig. E-3.

E4 References

[1] S. Smith, Lumen-side gas bubbling for enhancement of hollow fibre membrane filtration, Membrane Quarterly, 19, 2, (2004), pp. 12-16.

[2] American Society of Civil Engineers, Measurement of Oxygen Transfer in Clean Water, ANSI/ASCE 2-91, Published by the ASCE, New York 10017-2398, (1992) second edition, pp. 1-41.

[3] Metcalf & Eddy, edited by G. Tchobanoglous, and F. Burton, Wastewater Engineering, Treatment, Disposal and Reuse. McGraw-Hill, Boston, 3rd edition, (1991), ISBN 0-07-041690-7.

[4] B. Wilen and P. Balmer, The effect of dissolved oxygen concentration on the structure, size and size distribution of activated sludge flocs, Wat. Res., 32, 2, (1999), pp. 391-400.